Georgios Giannopoulos

The regulation of denitrification in *P. denitrificans*

A thesis submitted in fulfilment of the
requirements for the degree of
Doctor of Philosophy

School of Biological Sciences
University of East Anglia
Norwich, UK

The regulation of denitrification in *P. denitrificans*

At the time of printing this thesis, the following papers were published:

Andrew J. Thomson, Georgios Giannopoulos, Jules Pretty, Elizabeth M. Baggs and David J. Richardson (2012) Biological sources and sinks of nitrous oxide and strategies to mitigate emissions. Philosophical Transactions of the Royal Society B: Biological Sciences, Volume 367, Issue 1593, Pages 1157-1168. Dx.doi.org/10.1098/rstb.2011.0415

Heather Felgate, Georgios Giannopoulos, Matthew J. Sullivan, Andrew J. Gates, Thomas A. Clarke, Elizabeth Baggs, Gary Rowley and David J. Richardson (2012) The impact of copper, nitrate and carbon status on the emission of nitrous oxide by two species of bacteria with biochemically distinct denitrification pathways. Environmental Microbiology, Volume 14, Issue 7, pages 1788–1800. Dx.doi.org/10.1111/j.1462-2920.2012.02789.x

Acknowledgements

I am grateful to Professor David Richardson and Nicholas Watmough for their trust and providing me with the opportunity to make a huge step from soil biology to the core science of molecular biochemistry and regulatory transcriptomics to investigate my beloved topic of denitrification.

I would like to acknowledge the generous funding from the Norwich Research Park, the Biochemical Society and School of Biological Science, which without it I wouldn't be able to follow my passion.

I would like to thank Katherine Hartop for her passionate contribution to aerobic denitrification and support, and Marcus Edwards, Andy Gates and Matt Sullivan for sharing their passion in research and their effective help and discussions.

Our lab technicians, teaching lab technicians and UEA administration staff for their help making sure everything was running as smooth as possible. Also, I'd like to mention Professor Gary Rowley for his kind permission to have daily access in his advanced gene expression lab facilities.

It was a unique experience to meet and discuss my preliminary results with top specialists Professor Rob van Spanning (Vrije Universiteit van Amsterdam), Stuart Ferguson (Oxford University), Zhiguo Yuan (University of Queensland), Liz Baggs (University of Aberdeen) and Tim Donohue (Wisconsin-Madison University) during my study – thank you David for organising that!

Cheers goes to Ekow, Matt, Chris, Alice, Mr Willy-T, Arthur, Emma, Jon, Michael, Basti and Manuel for making every dull winter day in the lab fun! And I wish them good luck with their studies and future plans!

I won't forget the cheerful short chats with Colin when sharing that little storage writing room at the far end of the lab and the wonderful aroma of the properly brewed coffee of Professor Andrew Hemmings next to our coffee-break chats!

Lastly but equally I would like to thank my examiners Professor Stephen Spiro and Matt Hutchings for their time and effort spend reviewing this thesis and insightfully discussing the regulation of denitrification.

Nature does nothing uselessly.

Aristotle 384 BC – 7 March 322 BC

Abstract

Bacterial respiration generates the energy required for bacterial growth. Respiration is not only limited to oxygen but could be fuelled with nitrate in anaerobic environments. Upon signal reception bacteria adjust their respiratory pathway in short time by effectively regulating respiratory gene expression and subsequently engineering the complete removal of nitrite, nitric oxide and nitrous oxide from the cytoplasm. Comparison of anaerobic and aerobic gene expression data in continuous cultures of *Paracoccus denitrificans* revealed a majority of highly expressed genes were co-regulated by CPR/FNR type transcriptional regulators. Motif analysis of the upstream region showed similar patterns recognizable by FNR. *P. denitrificans* expresses three FNR type regulators that could potentially compete for cognate site binding. Three mutant strains of *fnr*P, *nnrR* and *narR* were used to investigate the transcriptional expression of genes involved in respiration. It was demonstrated that the transcriptional factor FnrP positively regulated the transcription of *nar*, *nor* and *nap* and repressed the expression of *nos* operon. NnrR positively regulated the *nir* and *nor* operons and inhibited the expression of the *nar* and *nos* operons, in the latter case due to substrate unavailability. Finally, NarR positively enhanced the expression of the *nar* operon durring the initial stage of anaerobicity. Additionally the expression of the *nir* and *nos* operons was repressed in the Δ*narR* strain suggesting that NarR may compete for the promoter binding sites and possibly repress the expression of those genes. Additionally, sub-optimal pH inhibited growth and repressed the expression of *nirS*, *norB* and *nosZ* resulting in detectable nitrous oxide emissions. Therefore, the transcription factors FnrP, NnrR and NarR compete for the binding sites upstream of the denitrification operons in a way that optimizes the metabolic rates of denitrification and subsequently eliminates the accumulation of toxic denitrification intermediates. Therefore a new model of regulation of denitrification in *P. denitrificans* is proposed and discussed.

Contents

Chapter 3

Chapter 4

Chapter 5

Chapter 6

Chapter 7

List of figures

Chapter 1

Chapter 2

Chapter 3

Chapter 4

Chapter 5

Chapter 6

Chapter 7

The regulation of denitrification in *P. denitrificans*

1. Introduction

General introduction for respiration, transcriptional regulation and the aims of this thesis.

Georgios Giannopoulos

Contents

1.1 General Introduction

Bacteria derive energy required for survival and growth from numerous biochemical reactions. The growth stage of the organism and environmental stimulus adjusts the utilisation of these metabolic pathways. These survival reactions can be classified into two groups; firstly, those pathways that form adenosine-tri-phosphate (ATP) by substrate level phosphorylation and secondly, those that synthesise ATP by oxidative and photo phosphorylation (White *et al.* 2012). For substrate level phosphorylation cytoplasmic enzymes catalyse reactions in which adenosine-di-phosphate (ADP) receives an inorganic phosphoryl group (PO_3) by direct transfer from a phosphorylated intermediate as part of glycolysis or the Krebs cycle. For oxidative phosphorylation ATP is formed during cellular respiration where redox reactions are coupled with the phosphorylation of ADP. Depending on the driving force of coupled ATP synthesis those reactions can be driven by light (phototrophs) or by the oxidation of organic (organotrophs) or inorganic compounds (lithotrophs). In the latter subgroup the negative redox potential of the electron donors is linked to the reduction of electron acceptors with more positive redox potential which drives the ATP synthesis. The overall process of electron transport and ATP synthesis is similar in bacteria and the mitochondria of higher organisms, although some differences may exist, for example branched vs. non-branched electron transport.

The bacterium *Paracoccus denitrificans* is classified as an organo-lithotroph organism and has a respiratory system of electron transport dependent ATP synthesis very similar to the animal mitochondrion (Otten *et al.* 1999, Kelly *et al.* 2006). Membrane bound and periplasmic enzymes catalyse the reactions of respiration and create an electrochemical gradient through a proton translocation coupled electron transfer. Protons and other ions co-exist either side of the membrane which is impermeable to most ions. Therefore the net result of ion or proton translocation is the generation of a relative proton and electrical potential gradient. Under physiological conditions the ATP synthase may react either way towards ATP synthesis or hydrolysis. The proton and membrane potential gradient form the proton-motive force which is further investigated in Chapter 5.

At this point it has to be noted that alternative configurations are possible in a way that the electron donor and acceptor interact with the respiratory enzyme complexes on different sides of the membrane and other stoichiometries than the 2 H^+ translocation per redox reaction can be expected, for example the oxidation of NO_2 by *Nitrobacter sp.*

So far it has been established that bacteria utilise ion gradients to transduce the energy required for survival and growth. Using the model organism *P. denitrificans* the processes and the enzymes involved in both aerobic and anaerobic respiration will be explored further. Usually, the term respiration refers to the electron transport systems occurring in the cell membrane. When oxygen is the terminal electron acceptor, then the respiratory system is referred to as aerobic. When the terminal electron acceptor is alternative to oxygen, such as nitrate, sulphate or fumarate, the respiratory system is referred to as anaerobic respiratory system. This work investigates the aerobic and anaerobic respiration on nitrate and the subsequent nitrogenous oxides. The latter compile the denitrification pathway of *P. denitrificans*.

During respiration, electrons flow through protein complexes via a series of cofactors that serve as electron carriers. These electron carriers are classified in four groups. Both flavins and quinones are organic cofactors that can carry one or two electrons. Flavoproteins contain a flavin prosthetic group and catalyse different oxidations at different redox potentials. Quinones are mobile lipid electron carriers located in the cell membrane. Iron-Sulfur proteins contain a non-heme iron-sulfur cluster and catalyse numerous redox reactions in the cytoplasm and membrane. Lastly, cytochromes are electron carriers that harbour a heme prosthetic group classified as *a*, *b*, *c*, *d*, and *o*. The letters denote the cytochrome heme group type. In the *a* group iron is chelated by cytoporphyrin IX and contains a methyl side chain, group *b* the iron is chelated by protoporphyrin IX but lacks a covalent bond between the porphyrin and the protein, in group *c* the protoheme vinyl side chain is covalently linked between either or both with a thioether, group *d* contains a tetrapyrrolic chelate of iron as a prosthetic group in which the degree of conjugation of the double bonds is less than in porphyrin (e.g. siroheme) and lastly *o* group uniquely contains pyridine hemochromes with a methyl residue. In a simplified illustration of a respiratory

system quinones accept electrons from the dehydrogenases and transfer them to the oxidases that reduce the terminal electron acceptor (Figure 1).

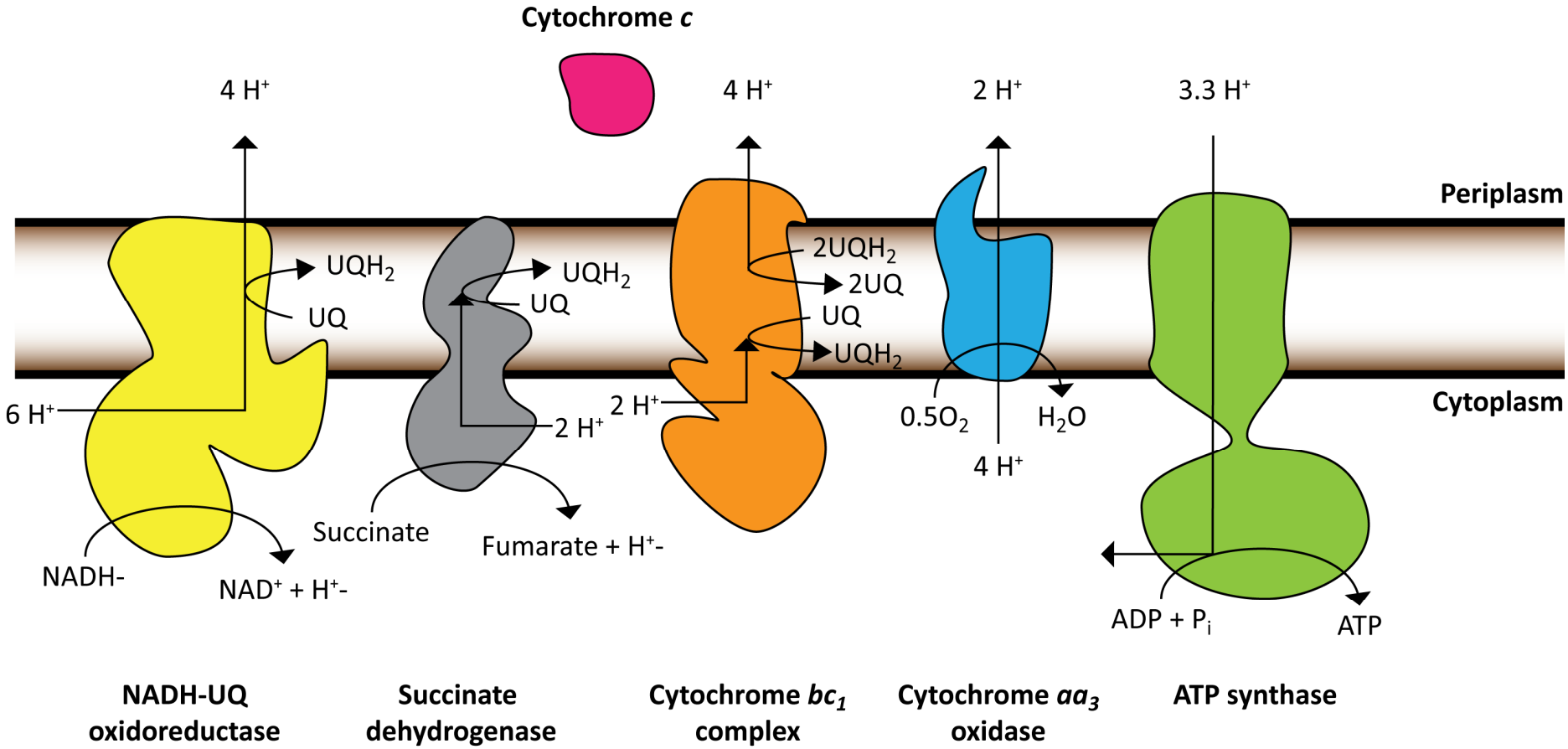

Figure 1 Oxidative phosphorylation pathway featuring the NADH-UQ oxidoreductase, succinate dehydrogenase, cytochrome bc_1 complex, cytochrome aa_3 oxidase and ATP synthase.

1.1.2 Paracoccus denitrificans as a model organism for respiration

1.1.2.1 Aerobic Respiration

Coupling the redox reactions of electron transport with proton translocation is the main process by which a proton gradient and proton motive force is created in bacteria and mitochondria (Otten *et al.* 1999). Cellular activities such as solute transport or ATP synthesis consume and lower the proton gradient (von Ballmoos *et al.* 2008). However, respiratory redox reactions in the bacterial cells generate a proton gradient that moves protons out of the cell to a greater potential. For example a common redox reaction in the respiratory chain is the oxidation of the reduced ubiquinone (UQH_2) by cytochrome *c* in the cytochrome bc_1 complex (Figure 1).

Generally, bacteria have a complex electron transport chain, which branches at either the quinone or cytochrome bc_1 level. The growth condition of *P. denitrificans* induces alterations to the electron transport chain. The aerobic pathway of *P. denitrificans* contains a number of primary dehydrogenases (see 1.1.3 Gene clusters involved in respiratory processes in *P. denitrificans*), ubiquinone, cytochrome bc_1 complex and a cytochrome aa_3 oxidase. In addition to the cytochrome aa_3 oxidase, it contains cytochrome cbb_3 and ba_3 oxidase. The genome of *P. denitrificans* also contains gene copies expressing a cytochrome *bd* oxidase, however little is known about its function. Furthermore, *P. denitrificans* expresses a respiratory peroxidase to detoxify any accumulating H_2O_2. Figure 2 illustrates a model of aerobic respiration system in *P. denitrificans*.

The cytochrome bc_1 complex (*fbcFBC*; pden_2305-2307) catalyses the electron transfer from ubiquinol to cytochrome *c* coupled to a two proton translocation across the membrane according to the proton motive Q-cycle originally proposed by Mitchell (1961). Proton pumping is achieved indirectly by movement of two negative charges across the membrane, carried by the electrons passing through the *b*-heme chain from Q_o to Q_i sites, and by release or uptake of protons on oxidation or reduction of quinone respectively, to give an overall yield of $2H^+$ pumped for each QH_2 oxidized (Crofts 2004, Crofts *et al.* 2006). This is summarized in the following equation:

$$QH_2 + 2cyt_c + 2H_N^+ \leftrightarrow Q + 2cyt_c + 2H_P^+ + 2H_{P(scalar)}^+$$

The *fbcFBC* operon encodes a Rieske iron sulphur cluster (*fbcF*), and the cytochrome c_1 and *b* subunits, *fbcB* and *fbcC* respectively. The cytochrome aa_3 oxidase is expressed by the *cta* operon. The *ctaEGBC* operon encodes the cytochrome aa_3 subunit II and III. Two copies of cytochrome aa_3 subunit I are expressed by *ctaDI* (pden_3028) and *ctaDII* (pden_1938). A second copy of the gene expressing the subunit IV of cytochrome aa_3 (pden_0432) was found in *P. denitrificans*. The cytochrome cbb_3 oxidase is encoded by the *ccoNOQPGHIS* operon and is expressed under oxygen limiting conditions; 3-22 nM oxygen (de Gier *et al.* (1994); Figure 3). The cytochrome cbb_3 has a K_m for oxygen of 7 nM. The catalytic subunit of cytochrome cbb_3 is expressed by *ccoN* (pden_1848). The *ccoO* (pden_1847), *ccoQ* (pden_1847) and *ccoP* (pden_1847) genes express the subunits II, IV and III respectively. The *ccoG* (pden_1844) gene is involved in the synthesis of a [4Fe-4S]. The *ccoI* (pden_1842) and *ccoS* (pden_1841) genes are involved in ATP-dependent Cu transport and cytochrome cbb_3 maturation respectively. The expression of the *cco* operon is controlled by of the transcription factor FnrP with a binding site of TTGACgcagATCAA found upstream of the *ccoN* (pden_1848) and TTGACgcagATCAA for *ccoG* (pden_1844).

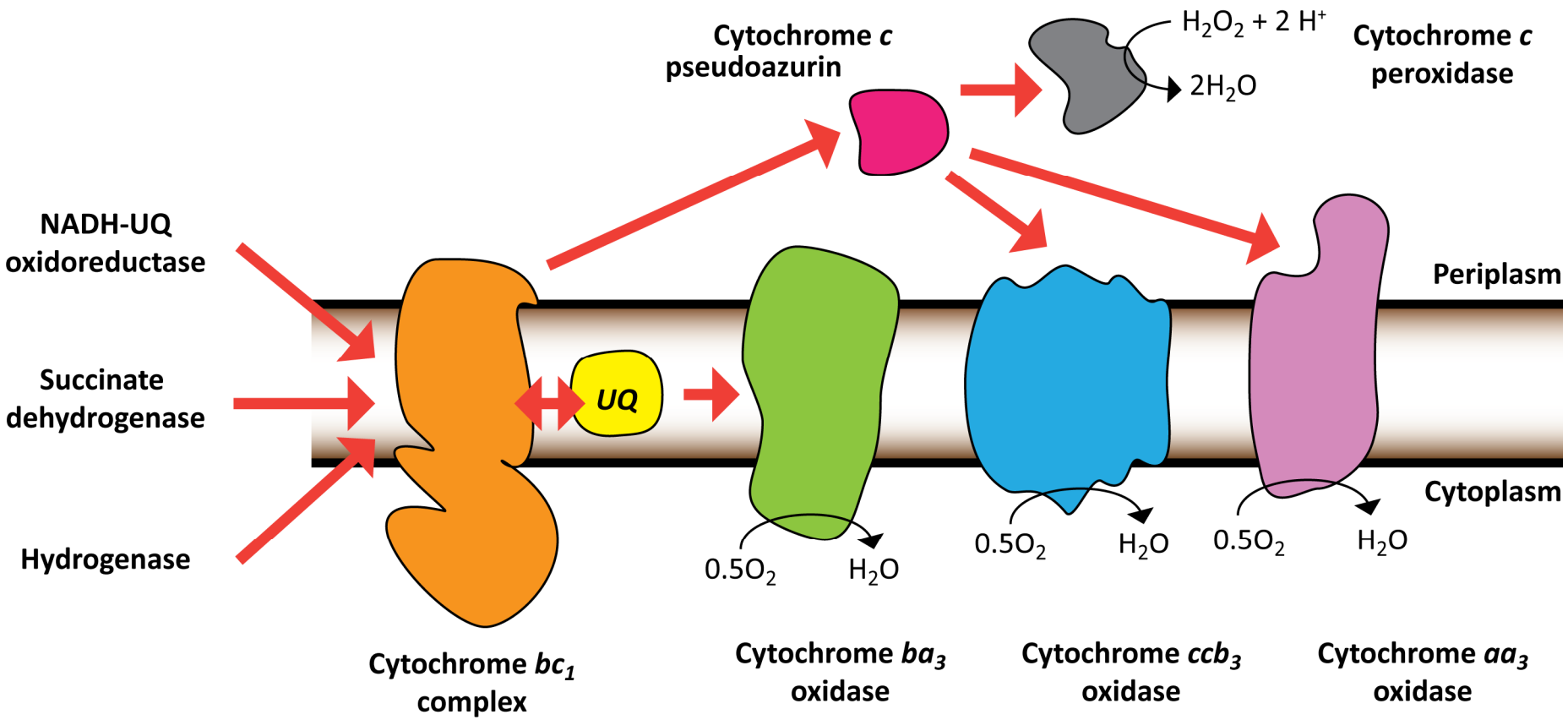

Figure 2 Illustration of the aerobic electron transport chain in *P. denitrificans*, orange arrows indicate electron transfer.

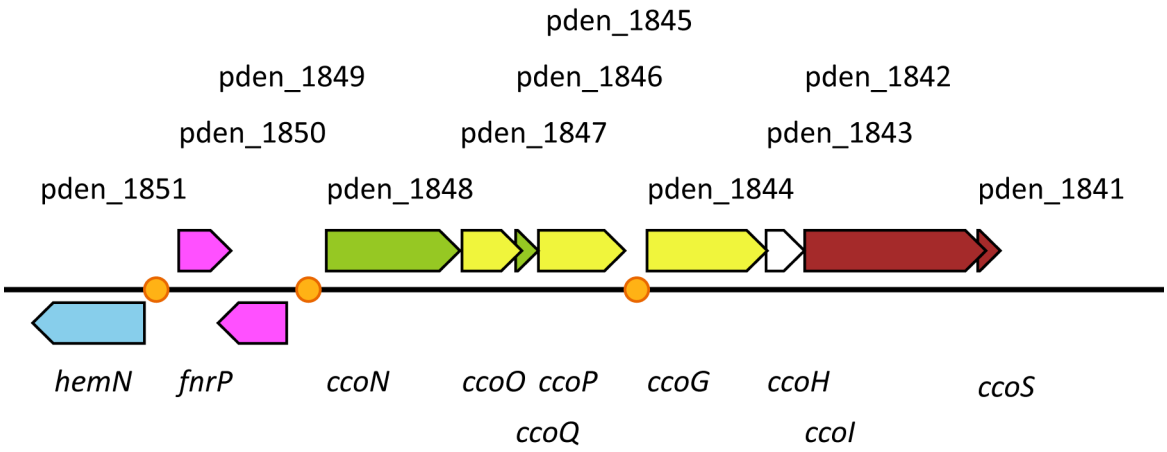

Figure 3 The *cco* operon of *P. denitrificans.* Orange dots indicate FnrP binding motifs; TTGACgcagATCAA for *fnrP* (pden_1850), TTGACgcagATCAA for *ccoN* (pden_1848) and TTGACgcagATCAA for *ccoG* (pden_1844).

1.1.2.2 Anaerobic respiration with nitrate

The absence of oxygen causes a switch in the metabolism of *P. denitrificans.* This switch changes the bacterial respiration from aerobic to anaerobic denitrification. This is very different to aerobic growth, however in anaerobic conditions, electrons are donated to the electron transport chain in exactly the same way via the same primary dehydrogenases. Nitrate is reduced to di-nitrogen gas in a bacterial process called denitrification (Tiedje *et al.* 1982, Zumft 1997). Denitrification can occur abiotically in a chemo-denitrifcation process. Chemo-denitrification is the chemical reduction of nitrate in alkaline solutions (pH 8) containing free iron (Fe^{2+}) and free copper ions (Cu^{2+}) in reducing conditions (van Cleemput 1998). Nitrate is reduced to nitrite in a reaction catalysed by nitrate reductase in a two electron transfer process. Nitrite is reduced to nitric oxide in a one electron transfer via nitrite reductase. Two moles of nitric oxide are reduced to one mole of nitrous oxide in a two electron reduction catalysed by the nitrous oxide reductase. Finally, nitrous oxide is reduced to di-nitrogen in a two electron per mole transfer via the nitrous oxide reductase. The balanced denitrification equations are listed in equations 1 - 4.

$$2NO_3^- + 4H^+ + 4e^- \xrightarrow{\text{NAR}} 2NO_2^- + 2H_2O \qquad \textbf{Equation 1}$$

$$2NO_2^- + 4H^+ + 2e^- \xrightarrow{\text{NIR}} 2NO + 2H_2O \qquad \textbf{Equation 2}$$

$$2NO + 2H^+ + 2e^- \xrightarrow{\text{NOR}} N_2O + H_2O \qquad \textbf{Equation 3}$$

$$N_2O + 2H^+ + 2e^- \xrightarrow{\text{NOS}} N_2 + H_2O \qquad \textbf{Equation 4}$$

P. denitrificans can express three different nitrate reductases, a membrane bound enzyme (Nar), a periplasmic enzyme (Nap) and a cytoplasmic assimilatory nitrate reductase (Nas). Each enables the bacterium to reduce nitrate for a specific purpose. Firstly, nitrate can be reduced as alternative electron acceptor to generate metabolic energy (nitrate respiration, Nar). Secondly, nitrate reduced to balance the excess redox potential associated with an over-reduced ubiquinone pool (nitrate dissimilation, Nap) and finally nitrate can be assimilated as a source of nitrogen for bacterial growth (assimilation, Nas).

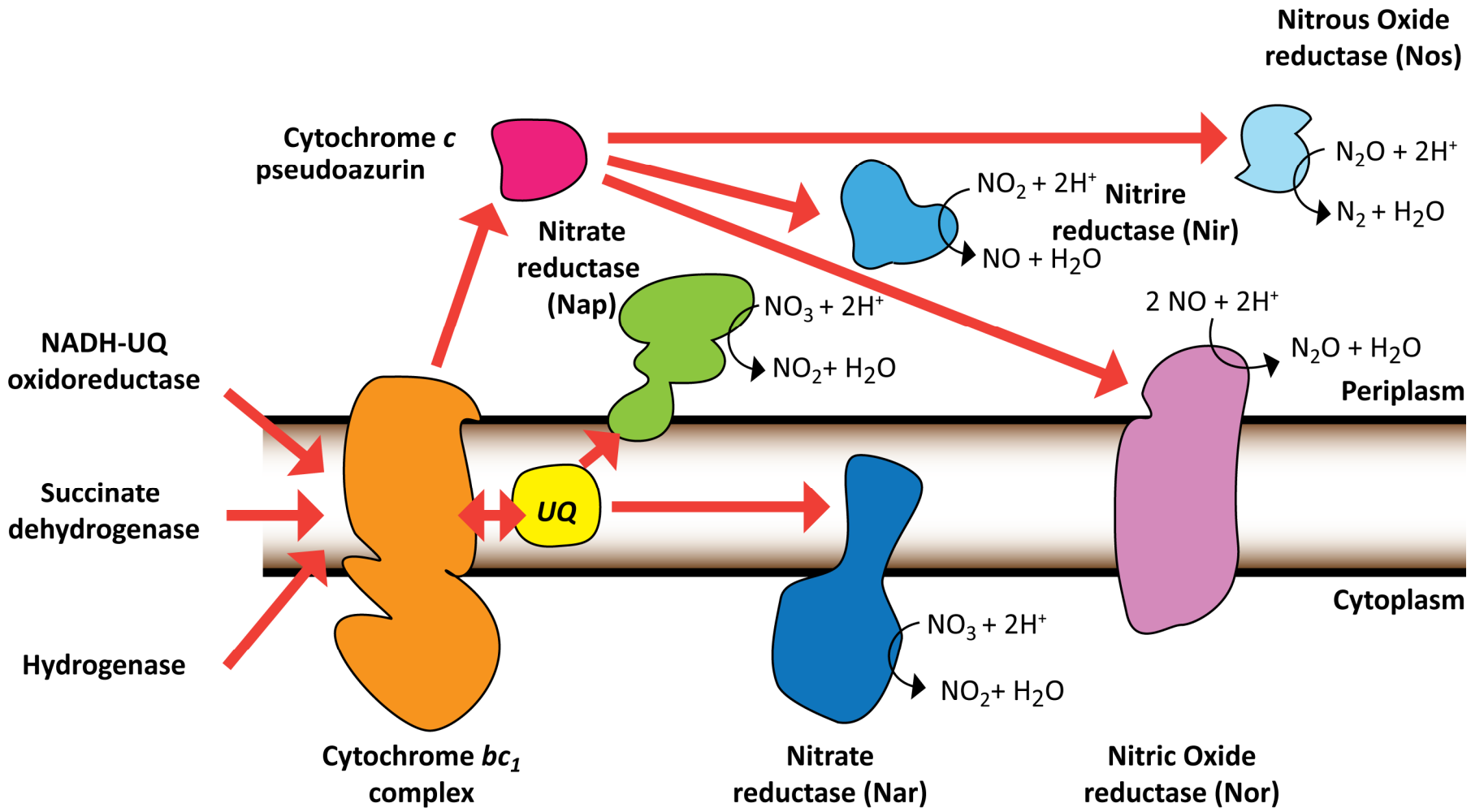

Figure 4 Illustration of the anaerobic electron transport chain in *P. denitrificans*, orange arrows indicate electron transfer (see 1.1.2.2 Anaerobic respiration with nitrate for details).

Nar, the membrane bound nitrate reductase of *P. denitrificans* is associated with the respiratory reduction of nitrate and comprises three subunits; the catalytic subunit α NarG (*narG*, pden_4233), the soluble subunit β NarH (*narH*, pden_4235) and the membrane bound subunit γ NarI (*narI*, pden_4236)(Bertero *et al.* 2003). NarG contains a MGD cofactor, NarH contains one [3Fe-4S] and three [4Fe-4S] centres and lastly the NarI subunit contains two *b*-type hemes. A fourth subunit NarJ is involved in the assembly and stability of the αβ complex of Nar. The *nar* gene cluster of *P. denitrificans* also contains *narK* (pden_4237) and *narR* (pden_4238) annotated downstream of *narG* as nitrate-nitrite transporter and nitrate transcriptional regulator respectively (Figure 5). Due to the location of the NarG in the cytoplasm nitrate has to be imported and nitrite has to be exported. Oxygen inhibits nitrate transport (NarK) via an indirect mechanism (Wood *et al.* 2001, Wood *et al.* 2002). However, the expression of this complex (Nar) is self-regulated by NarR (*narR*) and FNR (*fnrP*, pden_1850) that sense and respond to nitrate and oxygen respectively (van Spanning *et al.* 1997, Hutchings and Spiro 2000).

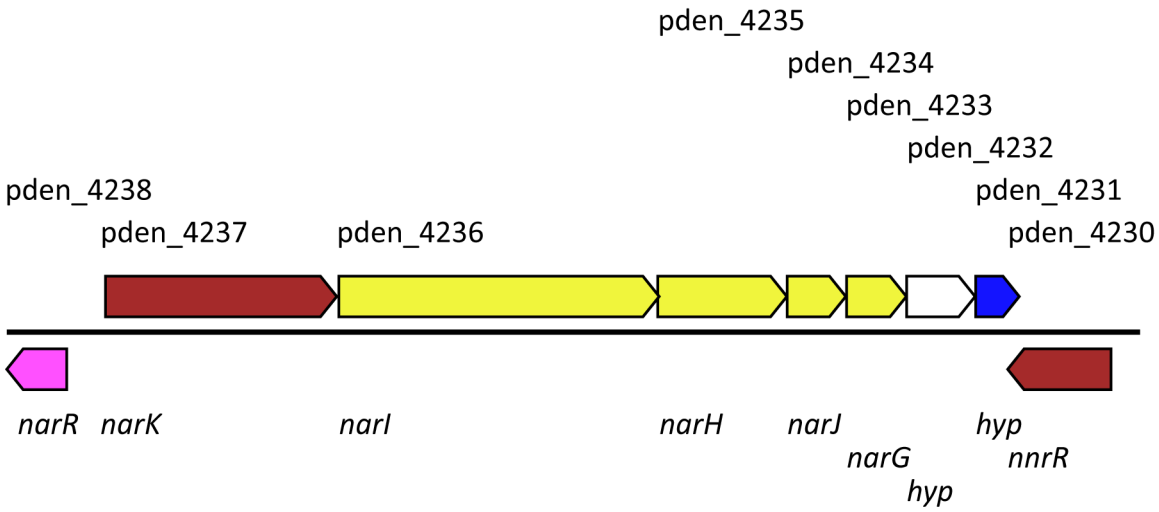

Figure 5 The *nar* gene operon of *P. denitrificans*

The periplasmic nitrate reductase (Nap) is not primarily involved in anaerobic respiration, although the nitrite formed could be used for the subsequent steps of nitrate anaerobic respiration (Sears *et al.* 1992). The *nap* gene operon is illustrated in figure 5 and consists of *napEDABC*. The catalytic subunit NapA (*napA*, pden_4721) contains a MGD cofactor and an

[4Fe-4S] cluster. The mass of NapA is 90 KDa. The NapB subunit contains a biheme cytochrome *c* and receives electrons from NapC (*napC*, pedn_4723). The NapC subunit is membrane bound and harbours a tetraheme cytochrome *c*. NapC is involved in the electron transfer between the ubiquinone pool and the periplasmic reductase NapAB. Therefore electron transfer to Nap is independent of the cytochrome bc_1 complex.

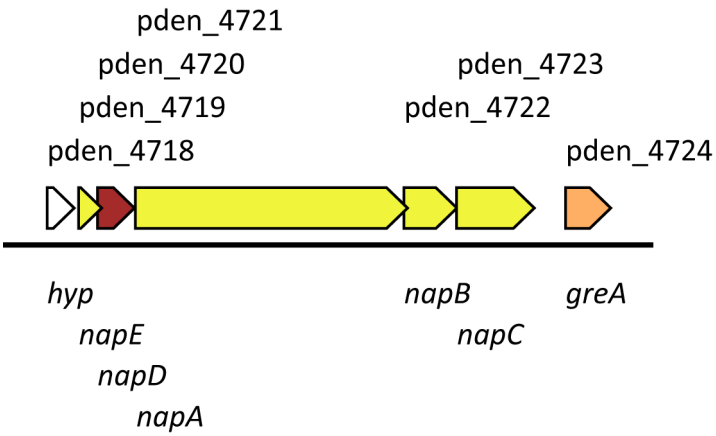

Figure 6 The *nap* gene operon of *P. denitrificans*

The expression of the *nap* operon is unaffected by the presence of ammonium and oxygen. Nap activity is induced by nitrate, however basal activity is observed either when nitrate is absent or when nitrate is mainly reduced by Nar. It has been confirmed that Nap is active when cells of *P. denitrificans* were grown aerobically without nitrate. Also it has been demonstrated that Nap is required for redox balancing during oxidative metabolism of highly reduced carbon sources such as butyrate (Sears *et al.* 1992). Refer to 5.3 Discussion for a detailed explanation of the redox balancing mechanism.

In the absence of ammonium *P. denitrificans* expresses an assimilatory nitrate reductase (Nas) and harvests the dissolved inorganic nitrogen (nitrate) for growth. The *nasTSABGHC* gene cluster (pden_4455 - pden_4449; Figure 7) in *P. denitrificans* expresses the assimilatory nitrate reductase. Electrons flow from the FAD-containing NasB subunit to NasG and finally to the catalytic bi-Mo-MGD containing subunit NasC, where nitrate is reduced to nitrite in a two-electron process (Equation 5) (Solomonson and Barber 1990). The completion of inorganic nitrogen assimilation requires the NasB subunit to reduce

nitrite to ammonium by a siroheme –dependent nitrite reductase in a six-electron reduction (Equation 6) (Gates *et al.* 2011). Nas is located in the cytoplasm therefore the membrane bound NasH and NasA subunits appear to be required for the transport of nitrate and nitrite.

$$NO_3^- + 2H^+ + 2e^- \xrightarrow{\text{NasC}} NO_2^- + H_2O \qquad \textbf{Equation 5}$$

$$NO_2^- + 8H^+ + 6e^- \xrightarrow{\text{NasB}} NH_4^+ + 2H_2O \qquad \textbf{Equation 6}$$

The *nasA* gene (pden_4453) encodes a putative major facilitator superfamily protein involved in the transport of the solute nitrate. NasH is proposed to be involved in nitrite transport. Downstream of *nasC* (pden_4449) a putative ABC transporter is identified (pden_4448). The *nas* gene cluster is repressed by ammonium and regulated by a two-component system, NasTS. The *nasT* deficient mutant of *P. denitrificans* was unable to grow in the presence of nitrate or nitrite and the growth was restored in an ammonium rich medium. The growth of the Δ*nasS* mutant of *P. denitrificans* was unaffected by the presence of nitrate, nitrite or ammonium. However, in the *nasS* deficient strain the activity of NasB was enhanced , indicating a role as a regulatory inhibitor of the *nas* operon (Luque-Almagro *et al.* 2013).

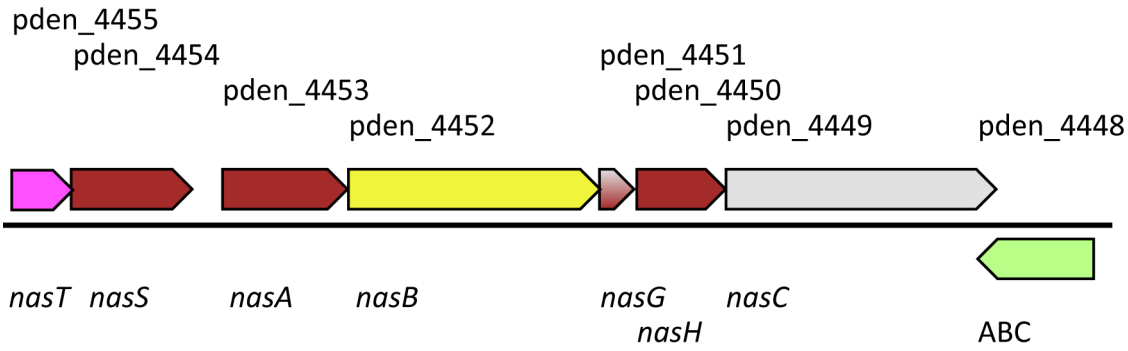

Figure 7 The *nas* gene operon of *P. denitrificans*

The dissimilatory nitrite reductase (Nir) is expressed by the *nir* genes of *P. denitrificans* (Figure 8). Bacterial nitrite reductases reduce nitrite to nitric oxide in a one-electron reaction catalysed either by a cytochrome cd_1 or Cu containing nitrite reductase (Equation 2). The nitrite reductase of *P. denitrificans* is located in the periplasm and is a cytochrome cd_1 nitrite reductase. So far, no bacterial strain has been reported to contain both types of nitrite reductase. The nitrite reductase of *P. denitrificans* contains two *c*-type heme and two d_1-type hemes in a functional dimer. Electrons flow from the cytochrome bc_1 to the catalytic d_1-type hemes via the *c*-type hemes.

The expression of the *nir* operon is under the control of the Nitrite and Nitric oxide Regulator (NNR) and is encoded by *nnrR* (pden_2478) in *P. denitrificans*. The NNR binding site is located downstream the *nir* and *nor* operon. It has also been demonstrated oxygen negatively regulates the expression of the *nir* and *nor* operons.

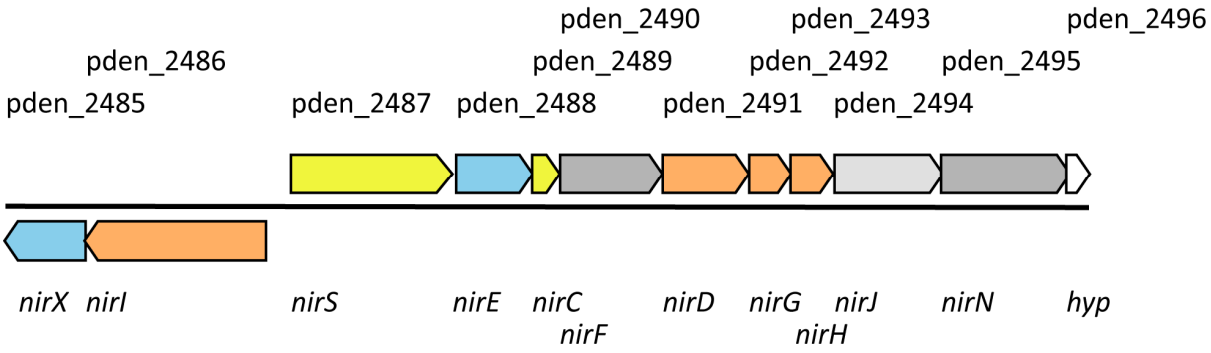

Figure 8 The *nir* gene operon of *P. denitrificans*

Nitric oxide, an intermediate of denitrification and potent molecule involved in cell signalling (Van Spanning *et al.* 1999, Hutchings and Spiro 2000, Spiro 2007, Bergaust *et al.* 2011) and host defence (Runkel *et al.* 2013) in other systems is reduced to nitrous oxide by the nitric oxide reductase (Equation 3). The functional subunits NorC (*norC*, pden 2484) and NorB (*norB*, pden_2483) of nitric oxide reductase of *P. denitrificans* contain a heme *c* and two *b*-type hemes with a non-heme iron (Fe_B) respectively. The NorB subunit is a transmembrane protein catalysing the nitric oxide reduction and the NorC subunit which is anchored on the membrane receives electrons from either cytochrome c_{550} or pseudoazurin

(*pasZ*, pden_4222) via the cytochrome bc_1 complex (Dermastia *et al.* 1991, Hendriks *et al.* 2000, Hino *et al.* 2010). The nitric oxide reductase of *P. denitrificans* is expressed by the *nor* operon (Figure 9).

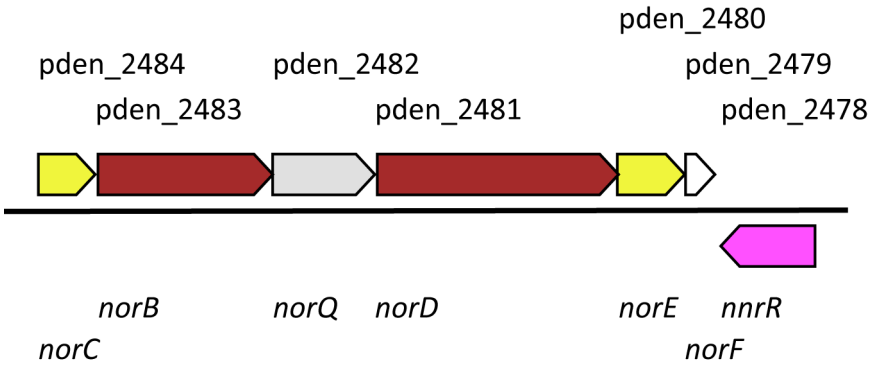

Figure 9 The *nor* gene operon of *P. denitrificans*

The greenhouse gas, nitrous oxide is reduced to di-nitrogen by a copper containing nitrous oxide reductase in *P. denitrificans*. In its functional form, nitrous oxide reductase is located in the periplasm as homo-dimer. Electrons are received from either cytochrome c_{550} or pseudoazurin (*pasZ*, pden_4222) via the cytochrome bc_1 complex by the bi-nuclear Cu_A electron input site. The catalytic site is a tetra-nuclear copper cluster Cu_Z, refer to Brown *et al.* (2000), Einsle and Kroneck (2004) for the crystal structure of NosZ. The functional enzyme requires 12 copper ions to reduce nitrous oxide to di-nitrogen. The C-terminal region of the NosZ, where the Cu_A is located, shares considerable similarities with the subunit II of the cytochrome aa_3 of *P. denitrificans*.

The *nos* operon encodes the nitrous oxide reductase of *P. denitrificans* (Figure 10) with the catalytic subunit expressed by *nosZ* (pden_4219). Downstream of *nosZ*, *nosR* (pden_4220), *nosC* (pden_4221) and *pasZ* (pden_4222) are found. Pseudoazurin (*pasZ*) and cytochrome c_{550} donate electrons via the the cytochrome bc_1 to Nos. The products of *nosR* and *nosC* are involved in the indirect transcriptional regulation of *nosZ* with a role in copper transport and NosZ assembly (Sullivan *et al.* 2013). The gene expressing NosX (*nosX*, pden_4214) is a homologue of *nirI* (pden_2486). The predicted amino acid motif indicates a twin arginine transport (TAT) system motif suggesting that NosX could be involved in metal ion transport

and NosZ assembly. Mutational insertions in either *nosX* or *nirI* of *P. denitrificans*, showed no distinct growth phenotype, however in the double mutant strain nitrous oxide activity was noticeably reduced. Further analysis of the NosZ of the double *nosX* - *nirI* mutant confirmed that the distinct signal of the Cu_A was undetectable, confirming the role of NosX in metal ion transport (Saunders *et al.* 2000). The remaining *nosDFYL* genes share sequence similarities with the equivalent genes from *Pseudomonas* species and are involved in NosZ maturation. The *nosD* product is annotated as a putative copper binding protein, the *nosF* gene product as an ATP-binding ABC transporter and the *nosY* and *nosL* are involved in the maturation of NosZ (Hoeren *et al.* 1993).

NosZ activity is repressed by oxygen and in principle could be regulated by an oxygen sensitive transcriptional regulator, the Fumarate and Nitrate Regulatory protein (FNR) which is encoded by *fnrP* in *P. denitrificans*. Upstream of *nosZ* two FNR-like binding sequences are detected, the first one has a sequence motif TTGAAGCTTAACCAG and is centred at position -21 in front of the start codon the second one is located at -126 with a motif of CCCGGTGGTCATCAAG. The latter binding motif is thought not to be involved in transcriptional binding due to the relatively long distance before the start codon.

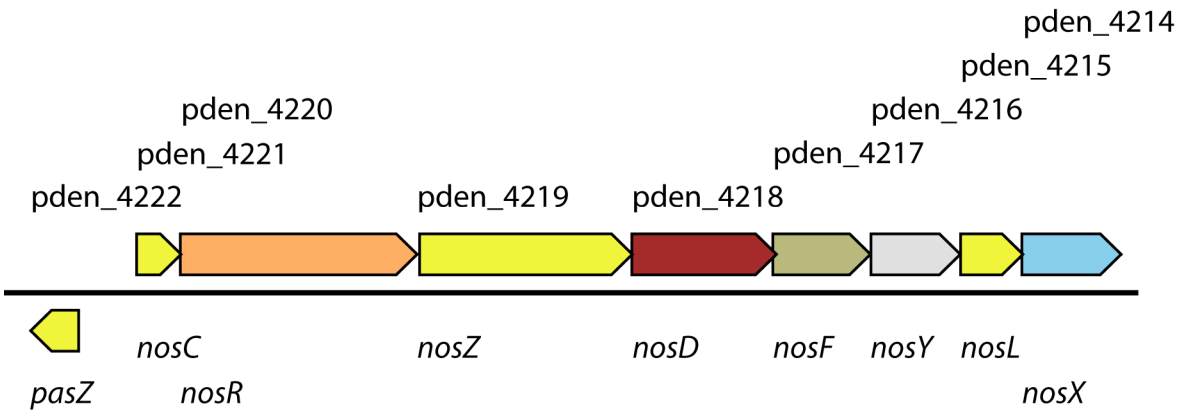

Figure 10 The *nos* gene operon of *P. denitrificans*

1.1.3 Gene clusters involved in respiratory processes in *P. denitrificans*

1.1.3.1 Genes involved in primary dehydrogenases

The genome of *P. denitrificans* encodes 12 primary dehydrogenases; succinate dehydrogenase (two gene clusters: *sdhCDAB* pden_0566-0572and *sdhDCB* pden_3020-3022) periplasmic quinone dependent formate dehydrogenase (*fdnGHI*; pden_2824-2830), NADH:quinone oxidoreductase (*nuo* operon; pden_2231-2250), Hydrogenase-I (*hypABCDEF* pden_3107-3113), hydrogenase-II NADH dependent (*hup* operon; pden_3093-3106), methanol dehydrogenase (*mxa* operon pden_2993-3003), methylamine dehydrogenase (mau operon; pden_4728-4738), glutathione-independent formaldehyde dehydrogenase (*fdh* operon; pden_1186-1189), glutathione-dependent formaldehyde dehydrogenase (*flh* operon; pden_0010-0011), formygluatathione hydrolase (*fgh* operon pden_0012-0023) and a sulphite dehydrogenase (*sox* operon; pden_4145-4161).

1.1.3.2 Genes involved in electron transport

As seen previously in aerobic and anaerobic respiration electrons flow from the electron donor though the cytochrome bc_1 complex to the terminal electron receptor via the quinone pool. The genome of *P. denitrificans* contains genes encoding cytochrome bc_1 ubiquinone cytochrome *c* oxidoreductase (*fbcFBC*; pden 2305-2307), cytochrome ba_3 ubiquinone oxidoreductase (*qoxABCD*; pden_5104-5108), cytochrome *bd* ubiquinone oxidoreductase (pden_4007-4012), electron transport flavoprotein (ETF) (*etfSL*; pden_2550-2551) and ETF:Ubiquinone oxidoreductase (*etfD*; pden_0425), pseudoazurin (*pasZ*; pden_4222), cytochrome c_{550} (*cycA*; pden_1937), cytochrome c_{552} (*cycM*; pden_1808), cytochrome c_{551i} (*mxaG*; pden_2995), cytochrome c_{553i} (*cycB*; pden_0021), cytochrome c_{551} (*soxD*; pden_4156) and cytochrome biogenesis (*cycH*; pden_0511 and *cycJ*; pden_3974).

1.1.4 The importance of growth medium and advantages of continuous culture in genomic studies

It has been firmly established that the ions of copper, molybdenum, cobalt, sulphur and iron play a fundamental role not only in the functional activity of the denitrification proteins, but

also in heme and [Fe-S] biosynthesis which is essential for bacterial growth and survival. Additionally the importance of ammonium in suppressing the nitrate assimilatory system has been explained. Nitrate, nitrite, nitric oxide and oxygen may serve as signalling compounds involved in transcriptional regulation of the denitrification pathway.

The minimal growth medium used in this study was based on the composition of Vishniac and Santer used for the experimental cultures of *Thiobacilli* species (or details see Chapter 7; Materials and Methods). The importance of copper availability in the growth medium specifically for a functional NosZ has been assessed in continuous cultures of *P. denitrificans* and *Achromobacter xylosoxidans* previously (Felgate *et al.* 2012). The continuous supply of ammonium, nitrate and succinate among other trace elements in continuous culture of denitrifying bacterial strains has been used successfully to investigate both physiological and transcriptional responses to denitrification (Sears *et al.* 1992, Baumann *et al.* 1996, Baumann *et al.* 1997, Baumann *et al.* 1997, Bergaust *et al.* 2011).

Continuous culture techniques have also been employed to effectively bio-synthesize or bio-transform various compounds of economic interest (Hoskisson and Hobbs 2005). Several studies utilize continuous cultures to investigate population or generation dynamics (Crécy *et al.* 2007, Panikov 2009). The concept of continuous culture lies on a steady state mass balance whereas the cellular biomass is removed at an equal rate of the apparent growth rate. In this balanced state, the cell biomass, the culture volume and the bacterial product levels should be kept constant. Additional growth controls could be added, in the case of chemostats the cell growth rate is determined by the input rate of the limiting substrate and subsequently to the outflow rate of the reaction vessel (Doran 2013); see Chapter 2 and 7 for a detailed modelling and system description respectively. A continuous culture with a single limiting substrate ensures that the remaining compounds in the medium will not be exhausted, eliciting stress related transcriptional and physiological bacterial responses. This concept is crucial to investigate the expression not only of the functional denitrification genes, but also the effect of the transcription factors involved. Under these conditions the dilution rate is equal to the specific growth rate, and the generation time of the culture can be calculated. Because of the overall impact of the dilution rate on the physiological state of the bacterial cell, the comparison and interpretation of continuous cultures with different

dilution rates should be done with extreme caution. The continuous inflow of sterile nutrient solution and the outflow of the waste solution eliminate the accumulation of toxic or inhibitory secondary metabolites that may mask any underlying processes when compared to experimental investigations performed in batch cultures. Additionally, the option to select lower dilution rates may be advantageous to study complicated bacterial metabolic pathways. It is therefore highly desirable to utilize such highly controlled systems to study the transcriptional profiles in a very well defined growth environment. Combined with recent advances in whole genome transcriptional techniques (microarray and RNA-seq), continuous cultures offer such defined and reproducible experimental growth environments to apply those techniques as explained previously (Hoskisson and Hobbs 2005). However, it should be noted that the long term continuous culture of bacterial species may stimulate spontaneous or evolutionary mutations (Helling *et al.* 1987, Doran 2013).

Therefore, the combination of steady-state chemostat cultures and molecular genomic techniques provides a solid experimental foundation for the analysis of biological processes in microorganisms; an approach which has not been used previously in the investigation of the whole genome transcriptional profile of *P. denitrificans* respiring anaerobically.

1.2 Regulation in proteobactria

1.2.1 The flow and replication of biological sequence information

Part of this thesis investigates the genetic regulation of denitrification which is complex but is known to involve a number of transcription factors. Genetic information stored in the sequence of alternating bases adenine, thymine, cytosine and guanine (DNA) is transcribed by RNA polymerase to readable genetic code as mRNA, that is subsequently used as an instruction script for the ribosomes to synthesize functional sequences of amino-acids

(proteins) (Figure 11). A simplified regulatory unit consists of the transcription factor (TF), the target gene (TG) and its binding site. TF are proteins that are predicted to bind to DNA binding sites (promoters), and to either up- or down-regulate gene transcription. TF may either bind on DNA recognizing specific and highly conserved DNA motifs or non-specifically. TF may control a single gene or a network of genes. However, every role or function of a TF in the energy dynamics and conformational changes of the DNA strain is not well understood but widely accepted that their presence has an instrumental role interacting with a wide variety of bacterial promoters subjected to positive or negative control.

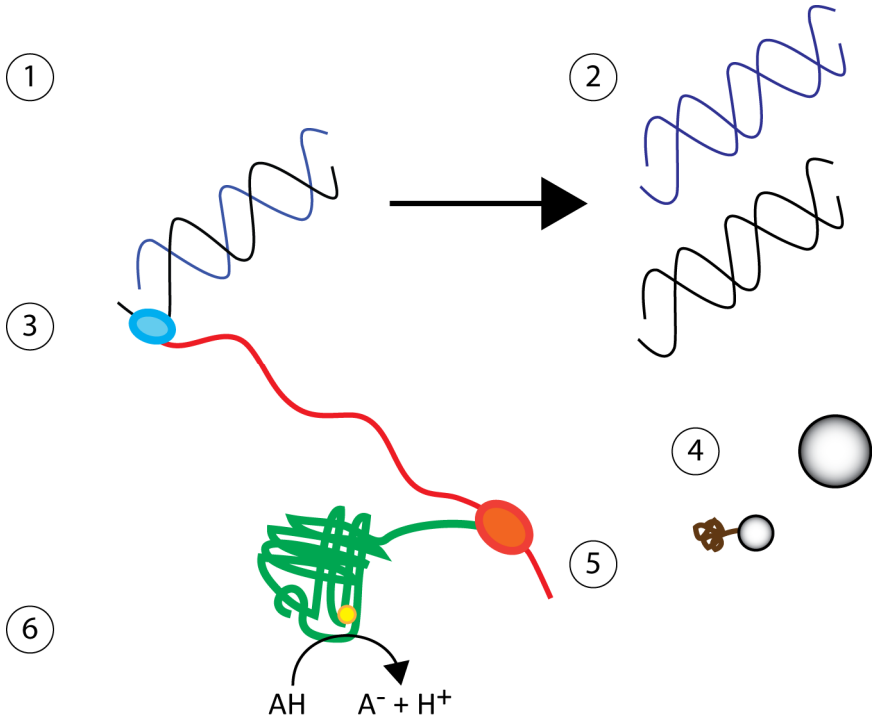

Figure 11 Schematic illustration of the central dogma in biology in prokaryotes. The genetic information is stored in nucleotide sequences (1) and the information is preserved by DNA replication (2). RNA polymerase (3) with the interaction of transcriptional factors that sense environmental signals (4) transcribes the genetic information to a genetic script (mRNA) that instructs the ribosomes (5) to construct functional sequences of amino-acids (6).

1.2.2 Regulation by FNR as an example of transcriptional regulation

Previously the flow of genetic information in prokaryotic cells has been briefly illustrated. The RNA polymerase consists of 5 subunits two α, β, β', and ω and is capable of synthesizing

mRNA based on a DNA template. The double stranded DNA is melted by another subunit known as the sigma (σ) factor. The σ factor enhances the binding between the RNA polymerase and the DNA template creating the RNA polymerase holoenzyme. Bacteria contain multiple σ factors for the regulation of a set of genes or operons when those genes are co-expressed. The σ^{70} class factors immediately activate the core RNA polymerase holoenzyme, however the σ^{54} class factors require an additional ATP-dependent activation event which is provided by AAA+ ATPase transcriptional activators. The σ^{54} transcription activators control the gene expression tightly and thus directing precise responses to an environmental change (Kazmierczak *et al.* 2005).

In *E. coli* the transcription activator Fnr binds to a consensus site of TTGAT-N4-ATCAA centered in the −40 to −50 region upon oxygen extinction (Spiro and Guest 1990). The Fnr becomes active as a dimer in anaerobic environments and induces gene clusters involved in anaerobic formate and nitrate respiration; the formate dehydrogenase-N, encoded by the *fdnGHI* operon and the nitrate reductase, encoded by the *narGHJI* operon in *E. coli* (Sutton *et al.* 2004, Kang *et al.* 2005, Constantinidou *et al.* 2006). Fnr contains a cyclic nucleotide (cAMP) binding domain and a C terminal CRP type helix-turn-helix domain. In the N terminal region the oxygen sensing domain exists, containing 5 cysteine residues that coordinate a iron-sulphur cluster. In vitro studies have shown that only four of the cysteine residues are essential for oxygen sensing. Upon oxygen depletion one [4Fe-4S] cluster per monomer is formed driving conformational changes and inducing dimerization and enhancing site-specific DNA binding to target promoters. When oxygen is available the $[4Fe\text{-}4S]^{2+}$ is oxidised to $[3Fe\text{-}4S]^{2+}$ and finally to [2Fe-2S] monomer of the apo-Fnr in a two-step reaction (Crack *et al.* 2008, Jervis *et al.* 2009).

In a σ^{54} initiated gene expression the transcription activator will bind to the enhancer sequences usually in distances less than 200 bp upstream of the target gene. The activated ligand of the transcriptional regulator, bound on the enhancer sequences assembles into the active conformation while where needed the integration host factor bends the DNA bringing the transcription activator into close contact with σ^{54} factor. The activated RNA polymerase holoenzyme opens the double stranded DNA and mRNA elongation begins.

P. denitrificans encodes the transcriptional regulator FnrP (*fnrP*, pden_1850) by a single gene located between the high-affinity cbb_3 oxidase operon *cco* and oxygen-independent coproporphyrinogen III oxidase (*hemN*) which is required for heme biosynthesis (Figure 3). In this genetic locus several FnrP DNA binding sequences (motifs) exist and van Spanning *et al.* (1997) has shown that FnrP acts as a *cis*-activator for *fnrP, ccoN* (pden_1848) and *ccoG* (pden_1844).

1.2.3 Background processes involved in transcriptional regulation

Transcription begins at a specific promoter site that interacts with the transcription factor enhancing the affinity of the RNA polymerase and with the interaction of σ factor forming d subsequently the RNA holoenzyme. The σ factor functions in such way that it ensures the recognition of specific sequences positioning the RNA polymerase holoenzyme upstream of the target gene facilitating the unwinding of the DNA duplex close to the start site. Bacteria may contain multiple σ factors; in *P. denitrificans rpoN* (Pden_4987) encodes a σ^{54} factor that recognizes two separate promoter regions between -35 and -10. However, the supply of RNA polymerase and σ factors is in short, distinct molecular mechanisms seem to ensure the prudent distribution of RNA polymerase between competing promoters. These involve promoter DNA sequences, σ factors, small ligands, the folded bacterial chromosome structure and transcription factors. Transcription factors may enhance the RNA holoenzyme interaction by stabilizing the open complex. Several transcription factors (CRP, FNR, AraC, NarL, LysR etc) control the regulation of gene operons in response to an environmental signal either by controlling the expression of target genes or the affinity of the RNA polymerase to initiate transcription. The mode of activation of simple promoters is done either by contraction of aCTD of RNA polymerase or by re-orientation and conformational changes to the DNA. In class I activation the TF binds to a target sequence that is located upstream of the promoter –35 element and recruits RNA polymerase to the promoter by directly interacting with the α carboxy-terminal domain (α-CTD) of RNA polymerase. In class II activation, the TF binds to a target sequence that overlaps the promoter –35 element and contacts domain 4 of the RNA polymerase σ subunit. This contact also results in recruitment of RNA polymerase to the promoter, but other steps in initiation can also be affected. The

third mechanism for activation involves conformational changes that re-orientate the promoter –10 and/or –35 elements to enable the interaction with RNA polymerase. Repression or prohibition of transcription may occur by 1) steric hindrance of RNA polymerase binding to promoter DNA, 2) interference with post-recruitment steps in transcription initiation and 3) functioning as an anti-activator.

However, cells need to modulate expression of multiple genes in response to an environmental perturbation, which involves complex multiple site regulation. Dictated by various mechanisms that allow variation in the level of expression of genes — known as 'fine tuning', transcriptional factors may bind synergistically or independently thus competing for binding sites in an oscillating dynamic system.

A transcription factor has to recognize its binding site among ~10^6 alternative sites in prokaryotic DNA sequences. This requires $I_{min} = log_2 N$ bits of information according to the information theory when searching for a unique object (Wunderlich and Mirny 2009). For a prokaryotic organism such as *P. denitrificans* with $5.2 * 10^6$ bp the I_{min} equals to ~22 bits, however the observed *I* for the CRP family of transcriptional factor is ~11 bits. Thus this low information content makes it rather challenging to find the cognate binding site. Additionally the low actual information content increases the number of spurious binding sites that may actually result in sequestering the transcription factor molecules lowering the active transcriptional factor copy numbers per cell. As an example the LacI repressor in *E. coli* has an average of 5-10 copies per cell (Glascock and Weickert 1998).

Besides the recognition process based on the sequence probability of actual and spurious cognate sites and the available information content for recognition of putative binding sites another physical process takes place in the cell that classifies the binding sites according to the energy potential they hold to associate with a transcription factor. For a binding motif with a length of 12 bp the energy contribution of each consensus base pair to the total sequence-specific energy was found ~ 2-3 k_BT=1-2 Kcal.mol^{-1} for prokaryotes. This process of energy binding does not discriminate the contribution of non-specific binding of proteins to DNA that may affect transcription. Experimental evidence has shown that competition between specific (high-affinity) and non-specific binding to a DNA sequence determines the

regulation of transcription (Kolesov *et al.* 2007). It was calculated that bacterial transcription factors have a probability 10^{-6} of binding non-specifically.

So far a probabilistic and thermodynamic model has been developed to interpret the difficulties of transcription factors finding and binding at a cognate site. The challenge of a transcription factor to find a cognate site in fractions of a second in a multi-dimensional cytoplasmic environment will be further developed with a kinetic approach. Three modes of transcription factor translocation along DNA sequences have been proposed: firstly, the transcription factor slides randomly without disassociating from the DNA sequence secondly, the transcription factor disassociates briefly and "hops" along the DNA sequence and lastly, the transcription factor disassociates and "jumps" to a nearby location. Having in mind those three modes of kinesis, the total cognitive site searching time required will be equal to the sum of the time used for sliding and disassociating in the total number of searching loops. This kinetic model suggests that the optimal strategy for locating a cognate binding site will be to involve frequent disassociations followed by re-associations and sliding along the DNA sequence. The binding to non-specific DNA sequences (low binding energy ~10-15 k_BT) could assist the transcription factor to slide along the sequences; however the stronger binding affinity of a specific site (~2-3 k_BT) will slow down and effectively engage the transcriptional factor. The existence of multiple cognate sites in the genome sequence may assist the transcription factor to jump to different DNA locations in a fast search mode. Additionally the multiple cognate sites may reserve part of the transcription factors by acting in stand-by mode (Tafvizi *et al.* 2011, Leith *et al.* 2012). The latter, could be of significance however is not well defined experimentally. Furthermore, maintaining hundreds of copies of transcription factor per cell and keeping them in a stand-by mode may increase the metabolic cost of the cell.

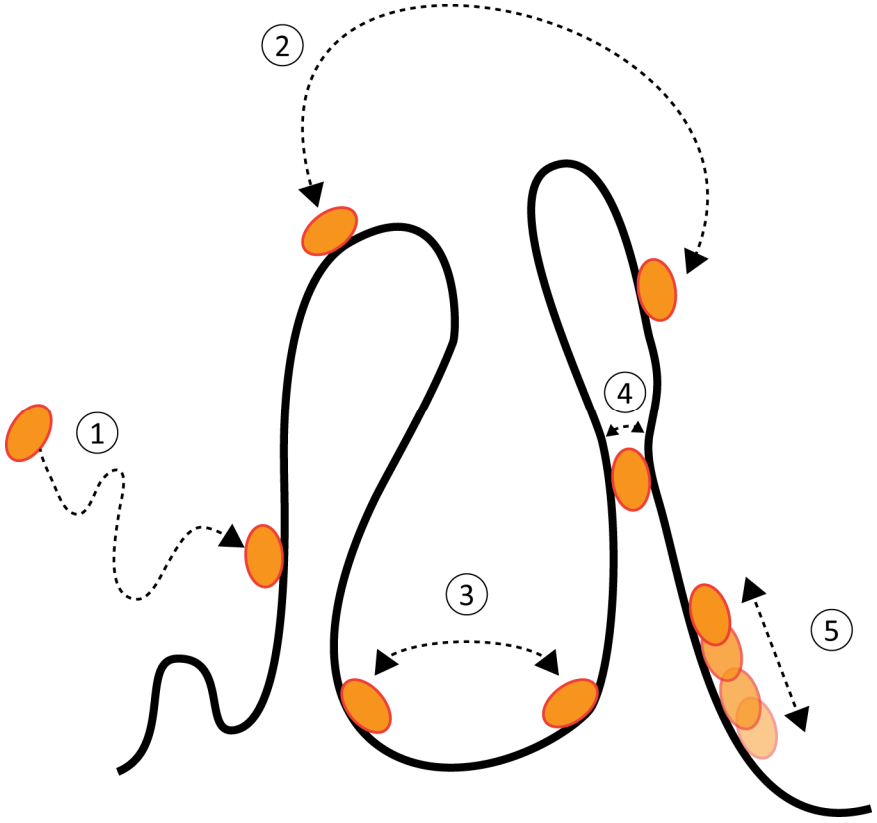

Figure 12 The kinesis dynamics of a transcription factor while searching for a cognate binding site. 1: Diffusion through the cytospace and binding to a putative site. 2: disassociation and jump to another DNA location. 3: disassociation and hop to another DNA location. 4: inter-segmental transfer via sliding and 5: random sliding along the DNA sequences.

To conclude, the previously described process of cognate site binding of a transcriptional factor challenges our current understanding of gene regulation that considers a single binding event per binding site per transcription factor takes place to regulate transcription based on previous experimental data. A clear competition between the transcription factor for a cognate site is possible and its balance determines the organism's response to an environmental signal.

1.2.4 Detection and quantification of transcription

Transcription is widely studied in various scales depending on the aim of the research. Currently there are numerous techniques to detect and assess the binding potential of a transcription factor to a known DNA sequence, including fluorescence microscopy,

chromatin immunoprecipitation and microarray technologies. Using total internal reflection fluorescence microscopy (TIRFM) single molecules of a transcription factor can be visualized sliding along individual DNA molecules, measuring the kinetics of this process (Harada *et al.* 1999). High throughput systems such as chromatin immunoprecipitation assays (ChIP) could be also used to study transcription factor-DNA binding interactions. ChIP assays are a robust way of capturing a snapshot of specific protein-DNA interactions, however high grade antibodies and additional qPCR assays are required to quantify the ChIP results. Type II microarray assays (DNA / RNA (cDNA)) offer a snapshot of genome expression. The gene expression is quantified by detecting the fluorescence levels of each probe. Microarray results can be coupled with qRT-PCR assays to quantify and verify the relative gene expression levels providing a confirmed snapshot of the organism genome expression at low cost (Suarez *et al.* 2009).

1.3 Regulation of denitrification in *Paracoccus denitrificans*

Earlier in the chapter the pathways of aerobic and anaerobic respiration in *P. denitrificans* were extensively summarized. The respiratory pathway that is followed depends on the external environmental gradients such as the oxygen tension. Those signals are sensed by transcription factor proteins that transcriptionally regulate or co-regulate the expression of genes encoding specific respiratory oxidoreductases. To illustrate this, it has been observed that the transcription of the *nar* operon was induced after oxygen depletion and the nitrate (*nar*) and nitrous oxide reductase (*nos*) mRNA transcripts were detected prior to those of the nitrite reductase (*nir*) (Baumann *et al.* 1997). In another study it was demonstrated that *nosZ* expression was induced twice, firstly when the batch culture depleted the dissolved oxygen and secondly when NO was detected in the growth medium of *P. denitrificans* (Bergaust *et al.* 2011). These observations suggest that different sensing and regulatory mechanisms are involved in the transcription gene expression *of P. denitrificans* under anaerobic conditions when nitrate is present as an alternative electron acceptor.

P. denitrificans encodes FnrP a protein that senses oxygen, its homologue in *E. coli* activates the transcription of genes involved in anaerobic respiration. A *fnrP* (pden_1850) deficient strain of *P. denitrificans* was unable to express the nitrate reductase (*nar* operon), cytochrome c peroxidase (*ccpA*) and the cytochrome cbb_3 (*cco* operon). In contrast the Δ*fnrP* mutant of *P. denitrificans* had increased levels of cytochrome ba_3 oxidase (*qox* operon) (van Spanning *et al.* 1997). The FnrP forms a dimer in its active form (in the absence of oxygen) and contains a helix-turn-helix domain that binds to the motif TTGATnnnnATCAA. Under aerobic conditions, the redox sensitive iron-sulphur cluster is destroyed, thus deactivating transcription (see 1.2.2 *Regulation* by FNR as an *example of* transcriptional regulation). FNR is rather sensitive to oxygen, with oxygen concentrations as low as 6 nM deactivating the dimer of FNR *in vitro* (Jervis *et al.* 2009). In a proteomic study genes induced by FnrP were the *fnrP* (pden_1850), *ccoG* (pden_1844), *ccoN* (pden_1848), *ompW* (pden_3636), *pasZ* (pden_4222), *narK* (pden_4237), *narG* (pden_4238) and *qoxA* (pden_5108) (Bouchal *et al.* 2010) These genes have similar FNR binding motifs with a simplified sequence of TTGnnnnnnnnCAA as illustrated in figure 13. See Chapter 2 for a detailed transcriptional investigation between aerobic and anaerobic respiration in *P. denitrificans*.

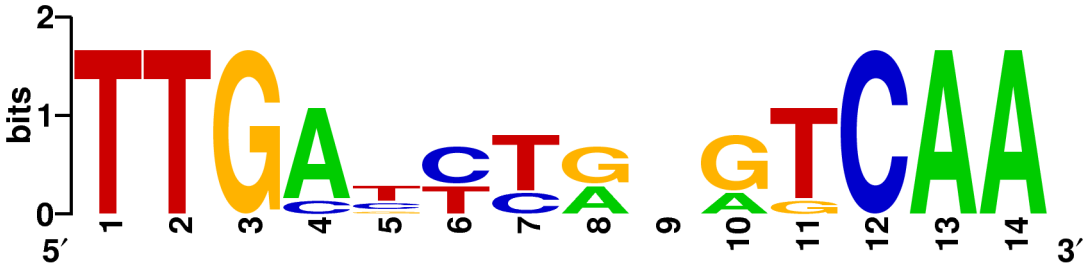

Figure 13 FNR binding motif logo based on promoter sequences of *fnrP* (pden_1850), *ccoG* (pden_1844), *ccoN* (pden_1848), *ompW* (pden_3636), pasZ (pden_4222), *narK* (pden_4237), *narG* (pden_4238) and qox (pden_5108). The logo was calculated with WebLogo (http://weblogo.berkeley.edu/logo.cgi).

The NnrR found in *P. denitrifcans* is very similar to the FnrP, it is deactivated by oxygen however it lacks the iron-sulphur cluster found in FnrP. Rapid deactivation of NnrR by oxygen is confirmed by low n*irS* mRNA transcripts of anaerobic cultures of *P. denitrificans* exposed to aerobic conditions (Baumann *et al.* 1996). It is believed that NnrR is activated in

response to a heme cofactor sensing nitric oxide. The *nnrR* gene of *P. denitrificans* (pden_2478) is found upstream the *nir* and *nor* operons (Figure 9). NnrR activates the expression of *nirS* (pden_2487) and *norC* (pden_2484) recognizing the TTAACaaagGTCAA and TTGACtttcATCAA motifs upstream of *nirS* and *norC* respectively (Hutchings and Spiro 2000). The *ΔnnrR* strain of *P. denitrificans* has a distinct anaerobic phenotype, nitrate reductase activity is induced by 3-4 times and nitrite accumulates in the medium (van Spanning *et al.* 1997). See Chapter 3 for a detailed transcriptional comparison of the Δ*fnrP* and Δ*nnrR* strain of *P. denitrificans* in anaerobic respiration.

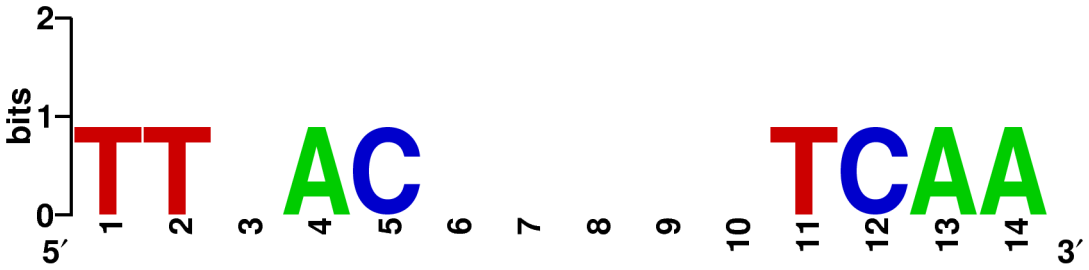

Figure 14 NNR binding motif logo based on promoter sequences of *nirS* (pden_2487) and *norC* (pden_2484). The logo was calculated with WebLogo (http://weblogo.berkeley.edu/logo.cgi).

Besides FnrP and NnrR, another FNR-like regulator exists in *P. denitrificans*. Upstream of *narK* (Figure 5), *narR* (pden_4238) encodes a nitrate/nitrite responsive transcriptional activator (Wood *et al.* 2001). The C terminal region of NarR contains a helix-turn-helix domain that shares a high degree of identity with NnrR that could enable NarR to bind to FNR-like cognate sites. Upstream of *narK* two putative FNR binding motifs exist, TTGATatttGTCAA and TTGATccagATCAA with the motif as illustrated in Figure 15. See Chapter 4 for a detailed transcriptional investigation of the Δ*narR* strain of *P. denitrificans* in anaerobic respiration.

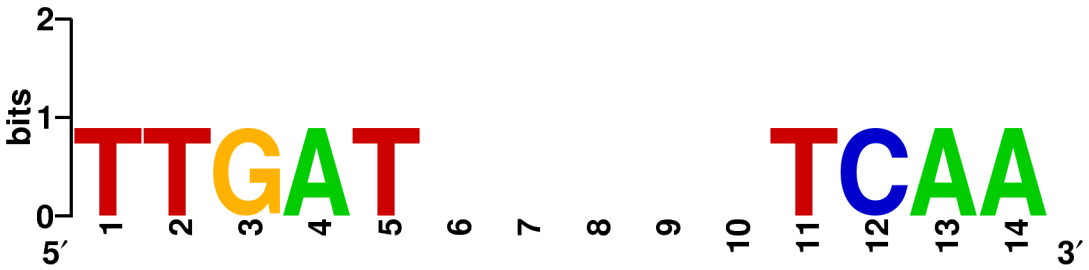

Figure 15 NarR binding motif logo based on two promoter sequences upstream of *narK* (pden_4237. The logo was calculated with WebLogo (http://weblogo.berkeley.edu/logo.cgi).

To summarize, the FnrP and NnrR are both activated in anaerobic environments. Additionally nitric oxide has the potential to bind to FnrP and NnrR (Mazoch and Kučera 2002, Mazoch *et al.* 2003, Lee *et al.* 2006). However, NnrR responds to micro level extracellular concentrations (>10 nM) of nitric oxide to activate the nitrite and nitric oxide reductase gene operons. Carbon monoxide, in vitro, could have a potential to bind on NnrR with a similar heme based sensing mechanism as in CooA from *Rhodospirillum rubrum* (Thorsteinsson *et al.* 2001, Crack *et al.* 2008, Jervis *et al.* 2009). A third FNR-like transcriptional activator exists in *P. denitrificans* and is involved in the auto-regulation of the *narK* and subsequently *nar* operon. It has also been observed that the activity of nitrous oxide reductase was unaffected by single mutants of either *fnrP* or *nnrR* strain of *P. denitrificans*. The double mutant *fnrP.nnrR* strain was unable to grow anaerobically and to reduce N_2O (Bergaust *et al.* 2011).

The FNR-like transcriptional regulators are highly conserved across the α-proteobactria. Dufour *et al.* (2010) using bioinformatic-based approaches showed that the amino-acid sequence of the helix-turn-helix motif of the FNR-like transcriptional regulators is highly conserved, that may suggest recognition of similar cognate sites. The analysis of experimental data showed practically identical binding site motifs with a logo as shown in Figure 16. Therefore it is highly likely that the FNR-like transcription regulators may compete for the cognate binding site and compensate for missing information. Previous studies however focused only on one transcriptional regulator and its effects on the regulation of single operons (Spiro 1992, van Spanning *et al.* 1997, Van Spanning *et al.* 1999, Hutchings and Spiro 2000, Wood *et al.* 2001, Hutchings *et al.* 2002, Zumft 2002, Spiro 2007) or whole genome (Dufour *et al.* 2010).The later approach did not consider the pleiotropic effects on

the genome transcriptional expression by comparatively altering the relative amounts of the different FNR-like transcription regulators.

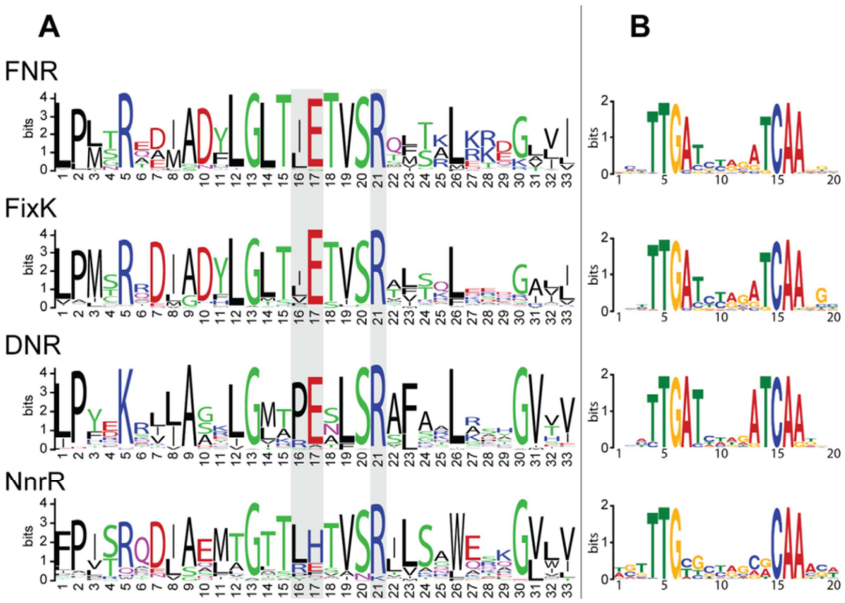

Figure 16 Protein binding domains and predicted DNA binding motifs of the CRP/FNR-type transcription regulators. Panel A illustrate logos of the amino-acid sequence alignments of the predicted helix-turn-helix domains of the CRP/FNR-type transcription regulators. B illustrates logos of the predicted DNA binding motifs of the CRP/FNR-type transcription regulators. Logo illustration taken from Dufour *et al.* (2010).

1.3.2 Significance of anaerobic respiration on nitrate

P. denitrificans possess several functional genes that are involved in nitrogen assimilation and denitrification, two major and very important pathways of the nitrogen cycle with ecological and industrial implications. The nitrogen cycle consists of nitrogen fixation, nitrification, denitrification, dissimilatory nitrate reduction to ammonia (DNRA), anaerobic ammonia oxidation (ANAMMOX), nitrogen assimilation and mineralization pathway (Thomson *et al.* 2012) (Figure 17).

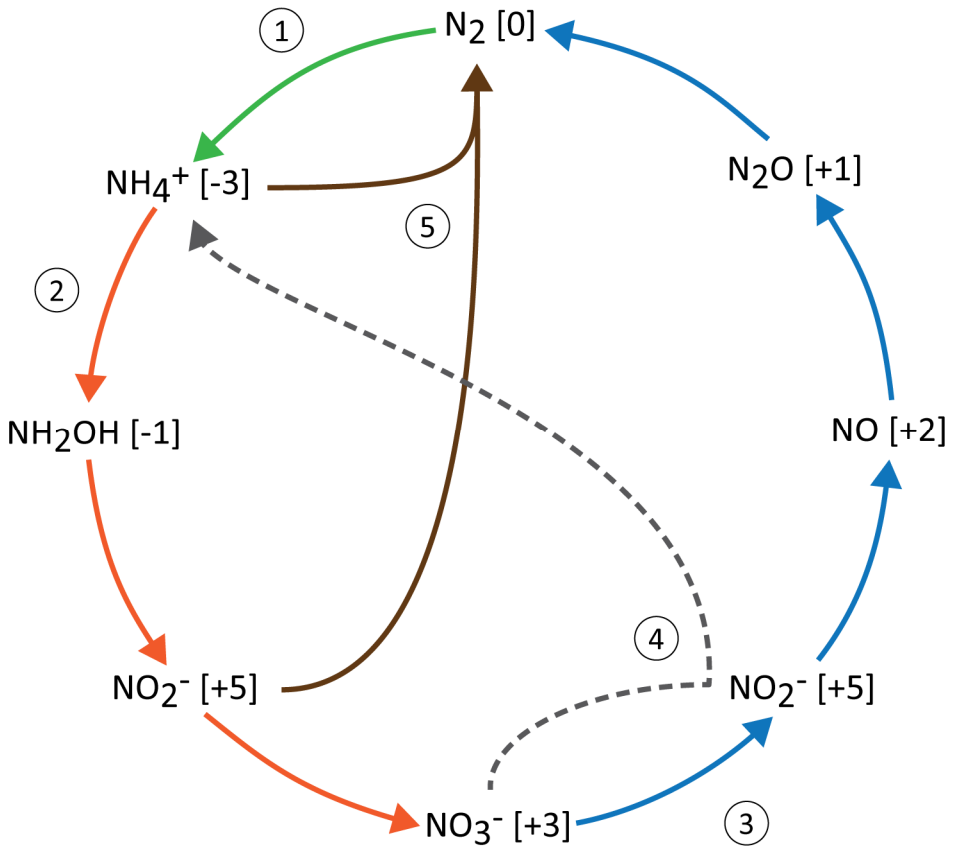

Figure 17 Simplified illustration of the nitrogen cycle (the oxidation states of the nitrogen are given in brackets). 1. Nitrogen fixation by nitrogenase 2. Nitrification 3. Denitrification 4. Dissimilatory nitrate reduction to ammonium (DNRA) and 5. Anaerobic ammonium oxidation (ANAMMOX). Not shown in the schematic are the processes of immobilization when ammonium, nitrate and nitrite are sequestered in biomass and the reverse process of mineralization.

The most potent greenhouse gas in the nitrogen cycle is undoubtedly nitrous oxide. Although nitrous oxide only accounts for ~0.03 percent of the global greenhouse gas emissions balance, it is ~300 times more potent for warming effects when compared to carbon dioxide. Nitrous oxide is the major anthropogenic cause of ozone depletion (Ravishankara *et al.* 2009), with ~62% of the total nitrous oxide emission originating from natural and agricultural soils; 6 and 4.2 Tg N-N2O.y^{-1} respectively (IPCC 2007, IPCC 2007), mainly due to microbial activity. Other anthropogenic sources of nitrous oxide besides agriculture and food production include the production of industrial chemicals, the fossil fuelled industry and vehicle emissions (Galloway 1998). With world population projections falling short of the actual 7.5 billion world population at the moment, there is even more societal pressure on agricultural systems for food security. Intensification of agriculture and the extensive use of nitrogen-based fertilizers will greatly contribute to the release of nitrous oxide. Unfortunately, very few organisms are able to reduce nitrous oxide to di-nitrogen. One of them is *P. denitrificans* a soil dwelling α-proteobacterium that synthesises an effective anaerobic nitrous oxide reductase (Zumft 1997, Kelly *et al.* 2006). However, the ecological disadvantageous effects of nitrous oxide are not only limited to its warming potential. Nitrous oxide is known to interfere with and inhibit methionine dependent pathways that subsequently affect the vitamin B_{12} synthesis and fatty acid metabolism (Sullivan *et al.* 2013). The latter may have deleterious effects in ecosystem functioning. Therefore, it is crucial to elucidate the mechanisms of nitrous oxide reduction, understand the effects of environmental signals to those mechanisms and perhaps master the regulation of those mechanisms at molecular level to provide the scientific knowledge that will tackle the problem of accumulating nitrous oxide emissions.

1.4 Aims and objectives

It has previously been shown that the successful binding of a transcription factor to a cognate site (DNA region) depends on various factors related to the potential binding affinity of the interaction, the relative availability of the transcriptional factor, the relative spacial configuration of the promoter and the target gene, the mode of search and the motif similarity. FnrP, NnrR and NarR of *P. denitrificans* have similar modes of DNA recognition based on a highly conserved helix-turn-helix domain, and their target genes have similar cognate site motifs, which suggests that FnrP, NnrR and NarR may compete for binding sites with a motif of TTG-N8-CAA that all three transcriptional factors recognize simultaneously. In this study, the abundance of the three FNR-like transcriptional regulators will be comparatively altered in *P. denitrificans* using strains in which the gene encoding a single transcriptional factor has been deleted. Combining this approach with highly reproducible continuous culture techniques and whole genome analysis the transcription profiles of each regulator and the degree to which they compete for cognate binding sites will be elucidated.

References

Baumann, B., M. Snozzi, J. R. Van Der Meer and A. J. B. Zehnder (1997). "Development of stable denitrifying cultures during repeated aerobic-anaerobic transient periods." Water Research **31**(8): 1947-1954.

Baumann, B., M. Snozzi, A. J. B. Zehnder and J. R. D. Van Meer (1996). "Dynamics of denitrification activity of *Paracoccus denitrificans* in continuous culture during aerobic-anaerobic changes." Journal of Bacteriology **178**(15): 4367-4374.

Baumann, B., J. R. Van Der Meer, M. Snozzi and A. J. B. Zehnder (1997). "Inhibition of denitrification activity but not of mRNA induction in *Paracoccus dentrificans* by nitrite at a suboptimal pH." Antonie van Leeuwenhoek, International Journal of General and Molecular Microbiology **72**(3): 183-189.

Bergaust, L., R. R. J. M. van Spanning, Å. Frostegård and L. R. Bakken (2011). "Expression of nitrous oxide reductase in *Paracoccus denitrificans* is regulated by oxygen and nitric oxide through FnrP and NNR." Microbiology.

Bertero, M. G., R. A. Rothery, M. Palak, C. Hou, D. Lim, F. Blasco, J. H. Weiner and N. C. J. Strynadka (2003). "Insights into the respiratory electron transfer pathway from the structure of nitrate reductase A." Nat Struct Mol Biol **10**(9): 681-687.

Bouchal, P., I. Struhárová, E. Budinská, O. Šedo, T. Vyhlídalová, Z. Zdráhal, R. van Spanning and I. Kučera (2010). "Unraveling an FNR based regulatory circuit in *Paracoccus denitrificans* using a proteomics-based approach." Biochimica et Biophysica Acta - Proteins and Proteomics **1804**(6): 1350-1358.

Brown, K., K. Djinovic-Carugo, T. Haltia, I. Cabrito, M. Saraste, J. G. Moura, I. Moura, M. Tegoni and C. Cambillau (2000). "Revisiting the Catalytic CuZ Cluster of Nitrous Oxide (N2O) Reductase." Journal of Biological Chemistry **275**(52): 41133-41136.

Constantinidou, C., J. L. Hobman, L. Griffiths, M. D. Patel, C. W. Penn, J. A. Cole and T. W. Overton (2006). "A reassessment of the FNR regulon and transcriptomic analysis of the effects of nitrate, nitrite, NarXL, and NarQP as *Escherichia coli* K12 adapts from aerobic to anaerobic growth." J Biol Chem **281**(8): 4802-4815.

Crack, J. C., A. J. Jervis, A. A. Gaskell, G. F. White, J. Green, A. J. Thomson and N. E. Le Brun (2008). "Signal perception by FNR: the role of the iron-sulfur cluster." Biochem Soc Trans **36**(Pt 6): 1144-1148.

Crécy, E., D. Metzgar, C. Allen, M. Pénicaud, B. Lyons, C. J. Hansen and V. Crécy-Lagard (2007). "Development of a novel continuous culture device for experimental evolution of bacterial populations." Applied Microbiology and Biotechnology **77**(2): 489-496.

Crofts, A. R. (2004). "Proton-coupled electron transfer at the Qo-site of the bc1 complex controls the rate of ubihydroquinone oxidation." Biochimica et Biophysica Acta (BBA) - Bioenergetics **1655**(0): 77-92.

Crofts, A. R., S. Lhee, S. B. Crofts, J. Cheng and S. Rose (2006). "Proton pumping in the bc1 complex: A new gating mechanism that prevents short circuits." Biochimica et Biophysica Acta (BBA) - Bioenergetics **1757**(8): 1019-1034.

de Gier, J. W. L., M. Lubben, W. N. M. Reijnders, C. A. Tipker, D. J. Slotboom, R. J. M. van Spanning, A. H. Stouthamer and J. van der Oost (1994). "The terminal oxidases of *Paracoccus denitrificans*." Molecular Microbiology **13**(2): 183-196.

Dermastia, M., T. Turk and T. C. Hollocher (1991). "Nitric oxide reductase. Purification from *Paracoccus denitrificans* with use of a single column and some characteristics." Journal of Biological Chemistry **266**(17): 10899-10905.

Doran, P. (2013). Bioprocess Engineering Priciples. MA, USA, Academic Press.

Dufour, Y. S., P. J. Kiley and T. J. Donohue (2010). "Reconstruction of the Core and Extended Regulons of Global Transcription Factors." Plos Genetics **6**(7).

Einsle, O. and P. M. Kroneck (2004). "Structural basis of denitrification." Biol Chem **385**(10): 875-883.

Felgate, H., G. Giannopoulos, M. J. Sullivan, A. J. Gates, T. A. Clarke, E. Baggs, G. Rowley and D. J. Richardson (2012). "The impact of copper, nitrate and carbon status on the emission of nitrous oxide by two species of bacteria with biochemically distinct denitrification pathways." Environ Microbiol **14**(7): 1788-1800.

Galloway, J. N. (1998). "The global nitrogen cycle: changes and consequences." Nitrogen, the Confer-N-S: 15-24.

Gates, A. J., V. M. Luque-Almagro, A. D. Goddard, S. J. Ferguson, M. D. Roldan and D. J. Richardson (2011). "A composite biochemical system for bacterial nitrate and nitrite assimilation as exemplified by *Paracoccus denitrificans*." Biochem J **435**(3): 743-753.

Glascock, C. B. and M. J. Weickert (1998). "Using chromosomal lacIQ1 to control expression of genes on high-copy-number plasmids in Escherichia coli." Gene **223**(1-2): 221-231.

Harada, Y., T. Funatsu, K. Murakami, Y. Nonoyama, A. Ishihama and T. Yanagida (1999). "Single-Molecule Imaging of RNA Polymerase-DNA Interactions in Real Time." Biophysical Journal **76**(2): 709-715.

Helling, R. B., C. N. Vargas and J. Adams (1987). "Evolution of Escherichia coli During Growth in a Constant Environment." Genetics **116**(3): 349-358.

Hendriks, J., A. Oubrie, J. Castresana, A. Urbani, S. Gemeinhardt and M. Saraste (2000). "Nitric oxide reductases in bacteria." Biochimica et Biophysica Acta (BBA) - Bioenergetics **1459**(2-3): 266-273.

Hino, T., Y. Matsumoto, S. Nagano, H. Sugimoto, Y. Fukumori, T. Murata, S. Iwata and Y. Shiro (2010). "Structural basis of biological N_2O generation by bacterial nitric oxide reductase." Science **330**: 1666.

Hoeren, F. U., B. C. Berks, S. J. Ferguson and J. E. G. McCarthy (1993). "Sequence and expression of the gene encoding the respiratory nitrous-oxide reductase from Paracoccus denitrificans." European Journal of Biochemistry **218**(1): 49-57.

Hoskisson, P. A. and G. Hobbs (2005). "Continuous culture – making a comeback?" Microbiology **151**(10): 3153-3159.

Hutchings, M. I., J. C. Crack, N. Shearer, B. J. Thompson, A. J. Thomson and S. Spiro (2002). "Transcription factor FnrP from *Paracoccus denitrificans* contains an Iron-Sulfur cluster and is activated by anoxia: Identification of essential cysteine residues." Journal of Bacteriology **184**(2): 503-508.

Hutchings, M. I. and S. Spiro (2000). "The nitric oxide regulated nor promoter of *Paracoccus denitrificans*." Microbiology **146**(10): 2635-2641.

IPCC (2007). Climate Change 2007: Synthesis Report. Contribution of Working Groups I, II and III to the Fourth Assessment Report of the Intergovernmental Panel on Climate Change. R. K. Pachauri and A. Reisinger. Geneva, Switzerland.

IPCC (2007). Summary for Policymakers. In: Climate Change 2007: The Physical Science Basis. Contribution of Working

Group I to the Fourth Assessment Report of the Intergovernmental Panel on Climate Change. S. Solomon, D. Qin, M. Manning et al. Cambridge, United Kingdom and New York, NY, USA.

Jervis, A. J., J. C. Crack, G. White, P. J. Artymiuk, M. R. Cheesman, A. J. Thomson, N. E. Le Brun and J. Green (2009). "The O_2 sensitivity of the transcription factor FNR is controlled by Ser24 modulating the kinetics of [4Fe-4S] to [2Fe-2S] conversion." Proceedings of the National Academy of Sciences **106**(12): 4659-4664.

Kang, Y., K. D. Weber, Y. Qiu, P. J. Kiley and F. R. Blattner (2005). "Genome-Wide Expression Analysis Indicates that FNR of Escherichia coli K-12 Regulates a Large Number of Genes of Unknown Function." Journal of Bacteriology **187**(3): 1135-1160.

Kazmierczak, M. J., M. Wiedmann and K. J. Boor (2005). "Alternative Sigma Factors and Their Roles in Bacterial Virulence." Microbiology and Molecular Biology Reviews **69**(4): 527-543.

Kelly, D., F. Rainey and A. Wood (2006). The Genus: *Paracoccus*. The Prokaryotes. M. Dworkin, S. Falkow, E. Rosenberg, K.-H. Schleifer and E. Stackebrandt, Springer New York**:** 232-249.

Kolesov, G., Z. Wunderlich, O. N. Laikova, M. S. Gelfand and L. A. Mirny (2007). "How gene order is influenced by the biophysics of transcription regulation." Proceedings of the National Academy of Sciences **104**(35): 13948-13953.

Lee, Y.-Y., N. Shearer and S. Spiro (2006). "Transcription factor NNR from *Paracoccus denitrificans* is a sensor of both nitric oxide and oxygen: isolation of nnr* alleles encoding effector-independent proteins and evidence for a haem-based sensing mechanism." Microbiology **152**(5): 1461-1470.

Leith, J. S., A. Tafvizi, F. Huang, W. E. Uspal, P. S. Doyle, A. R. Fersht, L. A. Mirny and A. M. v. Oijenf (2012). "Sequence-dependent sliding kinetics of p53." PNAS **109**(41): 16552.

Luque-Almagro, V. M., V. J. Lyall, S. J. Ferguson, M. D. Roldán, D. J. Richardson and A. J. Gates (2013). "Nitrogen Oxyanion-dependent Dissociation of a Two-component Complex That Regulates Bacterial Nitrate Assimilation." Journal of Biological Chemistry **288**(41): 29692-29702.

Mazoch, J. and I. Kučera (2002). "Control of gene expression by FNR-like proteins in facultatively anaerobic bacteria." Folia Microbiologica **47**(2): 95-103.

Mazoch, J., M. Kuňák, I. Kučera and R. J. M. van Spanning (2003). "Fine-tuned regulation by oxygen and nitric oxide of the activity of a semi-synthetic FNR-dependent promoter and expression of denitrification enzymes in *Paracoccus denitrificans*." Microbiology **149**(12): 3405-3412.

Mitchell, P. (1961). "Coupling of Phosphorylation to Electron and Hydrogen Transfer by a Chemi-Osmotic type of Mechanism." Nature **191**: 144-148.

Otten, M. F., W. N. M. Reijnders, J. J. M. Bedaux, H. V. Westerhoff, K. Krab and R. J. M. v. Spanning (1999). "The reduction state of the Q-pool regulates the electron flux through the branched respiratory network of *Paracoccus denitrificans*." Eur. J. Biochem **261**: 767-774.

Panikov, N. S. (2009). Kinetics, Microbial Groth. Encyclopedia of Bioprocess Technology: Fermentation, Biocatalysts and Bioseparation. M. C. Flickinger and S. W. Drew. New York, John Wiley & Sons**:** 1513-1543.

Ravishankara, A. R., J. S. Daniel and R. W. Portmann (2009). "Nitrous Oxide (N_2O): The dominant Ozone-depleting substance emitted in the 21st Century." Science **326**(5949): 123-125.

Runkel, S., H. C. Wells and G. Rowley (2013). "Living with Stress: A Lesson from the Enteric Pathogen Salmonella enterica." Adv Appl Microbiol **83**: 87-144.

Saunders, N. F. W., J. J. Hornberg, W. N. M. Reijnders, H. V. Westerhoff, S. de Vries and R. J. M. van Spanning (2000). "The NosX and NirX Proteins of *Paracoccus denitrificans* are functional homologues: their role in maturation of nitrous oxide reductase." Journal of Bacteriology **182**(18): 5211-5217.

Sears, H. J., S. Spiro and D. J. Richardson (1992). "Effect of carbon substrate and aeration on nitrate reduction and expression of the periplasmic and membrane-boundnitrate reductases in carbon-limited continuous cultures of *Paracoccus denitrificans* Pdl222." Microbiology **9971**: 3767-3774.

Solomonson, L. P. and M. J. Barber (1990). "Assimilatory Nitrate Reductase: Functional Properties and Regulation." Annual Review of Plant Physiology and Plant Molecular Biology **41**(1): 225-253.

Spiro, S. (1992). "An FNR-dependent promoter from *Escherichia coli* is active and anaerobically inducible in *Paracoccus denitrificans*." FEMS Microbiology Letters **98**(1-3): 145-148.

Spiro, S. (2007). "Regulators of bacterial responses to nitric oxide." FEMS Microbiology Reviews **31**(2): 193-211.

Spiro, S. and J. R. Guest (1990). "FNR and its role in oxygen-regulated gene expression in Escherichia coli." FEMS Microbiol Rev **6**(4): 399-428.

Suarez, E., A. Burguete and G. J. Mclachlan (2009). "Microarray Data Analysis for Differential Expression: a Tutorial." Puerto Rico Health Sciences Journal **28**(2): 89-104.

Sullivan, M. J., A. J. Gates, C. Appia-Ayme, G. Rowley and D. J. Richardson (2013). "Copper control of bacterial nitrous oxide emission and its impact on vitamin B12-dependent metabolism." Proceedings of the National Academy of Sciences.

Sutton, V. R., E. L. Mettert, H. Beinert and P. J. Kiley (2004). "Kinetic Analysis of the Oxidative Conversion of the [4Fe-4S]2+ Cluster of FNR to a [2Fe-2S]2+ Cluster." Journal of Bacteriology **186**(23): 8018-8025.

Tafvizi, A., L. A. Mirny and A. M. van Oijen (2011). "Dancing on DNA: kinetic aspects of search processes on DNA." Chemphyschem **12**(8): 1481-1489.

Thomson, A. J., G. Giannopoulos, J. Pretty, E. M. Baggs and D. J. Richardson (2012). "Biological sources and sinks of nitrous oxide and strategies to mitigate emissions." Philos Trans R Soc Lond B Biol Sci **367**(1593): 1157-1168.

Thorsteinsson, M. V., R. L. Kerby, H. Youn, M. Conrad, J. Serate, C. R. Staples and G. P. Roberts (2001). "Redox-mediated transcriptional activation in a CooA variant." J Biol Chem **276**(29): 26807-26813.

Tiedje, J. M., A. J. Sexstone, D. D. Myrold and J. A. Robinson (1982). "Denitrification: Ecological niches, competition and survival." Antonie van Leeuwenhoek **48**(1982): 569-583.

van Cleemput, O. (1998). "Subsoils: chemo-and biological denitrification, N2O and N2 emissions." Nutrient Cycling in Agroecosystems **52**(2-3): 187-194.

van Spanning, R. J. M., A. P. N. de Boer, W. N. M. Reijnders, H. V. Westerhoff, A. H. Stouthamer and J. van der Oost (1997). "FnrP and NNR of *Paracoccus denitrificans* are both members of the FNR family of transcriptional activators but have distinct roles in respiratory adaptation in response to oxygen limitation." Molecular Microbiology **23**(5): 893-907.

Van Spanning, R. J. M., E. Houben, W. N. M. Reijnders, S. Spiro, H. V. Westerhoff and N. Saunders (1999). "Nitric oxide is a signal for NNR-mediated transcription activation in *Paracoccus denitrificans*." Journal of Bacteriology **181**(13): 4129-4132.

von Ballmoos, C., G. M. Cook and P. Dimroth (2008). "Unique Rotary ATP Synthase and Its Biological Diversity." Annual Review of Biophysics **37**(1): 43-64.

White, D., J. Drummond and C. Fuqua (2012). The physiology and biochemistry of prokaryates. New York, Oxford University Press.

Wood, N. J., T. Alizadeh, S. Bennett, J. Pearce, S. J. Ferguson, D. J. Richardson and J. W. Moir (2001). "Maximal expression of membrane-bound nitrate reductase in *Paracoccus* is induced by nitrate via a third FNR-like regulator named NarR." J Bacteriol **183**(12): 3606-3613.

Wood, N. J., T. Alizadeh, D. J. Richardson, S. J. Ferguson and J. W. Moir (2002). "Two domains of a dual-function NarK protein are required for nitrate uptake, the first step of denitrification in *Paracoccus pantotrophus*." Mol Microbiol **44**(1): 157-170.

Wunderlich, Z. and L. A. Mirny (2009). "Different gene regulation strategies revealed by analysis of binding motifs." Trends in genetics : TIG **25**(10): 434-440.

Zumft, W. G. (1997). "Cell Biology and Molecular Basis of Denitrification." Microbiology and Molecular Biology Reviews **61**(4): 533-616.

Zumft, W. G. (2002). "Nitric Oxide Signaling and NO Dependent Transcriptional Control in Bacterial Denitrification by Members of the FNR-CRP Regulator Family." Journal of Molecular Microbiology and Biotechnology **4**(3): 277-286.

2. Comparison between the aerobic and anaerobic growth of P. denitrificans

Setting the scene; Aerobic and anaerobic metabolic and transcriptional profiles of *P. denitrificans*; a whole genome approach in continuous culture systems.

Contents

2.1 Introduction

2.1.1 Growth of *P.denitrificans* in anaerobic continuous cultures and gene regulation

In this chapter the metabolic profile of continuous cultures of *P. denitrificans* (PD1222) in anaerobic and aerobic steady states is established. Building upon the advantages of using chemostats (see 1.1.5 The importance of growth medium and advantages of continuous culture in genomic studies), transcriptional analysis was employed to investigate the (whole genome) transcriptome of *P. denitrificans* under those conditions. The use of such defined culture techniques aided the acquisition of metabolic and transcriptional data excluding the indirect effects of secondary metabolites, often accumulating in heterogeneous batch cultures that can mask subtle physiological differences and trends.

P. denitrificans is able to respire on various compounds by expressing certain oxyreductases as mentioned in detail in the 1.1 General introduction. The growth kinetics of continuous cultures of *P. denitrificans* have been studied extensively in the early 80's (Verseveld *et al.* 1977, Meijer *et al.* 1979, Verseveld *et al.* 1979, Schoen *et al.* 1985). The P/2 e^- and H^+/O was defined at 0.7 and 4.5 respectively for an anaerobic culture with succinate (limiting factor) and nitrate (Verseveld *et al.* 1977). Also it was observed that the accumulation of nitrite in excess of 10 mM increased membrane tension and inhibited growth of *P. denitrificans*. Excessive amounts of nitrite could act as a decoupling agent with cytotoxic effects to a cell in the form of free nitrous acid. The molar yield for ATP (Y_{ATP}^{max}) and succinate ($Y_{succinate}^{max}$) was 9.2 and 0.42 g.mol^{-1} respectively, defined by anaerobic growth on succinate (limiting factor) and nitrate (Meijer *et al.* 1979, Schoen *et al.* 1985).

A decade later, continuous culture systems were used again to understand the regulation of denitrification in *P. denitrificans*. The studies of Baumann *et al.* (1997) established the effect of sub-optimal pH and periodic aeration in continuous cultures of *P. denitrificans* with nitrate and acetate (limiting factor). The optimal rate of denitrification in *P. denitrificans* was observed at a pH range of 7.5 - 8.2. Baumann *et al.* (1997) compared two treatments with *P. denitrificans* continuous cultures; a control treatment with a pH of 7.5 and a sub-optimal treatment with a pH of 6.8. The sub-optimal treatment was unable to reduce nitrate to di-nitrogen and 35 mM of nitrite accumulated that resulted in growth inhibition. This inhibition was suggested to be

indirectly linked to the low pH of the culture and the increase of the free nitrous acid (protonated nitrite) concentration in the reactor vessel (17.5 µM). However, the lethal dose of nitrite or free nitrous acid has to be confirmed in such systems. In another study, investigating the transcription of mRNA during the incubation period, the authors revealed that oxygen depletion induced nitrate reduction and the mRNA transcripts of nitrate and nitrous oxide reductase were detectable prior to those of nitrite reductase. This observation suggests different modes of regulation for nitrate, nitrite and nitrous oxide reductase.

The denitrification pathway is induced after oxygen depletion and is regulated by multiple promoters and transcription factors. Promoter sequences are comparable across many orders of denitrifying bacteria, however the exact mechanism of regulation depends on the micro-organism (Rodionov *et al.* 2005, Dufour *et al.* 2010). External stimuli such as oxygen and the concentration of nitrogen oxides regulate gene expression globally or locally and various transcription factors and promoter sequences have been identified.

P. denitrificans is able to express three different cytochrome *c* oxidases; aa_3, ba_3 and cbb_3, the latter has a low K_m for oxygen and is expressed at low oxygen concentrations. The extent of expression is regulated by the oxygen concentration that is sensed by the transcriptional factor (TF) FNR (Fumarate and Nitrate Regulatory protein). It has been demonstrated that FNR acts as an activator in very low oxygen concentrations (< 6 µM in vitro; Crack *et al.* (2008), Jervis *et al.* (2009)). It was demonstrated that the expression of the cbb_3 operon (*ccoNOQP*) is under the control of FnrP which is encoded by *fnrP* (pden_1850) in *P. denitrificans* (de Gier *et al.* 1994).

Upon oxygen depletion, *P. denitrificans* utilises nitrogen oxyanions as alternative electron acceptors. Another homologue of FnrP which lacks the typical cysteine signature of the CRP family activates the expression of nitrite and nitric oxide reductase operons (Spiro and Guest 1990, Spiro 1992, Spiro 2007, Spiro 2012). Those substrates are products of nitrate reduction and could eventually be potent and cytotoxic if not removed rapidly. The Δ*nnrR* strain PD77.71 grew anaerobically reducing nitrate to nitrite and it was unable to further reduce the accumulating nitrite (van Spanning *et al.* 1997, Van Spanning *et al.* 1999); this finding demonstrates that NnrR (*nnrR*, pden_2348) acts as a *cis*-activator of nitrite reductase operon regulation.

The mode of action of FnrP and NnrR TF has been well characterized in batch cultures of *P. denitrificans*. However, little is known about the interaction of the afore-mentioned TF and the response of the total bacterial genome during the transition from aerobic to anaerobic conditions. This chapter aims to elucidate the effect of oxygen on the respirome of *P. denitrificans* and to identify putative promoter binding sites that could regulate the transition from aerobic to anaerobic respiration.

2.1.2 Medium composition and mass balances in continuous stirred tank reactors

This work mainly focuses on anaerobic respiration with nitrate as an alternative electron acceptor and for this reason a simple but defined growth medium was selected for the experimental work described herein. Succinate is provided as a carbon source, nitrate as an alternative electron acceptor, ammonium chloride for nitrogen assimilation, a mixture of mono and di-sodium ortho-phosphates for buffering the medium and trace elements to supplement growth and physiological functioning of the bacterium.

The medium contains 5 mM sodium succinate and 20 mM sodium nitrate (for a detailed medium composition see 7.1.1 Media). Succinate is stichiometricaly in excess of nitrate for the following two reasons. Firstly, succinate was selected as the limiting compound to control growth (assimilation and electron donor) in continuous cultures (Equation 6) and secondly to ensure that excess nitrate will be available for respiration (*electron* acceptor) at the event of a subsequent reduction step of denitrification is not occurring. The oxidation of 1 molecule of succinate yields 16 electrons and the complete reduction of 2 molecules of nitrate to one molecule di-nitrogen requires 10 electrons. However, not all of the carbon substrate is oxidized; approximately 40% is assimilated in bacterial biomass. Thus, the oxidation of 3 mM of succinate yields 48 mM electron equivalents and the reduction of 20 mM of NO_3^- to di-nitrogen requires 100 mM equivalents of electrons (Equation 1 and 2, respectively). Thus, the electron acceptor consumption rates were assumed to be limited by the maximum succinate oxidation rate and subsequently independent of the electron acceptor. Ammonium was added in the medium (10 mM) to be used for N assimilation and biomass incorporation.

$$C_4H_4O_4^{2-} + {}^7/_2\, O_2 \rightarrow 2OH^- + 4CO_2 + H_2O + 16e^-$$

Equation 1 Oxidation of succinate and electron yield

$$2NO_3^- + 12H^+ + 10e^- \rightarrow N_2 + 6H_2O$$

Equation 2 Reduction of nitrate to di-nitrogen and electron demand

A simplified continuous stirred tank reactor (CSTR) system consists of a culture vessel, an agitator and an inflow and an outflow port (Figure 1). Other controls and ports could be added depending on the requirements of the selected process. The accumulation of mass (X_{acc}) in such system is balanced by the inflow (X_{in}), the outflow (X_{out}) and the production (X_{prod}) of microbial mass. Equations 3 and 4 describe the mass balance in CSTR systems, with the incoming microbial biomass $\boldsymbol{X_{in} = 0}$ thus, $\boldsymbol{\frac{\partial X_{in}}{\partial t} = 0}$ by definition for sterile feed media. It is apparent that a relationship between microbial population, growth rate and dilution rate exists as seen in equation 6.

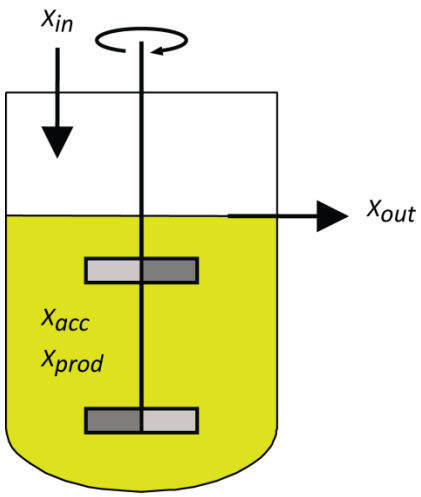

Figure 1 Simplified schematic of the microbial mass balance in a continuous stirred tank reactor (CSTR).

$$X_{Acc} = X_{In} + X_{Prod} - X_{Out}$$

Equation 3 The microbial population mass balance in the reactor at one time point, where X_{Acc} denotes the microbial population accumulating in the tank, X_{In} the input of microbial

population, X_{Prod} the increase of the microbial population via growth and X_{Out} the output of microbial population.

$$\frac{\partial(X_{In} + X_{Prod} - X_{Out})}{\partial t} = \frac{\partial X_{Acc}}{\partial t}$$

Equation 4 Microbial mass balance (Equation 3) factored per time units.

$$D = \frac{V}{F}$$

Equation 5 Equation calculating the dilution rate *D* (h^{-1}) of CSTR, when the culture volume V (ml) and nutrient media flow rate F ($ml.h^{-1}$) are known.

$$\frac{\partial X_{Acc}}{\partial t} = \frac{\partial X_{Prod}}{\partial t} - \frac{\partial X_{Out}}{\partial t} \; with \; \frac{\partial X_{Prod}}{\partial t} = \mu * X \; and \; \frac{\partial X_{Out}}{\partial t} = D * X \; thus,$$

$$\frac{\partial X_{Acc}}{\partial t} = (\mu - D)\mathrm{X}$$

Equation 6 The mass balance of the microbial population accumulating in the reactor's tank at steady state. Where $\frac{\partial X_{Acc}}{\partial t}$ denotes the rate of change of the microbial population, *μ the* specific growth rate and *D* the dilution rate of the CSTR.

When *D* is equal to the *μ*, the microbial population in the reactor tank will remain unchanged $\frac{\partial X_{Acc}}{\partial t} = 0$ because of the steady state (*D*= *μ*). However if the *D* exceeds *μ* the microbial population will decrease to the point of complete washing out of the culture. On the contrary, when *D* is smaller than *μ*, the microbial population will increase up to the point that is sustained with the level of nutrients available in the reactor. The latter principle describes a chemostatic continuous culture which is employed in this work. This principle is clearly illustrated when the Monod growth equation is combined with the mass balance.

$$\mu = \frac{\mu_{max} * [S]}{K_s + [S]} \; and \; D = \mu \; when \; \frac{\partial X_{Acc}}{\partial t} = 0 \; thus,$$

$$D = \frac{\mu_{max} * [S]}{K_s + [S]} \; or \; [S] = \frac{K_s * D}{\mu_{max} - D}$$

Equation 7 Solving the equations by linking growth, substrate concentration and the dilution rate in continuous culture systems; where μ *and* μ_{max} *denote the* specific growth and maximum specific growth rate respectively, [*S*] the concentration of the substrate, K_s the substrate half saturation coefficient and *D* the dilution rate of the CSTR.

2.2 Results

2.2.1 Primary investigations of *P. denitrificans* growth parameters

A set of batch experiments was conducted to monitor growth, nitrate and nitrite concentrations and subsequently to compare the dilution rate of the following experiments with the specific growth rate (μ_{max}) of the aerobic and anaerobic treatment. *P. denitrificans* has a μ_{max} of 0.45 h^{-1} when grown aerobically in agitated flasks. The culture reached maximal turbidity at ~ 11 h after inoculation, with an OD of ~1.12 that corresponds to a yield (*Y*) of 0.12 $g.L^{-1}.mM^{-1}$ succinate. The nitrate concentration was ~22 mM at the start of the incubation and increased slightly up to ~24 mM during exponential growth and remained at that level till the end of the incubation (35 h). At the mid-exponential growth nitrite accumulated to ~ 1 mM which was later removed (Figure 2). This observation may indicate firstly that agitation is not enough by itself to supply oxygen at a rate required during exponential growth to completely repress nitrate reduction, secondly nitrate could be reduced aerobically due to the basal activity of periplasmic nitrate reductases and thirdly that excess ammonia is oxidized to nitrite and nitrate.

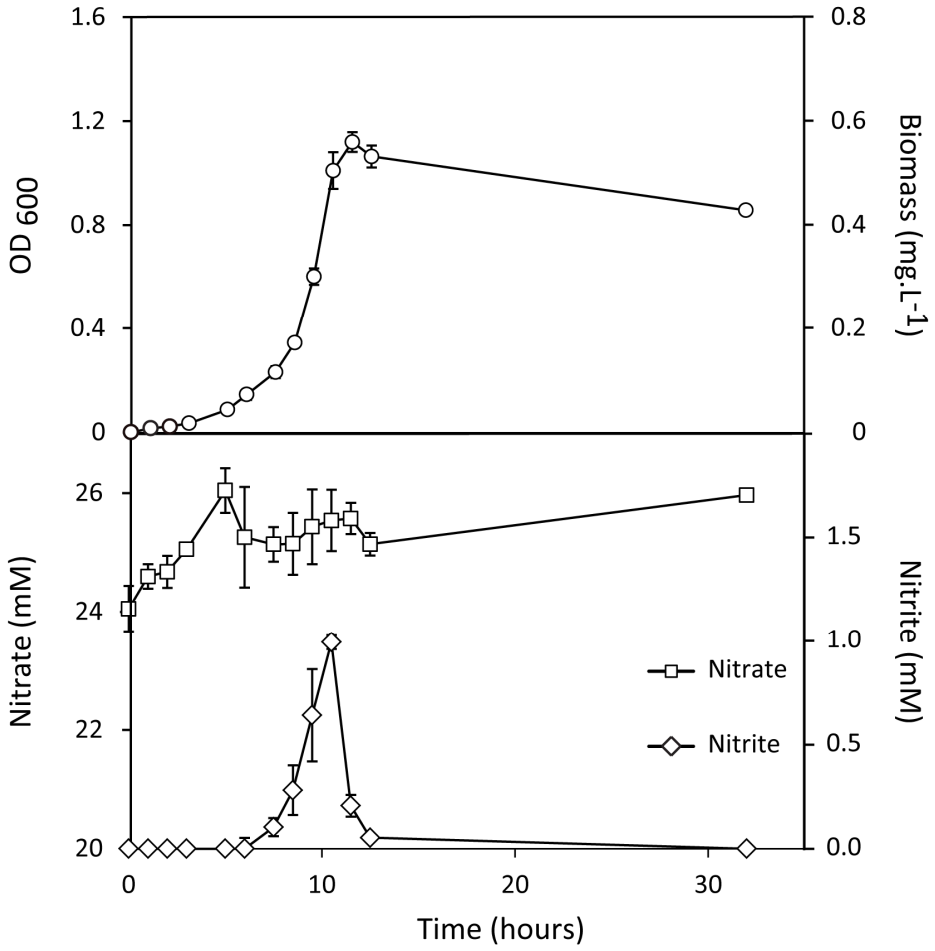

Figure 2 Aerobic batch growth of *P. denitrificans* (PD1222) at pH 7.5, 30°C in minimal media. Flasks were continually agitated to allow air diffusion through the medium; Panel A) Biomass (○) μ_{max}= 0.19 h^{-1} B) The concentration of nitrate (◇) and nitrite (□) during aerobic batch incubation. Error bars denote ± SEM (n=3).

In the anaerobic treatment it was observed that *P. denitrificans* has a slightly longer lag phase and a μ_{max} of 0.54 h^{-1}. The culture reached maximal turbidity at ~ 15 h, with an OD of ~0.6. Simultaneously with the initiation of the exponential growth phase a decrease in the nitrate concentration in the medium was observed. Approximately ~7 mM of nitrate are reduced, with a subsequent small and temporal accumulation of 1 mM nitrite (at 12 h) which at the end of the incubation was undetectable. The Y was 0.06 $g.L^{-1}.mM^{-1}$ succinate. The final product of the anaerobic respiration in this batch was di-nitrogen, as the headspace concentration of nitrous oxide was below the detection limit of gas chromatography. The remaining nitrate in the culture was ~14 mM (at 25 h; Figure 3).

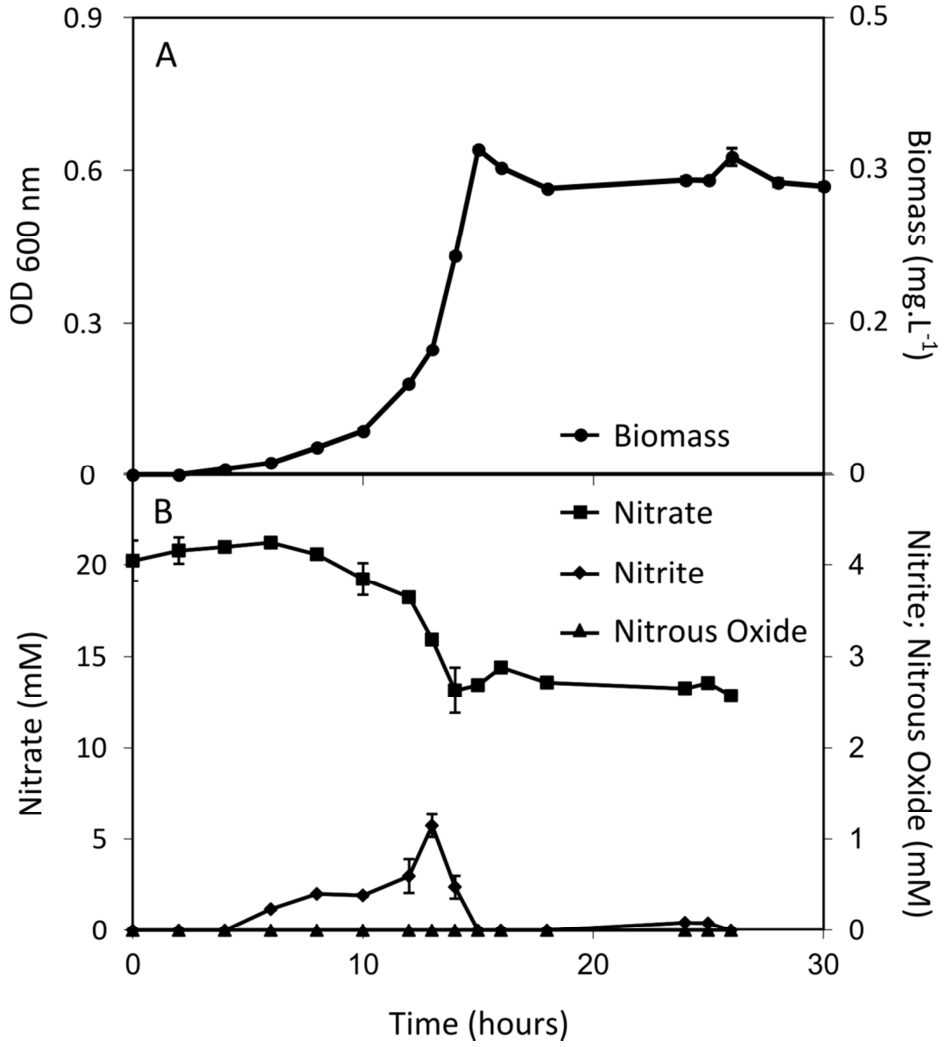

Figure 3 Anaerobic batch growth curve of *P. denitrificans* (PD1222) at pH 7.5, 30^{o}C in minimal media. Duran bottles sealed with custom septa to allow gas accumulation and sampling. Panel A illustrates the biomass (●) μ_{max}= 0.15 h^{-1} and B) the concentration of nitrate (■), nitrite (◆) and nitrous oxide (▲) during the anaerobic batch incubation. Error bars denote ±SEM (n=3).

Having defined the aerobic and anaerobic growth profiles of *P. denitrificans* in batch cultures, parameters for continuous growth were assessed and selected. Continuous culture of *P. denitrificans* was performed in CSTR.

Equations 6, 7 and 5 were solved with the kinetic parameters listed in table **1.** The results are presented graphically in figure 4. It is concluded that *P. denitrificans* could be cultured in minimal media with 5 mM succinate with D_{max}= 0.33 h^{-1}. Setting the dilution rate higher than the D_{max} will cause "washing out" of the culture (Figure 4).

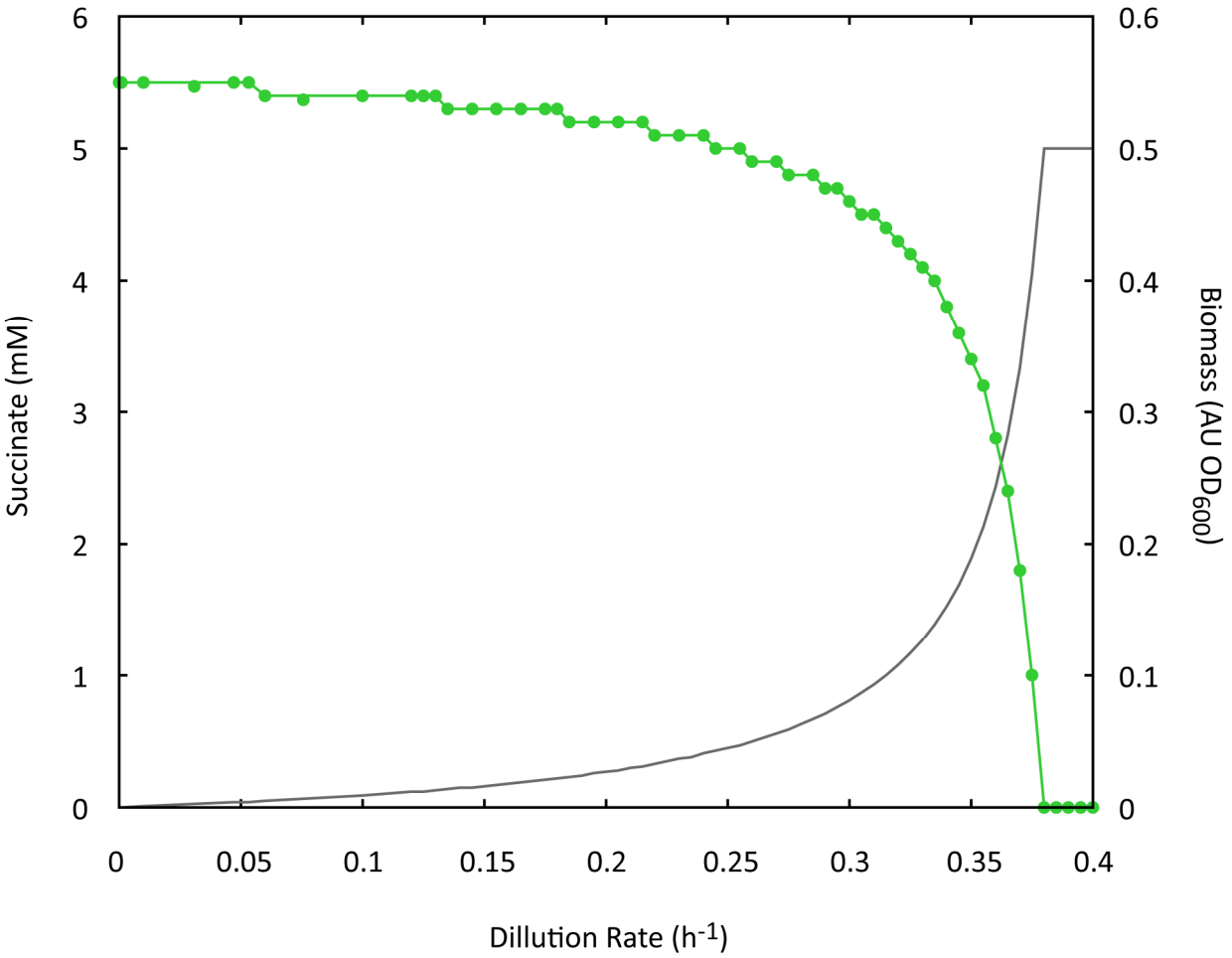

Figure 4 Graphical results of modelling the limiting substrate concentration; succinate (mM; –) and biomass (OD_{600}; ●) in an anaerobic CSTR of *P. denitrificans*. Table 1 lists the modelling parameters.

The feed flow was set at 80 $ml.L^{-1}$ in a culture volume 1.5 L, thus the dilution rate D=0.055 h^{-1} which is smaller than the μ_{max} of *P. denitrificans* (Equation 5). At this dilution rate, the calculated OD_{600} of the culture corresponds to 0.52 and approximately all of the substrate (succinate) is consumed (Figure 4).

Table 1 Parameters used to model growth of *P. denitrificans* in a CSTR system.

Definition	Symbol	Value	Units	Reference
Yield	$Y_{succinate}^{max}$	0.1-0.16	mM^{-1}	This work
Specific growth rate	μ_{max}	0.40-0.45	h^{-1}	This work
Monod saturation coefficient for succinate	K_s	0.27	mM	Dadák *et al.* (2009)

2.2.2 Metabolic profiles of *P. denitrificans* in aerobic and anaerobic CSTR cultures

Having defined the profiles of aerobic and anaerobic growth in batch and subsequently modelled the growth of *P. denitrificans* in CSTR, four sets of experiments were performed. The first set of experiments involved the growth of *P. denitrificans* aerobically at 30^{o}C, the second one anaerobically at 30^{o}C, the third one anaerobically at 37^{o}C. The final experiment was a control to assess the detection of nitrous oxide in CSTR from a mutant strain (PD10222) deficient in a functional copy of *nosZ*.

The first set of experiments involved culturing *P. denitrificans* aerobically at 30^{o}C. The temperature within the reactor and the pH remained at 30^{o}C and at pH 7.5 respectively throughout the 120 h incubation. Air was supplied at a rate of 3 SLPM during the length of the incubation. It was observed that the DO levels dropped by ~20% at ~20 h which coincided with the end of the exponential growth of the culture. At that point the feed pump was turned on at a rate of 80 $ml.h^{-1}$ and the DO levels recovered to 100% from this time point and onwards. Biomass was ~0.35 $g.L^{-1}$ towards the end of the incubation. The metabolic profile of this continuous culture incubation is depicted in Figure 5; E. Nitrate levels remained unchanged at ~ 21 mM, as expected in aerobic respiration, and oxygen was preferentially used as an *electron* acceptor. Nitrite and nitrous oxide were below detection levels.

The second set of experiments was performed under anaerobicity, similarly to the previous one, the temperature and the pH remained at 30^{o}C and at pH 7.5 respectively throughout the incubation. Air was supplied initially for ~20 h to allow the culture to grow in batch, then the air

inflow was restricted, the feed pump was set on, and the culture consumed any remaining dissolved oxygen (Figure 6; C, D). Contrary to the previous experiment, a reduction of the concentration of nitrate is observed at this point (~20 h onwards). Nitrate is consumed as an alternative electron acceptor to oxygen, with 15 mM out of ~22 mM remaining in the culture towards the end of the incubation. A minor but momentary increase of the concentration nitrite is observed at ~40 h. Nitrous oxide remained below detection limits and did not accumulate (Figure 6; E). Selected samples were taken and the concentration of succinate was determined. Succinate concentration in the aerobic and anaerobic culture treatments was below detection level and it was assumed that all succinate was oxidized as previously modelled. The reduction of 7 mM nitrate requires 35 mM electron equivalents and the oxidation of 5 mM succinate yields 70 mM electron equivalents. An assimilation coefficient for succinate was estimated to ~50%, based on this experiment.

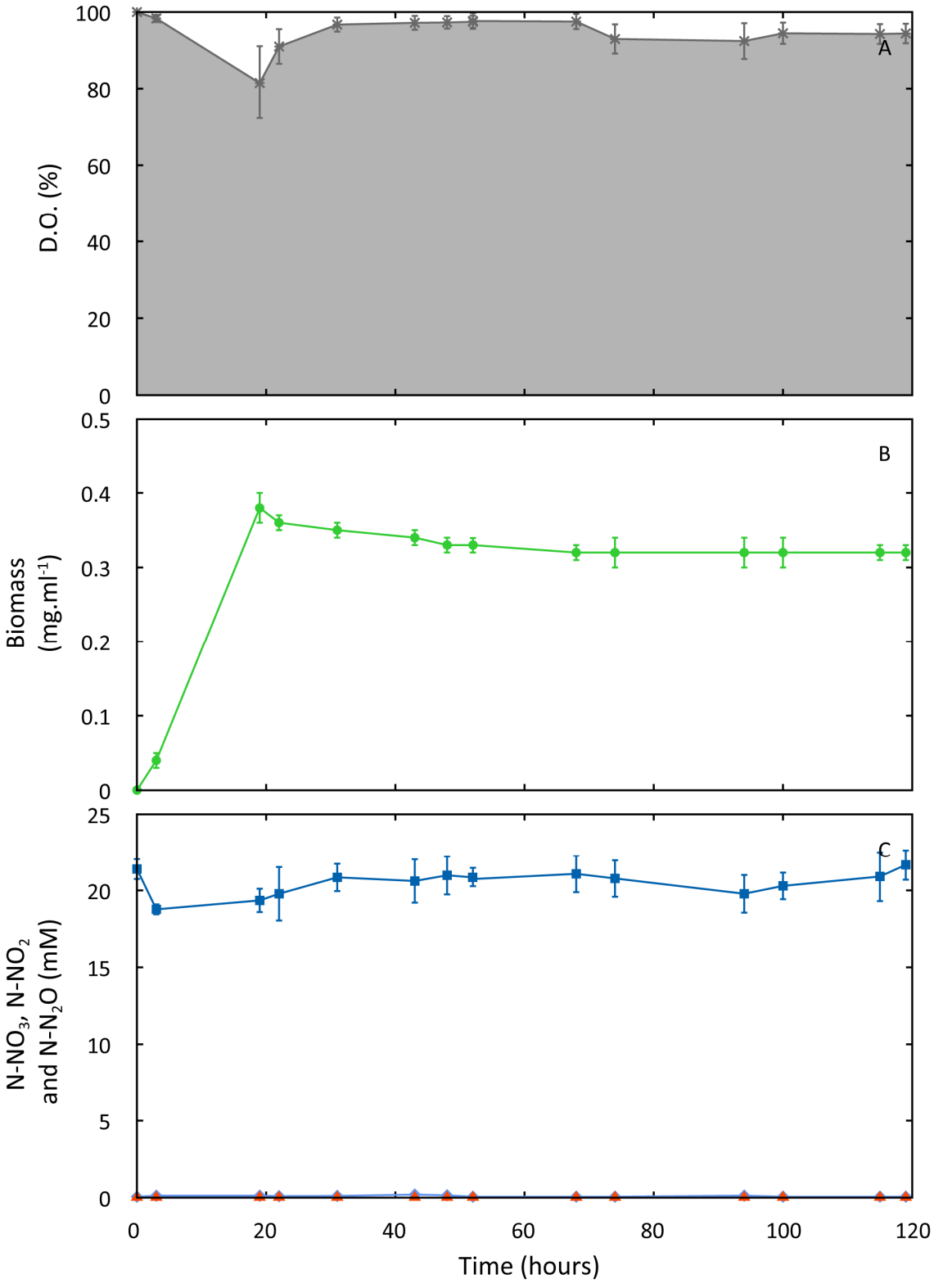

Figure 5 Aerobic continuous culture of *P. denitrificans* (PD1222) in CSTR. Panel A Illustrates the average dissolved oxygen concentration (D.O.; *) of the culture, B the average biomass (●) of the culture and C the average extracellular concentration of nitrate (■), nitrite (◆) and nitrous oxide (▲)during the continuous culture incubation (n=3; error bars denote ±SEM).

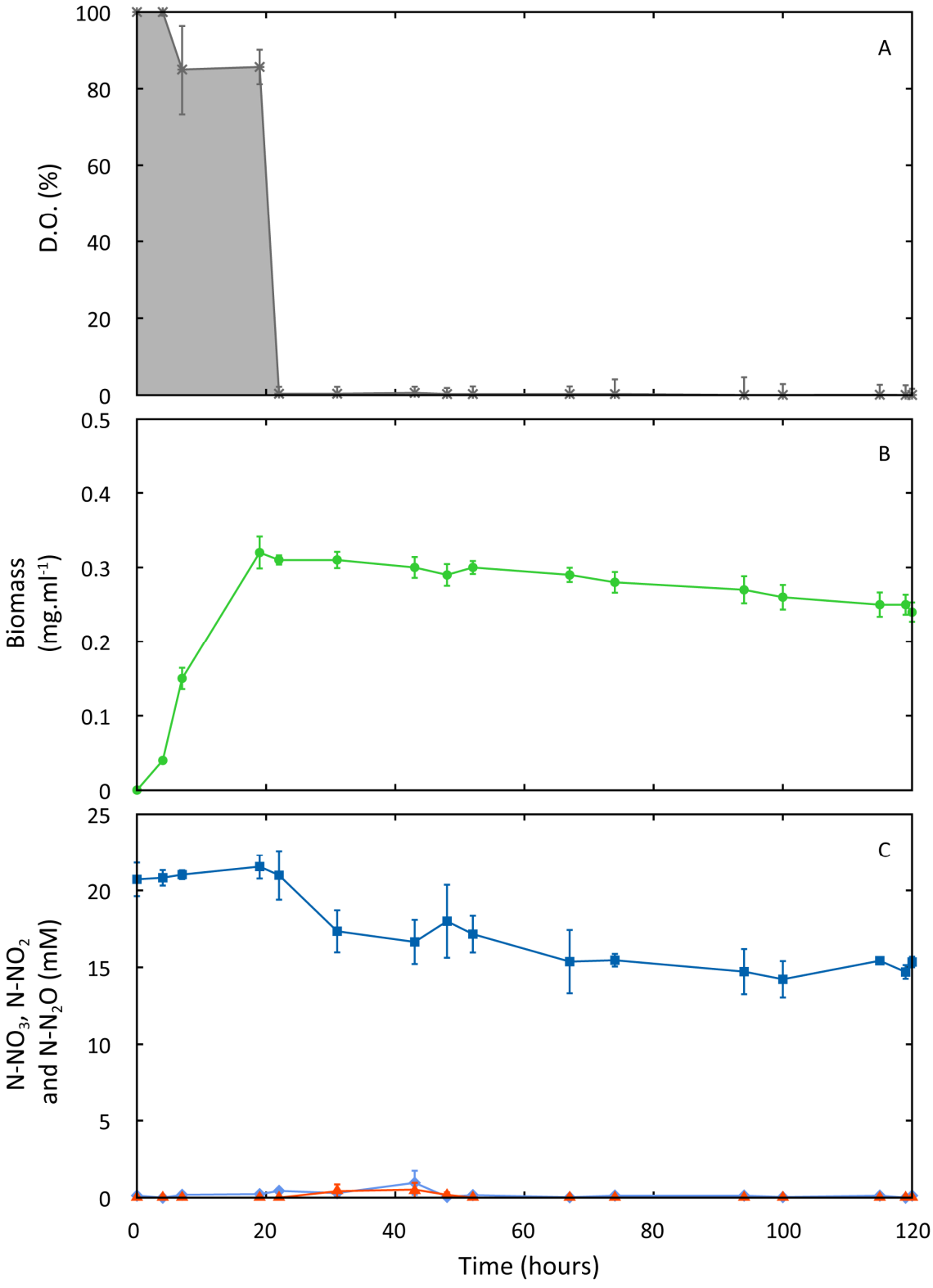

Figure 6 Anerobic continuous culture of *P. denitrificans* (PD1222) in CSTR. Panel A Illustrates the average dissolved oxygen concentration (D.O.; *) of the culture, B the average biomass (●) of the culture and C the average extracellular concentration of nitrate (■), nitrite (◆) and nitrous oxide (▲) during the continuous culture incubation (n=3; error bars denote ±SEM).

The third set of experiments involved the continuous culture of *P. denitrificans* at a higher temperature (37^{o}C) to assess and compare the reproducibility of similar cultures described in Felgate *et al.* (2012). The temperature and the pH remained unchanged during the incubation at 37^{o}C and pH 7.5 respectively (see Appendix). Air was supplied at the initial batch stage of the culture allowing the culture to increase in population (Figure 7; C, D; 0 - 22 h). After the initiation of the continuous culture mode, nitrate was consumed gradually up to ~15 mM of nitrate. Nitrite and nitrous oxide were below 200 µM throughout the incubation. These results corroborate with our experimental data (Figure 6) and those reported in Felgate *et al.* (2012).

Finally, an experiment was performed to assess the detection and the potential levels of nitrous oxide in the CSTR experimental system used. A strain of *P. denitrificans* deficient in a functional copy of *nosZ* was cultured at 37^{o}C and a pH of 7.5 (Figure 8; A, B). Similarly, as previously performed, air was injected to the vessel at for ~ 22 h, then the air supply was shut off and the continuous culture mode was initiated. Following that event, oxygen was consumed and nitrate was reduced with ~10 mM of nitrate remaining in the vessel at the end of the incubation (120 h). There was no nitrite accumulation in the vessel; however nitrous oxide emissions increased to ~9.8 mM (Figure 8; E; 120 h). This resulted in ~98% recovery of nitrogen mass (N-N_2O) in the mass balance.

The production and consumption quotients summarise the rates the aerobic and anaerobic metabolic profiles (Table 2)**.** The productivity quotients were calculated according to the methodology explained in the Materials and Methods. The concentration of oxygen in the culture affected directly the reduction of nitrate. The nitrate consumption quotient was 76 µmol.g^{-1}.h^{-1} in the aerobic treatment. On the contrary, in the anaerobic treatments the nitrate consumption quotient was ~1200 µmol.g^{-1}.h^{-1} comparable for the 30 and 37 ^{o}C incubations of *P. denitrificans*. The anaerobic incubations of the wild type strain (PD1222) produced di-nitrogen in comparable levels to the nitrate consumption quotient of ~ 1200 µmol.g^{-1}.h^{-1} at both temperatures. Notably the mutant strain PD10222, that was lacking a functional copy of *nosZ*, consumed 2 times more nitrate (Table 2; 2551 µmol.g^{-1}.h^{-1}) that was subsequently reduced to nitrous oxide and not to di-nitrogen, thus the nitrous oxide and di-nitrogen production quotient was 2466 and 323 µmol.g^{-1}.h^{-1}, respectively. The microbial yield productivity (*qX*) was higher in the aerobic (0.2 g.L^{-1}.h^{-1}) than in the anaerobic treatment ranging from 0.09 to 0.13 g.L^{-1}.h^{-1}, indicating the higher energy efficiency of aerobic respiration when compared to anaerobic

respiration. Furthermore the disruption of *nosZ* in the mutant strain PD10222 negatively affected the growth and microbial yield (0.09 $g.L^{-1}.h^{-1}$) of the bacterium. This observation and the accompanying increase in nitrate consumption quotient, indicates a notable change of the stoichiometry and electron use efficiency of the bacterial denitrification pathway, which will be further explained in the 2.3 Discussion: Towards the elucidation of the *regulation* of aerobic and anaerobic CSTR cultures of P. *denitrificans*.

Note: The microarray and respirome expression datasets are found in 2.4 Gene expression datasets.

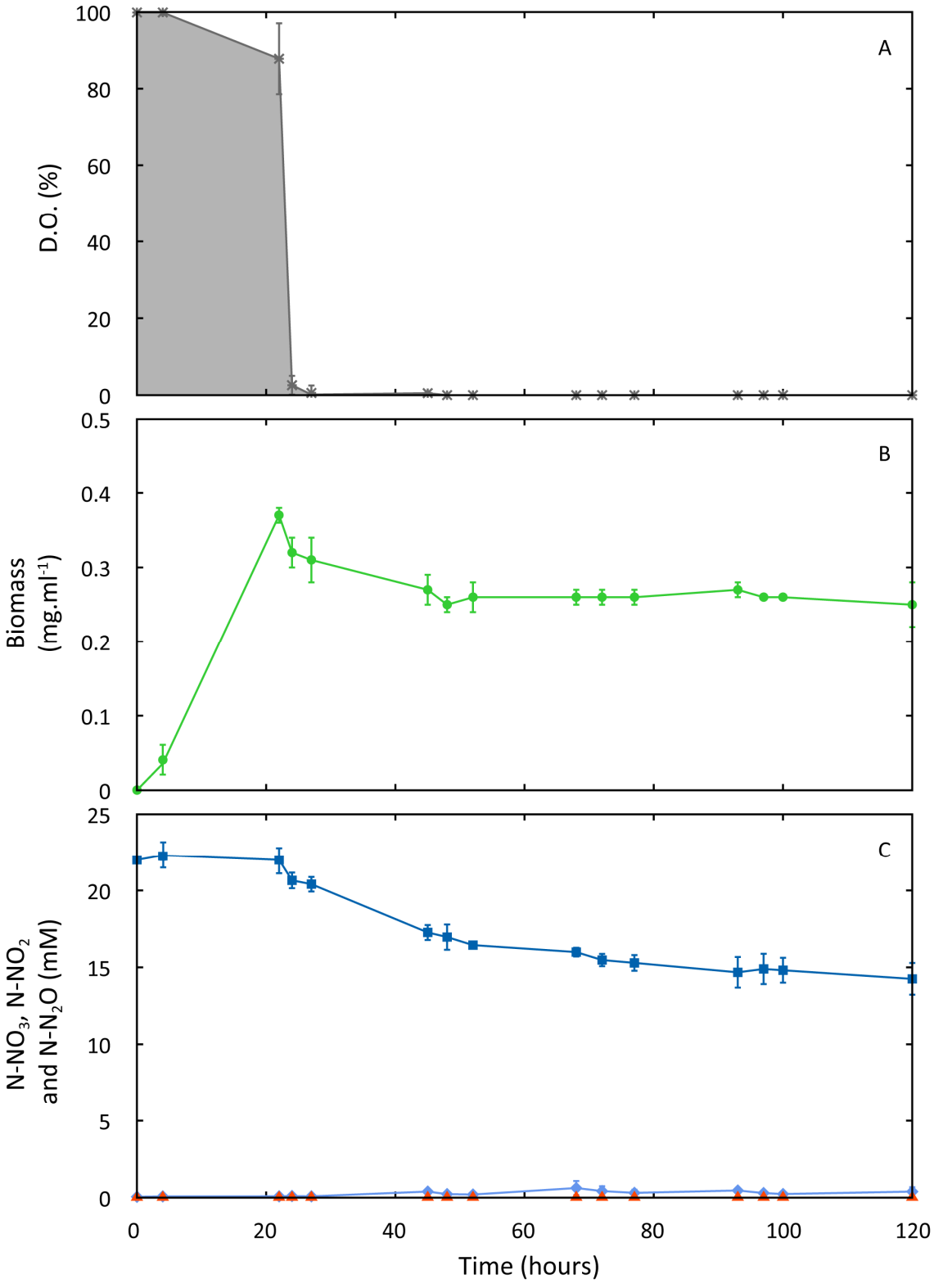

Figure 7 Anaerobic continuous culture of *P. denitrificans* (PD2221) at 37°C in CSTR. Panel A illustrate the average dissolved oxygen (D.O.; *) concentration of the culture, B the average biomass (●) concentration of the culture and C the average extracellular concentration of nitrate (■), nitrite (◆) and nitrous oxide (▲) during the continuous culture incubation (n=3; error bars denote ±SEM).

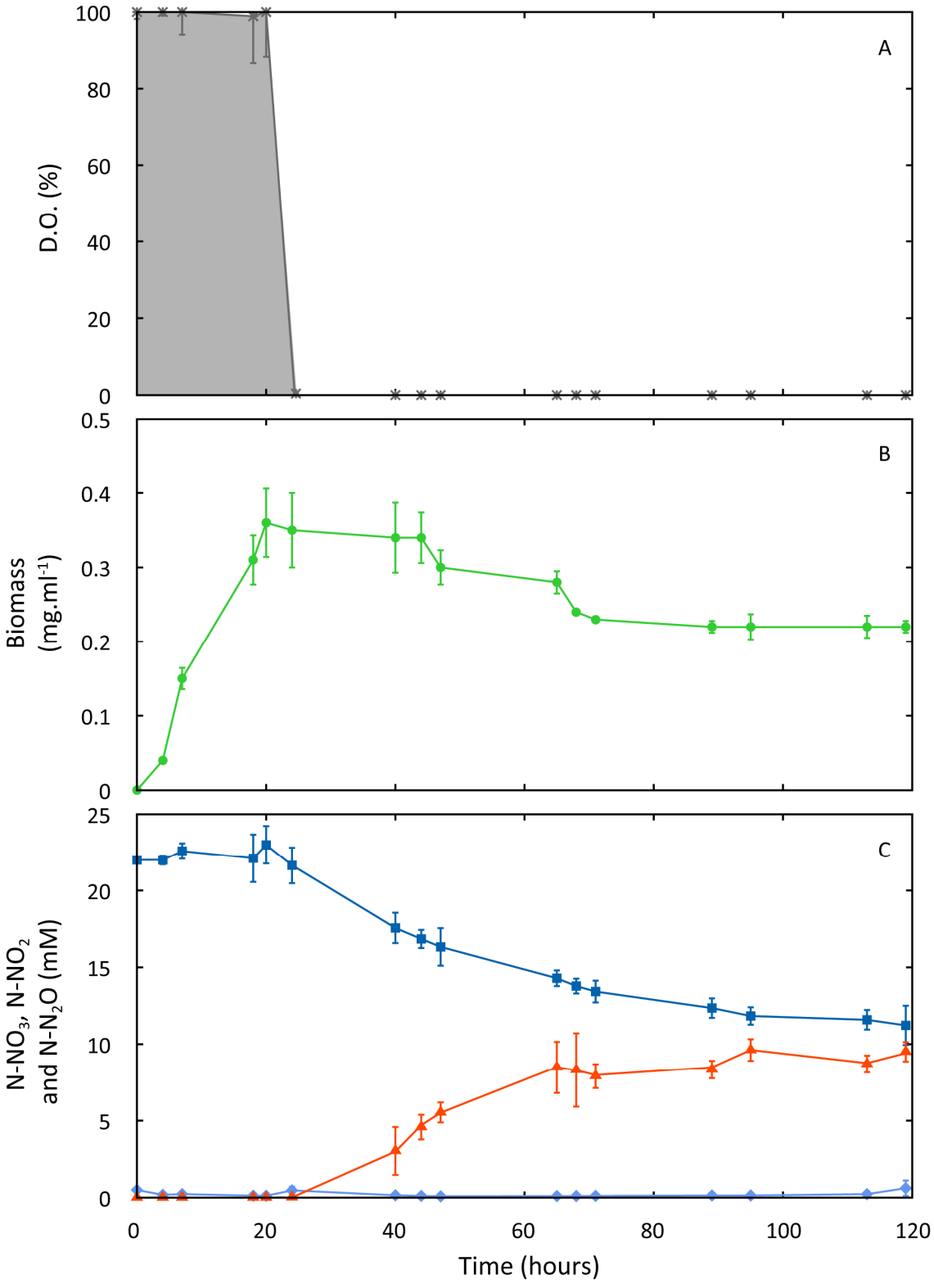

Figure 8 Anaerobic continuous culture of *P. denitrificans* (PD10.221) lacking a functional copy of *nosZ* (Pden_4219) at 37°C in CSTR. Panel A illustrate the average dissolved oxygen (D.O.; *) concentration of the culture, B the average biomass (●) concentration of the culture and C the average extracellular concentration of nitrate (■), nitrite (◆) and nitrous oxide (▲) during the continuous culture incubation (n=3; error bars denote ±SEM).

Table 2 Growth parameters and quotient rates of the aerobic and anaerobic continuous cultures (CSTR) (n=3).

#	Strain	Temp.	pH	D	OD	±SE	X		D/X	±SE	qX	±SE
		°C		h^{-1}			$g.L^{-1}$	±SE	$L.g^{-1}.h^{-1}$		$g.L^{-1}.h^{-1}$	
1	PD1222	30	7.5	0.05	0.61	0.03	0.32	0.01	0.17	0.01	0.20	0.02
2	PD1222	30	7.5	0.05	0.52	0.02	0.25	0.01	0.22	0.01	0.12	0.01
3	PD1222	37	7.5	0.05	0.50	0.02	0.26	0.01	0.21	0.01	0.13	0.01
4	PD10221	37	7.5	0.05	0.41	0.02	0.21	0.01	0.25	0.01	0.09	0.01

Table continues below; index number (#) defines the treatment.

#	Strain	Temp.	$[NO_3]_0$		$[NO_3]_t$	±SE	$[NO_2]_t$	±SE	$[N_2O]_t$	±SE	$[N_2]_t$	±SE
		°C	µM	±SE	µM		µM		µM		µM	
1	PD1222	30	21393	1095	20957	1144	67	38	0.07	0.07	370	0.07
2	PD1222	30	20723	647	15159	115	4745	44	0.33	0.11	5475	0.11
3	PD1222	37	20875	875	14653	942	311	140	1.54	0.22	5910	0.22
4	PD10221	37	22000	0	11678	786	327	199	8641.33	533.41	1354	533.41

Table continues below; index number (#) defines the treatment.

#	Strain	Temp.	$[NO_3]_c$		$[NO_2]_p$	±SE	$[NO_2]_c$	±SE	$[N_2O]_p$	±SE	$[N_2]_p$	±SE
		°C	$\mu mol.g^{-1}.h^{-1}$	SE	$\mu mol.g^{-1}.h^{-1}$		$\mu mol.g^{-1}.h^{-1}$		$\mu mol.g^{-1}.h^{-1}$		$\mu mol.g^{-1}.h^{-1}$	
1	PD1222	30	76	195	12	6.6	65	198	0.0	0.01	65	198
2	PD1222	30	1215	274	18	9.2	1196	283	0.2	0.03	1196	283
3	PD1222	37	1290	420	63	26.3	1228	446	0.3	0.06	1227	446
4	PD10221	37	2551	235	85	54.2	2466	202	2142.5	220.66	323	219

*Indexes **c** and **t** denote consumption and production respectively.

2.2.3 Validation of RT-PCR transcriptional analyses of *P. denitrificans*

The transcriptional profile of the aerobic and anaerobic continuous cultures was analysed at the 120 h time point. Genes involved in aerobic and anaerobic respiration and electron transport were selected. Additionally, four genes were selected to calibrate and normalize the amplification efficiency of RT-PCR; those are termed as housekeeping genes.

Table 3 Sequences of primer pairs for *gapdh*, *polB*, *rpoB* and *tpiA* selected as housing keeping genes for the normalization of RT-PCR expression values.

Gene ID	Annotation	Forward Primer	Reverse Primer
Pden_4465	*gapdh*	gctgaagggcatcctaggctata	actcgttgtcataccaggtcagg
Pden_0342	*polB*	catgtcgtgggtcagcatac	ctcgcgaccatgcatataga
Pden_0747	*rpoB*	ggtgtcttccagtcggtgtt	ggtactcctccacatcgtat
Pden_4305	*tpiA*	cgagaccgacgaacaggt	agatcacgtcgagcgtctg

Housekeeping gene (HKG) oligonucleotides were selected based on previously published transcriptional analyses and those genes were constitutively expressed under various conditions (Bouchal *et al.* 2010, Romanowski *et al.* 2011). The *gapdh* gene encodes glyceraldehyde phosphate dehydrogenase that catalyses the sixth step of glycolysis, *tpiA* expresses triose P-isomerase that catalyses the reversible inter-convertion of glyceraldehyde 3-phosphate and di-hydroxy-acetate phosphate, and is located upstream of *gapdh*. DNA polymerase B is involved in base excision and repair and is commonly annotated as the gap-filling-enzyme of DNA synthesis. The β subunit of RNA polymerase was also tested as a candidate HKG. These four candidate pairs were validated for specificity using standard PCR and genomic DNA from *P. denitrificans* as the PCR template. The PCR products were loaded on an Ethidum-bromide stained gel and had a single product ~ at 200 bp as expected (Figure 9). Then, the relative expression (anaerobic vs. aerobic treatment) of those four HKGs was compared using RT-PCR. From those four HKGs candidates, *polB* was selected for routine RT-PCR analyses having high specificity and an expression ratio of ~1 between the aerobic and anaerobic treatment (Figure 10).

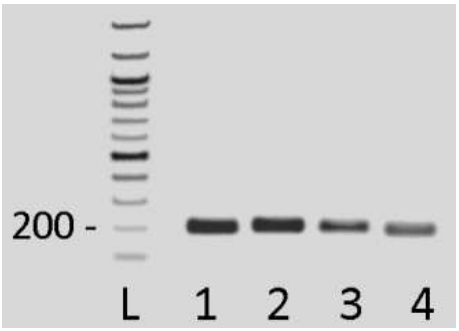

Figure 9 Agarose gel showing the PCR products of the primers selected for the housekeeping genes. L denotes 100 bp DNA ladder (NEB, UK); 1 *gadph*; 2 *rpob*; 3 *polB*; *tpiA*. Mark 200 indicates 200 bp DNA weight.

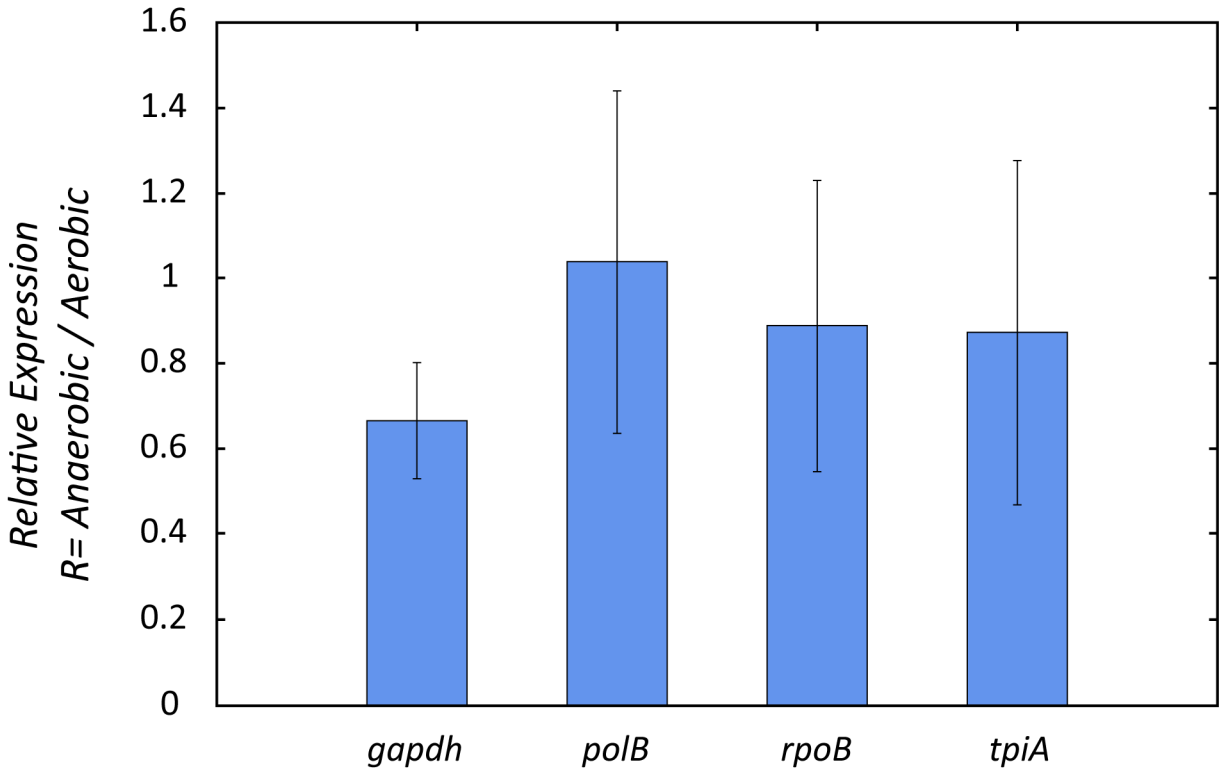

Figure 10 Relative expression of the housekeeping genes; *gapdh*, *polB*, *rpoB*, *tpiA* between the aerobic (reference) and anaerobic treatment.

Samples for RNA were taken from each reactor at 120 h of continuous culture. At this point it is assumed that the bacterial biomass has reached steady levels, as seen in figures 6 and 5. Total RNA was extracted and was quantified to 307 (SE ±46) and 257 (SE ±37) ng.µl^{-1} for the aerobic and anaerobic treatment respectively. RNA preps were tested for any residual DNA contamination with standard PCR and for RNA integrity with Experion electrophoresis. Any residual DNA contamination was treated with TurboDNAse; figure 11 shows the RNA purity of

the sample without any detectable DNA fragments. The integrity of the RNA was acceptable for further transcriptional analyses. In figure 12, all RNA samples, except sample 2, yielded distinct bands corresponding to the 23S, 16S and 5S rRNA species, a good indication that there was little if any degradation by RNase.

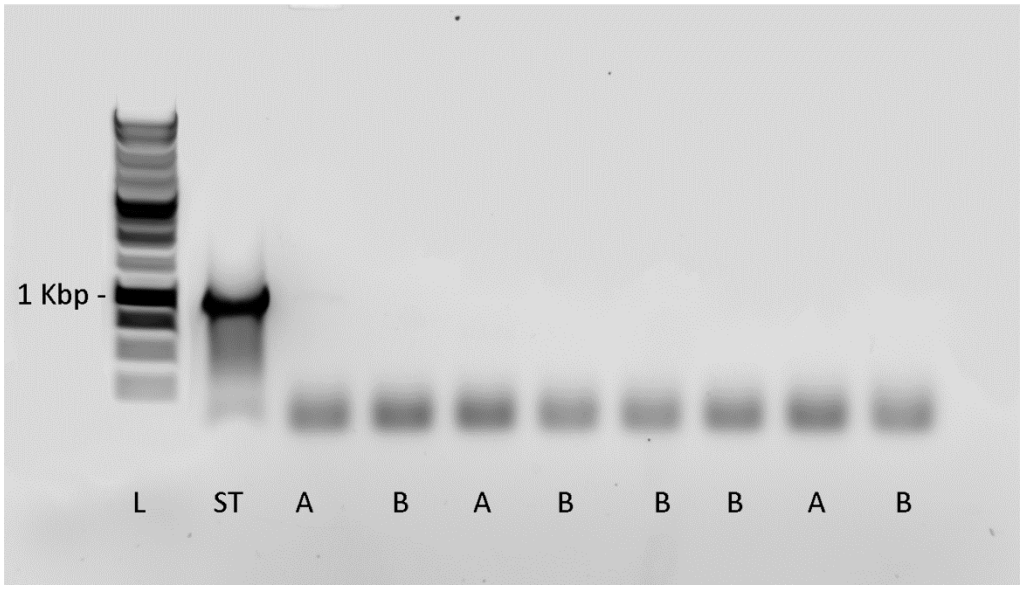

Figure 11 Agarose gel of the PCR products showing no DNA contamination in RNA preps from aerobic and anaerobic continuous cultures. L denotes DNA ladder; ST gDNA from *P. denitrificans*; A aerobic RNA preps and B anaerobic RNA preps. Mark 1 Kbp indicates 1 Kbp DNA weight**.**

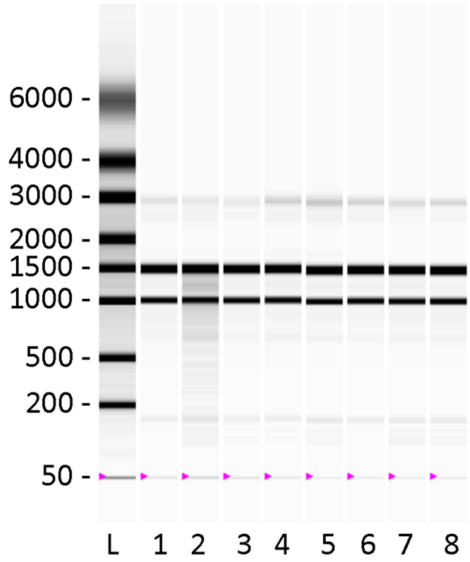

Figure 12 Experion (Bio-rad, UK) electrophoresis virtual gel showing RNA preps from aerobic and anaerobic continuous cultures; L denotes RNA ladder; 1-4 aerobic RNA preps and 5-8 anaerobic RNA preps. Numerical marks indicate DNA size in nt.

RNA was successfully extracted, purified and quantified from each reactor, a crucial step prior to any further transcriptional analyses. The next section of this results chapter will illustrate the relative expression of selected target genes between aerobic and anaerobic conditions and suggest the transcription factors involved in *cis*-acting regulatory pathways.

2.2.4 Transcriptional analyses with RT-PCR of *P. denitrificans* in aerobic and anaerobic CSTR cultures

RNA was reverse transcribed to cDNA that was subsequently used as template for quantitative real time polymerase chain reactions (qRT-PCR) to estimate expression of selected genes involved in the aerobic and anaerobic electron pathways. These target genes were *qoxB*, *ctaDI* and *ctaE* for aerobic respiration and the alternative oxidoreductases for anaerobic respiration on nitrate; *narG*, *nirS*, *norB*, and *nosZ*. Furthermore, genes of interest in electron transport were selected; *pasZ* and *cycA*, and additionally three more target genes involved in aerobic nitrate reduction were selected; *coxB*, *napA* and *nodA* respectively. *nodA* is suggested to be involved in NO detoxification (Hartop 2004) under nitrosative stress. For each target gene, the forward and

reverse primers were designed using primer3 software as described in 7.3.7 Primer design and validation. Upon arrival, the primers were hydrated and tested with standard PCR for performance and specificity. A selected agarose gel is enclosed depicting distinct single product for *pasZ* at ~200 bp and in contrast three non-specific products are depicted for the gene encoding cytochrome ba_3 (*coxB*) at ~ 200, ~ 400 and ~ 800 bp. For the above reason, new primers were designed for the target gene of cytochrome ba_3 oxidase and the existing pair of primers was excluded from any transcriptional analyses. The successful pairs of primers for the aforementioned genes are listed in table 4. Transcription of selected genes was quantified in real time with a SYBR-green fluorescent RT-PCR system (CFX-1000, Bio-rad, UK). The expression of *polB* was used to normalize the expression values of the target genes, and the aerobic treatment was used as a reference condition (7.3.11 RT-PCR comparative quantification).

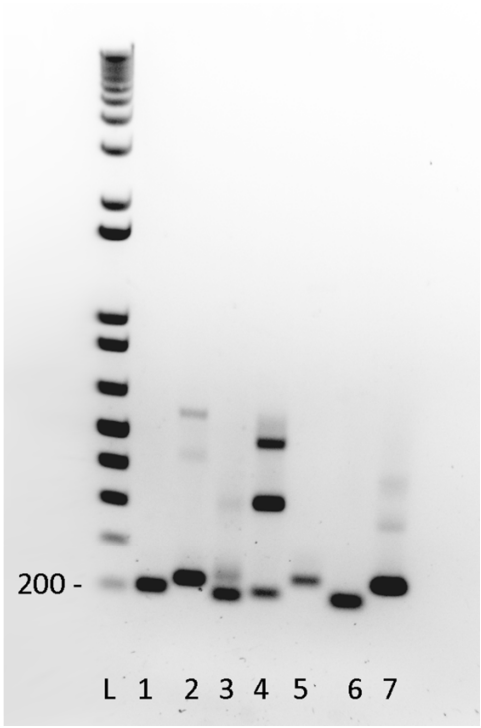

Figure 13 Selected agarose gel showing PCR products of candidate primer oligonucleotides. L denotes ladder; 1 *pasZ* (pden_4222); 2 *pasZ* (pden_4222); 3 *ctaE* (pden_4321); 4 *qoxB* (pden_5107); 5 *fbcC* (pden_2307); 6 (pden_4442); 7 (pden_4442). Primer *pasZ2* was discarded and primers for *ctaE* and *qoxB* were reordered. Mark 200 indicates 200 bp DNA weight**.**

Table 4 Sequences of primers used in RT-PCR to detect respiratory functional genes.

Gene ID	Annotation	Forward Primer	Reverse Primer
pden_4233	*narG*	gcgaggaggtctgctacaac	atccattcgtggtcctggta
pden_2487	*nirS*	aattcggcatgaaggagatg	tccagatcccagtcgttttc
Pden_4219	*nosZ*	cttttcgacctcctacaactcg	ccgttcagttcctgatagtcg
pden_1689	*nodA*	aggttccggtgcattacatc	gtctggtggaaatcggtgac
pden_2483	*norB*	tatgtcagcccgaacttcct	ttcgggcaggatgtaatagg
pden_4222	*pasZ*	tcgaagccatcaaggaaaa	catttcacgccgtaaagtcc
pden_1937	*cycA*	cagcatctatgccactctcg	caagccttgcacttgttgaa
pden_5107	*qoxB*	cgtgttttccgaagtcacct	gcccatggtgaagaagtgat
pden_3028	*ctaDI*	gctgatctcggtcacactca	taggtcacgacgacattcca
pden_4317	*ctaE*	cgtgctctacgtcatgttcg	acaggatgaagccgtattgc
pden_4721	*napA*	tggatccaggtgaacaacaa	gtccgagacgacgatgaaat

These RTPCR experiments showed that target genes *narG* (pden_4233), *nirS* (pden_2487), *nosZ* (Pden_4219), *nodA* (pden_1689), *norB* (pden_2483), *pasZ* (pden_4222), *cycA* (pden_1937), *qoxB* (pden_5107) and *ctaDI* (pden_3028) are relatively highly expressed in anaerobic conditions. However, one gene of interest *ctaE* (pden_4317) was up-regulated in aerobic conditions and *napA* (pden_4721) was less but notably up-regulated in the aerobic treatments as shown in figure 14. These values do not denote the absolute gene expression but the relative expression between two conditions; aerobic (reference condition) and anaerobic. However, it is clearly illustrated that in anaerobic conditions with nitrate present as an alternative electron acceptor, genes responsible for the reduction of nitrate to di-nitrogen were highly induced which is consistent with the flexibility of *P. denitrificans* to switch respiratory pathways (Richardson and Watmough 1999, Richardson 2008). The metabolic and transcriptional profile of *P. denitrificans* in aerobic and anaerobic environment is therefore well established. However a question remains open; how does *P. denitrifcans* sense the changes in its living environment and how is this complex network of genes regulated?

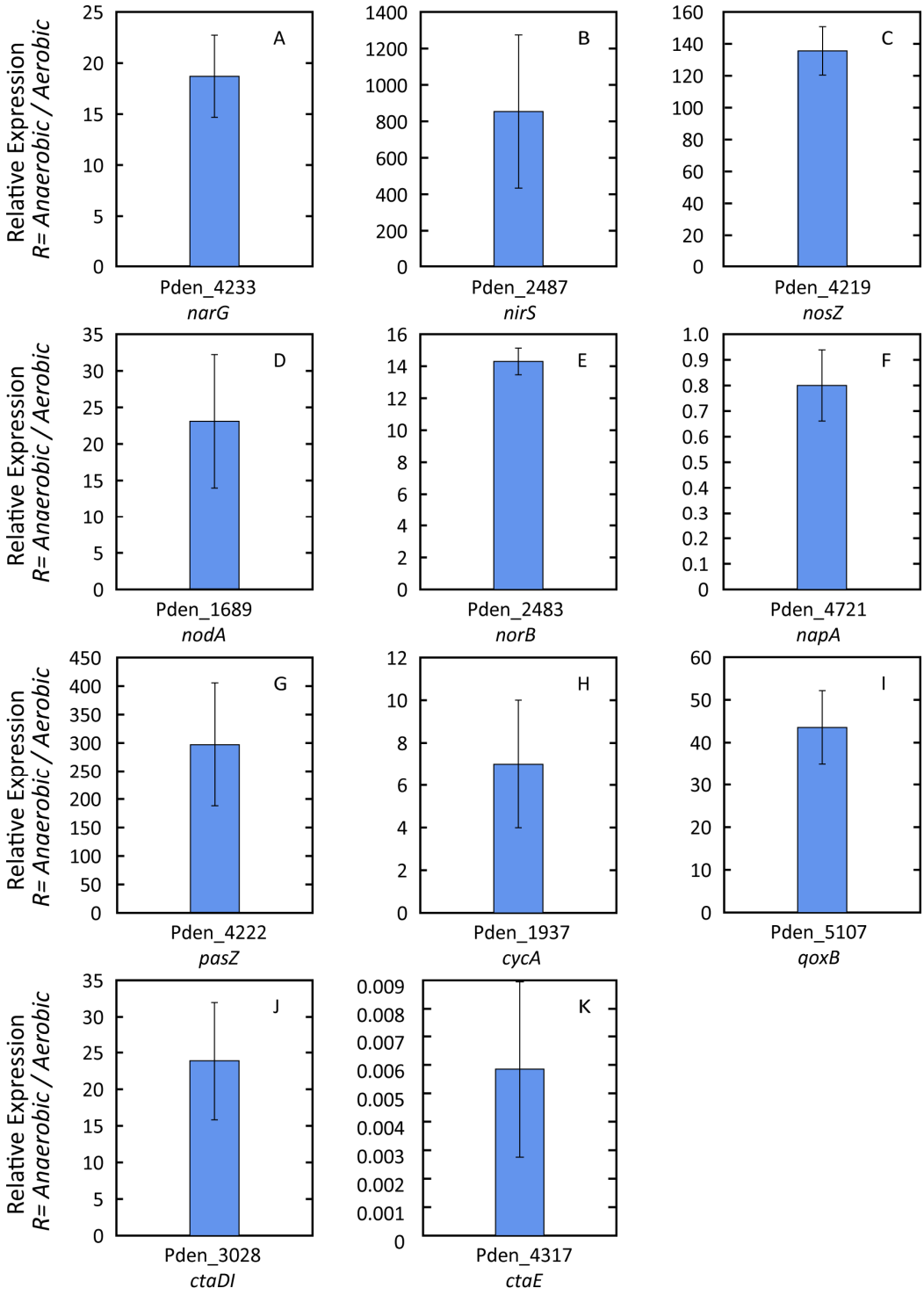

Figure 14 Average relative expression of target genes; A) *narG* (pden_4233), B) *nirS* (pden_2487), C) *nosZ* (pden_4219), D) *nodA* (pden_1689), E) *norB* (pden_2483), F) *napA* (pden_4721), G) *pasZ* (pden_4222), H) *cycA* (pden_1937), I) *qoxB* (pden_5107), J *ctaDI* (pden_3028) and K) *ctaE* (Pden_4317) detected with RT-PCR. Expression values are normalized on expression of *polB* and the relative ratio R is calculated using the aerobic treatment as reference based on the Pfaffl method (n=3, errorbars denote standard error).

2.2.5 Whole genome transcriptional analyses of *P. denitrificans* in aerobic and anaerobic CSTR cultures

Having established the metabolic profiles of aerobic and anaerobic continuous cultures micorarray technology was employed to investigate the transcriptional profile of the *P. denitrificans* genome. Investigation of the transcriptome of *P. denitrificans* could identify genes subject to coordinate regulation. Gene expression was estimated using a dual fluorescent dye system to label the mRNA, subsequently cDNA, and gDNA samples of the aerobic and anaerobic treatments. Oligonucleotide probes specific to the *P. denitrificans* genome were designed and printed on four-block arrays by Oxford Gene Technology. The samples were hybridized and arrays were scanned, the resulting images were analysed and the dye ratio was calculated. These results were normalised and imported in to GeneSpring GX 7.3 for further enrichment analyses. Expression values were filtered based on fold expression and significance, 2-fold and *p=0.05* respectively.

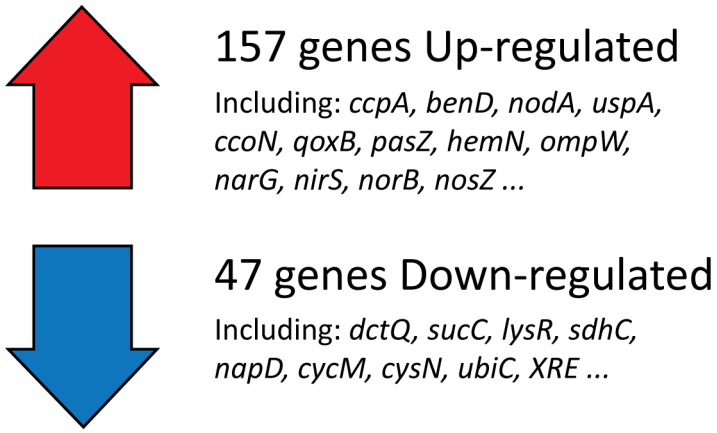

Figure 15 Schematic summarizing the volcano filtering (≥ 2 fold, *p=0.05*) of the microarray dataset.

Note: The microarray and respirome expression datasets are found in 2.4 Gene expression datasets.

The microarray analyses of the aerobic and anaerobic treatments revealed the significant regulation of genes comprising pathways involved in nitrate, nitrite, nitric oxide and nitrous oxide reduction, cytochrome ba_3 and cbb_3 oxidation, ubiquinone biosynthesis, *electron* transport and various outer membrane and ABC type transporters. A total of 204 genes showed significant regulation (*p=0.05*) with 47 being down-regulated and 157 being up-regulated (Figure 15). The relative expression values of selected genes of interest were compared between the microarray and the RT-PCR dataset (Table 5). A similar expression pattern was observed, that confirms the latter whole genome transcriptional analyses. It is interesting to note that Pden_1689 (*nodA*) is highly expressed in anaerobic conditions. Little is known about the function of this gene with a putative product of nitric oxide dioxygenase (Hartop et al. 2014 in prep.).

Gene clusters expressing the primary dehydrogenases; succinate dehydrogenase, lactate dehydrogenase, formate dehydrogenase, NADH-quinone oxidoreductase, hydrogenase, methylamine dehydrogenase, formaldehyde dehydrogenase and sulphite dehydrogenase remained unchanged. The methanol dehydrogenase gene cluster (*mxaFJRSACKL*) was induced anaerobically ~5-fold on average. The *mxaG* gene, expressing a cytochrome c_{551i} containing domain, also remained unchanged.

The genes encoding pseudoazurin and cytochrome c_{550} (pden_4222 and pden_1937 respectively) that are involved in electron transport were ~54 and ~2-fold induced in anaerobic conditions. Gene clusters involved in the biosynthesis of cytochrome c remained unchanged. Contrary, gene clusters involved in ubiquinone biosynthesis were highly induced ~30 fold on average.

The genes expressing the terminal oxidoreductase cbb_3 (*cco* gene cluster) was relatively up-regulated 5-fold in anaerobic conditions. Gene cluster *cta* expressing cytochrome aa_3 oxidoreductase was relatively down-regulated ~0.4 fold. The gene encoding cytochrome *c* peroxidase (*ccpA*) was 2-fold induced. The gene cluster expressing cytochrome ba_3 oxidoreductase (*qox*) was ~3-fold induced. The *napAB* cluster that encodes the periplasmic nitrate reductase remained unchanged and its absolute expression was relatively low. Gene clusters expressing the dissimilatory reductases for nitrate, nitrite, nitric oxide and nitrous oxide

were highly up-regulated. The functional genes for the aforementioned clusters *narG*, *nirS*, *norC* and *nosZ* induced ~10, 121, 15 and 20-fold respectively.

Other highly expressed genes were the putative second copy of succinate dehydrogenase (*sdhDCB* ~2-fold increase), the nitric oxide repressor (*nsrR* ~ 5-fold increase) and the putative universal stress protein (*uspA* ~7 fold increase).

Table 5 Relative expression values* of selected genes of interest from the microarray and RT-PCR datasets.

Gene_ID	Annotation	Microarray		RT-PCR	
		Average	±SE	Average	±SE
Pden_4233	*narG*	7.11	0.58	18.70	4.03
Pden_2487	*nirS*	128.76	23.69	854.00	420.55
Pden_4219	*nosZ*	24.04	8.93	135.60	15.16
Pden_1689	*nodA*	9.25	7.34	23.10	9.12
Pden_2483	*norB*	9.15	1.86	14.30	0.84
Pden_4721	*napA*	0.54	0.11	0.80	0.14
Pden_5107	*qoxB*	4.01	1.02	43.57	8.60
Pden_4222	*pasZ*	53.59	21.63	296.93	108.70
Pden_1937	*cycA*	2.02	0.41	7.00	3.01
Pden_3028	*ctaDI*	1.20	0.20	23.90	8.07
Pden_4317	*ctaE*	0.51	0.13	0.01	0.00

*Relative expression values are based on the ratio of anaerobic to aerobic gene expression

Note: The microarray and respirome expression datasets are found in 2.4 Gene expression datasets.

2.3 Discussion: Towards the elucidation of the regulation of aerobic and anaerobic CSTR cultures of *P. denitrificans*

A gene list based on the microarray data that contained sequences of 200 bp region upstream of the highly regulated genes was used to search for known and unknown highly enriched DNA sequences (motifs) that may represent protein binding sites. Motif analysis revealed sequence

logos similar to the FixK_FnrN motif involved in the dual regulation of nitrogen fixation and oxygen sensing. The FixK_FnrN motif is a binding site for members of the FNR/CRP family that respond to the oxygen concentration and control genes essential for respiration and central metabolism. It is evident that the anaerobic stimuli in these experiments induced genes involved in anaerobic respiration of nitrate that are regulated by transcription factors binding to FNR/CRP-like motifs.

A list of experimentally established genes of *P. denitrificans* involved in anaerobic respiration on nitrate was compiled and analysed for enriched motifs in a similar fashion as previously done. This search indicated a highly conserved sequence logo, TTGAnnnnnnTCAA, similar to FNR-like motifs (Figure 16) found previously.

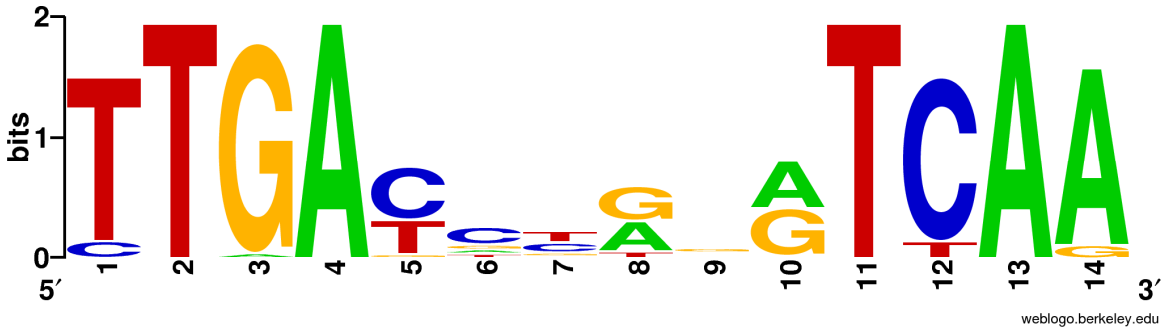

Figure 16 Sequence logo of highly conserved motif based on genes involved in anaerobic nitrate respiration (data from the van Spanning lab).

Similar FnrP binding motif sequences are found in transcription factors involved in nitrate reduction and nitrite and nitric oxide reduction. Table 7 lists the binding motifs of NarR, Nnr and FnrP in *P. denitrificans*. A high similarity of the binding motif is noted with a resulting sequence TTG-N8-CAA. This pattern was used for a wider search of any motifs occurring in the genome of *P. denitrificans.* A total of 116 genes had the TTG-N8-CAA pattern in the upstream flanking region. The regulatory genes *gntR, lysR, tetR, XRE, uspA, fis, marR, ftrB, narR* and *fnrR* were found in the vicinity of the pattern. Other genes found were various ABC type transporters, nitrite transporters, major facilitator transporters, di-carboxylate transporters, mono-oxygenases, ubiquinol oxygenases, pyrrolo-quinoline quinone, pseudoazurin, cytochrome cbb_3 oxidases, NADH oxidases and nitric oxide reductases. The pattern distance ranged for -13 to 1450 bp. Pattern hits falling in the intergenic region were discarded assuming no regulatory element for the current target gene (Table 8).

Interestingly, genes with a putative FNR pattern and involved in aerobic respiration or denitrification were highly induced. The highest up-regulation was observed in *pasZ* (~55 fold) followed by genes involved in nitric oxide and nitrous oxide regulation, *norC* and *nosC* with ~15 and ~17 fold induction respectively. The gene encoding a nitrite/nitrate transporter has ~9 fold induced, this gene is located in close vicinity of *narR* a transcriptional regulator involved in nitrate sensing. Genes expressing cytochrome cbb_3 and ba_3 oxydoreductases were also up-regulated ~6 and ~5 fold respectively. This pattern search also indicated other genes that were highly up-regulated; Pden_4105 with unknown function downstream of sulfonate ABC transporters and citryl-CoA lyase genes, *ompW* with unknown function downstream of genes involved in propionyl-CoA valine metabolism, and Pden_1835 with unknown function downstream of a DNA topoisomerase gene cluster.

Table 6 Relative expression of selected genes with a TTG-N8-CAA motif in the upstream flanking region

Gene ID	Ratio	Annotation	Product
Pden_1850	1.2	*fnrP*	Crp/Fnr family transcriptional regulator
Pden_3921	3.1		serine-glyoxylate transaminase
Pden_5103	3.1	*phbC1*	poly-beta-hydroxybutyrate polymerase domain
Pden_5108	4.7	*qoxA*	hypothetical protein
Pden_1844	6.1	*ccoG*	4Felectron4S ferredoxin
Pden_1848	6.3	*cooN*	cbb_3-type cytochrome c oxidase subunit I
Pden_4237	8.6	*narK*	nitrite transporter
Pden_1835	12.5		unknown, downstream of DNA topoisomerase
Pden_3636	13.4	*ompW*	unknown, downstream of propionyl-CoA valine
Pden_2484	15.1	*norC*	nitric-oxide reductase
Pden_4221	17.2	*nosC*	hypothetical protein
Pden_4105	32.4		unknown, downstream of sulfonate, citryl-CoA lyase
Pden_4226	32.8	*UbiD*	UbiD family decarboxylase
Pden_4222	54.8	*pasZ*	pseudoazurin

The relative expression of the genes encoding transcription factors *fnrP*, *nnrR* and *narR* was slightly induced in the anaerobic treatment and was on average 1.25 (SE ±0.10) as seen in figure 18. It is therefore concluded that the aforementioned transcriptional factors are constitutively expressed in both conditions. However, the mode of activation of each transcription factor is unique as explained in the Introduction. The absolute expression was on average 9 (SE ±0.6), 3 (SE ±0.2) and 0.9 (SE ±0.05) for the *fnrP*, *nnrR* and *narR* respectively. This indicates a higher relative abundance of transcripts according to the order *fnrP* > *nnrR* > *narR.* The relative higher abundance of *fnrP* in the cell could provide *fnrP* a higher probability to bind to other spurious motifs. The DNA binding domains of the regulatory proteins NarR, NNR and FNR were aligned (Figure 17) to test their potential to bind to similar motifs. The alignment shows high similarity of the helix-turn-helix domain and that could imply a similar binding specificity to the motifs of a TTG-N8-CAA pattern.

Table 7 Promoters and DNA binding motifs of genes regulated by NarR, NNR and FNR.

Promoter	Motif	Distance	Regulation	Reference
p*narG*	**TTG**ACttaaAT**CAA**	-52	*narR*	(Wood *et al.* 2001)
p*nirS*	**TTA**ACaaagGT**CAA**	-41.5	*nnrR*	(Zumft 2002)
p*norB*	**TTG**ACtttcAT**CAA**	-43.5	*nnrR*	Hutchings and Spiro (2000)
p*nosC*	**TTG**ACctaaGT**CAA**	-135	*nnrR*	Hutchings and Spiro (2000)
p*ccoN*	**TTG**ACGCAGAT**CAA**	-54	*fnrP*	(van Spanning *et al.* 1997)
p*fnrP*	**TTG**ACccaaAT**CAA**	-110	*fnrP*	(van Spanning *et al.* 1997)
p*nosZ*	**TTG**AAgcttAA**CCA**	-21	*fnrP-like*	(Hoeren *et al.* 1993)

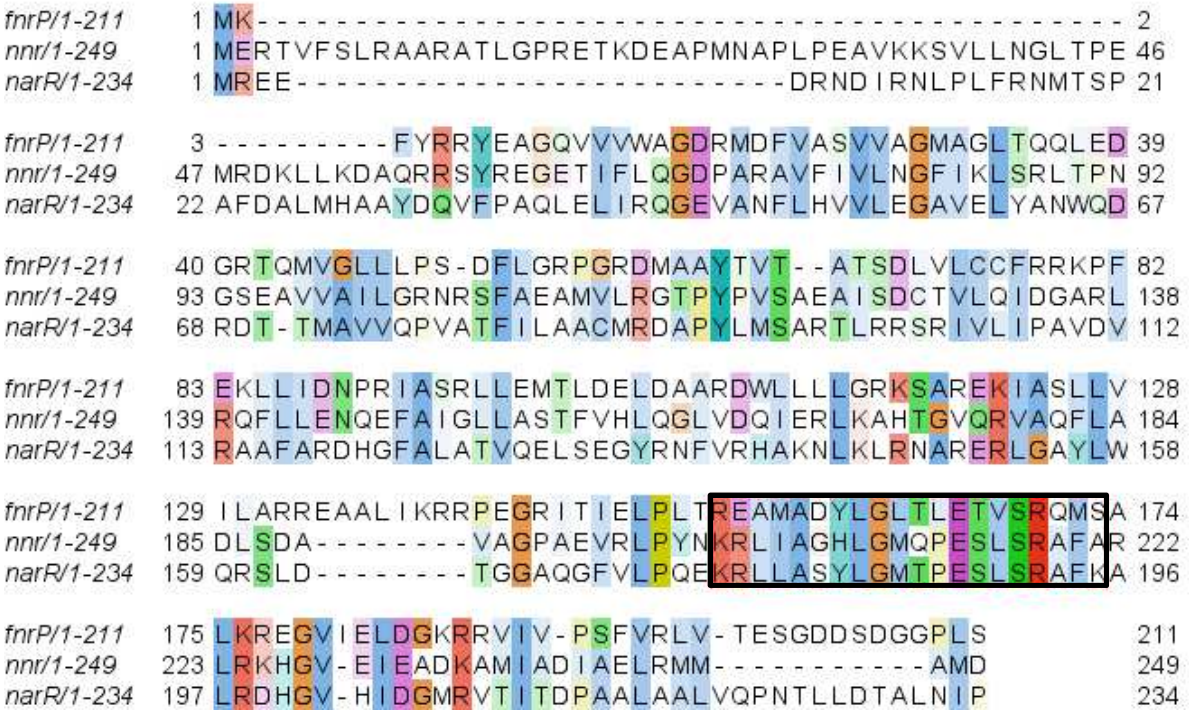

Figure 17 Amino-acid alignment of FnrP, NnrR and NarR from *P. denitrificans.* The boxed region indicates the DNA binding domain of the aligned regulatory proteins.

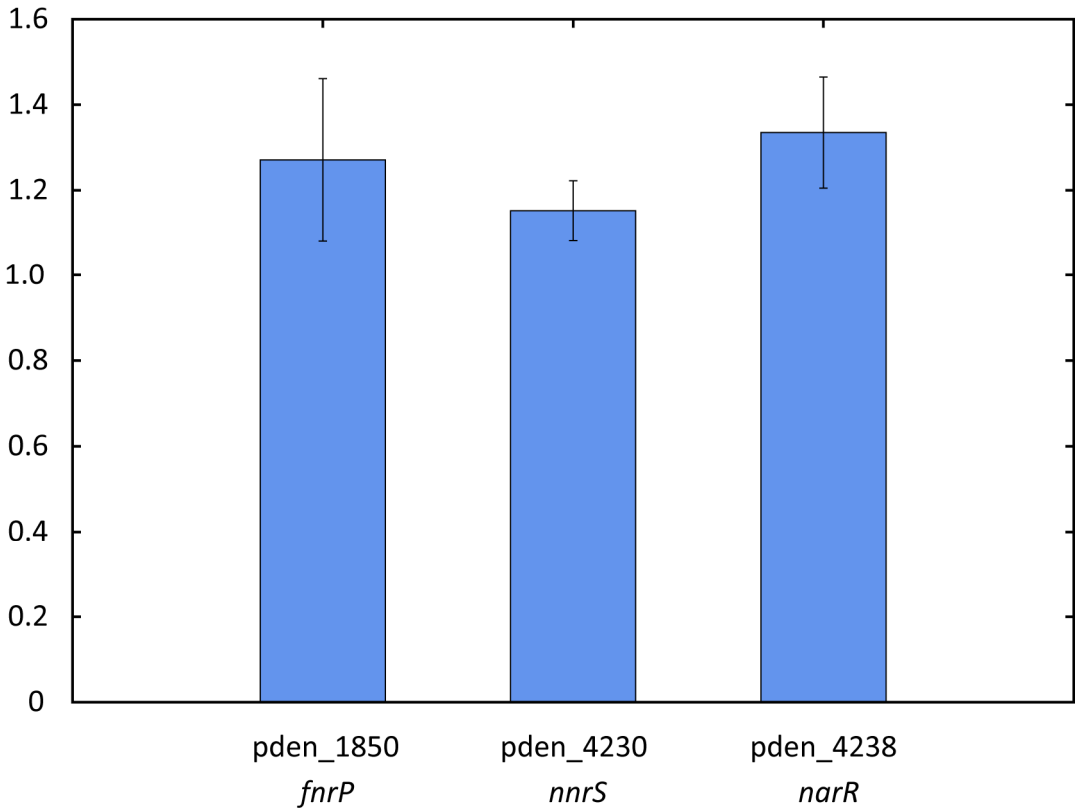

Figure 18 The relative expression of the transcriptional factors *fnrP*, *nnrR* and *narR* in aerobic and anaerobic CSTR cultures.

The next chapter (Chapter 3) investigates the role of three major regulatory DNA binding proteins, FNR, NNR and NarR in anaerobic respiration of nitrate in continuous cultures of *P.denitrificans*. Two well described strains of *P. denitrificans* lacking a functional copy of *fnrP* (Pden_1850) and *nnrR* (Pden_2478) were studied in continuous cultures systems for their metabolic and transcriptional profiles. Additionally a strain of *P. denitrificans* lacking a functional copy of *narR* (Pden_4238) was constructed in this study and subsequently analysed for its metabolic and transcriptional profile (Chapter 4). These results allow us to elucidate the genetic regulation of anaerobic respiration which is further examined in the 6. Discussion**.**

Table 8 Genes found downstream of a TTG-N8-CAA motif in *P. denitrificans*.

Gene	Sequence	nt	Annotation		Distance	Next Gene
Pden_0061	TTGAAAGGAGACAA	14	hypothetical protein	->	91…3	Pden_0062
Pden_0101	TTGCGCAAAGGCAA	14	hypothetical protein	<-	124...61	Pden_0102
Pden_0132	TTGAATCCGAACAA	14	putative replication protein A	->	116...127	Pden_0133
Pden_0174	TTGGGGGAGGACAA	14	maleylacetoacetate isomerase	->	11...2	Pden_0175
Pden_0278	TTGCTTCATGACAA	14	major facilitator transporter	->	170...-6	Pden_0279
Pden_0302	TTGCAGAGAATCAA	14	LysR family transcriptional regulator	<-	38...43	Pden_0303
Pden_0336	TTGTTCATTTTCAA	14	hypothetical protein	<-	-13...38	Pden_0337
Pden_0384	TTGATTCCGCGCAA	14	hypothetical protein	<-	59...47	Pden_0385
Pden_0451	TTGCCTCCCACCAA	14	hypothetical protein	<-	188...142	Pden_0452
Pden_0476	TTGCGCATCCGCAA	14	thioesterase superfamily protein	->	21...20	Pden_0477
Pden_0477	TTGCGCATTCGCAA	14	XRE family transcriptional regulator	->	65...108	Pden_0478
Pden_0477	TTGCTGATACGCAA	14	XRE family transcriptional regulator	->	89...84	Pden_0478
Pden_0532	TTGAAGCCATTCAA	14	UspA domain-containing protein	<-	81...63	Pden_0533

Table continues

Gene	Sequence	nt	Annotation		Distance	Next Gene
Pden_0566	TTGCGTGATCACAA	14	dehydratase	->	157...143	Pden_0567
Pden_0572	TTGCCGAAACGCAA	14	*sdhB*,succinate dehydrogenase iron-sulfur subunit	->	140...364	Pden_0573
Pden_0592	TTGGGCGGCCTCAA	14	inosinelectron5'-monophosphate dehydrogenase	->	136...176	Pden_0593
Pden_0614	TTGGGAAGCGTCAA	14	queA, ribosyltransferaselectronisomerase	<-	0...85	Pden_0615
Pden_0647	TTGGCCTTGCGCAA	14	peptide deformylase	<-	22...56	Pden_0648
Pden_0673	TTGCATGAATGCAA	14	regulatory protein, LacI	<-	57...28	Pden_0674
Pden_0744	TTGGCTCTTGGCAA	14	rplA,50S ribosomal protein L1	->	199...270	Pden_0745
Pden_0821	TTGATTTCGCACAA	14	hypothetical protein	->	-3...11	Pden_0822
Pden_0915	TTGACGCAAATCAA	14	entericidin EcnAB	<-	-8...55	Pden_0916
Pden_0924	TTGCGCGGGTTCAA	14	OsmC family protein	<-	49...46	Pden_0925
Pden_1010	TTGTTTTCAGTCAA	14	sulfoacetaldehyde acetyltransferase	<-	11...173	Pden_1011
Pden_1052	TTGCTGGCGCGCAA	14	aldehyde dehydrogenase	->	114...1347	Pden_1055
Pden_1197	TTGATGCCTCTCAA	14	NADH:flavin oxidoreductase/NADH oxidase	->	541...57	Pden_1198
Pden_1201	TTGTCACCCGCCAA	14	hypothetical protein	->	112...187	Pden_1202

Table continues

Gene	Sequence	nt	Annotation		Distance	Next Gene
Pden_1247	TTGCTTCGTGCCAA	14	glutathionylspermidine synthase	<-	136...57	Pden_1248
Pden_1339	TTGATGCGCGGCAA	14	hypothetical protein	->	-3...-10	Pden_1340
Pden_1345	TTGAGCCCGATCAA	14	methylisocitrate lyase	->	290...840	Pden_1347
Pden_1356	TTGGGCCGAGGCAA	14	hypothetical protein	->	899...311	Pden_1358
Pden_1356	TTGCCGTTGCTCAA	14	hypothetical protein	->	1143...67	Pden_1358
Pden_1376	TTGATCAACGCCAA	14	lipoyl synthase	<-	50...62	Pden_1377
Pden_1395	TTGAAGGCGAACAA	14	aminotransferase, class V	<-	111...16	Pden_1396
Pden_1457	TTGCGCCGAGCCAA	14	alpha/beta hydrolase	<-	69...86	Pden_1458
Pden_1486	TTGGTAATGTACAA	14	TonB-dependent receptor	->	-6...-7	Pden_1487
Pden_1548	TTGATTTACAACAA	14	HipA domain-containing protein	->	255...101	Pden_R0022
Pden_1616	TTGGCCTGGCGCAA	14	transposase IS3/IS911 family protein	<-	64...499	Pden_1618
Pden_1621	TTGATCGAACCCAA	14	hypothetical protein	<-	181...172	Pden_1622
Pden_1653	TTGGCGTCAATCAA	14	lytic murein transglycosylase	<-	149...-7	Pden_1654
Pden_1729	TTGCCGTTTCGCAA	14	alanine dehydrogenase	<-	48...341	Pden_1730

Table continues

Gene	Sequence	nt	Annotation		Distance	Next Gene
Pden_1789	TTGCGCCCGCCCAA	14	surface presentation of antigens, SPOA protein	->	144...28	Pden_1790
Pden_1796	TTGGGGAGGGGCAA	14	GCN5-related N-acetyltransferase	<-	136...130	Pden_1797
Pden_1822	TTGATACGCATCAA	14	5-aminolevulinate synthase	<-	24...88	Pden_1823
Pden_1835	TTGATCCGTGTCAA	14	hypothetical protein	<-	65...153	Pden_1836
Pden_1844	TTGATCTGCGTCAA	14	4Felectron4S binding domain-containing protein	<-	54...209	Pden_1845
Pden_1848	TTGATCTGCGTCAA	14	cbb3-type cytochrome c oxidase subunit I	<-	108...130	Pden_1849
Pden_1850	TTGATTTGGGTCAA	14	fnrR transcriptional regulator	<-	115...35	Pden_1851
Pden_1934	TTGTACTAGATCAA	14	translation initiation factor 2, gamma subunit, GTPase	<-	45...215	Pden_R0036
Pden_2009	TTGTTGTGTCGCAA	14	sulfotransferase	<-	11...53	Pden_2010
Pden_2010	TTGTTAAGCGGCAA	14	rimO,ribosomal protein S12 methylthiotransferase	<-	20...65	Pden_2011
Pden_2254	TTGCCGATGACCAA	14	moaA,molybdenum cofactor biosynthesis protein A	<-	119...-7	Pden_2255
Pden_2283	TTGCGGAAAGCCAA	14	hypothetical protein	<-	95...213	Pden_R0047
Pden_2285	TTGAAACGACCCAA	14	ABC-type glycine betaine transport system	->	1...-13	Pden_2286
Pden_2422	TTGTGCGCCTCCAA	14	hypothetical protein	<-	2144...140	Pden_2424

Table continues

Gene	Sequence	nt	Annotation		Distance	Next Gene
Pden_2484	TTGATGAAAGTCAA	14	nitric-oxide reductase	<-	65...-3	Pden_2485
Pden_2564	TTGCCGCCAGCCAA	14	entF,enterobactin synthase subunit F	->	184...23	Pden_2565
Pden_2614	TTGCGACAAGGCAA	14	5,10-methylenelectrontetrahydrofolate dehydrogenase	<-	186...35	Pden_2615
Pden_2643	TTGCCGACCAGCAA	14	hypothetical protein	->	22...386	Pden_2644
Pden_2742	TTGACCAATGCCAA	14	hypothetical protein	<-	32...297	Pden_2743
Pden_2742	TTGAGGCACGGCAA	14	hypothetical protein	<-	252...77	Pden_2743
Pden_2852	TTGCTTCGCACCAA	14	phosphoenolpyruvate carboxykinase	->	50...97	Pden_2853
Pden_2973	TTGGTTGCAGACAA	14	helicase domain-containing protein	->	433...1451	Pden_2975
Pden_2992	TTGGTATGGAACAA	14	hypothetical protein	<-	88...248	Pden_2993
Pden_3048	TTGCCGTCGGGCAA	14	hypothetical protein	->	408...493	Pden_3049
Pden_3072	TTGTCTGCGATCAA	14	GntR family transcriptional regulator	<-	77...-3	Pden_3073
Pden_3112	TTGGCTGCTTTCAA	14	hydrogenase expression/formation protein HypE	->	168...46	Pden_3113
Pden_3115	TTGCCTCGCGTCAA	14	hypothetical protein	<-	590...175	Pden_3116
Pden_3214	TTGCTCAGCGGCAA	14	hypothetical protein	->	13...105	Pden_3215

Table continues

Gene	Sequence	nt	Annotation		Distance	Next Gene
Pden_3248	TTGTAGGCACGCAA	14	regulatory proteins, IclR	<-	433...129	Pden_3249
Pden_3258	TTGTTTTCCTGCAA	14	TRAP dicarboxylate transporter- DctP subunit	->	308...95	Pden_3259
Pden_3265	TTGGGCGGCTGCAA	14	ABC-type nitrate/sulfonate/bicarbonate transport	<-	194...210	Pden_3266
Pden_3370	TTGAATCCGAACAA	14	putative replication protein A	->	116...127	Pden_3371
Pden_3388	TTGTTTGCATGCAA	14	SAF domain-containing protein	<-	180...88	Pden_3389
Pden_3389	TTGCAAGGCTTCAA	14	GntR family transcriptional regulator	->	80...162	Pden_3390
Pden_3392	TTGAGACCTCTCAA	14	hypothetical protein	<-	28...21	Pden_3393
Pden_3407	TTGAACTAGGACAA	14	ABC transporter related	->	-8...380	Pden_3408
Pden_3559	TTGAGTTGACCCAA	14	putative transport transmembrane protein	->	5...874	Pden_3561
Pden_3592	TTGGGACCTCTCAA	14	addiction module antitoxin	->	123...72	Pden_3593
Pden_3636	TTGATCTGGATCAA	14	OmpW family protein	<-	35...75	Pden_3637
Pden_3695	TTGTCAATTTGCAA	14	GCN5-related N-acetyltransferase	<-	116...67	Pden_3696
Pden_3709	TTGCAATGTGACAA	14	hypothetical protein	<-	36...15	Pden_3710
Pden_3783	TTGAGCATGCTCAA	14	hypothetical protein	<-	84...436	Pden_3784

Table continues

Gene	Sequence	nt	Annotation		Distance	Next Gene
Pden_3911	TTGCCTTGGATCAA	14	hypothetical protein	<-	367...13	Pden_3912
Pden_3921	TTGCTCTTTTCCAA	14	Serinelectron-glyoxylate transaminase	<-	118...54	Pden_3922
Pden_3923	TTGACTGGCGGCAA	14	hypothetical protein	->	43...33	Pden_3924
Pden_4094	TTGCGGGGCAGCAA	14	hypothetical protein	<-	36...260	Pden_4095
Pden_4100	TTGCCCGGTGACAA	14	hypothetical protein	->	208...82	Pden_4101
Pden_4105	TTGATAGGGATCAA	14	hypothetical protein	<-	56...101	Pden_4106
Pden_4221	TTGACTTAGGTCAA	14	hypothetical protein	<-	135...189	Pden_4222
Pden_4221	TTGACAATTCTCAA	14	hypothetical protein	<-	250...74	Pden_4222
Pden_4222	TTGCGCCATGGCAA	14	pseudoazurin	->	94...52	Pden_4223
Pden_4226	TTGACGAATATCAA	14	UbiD family decarboxylase	<-	73...35	Pden_4227
Pden_4237	TTGATCTGGATCAA	14	nitrite transporter	<-	72...189	Pden_4238
Pden_4237	TTGACTTAAATCAA	14	nitrite transporter	<-	208...53	Pden_4238
Pden_4303	TTGTCCTCTGGCAA	14	rpsD,30S ribosomal protein S4	<-	35...151	Pden_4304
Pden_4421	TTGATCTGGATCAA	14	phosphonate metabolism protein PhnM	->	36...55	Pden_4422

Table continues

Gene	Sequence	nt	Annotation		Distance	Next Gene
Pden_4459	TTGCCATTCACCAA	14	hypothetical protein	<-	-13...660	Pden_4460
Pden_4478	TTGCAGAAATGCAA	14	LysR family transcriptional regulator	<-	12...85	Pden_4479
Pden_4607	TTGACCGGCAGCAA	14	uracil-DNA glycosylase superfamily protein	->	47...13	Pden_4608
Pden_4648	TTGGCCCGGTCCAA	14	hypothetical protein	->	32...277	Pden_4649
Pden_4657	TTGTCGCGCGCCAA	14	two component, sigma54 specific, Fis l regulator	->	103...50	Pden_4658
Pden_4681	TTGAAGGAAGGCAA	14	TetR family transcriptional regulator	->	-3...822	Pden_4682
Pden_4684	TTGTCATGATCCAA	14	3-oxoacid CoA-transferase, B subunit	->	297...147	Pden_4685
Pden_4811	TTGAGGATGCGCAA	14	beta-ketoadipyl CoA thiolase	<-	117...16	Pden_4812
Pden_4883	TTGCCTTGCCGCAA	14	ABC transporter related	<-	97…91	Pden_4884
Pden_4921	TTGCGGAGGACCAA	14	alpha/beta hydrolase fold	<-	12...62	Pden_4922
Pden_4940	TTGTTGACAGACAA	14	histidine utilization repressor	<-	169...97	Pden_4941
Pden_5013	TTGTCAAAGACCAA	14	alkanesulfonate monooxygenase	<-	14...-10	Pden_5014
Pden_5033	TTGCCAATTGGCAA	14	BioY protein	->	296...6	Pden_5034
Pden_5036	TTGCCAATTGGCAA	14	parB-like partition proteins	->	6...158	Pden_5037

Table continues

Gene	Sequence	nt	Annotation		Distance	Next Gene
Pden_5086	TTGTCATGTCGCAA	14	3-hydroxybutyryl-CoA dehydrogenase	<-	-6...133	Pden_5087
Pden_5103	TTGATTCAAGTCAA	14	poly-β-hydroxybutyrate polymerase protein	<-	132...50	Pden_5104
Pden_5108	TTGATCTAGGTCAA	14	ubiquinol oxidase, subunit II	<-	79...130	Pden_5109
Pden_R0014	TTGGGGGACAGCAA	14	tRNA-Pro	->	224...511	Pden_0862
Pden_R0017	TTGATTTTACTCAA	14	tRNA-Ser	->	17...-3	Pden_0961

End of table

2.4 Gene expression datasets

2.4.1 Gene expression dataset of putative *fnr* regulated genes having a TTG-N8-CAA motif upstream.

Georgios Giannopoulos

Relative gene expression (Ratio) of aerobic and anaerobic cultures of *P. denitrificans*
Gene list based on TTG-N8-CAA (FNR-BOX) pattern upstream
20140129_wt_Aero_Anaero

Gene ID	Anaerobic Average	Aerobic Average	Ratio -O2 / +O2	Product
Pden_5108	1.43	0.31	4.68	qoxA hypothetical protein
Pden_5103	3.71	1.20	3.10	phbC1 poly-beta-hydroxybutyrate polymerase
Pden_5086	0.93	0.78	1.19	hypothetical protein
Pden_5036	1.57	2.46	0.64	parB-like partition proteins
Pden_5033	2.34	1.94	1.21	hypothetical protein
Pden_5013	0.37	0.35	1.06	alkanesulfonate monooxygenase
Pden_4940	0.63	0.67	0.95	histidine utilization repressor
Pden_4921	1.97	1.42	1.39	alpha/beta hydrolase
Pden_4883	0.58	0.44	1.31	ABC transporter related
Pden_4811	3.96	2.43	1.63	beta-ketoadipyl CoA thiolase
Pden_4684	4.53	6.96	0.65	3-oxoacid CoA-transferase subunit B
Pden_4681	0.56	0.56	1.01	TetR family transcriptional regulator
Pden_4657	0.95	1.10	0.87	two comp. σ54 specific Fis family regulator
Pden_4648	0.84	0.55	1.54	hypothetical protein
Pden_4607	0.48	0.36	1.33	uracil-DNA glycosylase
Pden_4478	1.53	1.55	0.99	LysR family transcriptional regulator
Pden_4459	0.54	0.93	0.59	hypothetical protein
Pden_4421	1.59	1.63	0.98	phosphonate metabolism protein PhnM
Pden_4303	15.76	33.94	0.46	30S ribosomal protein S4
Pden_4237	7.57	0.89	8.55	narK nitrite transporter
Pden_4226	11.72	0.36	32.81	UbiD UbiD family decarboxylase
Pden_4222	53.78	0.98	54.78	pasZ hypothetical protein
Pden_4221	13.50	0.79	17.19	nosC hypothetical protein
Pden_4105	11.83	0.37	32.37	hyp. protein downstream of sulfonate citryl-CoA lyase
Pden_4100	7.04	8.98	0.78	hypothetical protein

Pden_4094	0.42	0.21	2.01	hypothetical protein
Pden_3923	0.97	0.70	1.39	hypothetical protein
Pden_3921	2.74	0.90	3.06	serine-glyoxylate transaminase
Pden_3911	1.26	1.61	0.78	hypothetical protein
Pden_3783	1.51	0.69	2.20	hypothetical protein
Pden_3709	1.69	1.88	0.90	hypothetical protein
Pden_3695	3.62	3.66	0.99	N-acetyltransferase GCN5
Pden_3636	12.61	0.94	13.36	ompW
Pden_3592	8.01	7.79	1.03	addiction module antitoxin
Pden_3559	1.38	1.19	1.16	
Pden_3407	0.77	1.07	0.72	ABC transporter
Pden_3392	0.63	0.51	1.23	hypothetical protein
Pden_3389	0.37	0.54	0.68	GntR family transcriptional regulator
Pden_3388	0.41	0.30	1.39	SAF domain-containing protein
Pden_3370	0.40	0.28	1.45	replication protein A
Pden_3265	0.19	0.19	0.99	hypothetical protein
Pden_3258	0.29	0.44	0.66	hypothetical protein
Pden_3248	0.69	1.02	0.67	regulatory proteins IclR
Pden_3214	0.32	0.45	0.71	hypothetical protein
Pden_3115	1.16	0.81	1.43	hypothetical protein
Pden_3112	0.85	0.68	1.25	hydrogenase expression/formation protein HypE
Pden_3072	0.68	0.85	0.79	GntR family transcriptional regulator
Pden_3048	0.43	0.38	1.13	hypothetical protein
Pden_2992	6.84	3.97	1.72	hypothetical protein
Pden_2973	0.18	0.23	0.80	
Pden_2852	6.29	8.47	0.74	phosphoenolpyruvate carboxykinase
Pden_2742	2.51	7.93	0.32	hypothetical protein
Pden_2643	0.16	0.44	0.37	hypothetical protein
Pden_2614	1.22	1.62	0.75	5-10-methylene-tetrahydrofolate dh
Pden_2564	1.16	1.28	0.91	enterobactin synthase subunit F
Pden_2484	44.60	2.95	15.11	norC nitric-oxide reductase
Pden_2422	0.31	0.60	0.52	
Pden_2285	3.28	5.14	0.64	ABC-type glycine betaine transport system

Pden_2283	0.24	0.32	0.74	hypothetical protein
Pden_2254	2.19	2.82	0.78	molybdenum cofactor biosynthesis protein A
Pden_2010	1.14	1.72	0.66	30S ribosomal protein S12 methylthiotransferase
Pden_2009	0.79	1.82	0.43	sulfotransferase
Pden_1934	0.88	0.65	1.35	translation initiation factor 2 subunit gamma GTPase
Pden_1850	10.01	6.63	1.51	Crp/Fnr family transcriptional regulator
Pden_1848	12.66	2.00	6.35	cooN cbb3-type cytochrome c oxidase subunit I
Pden_1844	6.51	1.07	6.09	ccoG 4Fe-4S ferredoxin
Pden_1835	10.86	0.87	12.53	hypothetical protein downstream of DNA topoisomerase
Pden_1822	27.81	17.74	1.57	5-aminolevulinate synthase
Pden_1796	0.74	1.36	0.54	N-acetyltransferase
Pden_1789	1.15	2.12	0.54	surface presentation of antigens (SPOA) protein
Pden_1729	3.55	5.26	0.68	alanine dehydrogenase
Pden_1653	6.09	5.10	1.19	lytic murein transglycosylase
Pden_1621	0.11	0.18	0.64	hypothetical protein
Pden_1616	0.14	0.15	0.98	
Pden_1548	0.70	0.89	0.79	HipA domain-containing protein
Pden_1486	0.07	0.09	0.84	TonB-dependent receptor
Pden_1457	0.14	0.22	0.64	alpha/beta hydrolase
Pden_1395	6.76	5.81	1.16	class V aminotransferase
Pden_1376	8.41	10.49	0.80	lipoyl synthase
Pden_1356	0.13	0.13	1.07	
Pden_1345	0.28	0.16	1.80	
Pden_1339	0.27	0.25	1.09	hypothetical protein
Pden_1247	4.29	4.38	0.98	glutathionylspermidine synthase
Pden_1201	0.49	0.42	1.17	hypothetical protein
Pden_1197	0.76	0.94	0.81	NADH:flavin oxidoreductase
Pden_1052	4.25	6.42	0.66	
Pden_1010	0.44	0.50	0.88	sulfoacetaldehyde acetyltransferase
Pden_0924	1.82	2.94	0.62	OsmC family protein
Pden_0915	0.91	1.08	0.85	entericidin A/B
Pden_0821	1.06	0.94	1.12	hypothetical protein
Pden_0744	20.74	22.94	0.90	50S ribosomal protein L1

Pden_0673	1.15	0.88	1.31	regulatory protein LacI
Pden_0647	3.94	5.89	0.67	peptide deformylase
Pden_0614	2.61	3.29	0.79	S-adenosylmethionine-tRNA ribosyltransferase-isomerase
Pden_0592	2.12	3.48	0.61	inosine-5'-monophosphate dehydrogenase
Pden_0572	4.58	9.64	0.48	sdhB succinate dehydrogenase iron-sulfur subunit
Pden_0566	1.74	2.49	0.70	dehydratase
Pden_0532	3.75	4.74	0.79	UspA domain-containing protein
Pden_0477	0.34	0.36	0.97	XRE family transcriptional regulator
Pden_0476	0.31	0.29	1.07	thioesterase
Pden_0451	0.29	0.93	0.31	hypothetical protein
Pden_0384	1.77	1.70	1.04	hypothetical protein
Pden_0336	0.44	0.33	1.34	hypothetical protein
Pden_0302	0.61	0.85	0.72	LysR family transcriptional regulator
Pden_0278	0.22	0.19	1.17	major facilitator superfamily transporter
Pden_0174	0.60	0.71	0.84	maleylacetoacetate isomerase
Pden_0132	0.30	0.23	1.33	replication protein A
Pden_0101	0.21	0.36	0.58	hypothetical protein
Pden_0061	2.13	1.81	1.18	hypothetical protein

2.4.2 Volcano enrichment expression dataset

Georgios Giannopoulos

Volcano enrichment
Microarray expression in aerobic and anaerobic cultures of *P. denitrificans*

Gene ID	WT Aerobic Average	SE Norm	WT Anaerobic Average	SE Norm	Annotation	Ratio -O2/+O2
Pden_0338	0.20	0.02	0.84	0.32		4.28
Pden_0409	0.38	0.10	1.76	0.71		4.58
Pden_0893	1.03	0.09	14.92	3.96		14.43
Pden_1180	0.92	0.30	19.06	13.92	*benD*	20.73
Pden_1204	0.21	0.04	0.99	0.26		4.63
Pden_1350	0.86	0.18	3.74	2.55		4.33
Pden_1352	0.32	0.08	1.56	0.90		4.91
Pden_1664	0.71	0.10	3.33	1.40		4.68
Pden_1689	0.40	0.05	2.60	1.35	*nodA*	6.53
Pden_1835	0.88	0.11	11.09	3.27		12.62
Pden_1842	1.38	0.20	5.54	0.37		4.01
Pden_1844	1.11	0.10	7.16	1.22		6.47
Pden_1845	4.15	0.64	23.15	2.63		5.58
Pden_1846	2.95	0.99	21.05	6.85		7.14
Pden_1847	2.32	0.30	14.19	1.92	*ccoO*	6.10
Pden_1848	2.13	0.32	15.33	2.89	*ccoN*	7.20
Pden_1849	8.99	2.12	71.05	31.33	*uspA*	7.91
Pden_1851	1.33	0.16	30.78	10.96		23.15
Pden_2068	0.26	0.03	2.76	3.42		10.53
Pden_2278	0.55	0.36	2.85	1.04		5.14
Pden_2387	0.30	0.05	1.34	1.05		4.47
Pden_2406	0.26	0.06	1.09	0.28		4.14
Pden_2408	0.40	0.03	2.14	0.33		5.32
Pden_2409	0.33	0.04	2.82	0.78		8.64
Pden_2410	0.35	0.04	3.54	0.86		10.17
Pden_2411	0.44	0.07	6.53	1.76		14.72
Pden_2412	0.42	0.05	6.48	2.52		15.32
Pden_2413	0.46	0.03	5.97	1.56		12.90
Pden_2414	1.73	0.24	76.90	24.81	*nosX*	44.45
Pden_2415	1.62	0.46	44.22	19.65	*nosL*	27.31
Pden_2480	1.96	0.55	7.96	1.14	*norE*	4.07
Pden_2481	3.76	1.12	22.44	2.78	*norD*	5.97
Pden_2482	5.50	1.39	44.12	5.58	*norQ*	8.02
Pden_2483	3.14	0.45	31.60	3.17	*norB*	10.05
Pden_2484	3.18	0.54	53.98	12.23	*norC*	16.96
Pden_2485	0.31	0.04	3.45	0.31	*nirX*	11.07
Pden_2486	0.27	0.04	3.28	0.29	*nirI*	12.07
Pden_2487	0.25	0.06	43.98	4.40	*nirS*	172.88
Pden_2488	0.23	0.05	6.61	0.80	*nirE*	28.73
Pden_2489	0.29	0.07	5.23	1.21	*nirC*	17.85
Pden_2490	0.51	0.14	6.29	0.93	*nirF*	12.40
Pden_2491	0.23	0.04	5.59	0.60	*nirD*	24.78

Pden_2492	0.59	0.14	4.33	0.62	*nirG*	7.29
Pden_2493	0.15	0.05	2.59	0.31	*nirH*	16.90
Pden_2494	0.36	0.04	4.05	0.59	*nirJ*	11.23
Pden_2495	0.58	0.07	2.63	0.17	*nirN*	4.55
Pden_2611	0.77	0.13	3.69	1.64		4.77
Pden_2910	1.20	0.24	5.22	3.61		4.35
Pden_2944	12.56	1.49	2.49	2.05		0.20
Pden_2982	0.32	0.04	1.41	0.91		4.45
Pden_2993	4.02	1.79	22.05	8.24		5.49
Pden_2994	2.39	1.00	11.01	3.33		4.60
Pden_2995	2.23	1.44	10.87	2.37		4.88
Pden_2996	6.34	3.61	32.31	7.95		5.10
Pden_3011	0.61	0.13	2.83	1.78		4.65
Pden_3023	0.86	0.18	4.94	3.12		5.76
Pden_3024	1.18	0.26	7.45	3.12		6.34
Pden_3025	1.28	0.37	14.30	7.09		11.18
Pden_3026	0.95	0.20	11.26	6.05		11.81
Pden_3027	0.63	0.08	4.76	2.30		7.62
Pden_3339	0.55	0.14	5.04	5.74		9.19
Pden_3383	0.65	0.12	5.67	7.36		8.77
Pden_3430	0.49	0.11	2.57	2.56		5.20
Pden_3454	2.15	0.28	0.54	0.13	*LysR*	0.25
Pden_3490	1.57	0.34	6.92	6.85		4.42
Pden_3534	0.70	0.13	4.45	2.27		6.36
Pden_3636	1.00	0.12	17.88	3.60		17.95
Pden_3834	1.83	1.00	0.30	0.07		0.16
Pden_4105	0.37	0.04	10.05	7.06		27.29
Pden_4120	19.84	3.82	4.13	0.91		0.21
Pden_4121	26.93	8.39	4.94	1.49		0.18
Pden_4161	0.42	0.06	3.62	2.38		8.65
Pden_4167	0.28	0.03	1.22	0.29		4.42
Pden_4169	0.32	0.06	3.82	2.42		11.91
Pden_4173	0.64	0.18	4.06	1.75		6.37
Pden_4214	1.04	0.29	7.64	1.15	*nosX*	7.37
Pden_4215	0.44	0.09	6.27	0.63	*nosL*	14.34
Pden_4216	0.61	0.09	8.13	0.96	*nosY*	13.23
Pden_4217	0.58	0.09	6.79	1.07	*nosF*	11.75
Pden_4218	0.98	0.20	18.76	7.68	*nosD*	19.14
Pden_4219	1.26	0.51	34.83	3.92	*nosZ*	27.64
Pden_4220	0.44	0.09	10.29	2.07	*nosR*	23.48
Pden_4221	0.78	0.17	14.24	4.76	*nosC*	18.37
Pden_4222	1.00	0.27	57.53	32.93	*pasZ*	57.64
Pden_4223	2.85	0.59	11.84	3.46		4.16
Pden_4224	0.58	0.08	30.57	7.51		53.03
Pden_4225	0.33	0.07	8.58	1.76		25.84
Pden_4226	0.36	0.06	11.62	4.36	*UbiD*	32.42
Pden_4227	0.33	0.04	12.74	3.47		38.66
Pden_4228	0.36	0.06	11.48	3.32		32.05
Pden_4229	0.78	0.15	13.26	3.56		16.91
Pden_4230	0.67	0.09	7.26	1.18	*nnrS*	10.86

Pden_4231	2.18	0.68	18.36	2.82		8.43
Pden_4232	3.41	0.91	26.13	4.56		7.66
Pden_4233	2.43	0.33	17.73	2.35	*narG*	7.30
Pden_4234	3.35	0.47	34.54	4.14	*narJ*	10.30
Pden_4235	2.05	0.20	17.74	1.61	*narH*	8.64
Pden_4236	1.88	0.23	18.22	1.53	*narI*	9.70
Pden_4237	0.91	0.05	7.77	0.97	*narK*	8.57
Pden_4741	1.02	0.16	6.66	4.73		6.51
Pden_5106	0.23	0.05	1.04	0.16	*qoxC*	4.48
Pden_5107	0.28	0.09	1.18	0.18	*qoxB*	4.17
Pden_5108	0.29	0.05	1.22	0.51	*qoxA*	4.18
Pden_5109	0.92	0.09	5.44	0.75	*mfs_1*	5.92

2.4.3 Microarray expression dataset

Note: The microarray dataset is enclosed in the CD-ROM attached

References

Baumann, B., J. R. Van Der Meer, M. Snozzi and A. J. B. Zehnder (1997). "Inhibition of denitrification activity but not of mRNA induction in *Paracoccus dentrificans* by nitrite at a suboptimal pH." Antonie van Leeuwenhoek, International Journal of General and Molecular Microbiology **72**(3): 183-189.

Bouchal, P., I. Struhárová, E. Budinská, O. Šedo, T. Vyhlídalová, Z. Zdráhal, R. van Spanning and I. Kučera (2010). "Unraveling an FNR based regulatory circuit in *Paracoccus denitrificans* using a proteomics-based approach." Biochimica et Biophysica Acta - Proteins and Proteomics **1804**(6): 1350-1358.

Crack, J. C., A. J. Jervis, A. A. Gaskell, G. F. White, J. Green, A. J. Thomson and N. E. Le Brun (2008). "Signal perception by FNR: the role of the iron-sulfur cluster." Biochem Soc Trans **36**(Pt 6): 1144-1148.

Dadák, V., J. Dudák and P. Zbořil (2009). "Electron transfer in *Paracoccus denitrificans* with the modified *fbc* operon." Folia Microbiologica **54**(6): 475-482.

de Gier, J. W. L., M. Lubben, W. N. M. Reijnders, C. A. Tipker, D. J. Slotboom, R. J. M. van Spanning, A. H. Stouthamer and J. van der Oost (1994). "The terminal oxidases of *Paracoccus denitrificans*." Molecular Microbiology **13**(2): 183-196.

Dufour, Y. S., P. J. Kiley and T. J. Donohue (2010). "Reconstruction of the Core and Extended Regulons of Global Transcription Factors." Plos Genetics **6**(7).

Felgate, H., G. Giannopoulos, M. J. Sullivan, A. J. Gates, T. A. Clarke, E. Baggs, G. Rowley and D. J. Richardson (2012). "The impact of copper, nitrate and carbon status on the emission of nitrous oxide by two species of bacteria with biochemically distinct denitrification pathways." Environ Microbiol **14**(7): 1788-1800.

Hartop, K. (2004). The impact of nitrite on aerobic growth of *Paracoccus denitrificans* PD1222. PhD, University of East Anglia.

Hoeren, F. U., B. C. Berks, S. J. Ferguson and J. E. G. McCarthy (1993). "Sequence and expression of the gene encoding the respiratory nitrous-oxide reductase from Paracoccus denitrificans." European Journal of Biochemistry **218**(1): 49-57.

Hutchings, M. I. and S. Spiro (2000). "The nitric oxide regulated nor promoter of *Paracoccus denitrificans*." Microbiology **146**(10): 2635-2641.

Jervis, A. J., J. C. Crack, G. White, P. J. Artymiuk, M. R. Cheesman, A. J. Thomson, N. E. Le Brun and J. Green (2009). "The O_2 sensitivity of the transcription factor FNR is controlled by Ser24 modulating the kinetics of [4Fe-4S] to [2Fe-2S] conversion." Proceedings of the National Academy of Sciences **106**(12): 4659-4664.

Meijer, E. M., J. W. Van Der Zwaan, A. H. Stouthamer and R. Wever (1979). "Anaerobic Respiration and Energy Conservation in *Paracoccus denitrficans*." European Journal of Biochemistry **96**(1): 69-76.

Richardson, D. J. (2008). Structural and functional flexibilty of bacterial respirome. Bacterial Physiology: A molecular approach. W. El-Sharoud. Berlin Heidelberg, Springer-Verlag**:** 97-128.

Richardson, D. J. and N. J. Watmough (1999). "Inorganic nitrogen metabolism in bacteria." Current Opinion in Chemical Biology **3**(2): 207-219.

Rodionov, D. A., I. L. Dubchak, A. P. Arkin, E. J. Alm and M. S. Gelfand (2005). "Dissimilatory metabolism of nitrogen oxides in bacteria: Comparative reconstruction of transcriptional networks." PLoS Comput Biol **1**(5): e55.

Romanowski, K., A. Zaborin, H. Fernandez, V. Poroyko, V. Valuckaite, S. Gerdes, D. Liu, O. Zaborina and J. Alverdy (2011). "Prevention of siderophore- mediated gut-derived sepsis due to P. aeruginosa can be achieved without iron provision by maintaining local phosphate abundance: role of pH." BMC Microbiology **11**(1): 212.

Schoen, E. D., J. C. Jager and H. W. van Verseveld A. H. Stouthamer (1985). "Statistical analysis of growth limitations in *Paracoccus denitrificans*: An experiment with a completely randomized two-way factorial design with replications." Antonie van Leeuwenhoek **51**(1985): 11-24.

Spiro, S. (1992). "An FNR-dependent promoter from *Escherichia coli* is active and anaerobically inducible in *Paracoccus denitrificans*." FEMS Microbiology Letters **98**(1-3): 145-148.

Spiro, S. (2007). "Regulators of bacterial responses to nitric oxide." FEMS Microbiology Reviews **31**(2): 193-211.

Spiro, S. (2012). "Nitrous oxide production and consumption: regulation of gene expression by gas-sensitive transcription factors." Philos Trans R Soc Lond B Biol Sci **367**(1593): 1213-1225.

Spiro, S. and J. R. Guest (1990). "FNR and its role in oxygen-regulated gene expression in *Escherichia coli*." FEMS Microbiology Letters **75**(4): 399-428.

van Spanning, R. J. M., A. P. N. de Boer, W. N. M. Reijnders, H. V. Westerhoff, A. H. Stouthamer and J. van der Oost (1997). "FnrP and NNR of *Paracoccus denitrificans* are both members of the FNR family of transcriptional activators but have distinct roles in respiratory adaptation in response to oxygen limitation." Molecular Microbiology **23**(5): 893-907.

Van Spanning, R. J. M., E. Houben, W. N. M. Reijnders, S. Spiro, H. V. Westerhoff and N. Saunders (1999). "Nitric oxide is a signal for NNR-mediated transcription activation in *Paracoccus denitrificans*." Journal of Bacteriology **181**(13): 4129-4132.

Verseveld, H. W., J. P. Boon and A. H. Stouthamer (1979). "Growth yields and the efficiency of oxidative phosphorylation of *Paracoccus denitrificans* during two- (carbon) substrate-limited growth." Archives of Microbiology **121**(3): 213-223.

Verseveld, H. W., E. M. Meijer and A. H. Stouthamer (1977). "Energy conservation during nitrate respiration in *Paracoccus denitrificans*." Archives of Microbiology **112**(1): 17-23.

Wood, N. J., T. Alizadeh, S. Bennett, J. Pearce, S. J. Ferguson, D. J. Richardson and J. W. Moir (2001). "Maximal expression of membrane-bound nitrate reductase in *Paracoccus* is induced by nitrate via a third FNR-like regulator named NarR." J Bacteriol **183**(12): 3606-3613.

Zumft, W. G. (2002). "Nitric Oxide Signaling and NO Dependent Transcriptional Control in Bacterial Denitrification by Members of the FNR-CRP Regulator Family." Journal of Molecular Microbiology and Biotechnology **4**(3): 277-286.

The regulation of denitrification in *P. denitrificans*

3. The metabolic and transcriptional profiles of the fnrP and nnrR mutants of P. denitrificans in anaerobic CSTR cultures.

Evidence for a novel role of the transcriptional activators *fnrP* and *nnrR* of *P. denitrificans*; a whole genome approach in continuous culture systems.

Contents

3.1 Introduction

Previously, in Chapter 2 the aerobic and anaerobic metabolic and transcriptional profiles were established in continuous cultures using continuous stirred tank reactors (CSTR) applying high through-put metabolic and transcriptional analysis. Continuous cultures of *P. denitrificans* (PD1222) oxidised 5 mM succinate in both aerobic and anaerobic treatment. Further metabolic analysis revealed that the concentration of nitrite and nitrous oxide in both cultures was ~0 mM. Extracellular nitrate concentration remained ~20 mM through the aerobic incubation, however, during the anaerobic incubation the nitrate concentration decreased from an initial concentration of 20 to a steady state concentration of ~15 mM. Based on this observation, it has been suggested that *P. denitrificans* reduced 5 mM nitrate to di-nitrogen in the anaerobic treatment. The comparison of the gene expression profiles of the aerobic and anaerobic growth treatments revealed 204 genes with significant changes (Volcano filter; relative expression ≥2 fold, $p \leq 0.05$). A motif search performed in the upstream regions (200 bp) of the highly regulated genes indicated sequence logos with cognate sites of CRP/FNR family transcriptional factor (TF) binding. The amino-acid sequence of TF FnrP (*fnrP*; pden_1850) was blast compared against the genome of *P. denitrificans* and revealed an additional gene with close sequence similarity. This protein is the TF NnrR (*nnrR*; pden_2478) with 85% (*E*= 2e-05) similarity. In this chapter, using the well-established CSTR, mutants lacking a functional copy of *fnrP* and *nnrR* were analysed for their metabolic and transcriptional profile in anaerobicity. This holistic approach allowed us to decode the putative network of regulation of the aforementioned TF.

The TF FnrP (encoded by *fnrP,* pden_1850) belongs to the CRP/FNR family with a binding site motif of TTGAC-N4-GTCAA.The *fnrP* acts as an activator in *cis*-regulation when an active dimer of FNR is formed under anaerobic conditions (see 1. Introduction). It has been shown by de Gier *et al.* (1994) that FnrP activates the expression of the *cco* operon (cbb_3 oxidase) binding at the TTGATctgcGTCAA box found upstream of *ccoN* (pden_1848). Interestingly, upstream of *fnrP*, a TTGATttggGTCAA box exists indicating self-regulation of FnrP (pden_1850) or of the neighbouring gene expressing a putative coproporphyrinogen III oxidase (*hemN*; pden_1851) that is involved in heme synthesis. Binding sites similar to the consensus of FNR are also found upstream of the nitrate/nitrite transporter gene *narK*

(pden_4237); TTGATctggATCAA and TTGACttaaATCAA. It was also shown that the cytochrome *c* peroxidase gene *ccpA* (pden_0893) could be under FNR regulation as it was highly induced in the anaerobic treatment. Upstream of *ccpA* there are two putative FNR binding sites with motifs TTcAacggccggCAA and caaTTagCcgctgctTCAA.

It has been also demonstrated that *nirS* (pden_2487) which encodes nitrite reductase is under the regulation of NnrR (expressed by *nnrR*, pden_2478) which is highly similar to FnrP. TF *nnrR* activates both nitrite reductase (*nirI, nirS*; pden_2486, pden_2487; Saunders *et al.* (2000)) and nitric oxide reductase (*norCB*; pden_2483 and pden_2484; Hutchings and Spiro (2000)). However the promoter binding sites are different to each other; TTAACaaagGTCAA and TTGATgaaaGTCAA for *nirS* and *norC* respectively. The latter motif is closely related to those under the regulation of FNR. This could indicate that in the absence of a TF (eg NnrR), others (eg FnrP) may substitute the regulation of a gene either as an activator or repressor.

To conclude, the regulatory network of anaerobic nitrate respiration in *P. denitrificans* could be exemplified as follows (Figure 1). FNR is a typical CRP/FNR family regulatory protein that upon oxygen depletion dimerises forming an oxygen sensitive [4Fe-4S] cluster (Jervis *et al.* 2009). During this phenomenon FNR has increased affinity for DNA. It has also been documented that the [4Fe-4S] cluster may react with NO, however the product or the mode of action of the FNR-NO ligand is still unknown. NO reacts anaerobically with the Fe–S cluster of purified FNR, generating spectral changes consistent with formation of a dinitrosyl-iron–cysteine complex. In vitro experiments incubating purified Fnr (*E.coli*) with NO showed a mixture of monomeric and dimeric dinitrosyl-iron–cysteine complexes. The NO-treated Fnr remained native and could be reconstituted (Cruz-Ramos *et al.* 2002, Crack *et al.* 2013). This interaction may indicate new roles of a molecular NO switch in Fnr-regulated genes. It is speculated that NO disables the DNA binding capacity of FNR (Crack *et al.* 2008).

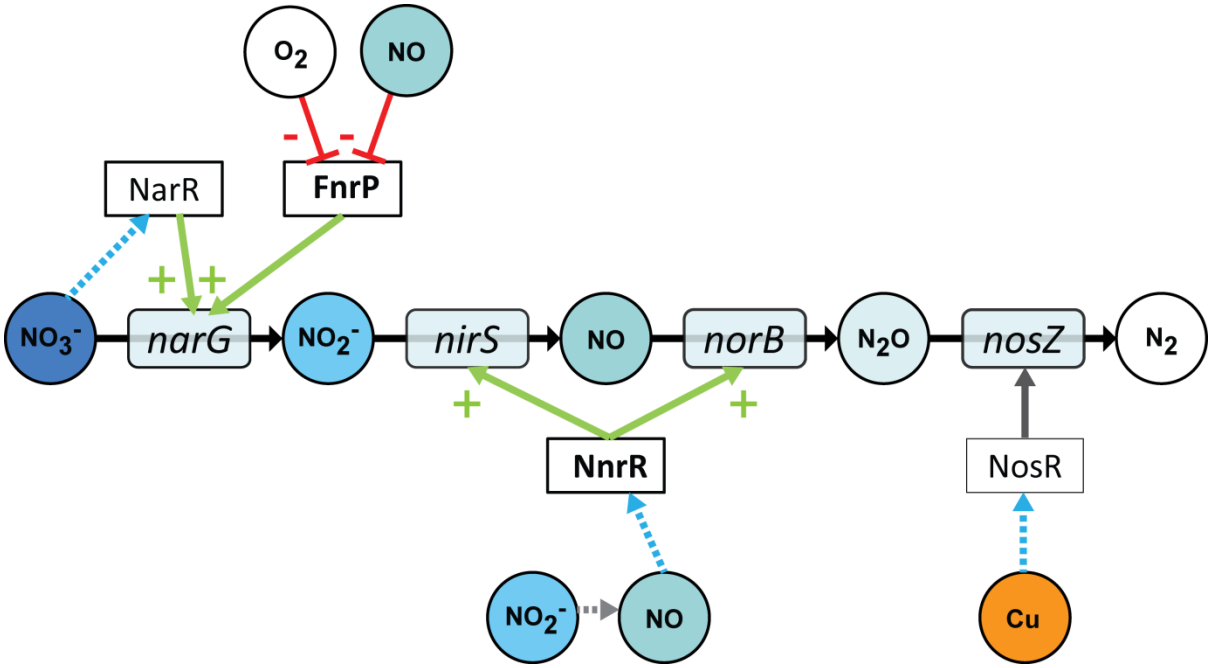

Figure 1 Simplified illustration of the regulatory network controlling expression of denitrification genes in *P. denitrificans.* The solid arrows represent positive activating events between the transcription factor (TF) and the target gene. Dashed arrows indicate positive signalling between the metabolites and the TF. The lines with a bar end indicate inhibition events between the TF and the signal metabolite. The TF and subsequently the regulatory proteins are boxed by clear layers; those are the FNR (Fumarate and Nitrate Regulatory), NNR (Nitrite and Nitric Oxide Regulatory), NarR (Nitrate reductase Regulatory) and NosR (Nitrous oxide reductase Regulatory protein). The target genes are boxed by a shaded layer; those are the membrane nitrate reductase *narG* (pden_4233), the nitrite reductase *nirS* (pden_2487), the nitric oxide reductase *norB* (pden_2483) and the nitrous oxide reductase *nosZ* (pden_4219). The metabolites are represented in circles.

Two other regulatory proteins involved in nitrate respiration are the NnrR and NarR, which are also members of the wider CRP/FNR family. NnrR is postulated to sense nitric oxide via a heme interaction and NarR to sense nitrate (van Spanning *et al.* 1997, Van Spanning *et al.* 1999, Hutchings *et al.* 2000, Veldman *et al.* 2006). The method of heme-NO interaction and its role in the conveyance of nitric oxide sensitivity to NnrR is not well known. Also, the method of nitrate sensing carried out by NarR has yet to be resolved, but is suspected to be subsequently sensed as the reduced product of nitrite (nitric oxide).

The most well understood of these proteins is FnrP. FnrP senses oxygen depletion and activates the expression of the *nar* and *nos* operons. The latter has only been demonstrated in anaerobic cultures respiring nitrate and not nitrous oxide. This may mask any potential elucidation of the regulation of the *nos* cluster. NnrR acts as an activator of the *nir* and *nor* operon. TF *nnrR* (pden_2478) is found in close proximity of its target genes *norB* (pden_2483) and *nirS* (pden_2487) in *P. denitrificans*, co-localisation of NnrR may aid in efficient or rapid associated gene regulation in the presence of cytotoxic NO (Kolesov *et al.* 2007). NarR is required for the expression of the *nar* operon and most likely responds to nitrite and nitrate. It is postulated that NarR may sense any nitrate or nitrite molecules from the low but existing expression of the *nar* or *nap* operons to subsequently induce progressively the *nar* expression (Wood *et al.* 2001, Wood *et al.* 2002). Another gene possibly involved in the regulation of nitrate respiration in *P. denitrificans* is *nosR* which was previously thought to be involved in the regulation of the *nos* operon, however it has recently been shown to be involved in copper sensing (Sullivan *et al.* 2013).

This chapter investigates the metabolic and transcription profiles of the Δ*fnrP* and Δ*nnrR* strains of *P. denitrificans* in the anaerobic respiration of nitrate. It was hypothesised that in the absence of the associated transcription factor, gene expression may be repressed or induced by another transcription factor recognising a similar motif. This hypothesis would assist towards the comprehension of a complex interaction within the regulation of anaerobic respiration on nitrate of *P. denitrificans*.

3.2 Results

3.2.1 Description and validation of the Δ*fnrP* and Δ*nnrR* strains of *P. denitrificans*

The *fnrP* and *nnrR* deficient mutants (PD29.21 and PD77.21; van Spanning *et al.* (1997) and Saunders *et al.* (2000) respectively) were acquired from the van Spanning lab of the Vrije University of Amsterdam, NL. Confirmation of the mutation was carried out by colony PCR taken from colonies grown on LB agar with the appropriate antibiotic associated with the mutation (see Chapter 7). The successful primers used in the mutant validation are listed in table 1. Gel electrophoresis of the colony PCR amplification revealed the product sizes expected for a gene disruption mutation via antibiotic cassette resistance insertion. The expected product size (PCR amplification) for the wild type (genomic DNA) and mutant strain is ~1 Kbp and ~2.5Kbp respectively (Figure 2). That was experimentally confirmed, indicating a strain deficient in *fnrP* (Figure 3) as described in van Spanning *et al.* (1997).

Table 1 Primers used to confirm disruption of *fnrP* with a kanamycin resistance insert in Δ*fnrP* (PD2921).

Primer ID	Target	Sequence
fnr_checkF1	Pden_1850	ggaaccttgacccaaatcaa
fnr_checkR1	Pden_1850	ctatggccattcccgcttcc
fnr_intF1	Pden_1850	ggagatgacgctggacga
fnr_intR1	Pden_1850	tcgtccagcgtcatctcc
kanR_intF1	Kan^R insert	gggaaaacagcattccaggt
kanR_intR1	Kan^R insert	acctggaatgctgttttccc

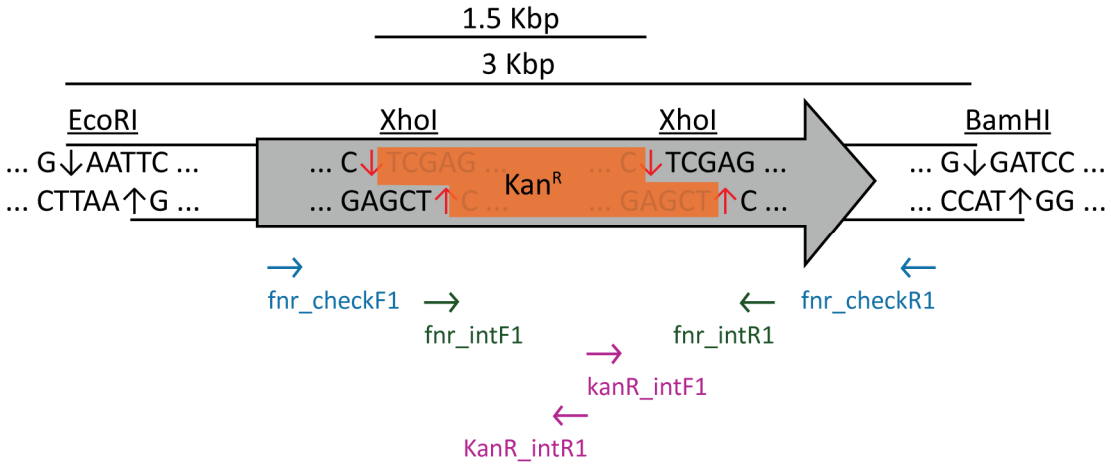

Figure 2 Schematic representation of *fnrP* disruption with a kanamycin resistance cassette in *P. denitrificans*. Restriction sites of *Eco*RI, *Xho*I and *BamH*I and PCR primers used are depicted in the above illustration.

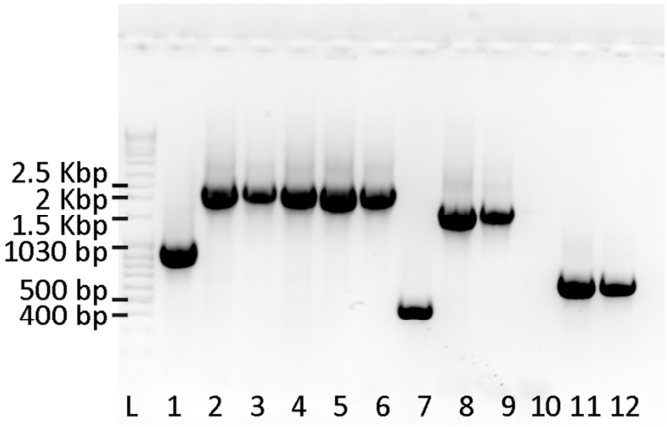

Figure 3 Gel electrophoresis presenting the PCR amplified DNA fractions of genomic DNA (PD1222) and Δ*fnrP* (PD2921). L denotes the DNA ladder (MassRuler Ready-to-use ™), 1 genomic DNA from PD1222, 2

3.2.2 Investigating the metabolic profiles of the *fnrP* and *nnrR* mutants of *P. denitrificans.*

Having ensured the identity of the mutant strain, the growth parameters were defined. The Δ*fnrP* strain grew aerobically in spinning flasks within 12 hours. Figure 4 depicts the anaerobic growth curve of the Δ*fnrP* mutant acquired with a high-throughput system (described Chapter 7); the μ_{max} was 0.08 h^{-1} and the Y was 0.07 $g.L^{-1}.mM^{-1}$ succinate for this batch treatment. The dilution rate of the CSTR system is 0.05 h^{-1}, which is lower than the anaerobic μ_{max} of this strain. This indicates that it is possible to culture the Δ*fnrP* strain with the current CSTR setup.

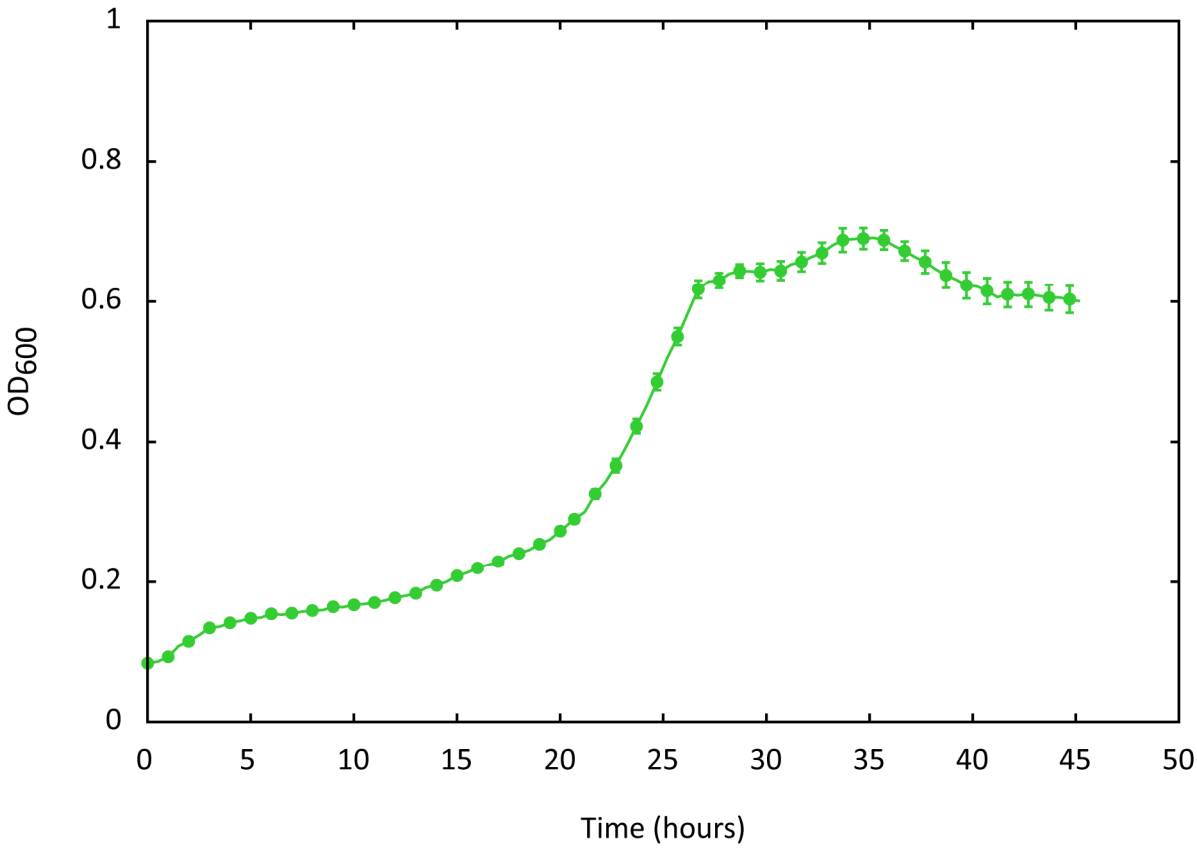

Figure 4 Anaerobic batch growth profile of the Δ*fnrR* strain (PD2921). Biomass was measured indirectly by determining the optical density (OD) at 600 nm with a high through put system (n=12, error bars denote ± SEM).

The incubation procedure of the mutant strain in CSTR was similar to the previous experiments as described in the Materials and Methods. The mutant strain was initially incubated aerobically for ~20 h and then the air supply was restricted allowing the bacterial culture to consume any remaining oxygen in the medium. At that point, the feed pump was set on a rate of 80 ml.h^{-1} corresponding to a dilution rate of 0.05 h^{-1}. The temperature and pH were controlled and adjusted to their defined values of 30^{o}C and 7.5 respectively throughout the incubation period. Interestingly, a prolonged phase of a low oxygen consumption rate was observed (~5 hours; Figure 7 A; see also a detailed illustration in Figure 9). The extracellular concentration of nitrate decreased from ~ 20 to a steady state concentration 15 mM towards the end of the incubation period. The levels of nitrite and nitrous oxide were below the detection limit at that point (Figure 7; C). This fact leads to the assumption that ~ 5 mM nitrate was reduced to di-nitrogen without the accumulation of any intermediate metabolites.

The second mutant cultured in anaerobic CSTR was a mutant lacking a functional copy of *nnrR* (PD7721). Figure 5 presents the batch growth curve of the Δ*nnrR* mutant incubated aerobically and anaerobically in minimal media with nitrate and succinate. The Δ*nnrR* strain has a μ_{max} of 0.57 h^{-1} and a Y of 0.07 g.L^{-1}.mM^{-1} succinate when incubated aerobically. The aerobic growth of Δ*nnrR* in batch is comparable with the wild type strain (PD1222). During anaerobic incubation a μ_{max} of 0.23 h^{-1} and a Y of 0.06 g.L^{-1}.mM^{-1} succinate were observed (Figure 5; B). The Δ*nnrR* strain is known to reduce nitrate to nitrite only as the nitrite reductase operon is not expressed. Based on this previously defined phenotype (van Spanning *et al.* 1997), the concentrations of nitrate and nitrite in the culture medium were determined. At the end of the batch growth the Δ*nnrR* strain had reduced ~20 mM of nitrate to of nitrite. The extracellular concentration of nitrate, nitrite and nitrous oxide enclosed in the Hungate tubes was 0.7, 20 and 0.05 mM respectively (Figure 6). The electron balance of the nitrate reduction to nitrite requires 2 mM electron equivalents per mM nitrate (thus 40 mM electron equivalents in total; Equation 1). The oxidation of 5 mM succinate yields ~ 48 mM electron equivalents assuming that the assimilation coefficient set at 40% (Felgate *et al.* 2012). Thus, it is theoretically possible to culture the Δ*nnrR* strain with this current CSTR approach.

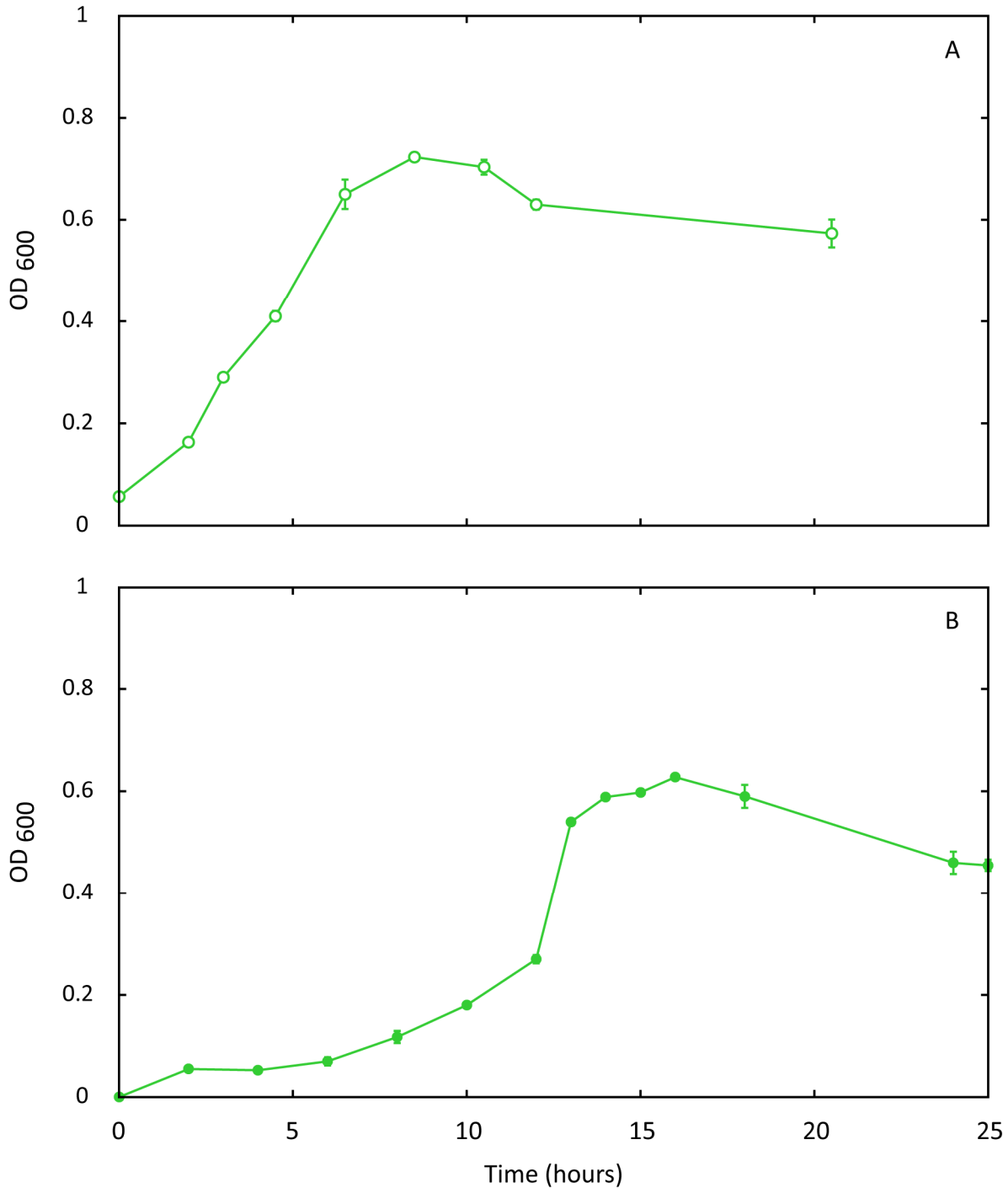

Figure 5 Growth profiles of the Δ*nnrR* strain (PD77.21) in batch cultures; A) Aerobic treatments and B) Anaerobic treatment. Biomass was measured indirectly by determining the optical density (OD) at 600 nm (n=3, error bars denote standard error).

$$NO_3^- + 2e^- + 2H^+ \rightarrow NO_2^- + H_2O$$

Equation 1 The reduction of nitrate to nitrite; note that only 2 e^- are required.

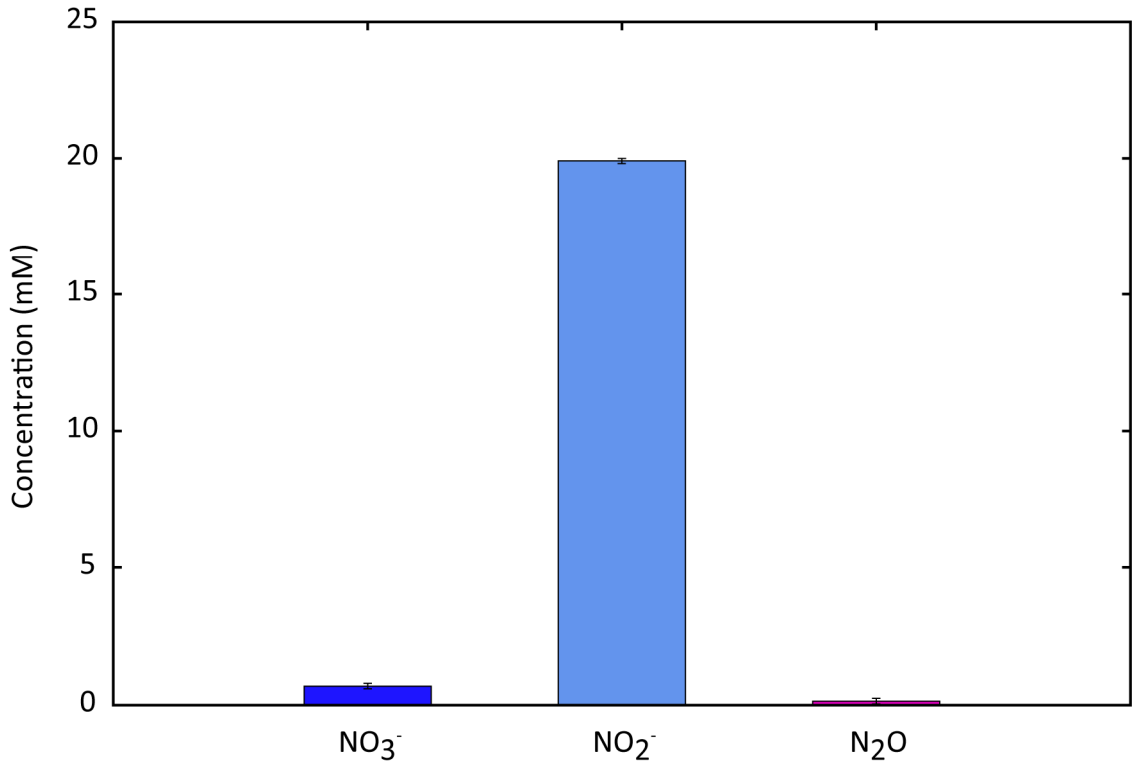

Figure 6 Average concentration of nitrate, nitrite and nitrous oxide at the end of a 28 h anaerobic batch incubation of the Δ*nnrR* strain (PD7722; n=3, error bars denote ±SEM). The culture was supplied initially with 20 mM nitrate and 5 mM succinate.

Based on the previous observations from the batch growth experiments, continuous culture experiments with the Δ*nnrR* strain were successfully performed in triplicate. Temperature and pH were 30^{o}C and 7.5 respectively throughout the incubation period. The dissolved oxygen in the culture was completely consumed when the air supply was shut off (after 20 h, Figure 8; A). Contrary to the continuous culture of the Δ*fnr*P strain; the concentration of nitrate in the steady state of the Δ*nnrR* culture decreased notably from 20 to 1 mM. Subsequently, 19 mM of nitrite has accumulated in the medium towards the end of the incubation (120 h, Figure 8; C). The concentration of nitrous oxide was below detection limit (Figure 8; C) throughout the incubation in the CSTR system. This phenotype of extensive nitrate consumption and subsequent nitrite accumulation is characteristic and typical of a Δ*nnrR* mutant that is unable to reduce nitrite to di-nitrogen (van Spanning *et al.* 1997).

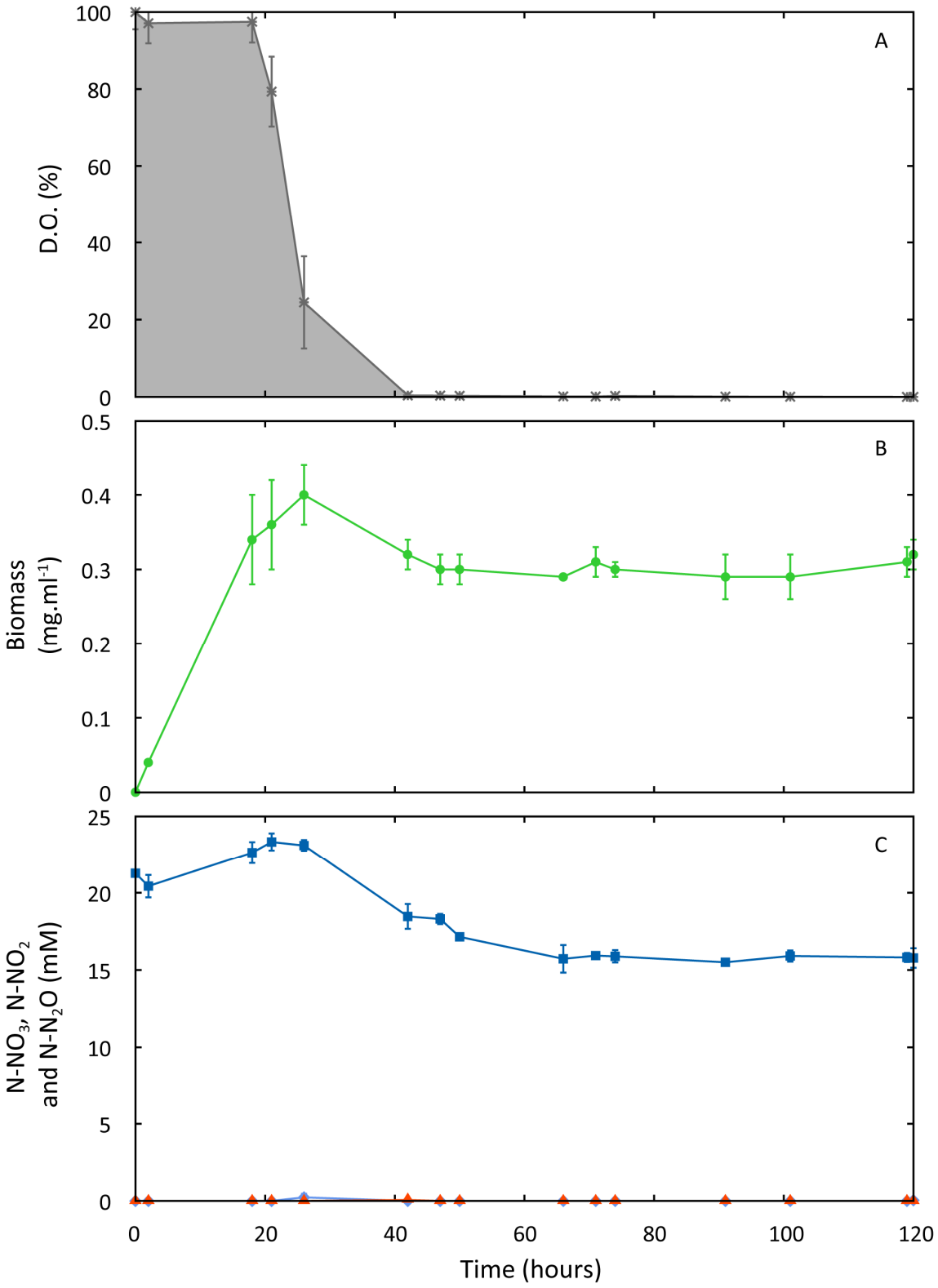

Figure 7 Anaerobic continuous culture of *P. denitrificans* (PD2921) lacking a functional copy of *fnrP* (Pden_1850) at 30°C in CSTR. A) Average dissolved oxygen (D.O.; *) concentration of the culture, B) Average biomass (●) of the culture and C) Average nitrate (■), nitrite (◆) and nitrous oxide (▲) concentration of the culture (n=3; error bars denote ±SEM).

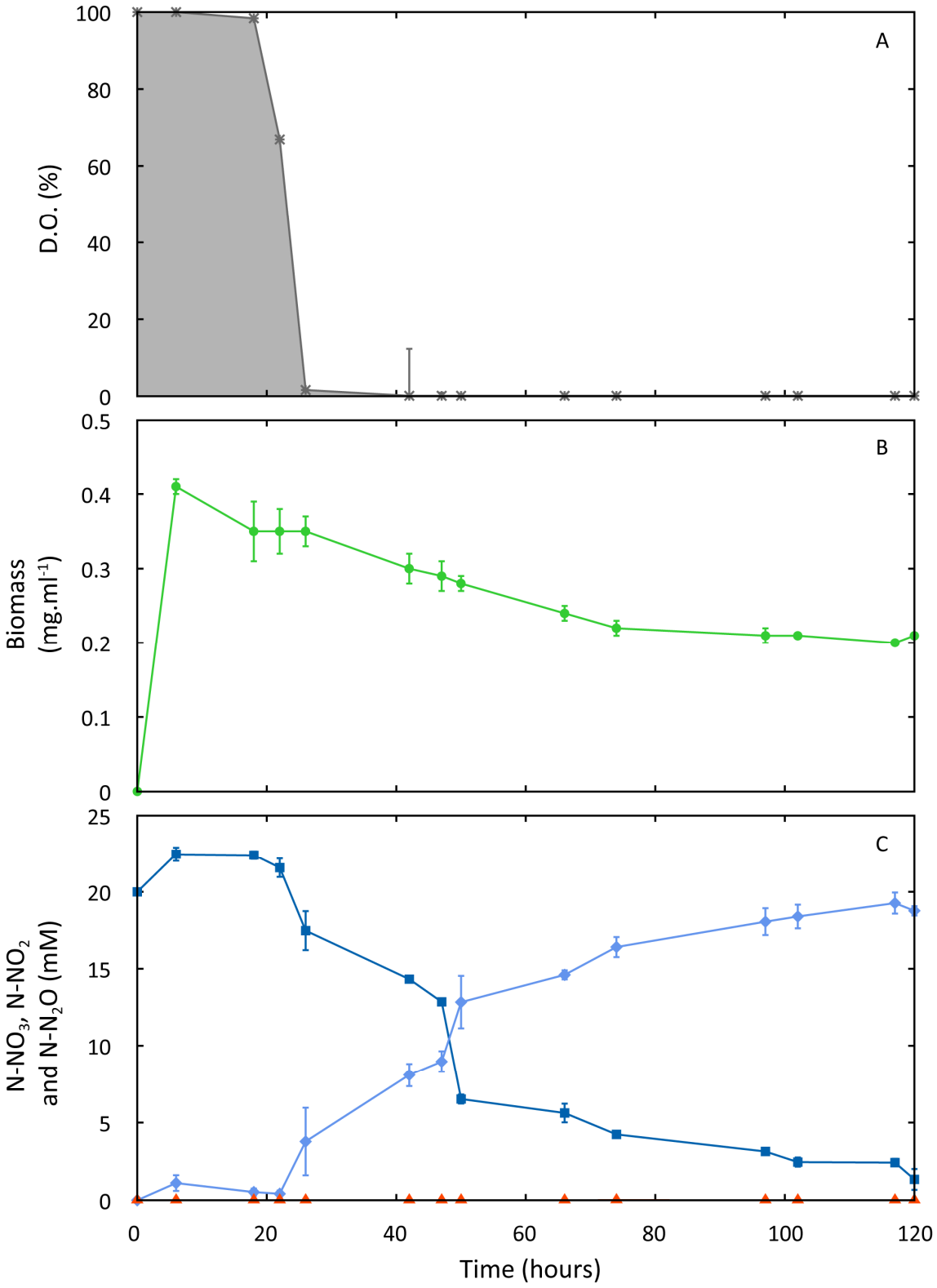

Figure 8 Anaerobic continuous culture of *P. denitrificans* (PD7722) lacking a functional copy of *nnrR* (Pden_2478) at 30°C in CSTR. A) Average dissolved oxygen (D.O.; *) concentration of the culture, B) Average biomass (●) of the culture and C) Average nitrate (■), nitrite (◆) and nitrous oxide (▲) concentration of the culture (n=3; error bars denote ±SEM).

Table 2 Average growth parameters and quotients for metabolite consumption and production at steady state anaerobic continuous cultures (n=3).

#	Strain	Temp. °C	pH	D h^{-1}	OD	±SE	X $g.L^{-1}$	±SE	D/X $L.g^{-1}.h^{-1}$	±SE	qX $g.L^{-1}.h^{-1}$	±SE
1	PD1222	30	7.5	0.05	0.52	0.02	0.25	0.01	0.22	0.01	0.12	0.01
2	PD2921	30	7.5	0.05	0.60	0.05	0.31	0.02	0.17	0.01	0.19	0.03
3	PD7721	30	7.5	0.05	0.40	0.00	0.21	0.00	0.25	0.00	0.08	0.00

Table continues below; index number (#) defines the treatment

#	Strain	Temp. °C	$[NO_3]_0$ µM	±SE	$[NO_3]_t$ µM	±SE	$[NO_2]_t$ µM	±SE	$[N_2O]_t$ µM	±SE	$[N_2]_t$ µM	±SE
1	PD1222	30	20723	1096	15159	115	4745	44	0.3	0.11	5475	1078
2	PD2921	30	20000	0	15831	104	15	15	0.2	0.08	4154	119
3	PD7721	30	20000	0	2058	246	18810	572	0.4	0.06	-868	479

Table continues below; index number (#) defines the treatment

#	Strain	Temp. °C	$[NO_3]_c$ $\mu mol.g^{-1}.h^{-1}$	±SE	$[NO_2]_p$ $\mu mol.g^{-1}.h^{-1}$	±SE	$[NO_2]_c$ $\mu mol.g^{-1}.h^{-1}$	±SE	$[N_2O]_p$ $\mu mol.g^{-1}.h^{-1}$	±SE	$[N_2]_p$ $\mu mol.g^{-1}.h^{-1}$	±SE
1	PD1222	30	1215	274	18	9.2	1196	283	0.2	0.03	1196	283
2	PD2921	30	717	46	3	2.8	714	45	0.0	0.01	714	45
3	PD7721	30	4553	81	4774	159.7	-221	122	0.1	0.01	-221	122

Strains of *P. denitrificans* used: #1 wild type (PD1222), #2 Δ*fnrP* (PD2921) and #3 Δ*nnrR* (PD7721).

The average metabolic rates and CSTR parameters of the mutants and the wild type strain are summarized in Table 2. It is notable that the biomass optical density and subsequently the biomass quotient differ substantially between each treatment. The biomass quotient in the Δ*fnrP* strain (0.19 ±0.03 $g.L^{-1}.h^{-1}$) was higher than the reference treatment (PD1222; 0.12 ±0.01 $g.L^{-1}.h^{-1}$). The Δ*nnrR* strain had a lower biomass quotient (0.08 ±0.004 $g.L^{-1}.h^{-1}$) when compared with the Δ*fnrP* and PD122 strain. The steady state nitrate consumption by the wild type (PD1222) and the Δ*fnrP* strain are comparable (~ 5 mM). The steady state nitrate consumption in the Δ*nnrR* treatment is ~ 18 mM. The consumption quotient of the Δ*fnrP* and the Δ*nnrR* is 1.7 lower and 3.7 greater respectively than the control treatment. Notably, the nitrite production quotient of the Δ*nnrR* strain is 265 times higher than the control treatment and the nitrite consumption quotient of the same strain is ~ 0 mM indicated by a negative rate in table 2. The quotients of nitrite consumption and nitrous oxide and di-nitrogen production in the wild type and Δ*fnrP* strain are comparable to their nitrate consumption quotients, namely ~ 1200 and ~ 715 $\mu mol.g^{-1}.h^{-1}$. Based on the quotient analyses it is evident that lack of *fnrP* in *P. denitrificans* repressed 1.7 times the total nitrate reduction and the lack of *nnrR* induced nitrate reduction 3.7 times and completely inhibited nitrite reduction. The truncated denitrification pathway in the Δ*nnrR* strain resulted in lower biomass quotients.

Another interesting observation retrieved from the CTSR data-logging unit is the high resolution oxygen tension curve after the air flow restriction (Figure 9). The wild type and the Δ*nnrR* strain consume the remaining dissolved oxygen in the medium within ~1 hour. However, the Δ*fnrP* strain requires ~5 hours to consume the remaining dissolved oxygen possibly due to *ccoN* inhibition (van Spanning *et al.* 1997). The lower oxygen consumption rate of Δ*fnrP* is observed at oxygen concentrations lower than ~100 µM. The affinity of the *Bradyrhizobium japonicum* cbb_3 oxidase is ~7 µM (Preisig *et al.* 1996, Bueno *et al.* 2009). This physiological observation suggests a wider role of FnrP, besides regulation of *fnrP*, *ccoN* and *narG*, in regulating the aerobic respiration in *P. denitrificans*.

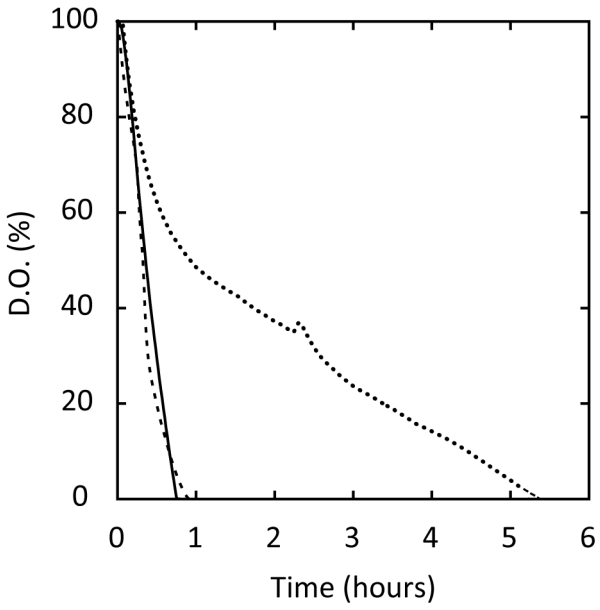

Figure 9 Detailed illustration of the dissolved oxygen tension during the initiation of anaerobic continuous culture in CSTR. The solid line denotes the wild type strain (PD1222), the dotted line the Δ*fnrP* strain (PD2921) and the dashed line the Δ*nnrR* (PD7721). Selected data are presented from each treatment.

3.2.3 Transcriptional analyses with RT-PCR of *fnrP*, *nnrR* and *narR* mutants of *P. denitrificans* in anaerobic CSTR cultures

At 120 hours of continuous cultures samples were taken for total RNA extraction from the Δ*fnrP* strain. Total RNA was extracted, tested for DNA contamination and checked for RNA integrity. Figure 10 depicts the electrophoresis of the PCR products on an agarose gel stained with ethidium bromide. The lack of bands in lanes A and B indicates the absence of any DNA contamination. Lane S shows the PCR product with genomic DNA used as a template (positive control). Having confirmed the purity of the total RNA samples, the RNA quality was assessed with Experion electrophoresis. All total RNA samples had distinct bands at 1500 and 1000 nt, indicating solid RNA fragments (Figure 11). The RNA yield from the CTSR samples was 145 ng.μL^{-1} on average.

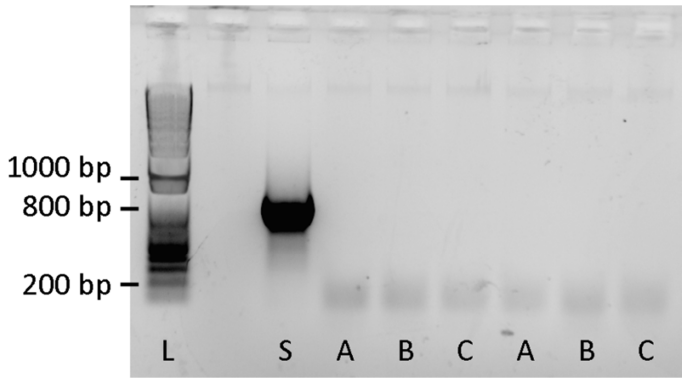

Figure 10 DNA Electrophoresis gel loaded with the PCR products of total RNA samples taken from the Δ*fnrP* continuous culture treatment. Lane L indicates the ladder in bp, S the standard positive control with genomic DNA (Pd1222) as template and A, B and C total RNA samples taken from three biological replicates.

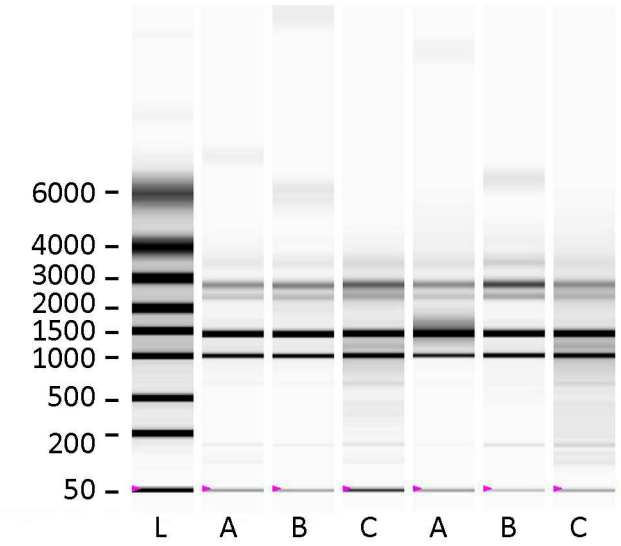

Figure 11 Experion electrophoresis gel evaluating the RNA integrity for the Δ*fnrP* treatment. Lane L indicates the ladder in nt and A, B and C the total RNA samples (5s: 120 nt, 16s: 1542 nt and 23s: 2906 nt).

The same approach was used to assess the purity and assess the overall quality of the total RNA samples for the Δ*nnrR* mutant. Total RNA samples from the Δ*nnrR* strain were free of any DNA contamination (Figure 12). Similarly to the Δ*fnrP* treatment, the integrity of total RNA was acceptable for further transcriptional analyses as indicated by the solid and distinct fragments (Figure 12).

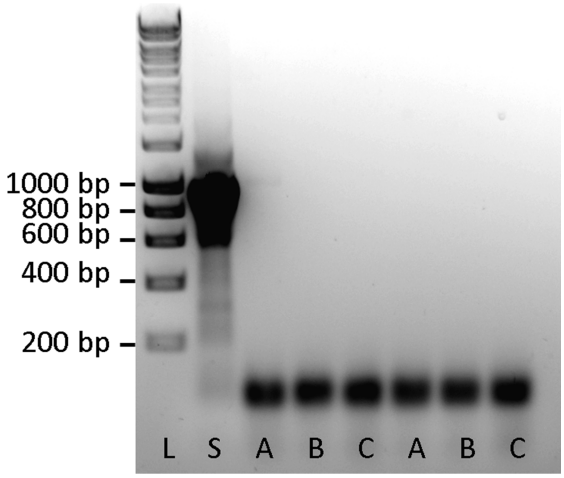

Figure 12 Electrophoresis gel evaluating the RNA purity from DNA contamination. Total RNA samples were taken from the Δ*nnrR* continuous culture treatment. Lane L indicates the ladder, S the standard positive control with genomic DNA as template and A, B and C total RNA samples taken from three biological replicates. Products below the 200 bp mark are primer dimmers.

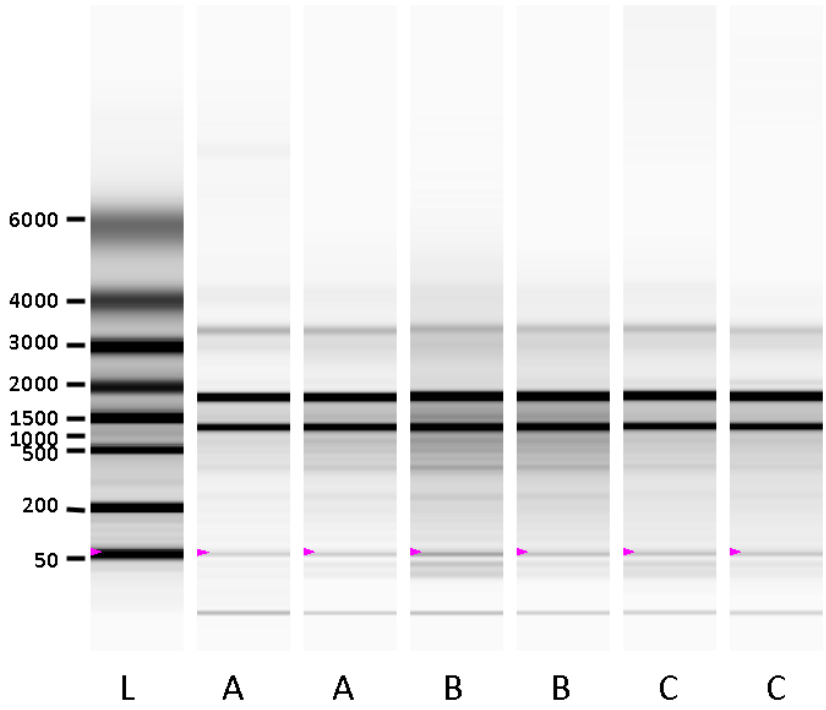

Figure 13 Experion electrophoresis gel of total RNA samples from CSTR cultures of Δ*nnrR* (PD2921). L denotes ladder in nt and A, B and C total RNA samples from Δ*narR* (PD2345) treatment (5s: 120 nt, 16s: 1542 nt and 23s: 2906 nt).

Total RNA samples of all three treatments were stored at -80^{o}C until further use. A 2 µg of RNA aliquot was reversed transcribed and was used to determine the expression of selected genes with RT-PCR.

The genes *nirS*, *norB*, *nosZ*, *cycA* and *pasZ* were relatively up-regulated in the Δ*fnrP* strain when compared to the expression levels of the wild type treatment (PD1222) (Figure 14; C, D, E, F and G). Contrary to this, the expression of *napA* and *narG* was down-regulated ~2 and 10 times (Figure 14; A and B). Interestingly, *ccbS* (pden_1700) was highly induced in the Δ*fnrP* strain (Figure 15; A). This gene encodes the small chain of ribulose-bisphosphate carboxylase, an enzyme involved in CO_2 scavenging and assimilation in the Calvin-Benson-Bassham cycle (CBB). Formate dehydrogenase (*fdhA*) and cytochrome aa_3 oxidase (*ctaDI*) were down-regulated by ~2 times, whereas genes encoding cytochrome ba_3, cbb_3, *bd* and bc_1 oxidase were up-regulated in the Δ*fnrP* treatment (Figure 15; I, K, L, M, N, O). The gene encoding the universal stress protein (*uspA*) upstream of *fnrP* remained unchanged.

In the Δ*nnrR* treatment, target genes involved in the reduction of nitrite, nitric oxide and nitrous oxide were notably down-regulated compared to the wild type treatment. Contrary to this, *narG* was relatively up-regulated (Figure 18). This transcriptional observation is consistent with the metabolic profile of the Δ*nnrR* strain (Figure 8; A, B, C and D). The nitrite concentration of the culture increased towards the incubation and all available nitrate was reduced. The genes for pseudoazurin (*pasZ*) and cytochrome c_{550} (*cycA*) were relatively up and down-regulated respectively (Figure 8; E and F).

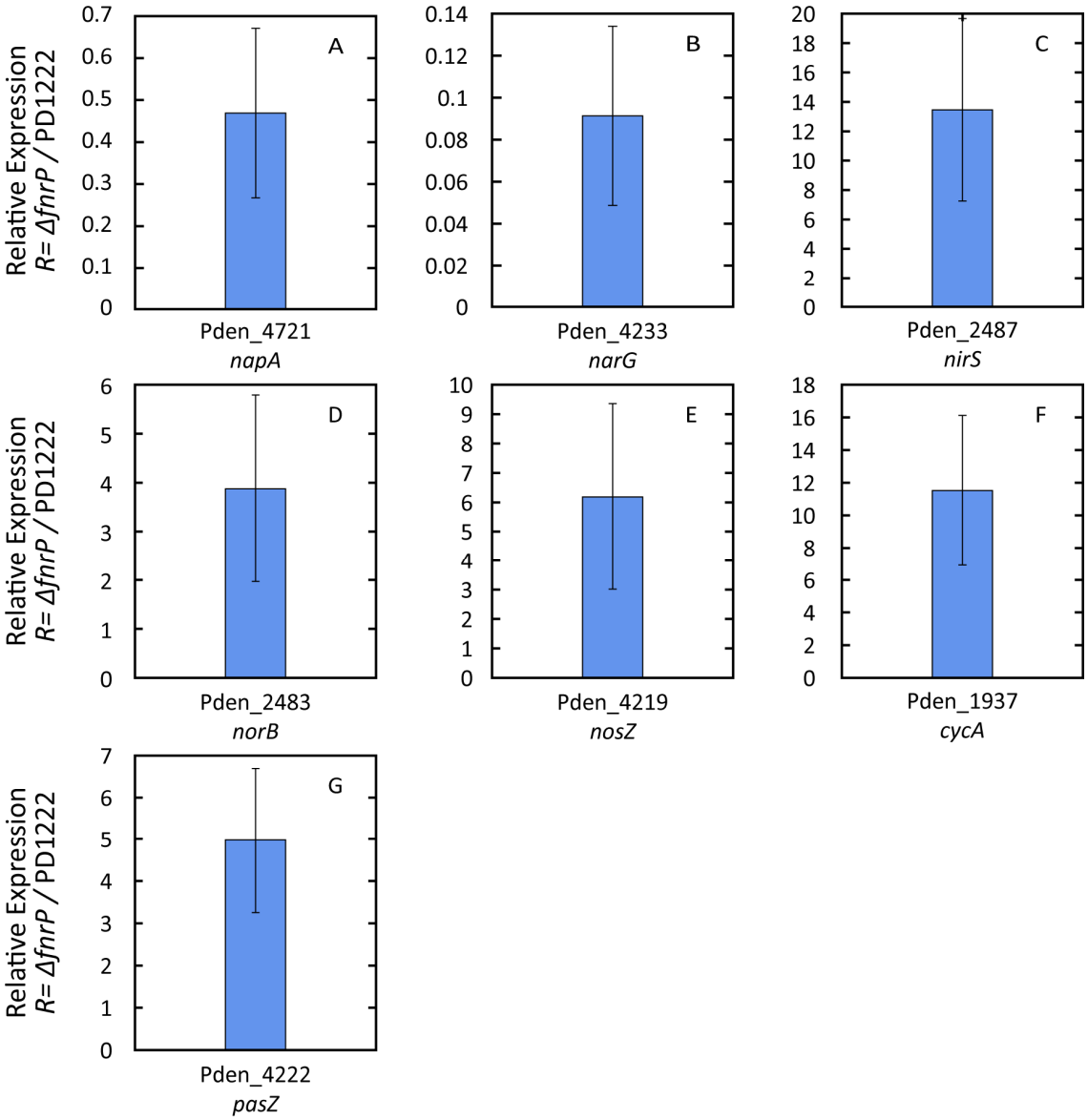

Figure 14 Average relative expression of target genes in Δ*fnrP*; A) *napA* (pden_4721), B) *narG* (pden_4233), C) *nirS* (pden_2487), D) *norB* (pden_2483), E) *nosZ* (pden_4219), F) *cycA* (pden_1937) and G) *pasZ* (pden_4222) detected with RT-PCR. Expression values were normalized on expression of *polB* and the relative ratio *R* is calculated using the anaerobic treatment of the PD1222 strain as a reference based on the Pfaffl method (n=3, error bars denote ±SEM).

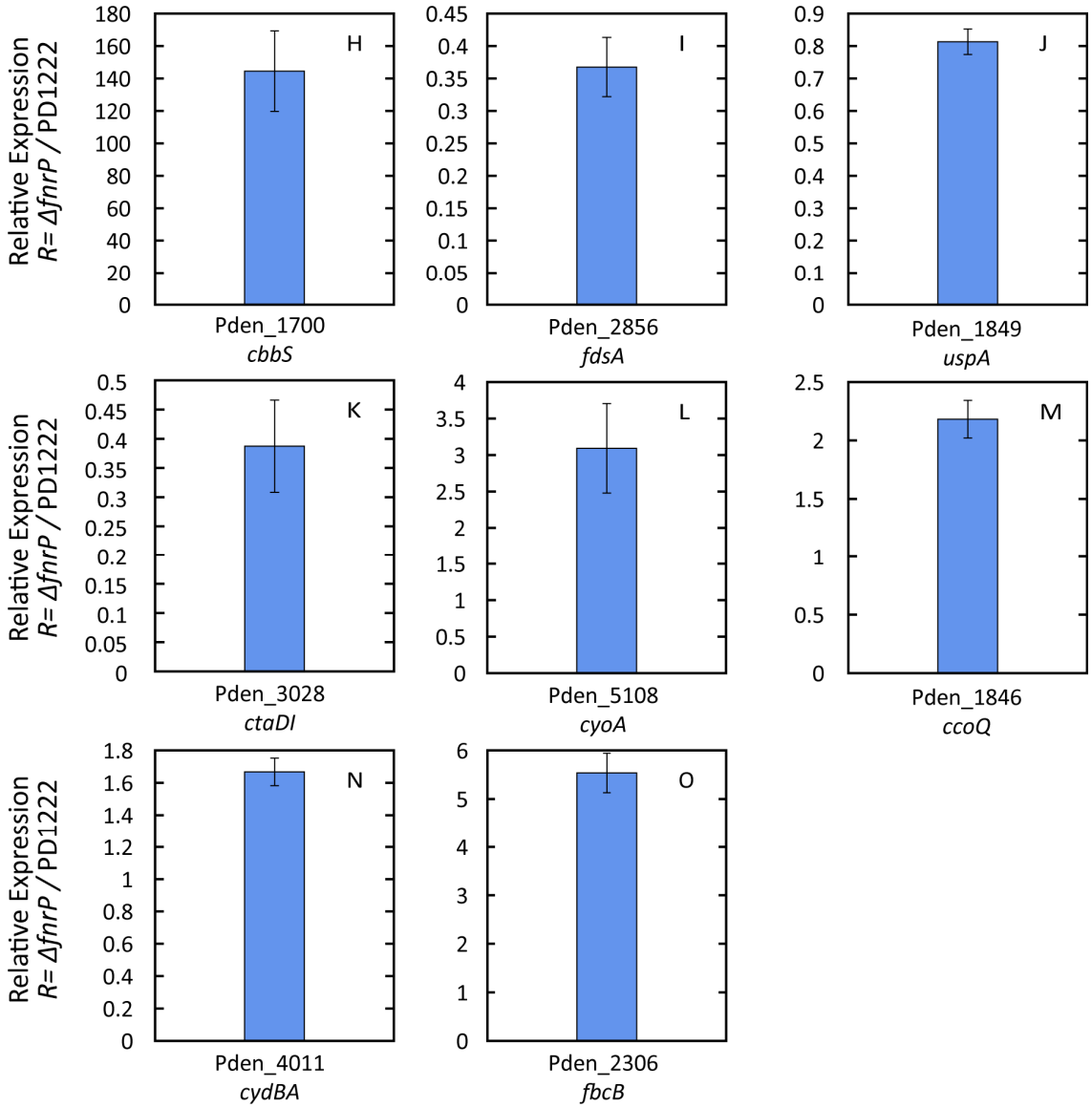

Figure 15 Average relative expression of target genes in Δ*fnrP*; H) *cbbS* (pden_1700), I) *fdsA* (pden_2856), J) *uspA* (pden_1849), K) *ctaDI* (pden_3028), L) *cyoA* (pden_5108), M) *ccoQ* (pden_1846), N) *cydBA* (pden_4011) and O) *fbcB* (pden_2306) detected with RT-PCR. Expression values were normalized on expression of *polB* and the relative ratio *R* is calculated using the anaerobic treatment of the PD1222 strain as a reference based on the Pfaffl method (n=3, error bars denote ±SEM).

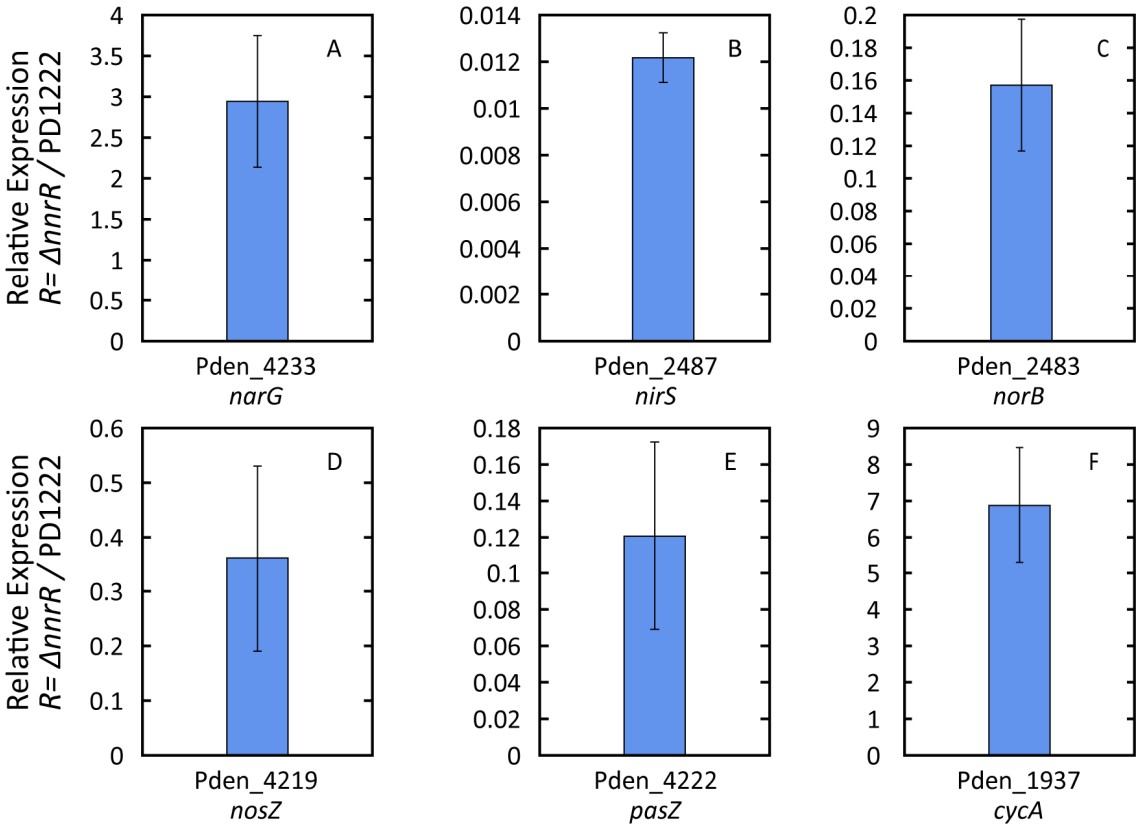

Figure 16 Average relative expression of target genes in Δ*nnrR*; A) *narG* (pden_4233), B) *nirS* (pden_2487), C) *norB* (pden_2483), D) *nosZ* (pden_4219), E) *pasZ* (pden_4222) and F) *cycA* (pden_1937) detected with RT-PCR. Expression values were normalized on expression of *polB* and the relative ratio *R* is calculated using the anaerobic treatment of the PD1222 strain as a reference based on the Pfaffl method (n=3, error bars denote ±SEM).

3.2.4 Whole genome transcriptional analyses of *fnrP* and *nnrR* mutants of *P.denitrificans* in anaerobic CSTR cultures.

Whole genome transcriptome of the *fnrP* and *nnrR* mutants of *P. denitrificans* cultured in anaerobic continuous systems (CSTR) were analysed with type *II* microarray technology. The normalized results were compared against the wild type (PD1222) anaerobic treatment and the relative expression was calculated. 897 and 727 genes for the Δ*fnrP* and Δ*nnrR* treatment respectively showed significant changes ≥ 2 fold (Volcano test, $p \leq 0.05$,). In summary, genes involved in the rubisco pathway, methanol oxidation, cytochrome *c* biogenesis and maturation, cytochrome cbb_3 and ba_3 oxidase expression, nitrite, nitric oxide and nitrous oxide reduction pathways were highly regulated in the Δ*fnrP* strain (Figure 17). For the Δ*nnrR* strain genes involved in nitrate reduction and assimilation, nitrite and nitric oxide reduction, methanol and sulphate oxidation, cytochrome cbb_3 and ba_3 oxidation gene expression were highly up- or down- regulated (Figure 18).

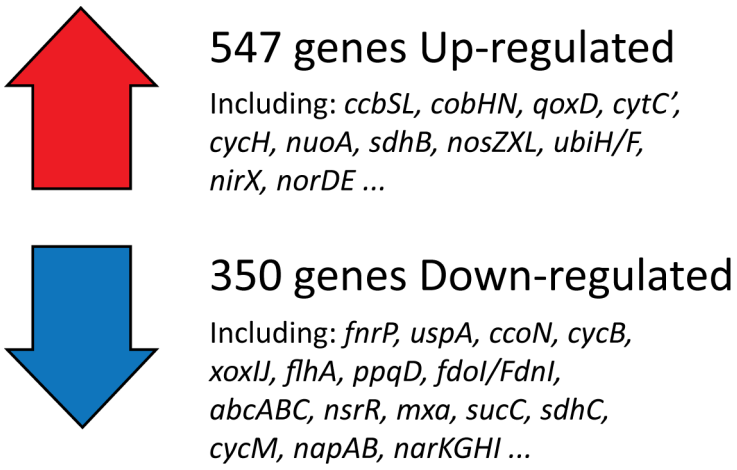

Figure 17 Simplified illustration summarizing the volcano test results (≥2 fold expression and $p \leq 0.05$) in the Δ*frnP* treatment.

Note: The microarray and respirome gene expression datasets for the Δ*fnrR* and Δ*nnrR* strains are presented in 3.4 Gene Expression datasets**.**

Specifically, the ba_3 oxidase operon (*qox* operon; on average 2 fold) and bc_1 oxidase operon (*fbc* operon; on average 1.5 fold) were relatively up-regulated in the absence of the transcriptional factor FnrP in *P. denitrificans* (Δ*fnrP* strain). Contrary, the expression of

cytochrome cbb_3 (*cco* operon; ~3 fold), aa_3 oxidase operon (c*ta* operon; ~2 fold) and cytochrome *c* peroxidase (*ccpA*; 11 fold) were down-regulated. Interestingly, putative genes annotated as cytochrome *c*' (pden_4700) and as cytochrome B_{561} (pden_4699) were on average 5 fold up-regulated.

Genes and operons involved in anaerobic nitrate respiration showed notable induction or repression in the Δ*fnrP* treatment. The operons involved in the reduction of nitrite (*nir*), nitric oxide (*nor*) and nitrous oxide (*nos*) were on average induced ~2, 2 and 3 fold respectively. However, the respiratory nitrate reductase operon in the membrane (*nar*) and periplasmic (*nap*) domain were repressed by ~2 fold in the Δ*fnrP* treatment.

Other operons or genes synthesising the respirome of *P. denitrificans* with a notable regulation were the methylamine metabolism operon (*mau operon*; 2 fold up-regulated), methanol oxidation (*mxa*; 50 fold repressed) and formate dehydrogenase (*fds*; 5 fold repressed). It was also observed that the relative expression for pseudoazurin (*pasZ*; pden_4222) and cytochrome c_{550} (*cycA*; pden_1937) involved in e^- transport remained unchanged and was induced by 2.6 fold respectively.

The nitrate assimilation operon, although not involved in the respiration network directly, had a mixed pattern of induction. Genes expressing an ABC transporter (pden_4448), nitrate transporter (*nasH*; pden_4450) and the small subunit of the nitrate reductase (*nasG*; pden_4451) were induced 1.5 times. Genes expressing a molybopterin oxidoreductase (*nasC*; pden_4449) and a major facilitator transporter (*nasA*; pden_4453) were inhibited 2 fold.

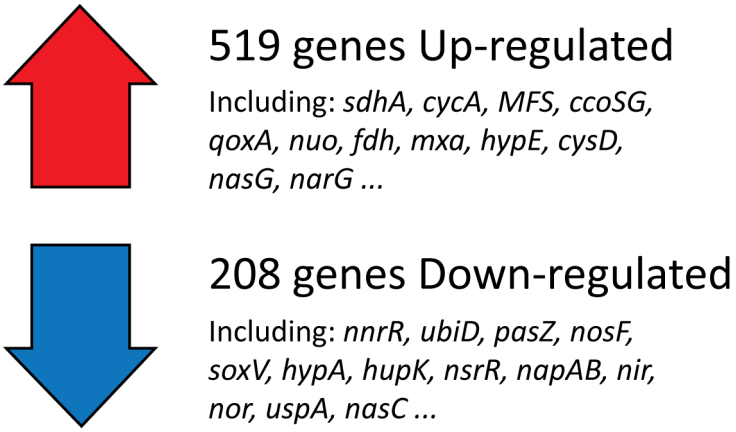

Figure 18 Simplified illustration summarizing the volcano test results (≥2 fold expression and p≤0.05) in the Δ*nnrR* treatment.

Note: The microarray and respirome gene expression datasets for the Δ*fnrR* and Δ*nnrR* strains are presented in 3.4 Gene Expression datasets**.**

Turning now to the transcriptional results of the Δ*nnrR* strain treatment, the ba_3 oxidase operon (*qox*) was on average induced 3 fold, the bc_1 complex operon was also induced (*fbc*; 2 fold), the aa_3 oxidase operon (*cta*) remained unchanged and the cbb_3 oxidase was induced on average 2 fold. In contrast to the Δ*fnrP* strain the cytochrome *c* peroxidase (*ccpA*; pden_0893) remained unchanged in the Δ*nnrR* mutant. The putative genes for cytochrome *c*' (pden_4700) and as cytochrome B_{561} (pden_4699) were on average 1.5 and 3 fold induced.

The expression of key operons involved in anaerobic nitrate respiration in the Δ*nnrR* strain corresponds consistently with the metabolic results of this treatment. The relative expression of the membrane nitrate reductase operon (*narG*) and unchanged when compared to the control treatment, however still expressed at absolute levels. The periplasmic nitrate reductase (*napA*) was repressed on average 5 fold. The nitrite, nitric oxide and nitrous oxide reductase operons were relatively down-regulated 10, 11 and 4 fold respectively. Interestingly, the assimilatory nitrate transporter (*nasH*; pden_4450) and nitrate reductase (*nasG*; pden_4451) were induced 1.5 and 2.4 fold when compared to the control.

Other interesting transcriptional observations in the respirome of the Δ*nnrR* strain of *P. denitrificans* were the relative induction of methanol oxidation operon (*mxa*) by 3 fold, the NADH dependent formate dehydrogenase operon (*fdh*) by 3 fold, the NADH dehydrogenase operon (*nuo*) by 2 fold on average.

Lastly, the relative gene expression for pseudoazurin (*pasZ*; pden_4222) and cytochrome c_{550} (*cycA*; pden_1937) involved in electron transport was relatively repressed by ~10 fold and induced by ~5 fold respectively.

Overall, these results show unique transcriptional responses of the respirome of *P. denitrificans* in the absence of FnrP (Δ*fnrP*) and NnrR (Δ*nnrR*) that have not been previously reported. The target gene for the respiratory nitrate reductase *narG* gene (pden_4233) was repressed under the lack of TF *fnrP* and remained unchanged in the Δ*nnrR* treatment. Functional genes for the nitrite reductase *nirS* (pden_2487) and nitric oxide reductase *norCB* (pden_2483-4) were induced (1.5 fold) and repressed (~30 and 10 fold respectively) for the Δ*fnrP* and the Δ*nnrR* treatment respectively. The nitrous oxide reductase catalytic target gene *nosZ* (pden_4219) was induced in the Δ*fnrP* strain and in contrast was repressed in Δ*nnrR* strain. The above findings reveal unknown interactions of the TF *fnrP* and *nnrR* with target genes involved in the anaerobic nitrate respiration. These interactions will be discussed in the next section and a new regulation network of denitrification in *P. denitrificans* will be proposed.

3.3 Discussion

3.3.1 Towards the elucidation of the nitrate respiration regulon of FnrP and NnrR of *P. denitrificans* in anaerobic continuous culture systems.

The denitrification profiles of the Δ*fnrP* and Δ*nnrR* in continuous culture systems have been confirmed and are consistent with the phenotypes reported previously in van Spanning *et al.* (1997). The Δ*fnrP* strain showed a distinct oxygen consumption pattern when the air supply was turned off in the CTRS (Figure 9). The consumption and production quotient of nitrate and nitrous oxide respectively was 1.7 times lower when compared to the wild type treatment (PD1222). This shows that in the Δ*fnrP* strain, cells reduced nitrate to di-nitrogen with a notably slower rate. The expression of nitrate reductase (*narG*; pden_4233) was ~10 fold lower (RT-PCR; Figure 14 B) and a similar pattern was found with microarray analysis. Contrary to the expression of *narG* (pden_4238), the expression of the nitrite, nitric oxide and nitrous oxide reductase genes was relatively induced ~13, 4 and 6 fold (RT-PCR; Figure 14 C, D, E) and a similar pattern was also observed with microarray analysis (Table 3). FnrP has been shown previously to act as an activator for the *nar* operon (*narG*; pden_4233) and this has been confirmed in this study. The most striking result to emerge from this dataset is that when FnrP is absent (Δ*fnrP* treatment) a positive induction of the *nir*, *nor* and *nos* operons was observed when compared to the control wild type (PD1222) strain. This suggests a new putative role for FnrP repressing the expression by competing with NnrR and perhaps NarR for the same promoter binding site of the aforementioned operons in the wild type strain of *P. denitrificans.*

The Δ*nnrR* strain of *P. denitrificans* has been previously described to accumulate nitrite. It has been previously demonstrated that NnrR, a homologue of FnrP, activates the expression of nitrite and nitric oxide operons. The metabolic profile of the Δ*nnrR* strain cultured in continuous culture is consistent with the previous findings of (van Spanning *et al.* 1997, Van Spanning *et al.* 1999, Bergaust *et al.* 2010). A 3.7 fold increase in the nitrate consumption quotient was observed when compared to the wild type treatment. Subsequently the nitrite production quotient had a comparable magnitude with the nitrate consumption quotient

(~4500 µmol.g^{-1}.h^{-1}) in the Δ*nnrR* strain. The nitrate reductase *narG* gene (pden_4233) was induced 3 fold and the nitrite (*nirS*; pden_2487), nitric oxide (*norB*; pden_2483), and nitrous oxide operons (*nosZ*; pden_4219) were relatively repressed ~100, 7 and 3 fold when the NnrR (Δ*nnrR* strain) was absent. A similar transcriptional pattern was observed in the microarray dataset (Table 4). These results confirm the role of NnrR as an activator for the nitrite (*nor*) and subsequently for the nitric oxide (*nor*) operon. Interestingly, the above observation by disrupting the expression of a functional NnrR, suggest a new role for NnrR it may repress the expression of the *nar* operon by partly binding on the FnrP motifs of the *nar* operon in the wild type strain of *P. denitrificans.*

Table 3 Relative expression values of selected genes of interest from the microarray and RT-PCR datasets in the Δ*fnrP* treatment.

Gene ID	Annotation	Microarray Average	SE	RT-PCR Average	SE
Pden_4721	*napA*	0.26	0.01	0.47	0.20
Pden_4233	*narG*	0.14	0.01	0.09	0.04
Pden_2487	*nirS*	1.77	0.35	13.46	6.21
Pden_2483	*norB*	1.60	0.23	3.88	1.91
Pden_4219	*nosZ*	2.76	0.30	6.19	3.17
Pden_1937	*cycA*	2.96	1.14	11.52	4.60
Pden_4222	*pasZ*	1.42	0.42	4.97	1.72
Pden_1700	*ccbS*	62.84	17.72	144.50	24.84
Pden_2856	*fdsA*	0.21	0.05	0.37	0.05
Pden_1849	*uspA*	0.11	0.04	0.81	0.04
Pden_3028	*ctaDI*	0.67	0.11	0.39	0.08
Pden_5108	*cyoA*	2.74	1.23	3.09	0.61
Pden_1846	*ccoQ*	0.35	0.06	2.18	0.16
Pden_4011	*cydBA*	0.95	0.28	1.67	0.08
Pden_2306	*fbcB*	1.72	0.23	5.54	0.41

*The relative gene expression values are expressed as the fold change gene expression of the Δ*fnrP* to wild type strain (PD1222) ratio.

Table 4 Relative expression values of selected genes of interest from the microarray and RT-PCR datasets in the Δ*nnrR* treatment.

Gene ID	Annotation	Microarray Average	±SE	RT-PCR Average	±SE
Pden_4233	*narG*	1.30	0.01	2.94	0.81
Pden_2487	*nirS*	0.03	0.00	0.01	0.00
Pden_2483	*norB*	0.12	0.01	0.16	0.04
Pden_4219	*nosZ*	0.99	0.07	0.36	0.17
Pden_4222	*pasZ*	0.14	0.05	0.12	0.05
Pden_1937	*cycA*	6.38	1.89	6.88	1.59

*The relative gene expression values are expressed as the fold change gene expression of the Δ*fnrP* to wilt type strain ratio.

The newly established roles of the transcriptional regulators FnrP and NnrR as a result of a possible motif binding interplay, based on the transcriptional expression of the target operons, could be further explained by taking into account the physiochemical attributes of the respective enzymes expressed. Table 5 summarises the kinetic parameters of Nar, Nir, Nor and Nos of *P. denitrificans.* Results illustrate that NnrR competes with FnrP to activate the target operon *nar*. FnrP acts as an activator and NnrR as a repressor, this observation may have a mechanistic causality based on the enzyme kinetics. Nar has a similar to Nir K_M value of ~ 12 μM, however the turnover number K_{cat}, thus the number of reactions per time unit, is 174 and 74 s^{-1} respectively. In another perspective Nar reduces 2.3 times more nitrate molecules that Nir reduces nitrite. Thus, to remove the Nar-produced nitrite effectively and maintain a stoichiometric balance with the cell, there are three possible mechanisms that *P. denitrificans* may utilize on transcriptional level; i) to express more *nirS* gene copies, ii) to slow down the expression of *narG* or iii) utilize both of the above mechanisms. In results Chapter 1 metabolic analysis showed that nitrate reduction was balanced with nitrite consumption (~ 1200 $\mu mol.g^{-1}.h^{-1}$) and the extracellular nitrite concentration was bellow detection limits in the CTST system. The transcriptional analysis showed that *nirS* is relatively expressed 18 times more than *narG.* The mechanisms of the above regulatory approach will be further explained in 6. Discussion, taking into account the

latest research finding on biophysical transcriptional regulation. Therefore, it is plausible that the new roles for FnrP and NnrR are actually employed by *P. denitrificans* and the current model of transcriptional regulation of denitrification can be updated as illustrated in Figure 19.

Table 5 Kinetic parameters for the Nar, Nir, Nor and Nos of *P. denitrificans*

Enzyme	Parameter	Value	Units	Reference
Nar	K_M	13	μM	**Craske and Ferguson 1986**
	K_{cat}	174	s^{-1}	
Nir	K_M	12	μM	**Richter *et al.* 2002**
	K_{cat}	74	s^{-1}	
Nor	K_M	35	μM	**Thorndycroft *et al.* 2007**
	K_{cat}	81	s^{-1}	
Nos	K_M	6.7	μM	**Snyder and Hollocher 1987**
	K_{cat}	264	s^{-1}	

To conclude, the present results are significant in at least two major respects i) new putative roles of the transcription factors FnrP and NnrR have been demonstrated and ii) an interactive association between the two TF may exist in a way that optimizes the reduction rates of the denitrification metabolites in *P. denitrificans*.

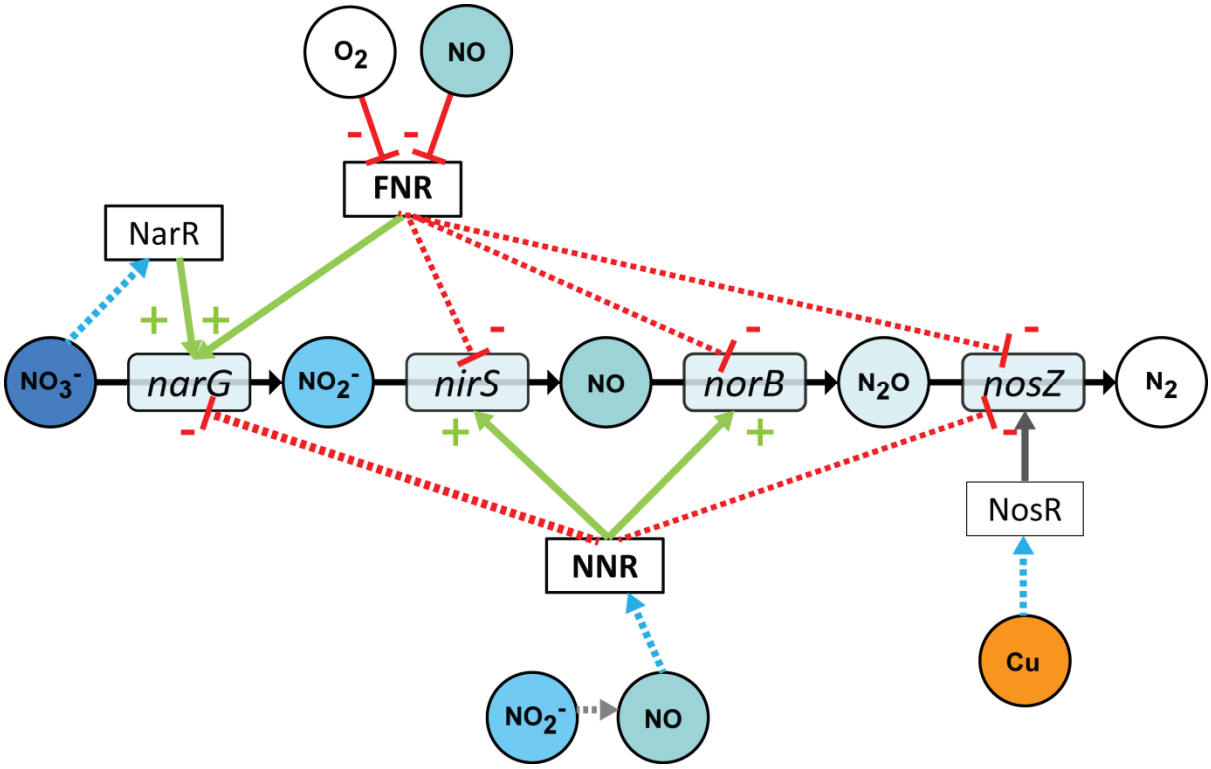

Figure 19 Updated version of the simplified illustration of the regulatory network controlling expression of denitrification genes in *P. denitrificans* with the newly proposed roles of the transcription factors (TF) *fnrP* and *nnrR.* The solid arrows represent positive activating events between the TF and the target gene. Dashed arrows indicate positive signalling between the metabolites and the TF. The lines with a bar end indicate inhibition events between the TF and the signal metabolite. The dashed lines with a bar end indicate inhibition events between the TF and the target genes.The TF and subsequently the regulatory proteins are boxed by clear layers; those are the FNR (Fumarate and Nitrate Regulatory), NNR (Nitrite and Nitric Oxide Regulatory), NarR (Nitrate reductase Regulatory) and NosR (Nitrous oxide reductase Regulatory protein). The target genes are boxed by a shaded layer; those are the membrane nitrate reductase *narG* (pden_4233), the nitrite reductase *nirS* (pden_2487), the nitric oxide reductase *norB* (pden_2483) and the nitrous oxide reductase *nosZ* (pden_4219). The metabolites are represented in circles.

3.4 Gene Expression datasets

3.4.1 Respirome gene expression dataset for the Δf*nrP* strain

Georgios Giannopoulos

Respirome Relative Expression WT *vs* . Δ*fnrP*
20140214_wt_fnrP

Gene ID	Δ*fnrP*		WT		Ratio	Gene ID	Annotation
	Average	SE Norm	Average	SE Norm	Δ*fnrP* /WT		
Pden_5108	3.67	0.43	1.64	0.64	2.24	Pden_5108	qoxA ba3 subunit II
Pden_5107	2.78	0.24	1.36	0.17	2.04	Pden_5107	qoxB ba3 subunit I
Pden_5106	3.21	0.32	1.10	0.27	2.91	Pden_5106	qoxC ba3 subunit III
Pden_5105	3.80	0.82	1.10	0.23	3.47	Pden_5105	qoxD ba3 subunit IV
Pden_5104	7.52	1.15	2.76	0.42	2.73	Pden_5104	surF1 surfeit family
Pden_5063	1.41	0.17	1.27	0.35	1.11	Pden_5063	Alcohol dh
Pden_5062	0.46	0.04	0.40	0.08	1.15	Pden_5062	L-Lactate dh
Pden_5013	0.34	0.03	0.33	0.03	1.04	Pden_5013	peroxidase
Pden_4938	0.40	0.05	0.53	0.14	0.76	Pden_4938	ubiX
Pden_4877	0.39	0.05	0.50	0.08	0.77	Pden_4877	L-lactate dh
Pden_4866	0.49	0.07	0.64	0.21	0.76	Pden_4866	Malate/lactate dh
Pden_4855	0.30	0.03	0.41	0.04	0.72	Pden_4855	Malate/lactate dh
Pden_4738	0.64	0.09	0.43	0.07	1.48	Pden_4738	mauN ferrodoxin nap
Pden_4737	0.53	0.12	0.46	0.07	1.16	Pden_4737	mauM ferrodoxin nap
Pden_4736	0.56	0.10	0.35	0.19	1.58	Pden_4736	mauG diheme c perox
Pden_4735	0.69	0.14	0.32	0.05	2.13	Pden_4735	mauJ
Pden_4734	0.29	0.04	0.22	0.03	1.31	Pden_4734	mauC amicyamin
Pden_4733	0.31	0.06	0.33	0.09	0.96	Pden_4733	mauA small subnit
Pden_4732	0.48	0.09	0.58	0.38	0.82	Pden_4732	mauD accessory prot
Pden_4731	0.41	0.05	0.18	0.09	2.26	Pden_4731	mauE ma utilization
Pden_4730	0.66	0.08	0.30	0.04	2.19	Pden_4730	mauB MADH heavy ch
Pden_4729	1.40	0.40	0.40	0.07	3.51	Pden_4729	mauF big subunit
Pden_4728	0.46	0.06	0.30	0.07	1.55	Pden_4728	lysR
Pden_4727	2.59	0.21	1.76	0.18	1.47	Pden_4727	sndhA
Pden_4726	0.46	0.06	0.86	0.28	0.53	Pden_4726	mscS-aldose dh
Pden_4724	1.45	0.33	8.99	7.65	0.16	Pden_4724	GreA kinase regulat

Pden_4723	0.41	0.03	1.66	0.15	0.24	Pden_4723	napC
Pden_4722	0.61	0.10	3.25	0.59	0.19	Pden_4722	napB cyt c
Pden_4721	0.63	0.03	2.49	0.18	0.25	Pden_4721	napA catalytic
Pden_4720	0.78	0.13	1.69	0.42	0.46	Pden_4720	napD
Pden_4719	1.09	0.13	3.51	0.47	0.31	Pden_4719	napE
Pden_4718	0.70	0.12	0.71	0.26	0.99	Pden_4718	Hypotherical
Pden_4700	2.97	0.69	0.50	0.07	5.96	Pden_4700	CytCP
Pden_4699	1.09	0.14	0.25	0.06	4.31	Pden_4699	B651
Pden_4511	5.69	0.79	4.29	3.50	1.33	Pden_4511	ubiE
Pden_4510	5.37	0.71	1.66	0.14	3.24	Pden_4510	ubiB
Pden_4397	2.69	0.34	2.88	0.38	0.93	Pden_4397	hypothetical
Pden_4396	5.09	0.43	2.89	0.39	1.76	Pden_4396	cysN/cysC
Pden_4395	4.87	0.53	2.24	0.70	2.18	Pden_4395	cysD
Pden_4394	0.71	0.20	0.35	0.07	2.04	Pden_4394	hypothetical protein
Pden_4393	0.53	0.18	1.03	0.26	0.52	Pden_4393	glpD homodimeric quin
Pden_4392	0.56	0.23	0.95	0.14	0.58	Pden_4392	ABC transporter ATP
Pden_4391	0.67	0.23	0.85	0.14	0.79	Pden_4391	ABC transporter ATP
Pden_4390	0.67	0.10	0.69	0.17	0.98	Pden_4390	ABC transporter
Pden_4389	0.79	0.15	0.72	0.11	1.10	Pden_4389	ABC transporter
Pden_4388	0.66	0.19	1.70	0.60	0.39	Pden_4388	hypothetical
Pden_4387	2.66	1.09	6.64	0.54	0.40	Pden_4387	ABC transporter
Pden_4386	1.94	0.29	1.48	0.09	1.31	Pden_4386	glycerol kinase
Pden_4356	1.70	0.26	2.06	0.58	0.83	Pden_4356	b561?
Pden_4323	0.80	0.08	0.48	0.04	1.66	Pden_4323	DprA
Pden_4322	6.58	0.78	4.95	0.82	1.33	Pden_4322	TldD
Pden_4321	18.51	1.93	26.26	5.07	0.70	Pden_4321	ctaC subunit II
Pden_4320	5.86	0.73	10.11	1.91	0.58	Pden_4320	ctaB
Pden_4319	6.17	1.23	12.41	2.40	0.50	Pden_4319	hypothetical
Pden_4318	4.30	0.59	7.47	1.14	0.58	Pden_4318	ctaG assembly protein
Pden_4317	7.91	1.28	8.58	1.77	0.92	Pden_4317	ctaE subunit III
Pden_4316	2.82	0.22	2.98	0.29	0.95	Pden_4316	surF1
Pden_4315	4.58	0.46	5.67	0.75	0.81	Pden_4315	thrC
Pden_4238	0.95	0.11	1.00	0.13	0.94	Pden_4238	narR

Pden_4237	0.70	0.05	7.70	1.34	0.09	Pden_4237	narK
Pden_4236	0.96	0.05	17.18	1.49	0.06	Pden_4236	narI
Pden_4235	1.36	0.11	16.67	1.81	0.08	Pden_4235	narH
Pden_4234	2.31	0.41	32.81	4.46	0.07	Pden_4234	narJ
Pden_4233	2.44	0.33	17.62	2.81	0.14	Pden_4233	narG
Pden_4232	7.06	1.06	23.77	3.57	0.30	Pden_4232	
Pden_4231	7.24	0.73	17.83	3.13	0.41	Pden_4231	
Pden_4230	19.62	4.12	6.94	1.40	2.83	Pden_4230	nnrS
Pden_4226	14.84	2.42	10.39	4.87	1.43	Pden_4226	ubiD
Pden_4225	8.32	1.69	7.69	1.57	1.08	Pden_4225	ubiD
Pden_4222	51.28	14.93	40.77	33.18	1.26	Pden_4222	pasZ
Pden_4221	21.60	5.09	13.42	6.48	1.61	Pden_4221	nosC
Pden_4220	15.80	2.39	9.35	2.22	1.69	Pden_4220	nosR
Pden_4219	73.97	10.65	27.17	2.10	2.72	Pden_4219	nosZ
Pden_4218	16.08	4.23	13.70	5.11	1.17	Pden_4218	nosD
Pden_4217	15.91	2.92	6.22	1.01	2.56	Pden_4217	nosF
Pden_4216	28.83	6.41	7.85	0.99	3.67	Pden_4216	nosY
Pden_4215	17.82	3.22	6.06	0.67	2.94	Pden_4215	nosL
Pden_4214	28.61	5.49	7.00	1.01	4.09	Pden_4214	nosX
Pden_4161	0.61	0.08	3.02	2.89	0.20	Pden_4161	hypothetical
Pden_4160	0.70	0.10	1.03	0.32	0.68	Pden_4160	soxH
Pden_4159	0.99	0.09	0.94	0.09	1.06	Pden_4159	soxG β-lactamase
Pden_4158	1.50	0.31	0.90	0.15	1.67	Pden_4158	SoxF FAD disulfide ox
Pden_4157	0.65	0.07	0.56	0.11	1.15	Pden_4157	SoxE cyt c-I
Pden_4156	0.93	0.13	0.71	0.17	1.30	Pden_4156	soxD cyt c551
Pden_4155	0.66	0.06	0.46	0.03	1.43	Pden_4155	soxC Mo-oxidase
Pden_4154	0.34	0.03	0.42	0.05	0.81	Pden_4154	soxB Rden
Pden_4153	0.78	0.09	2.28	0.43	0.34	Pden_4153	socA di-heme cyt c
Pden_4152	0.80	0.10	1.73	0.48	0.46	Pden_4152	soxZ sulfur oxidase
Pden_4151	1.47	0.27	2.89	0.50	0.51	Pden_4151	soxY sulfur oxidase
Pden_4150	0.46	0.06	1.31	0.39	0.35	Pden_4150	soxX cyt c
Pden_4149	0.24	0.03	0.41	0.06	0.58	Pden_4149	soxW thioredoxin
Pden_4148	0.43	0.07	0.75	0.14	0.57	Pden_4148	soxV cyt c

Pden_4147	0.35	0.04	0.63	0.22	0.55	Pden_4147	soxS cyt c biogenesis
Pden_4146	2.03	0.46	2.21	0.55	0.92	Pden_4146	ArsR regulatory
Pden_4145	1.55	0.16	2.41	0.27	0.64	Pden_4145	Hypothetical (YeeD)
Pden_4075	4.86	0.65	3.67	0.96	1.33	Pden_4075	L-Lactate dh cyt c
Pden_4012	0.35	0.03	0.62	0.05	0.57	Pden_4012	ATPase
Pden_4011	0.21	0.02	0.24	0.05	0.87	Pden_4011	d subunit II
Pden_4010	0.42	0.05	0.36	0.06	1.17	Pden_4010	bd subunit I
Pden_4009	0.40	0.05	0.47	0.06	0.86	Pden_4009	Mo-pterin α subunit
Pden_4008	0.30	0.02	0.42	0.04	0.73	Pden_4008	σ54 Fis transcript reg
Pden_4007	0.38	0.04	0.54	0.12	0.71	Pden_4007	Membrane sensor kina
Pden_3985	0.68	0.11	0.71	0.09	0.96	Pden_3985	p450
Pden_3978	9.42	1.56	4.11	0.63	2.29	Pden_3978	ccmH
Pden_3977	11.83	1.14	6.60	0.58	1.79	Pden_3977	ccmF
Pden_3974	4.59	0.64	5.00	0.93	0.92	Pden_3974	cycJ
Pden_3942	12.67	1.63	8.31	1.34	1.52	Pden_3942	ubiH/F
Pden_3543	0.61	0.09	0.48	0.04	1.28	Pden_3543	Short Chain Reductase
Pden_3286	0.42	0.06	0.47	0.07	0.90	Pden_3286	b561?
Pden_3113	0.44	0.06	0.36	0.08	1.22	Pden_3113	hypothetical
Pden_3112	0.59	0.18	0.69	0.28	0.86	Pden_3112	hypE
Pden_3111	0.55	0.04	0.77	0.09	0.71	Pden_3111	hypD
Pden_3110	0.34	0.10	0.55	0.15	0.61	Pden_3110	hypC
Pden_3109	0.41	0.06	0.43	0.08	0.94	Pden_3109	hypothetical
Pden_3108	0.57	0.06	0.73	0.13	0.78	Pden_3108	hypB
Pden_3107	0.84	0.03	0.85	0.08	0.99	Pden_3107	hypA
Pden_3106	0.56	0.10	1.10	0.40	0.50	Pden_3106	HupK
Pden_3105	0.29	0.04	0.38	0.04	0.76	Pden_3105	HupJ Rubredoxin
Pden_3104	0.40	0.05	0.61	0.09	0.65	Pden_3104	HupH
Pden_3103	0.33	0.04	0.50	0.08	0.67	Pden_3103	HupG
Pden_3102	0.79	0.10	1.20	0.20	0.66	Pden_3102	hupF
Pden_3101	0.45	0.06	0.43	0.05	1.05	Pden_3101	HupD
Pden_3100	0.27	0.04	0.21	0.04	1.30	Pden_3100	hupC cyt b
Pden_3099	0.33	0.05	0.31	0.13	1.05	Pden_3099	hupE
Pden_3098	0.21	0.02	0.22	0.02	0.94	Pden_3098	hupL large subunit

Pden_3097	0.19	0.02	0.19	0.02	1.01	Pden_3097	hupA/S small subunit
Pden_3096	0.49	0.03	0.73	0.08	0.67	Pden_3096	hupF maturation
Pden_3095	0.75	0.06	1.07	0.09	0.70	Pden_3095	hupV
Pden_3094	0.84	0.09	1.18	0.16	0.72	Pden_3094	hupU
Pden_3093	0.90	0.07	1.28	0.13	0.70	Pden_3093	hupT hist-kinase sensor
Pden_3028	2.85	0.32	4.34	0.52	0.66	Pden_3028	ctaDI
Pden_3027	1.25	0.23	4.68	3.51	0.27	Pden_3027	ahpD Alkylhydroperoxidase
Pden_3026	2.12	0.40	11.35	9.49	0.19	Pden_3026	Hypothetical
Pden_3025	3.32	0.57	14.24	10.80	0.23	Pden_3025	NO & morphol reg
Pden_3024	1.63	0.33	6.77	4.27	0.24	Pden_3024	nsrR NO repressor
Pden_3023	1.24	0.21	5.53	5.47	0.22	Pden_3023	hypothetical
Pden_3022	0.65	0.12	1.93	1.25	0.34	Pden_3022	sdhB
Pden_3021	0.89	0.14	1.33	0.51	0.67	Pden_3021	sdhC
Pden_3020	0.52	0.06	1.06	0.29	0.49	Pden_3020	sdhD
Pden_3019	0.71	0.11	1.26	0.35	0.56	Pden_3019	Signal protein
Pden_3003	0.64	0.07	3.15	0.53	0.20	Pden_3003	mxaD
Pden_3002	0.67	0.08	1.37	0.12	0.49	Pden_3002	mxaL
Pden_3001	1.70	0.31	2.25	0.43	0.75	Pden_3001	mxaK
Pden_3000	2.22	0.32	2.93	0.64	0.76	Pden_3000	mxaC von Willebr.
Pden_2999	3.15	0.67	2.63	0.39	1.20	Pden_2999	mxaA
Pden_2998	1.69	0.40	2.89	0.54	0.58	Pden_2998	mxaS unknown
Pden_2997	0.86	0.13	5.20	0.95	0.16	Pden_2997	mxaR unknown
Pden_2996	0.87	0.28	37.72	10.45	0.02	Pden_2996	mxaI β subunit
Pden_2995	0.59	0.13	12.34	2.87	0.05	Pden_2995	mxaG cyt C-L c551i
Pden_2994	0.44	0.06	12.81	4.29	0.03	Pden_2994	mxaJ binding prot.
Pden_2993	0.33	0.03	26.43	10.76	0.01	Pden_2993	mxaF α subunit
Pden_2929	2.05	0.28	3.04	0.73	0.68	Pden_2929	lctR Lactate Regulator
Pden_2928	0.81	0.06	1.23	0.09	0.66	Pden_2928	Dld D-Lactate dh
Pden_2927	1.94	0.23	4.03	0.63	0.48	Pden_2927	lctP L-Lactate permeas
Pden_2859	2.03	0.29	1.66	0.33	1.23	Pden_2859	LysR family
Pden_2858	1.26	0.20	4.58	1.58	0.28	Pden_2858	Fdh γ subunit
Pden_2857	1.18	0.09	6.32	1.89	0.19	Pden_2857	NADH dh (quinone)
Pden_2856	1.33	0.25	6.76	1.05	0.20	Pden_2856	Fdh α subunit

Pden_2855	2.64	0.28	4.35	0.79	0.61	Pden_2855	FdhD family
Pden_2854	2.15	0.67	2.16	0.27	1.00	Pden_2854	NAD-fdh δ subunit
Pden_2853	2.67	0.21	2.65	0.26	1.01	Pden_2853	ribonuclease R
Pden_2830	1.82	0.32	10.23	2.27	0.18	Pden_2830	4Fe-4S
Pden_2829	0.41	0.04	0.94	0.09	0.44	Pden_2829	fdnG α subunit
Pden_2828	0.40	0.05	1.10	0.23	0.36	Pden_2828	fdnH β subunit
Pden_2827	0.56	0.06	1.21	0.21	0.47	Pden_2827	fdnI γ subunit
Pden_2826	1.79	0.26	2.72	0.39	0.66	Pden_2826	fdhE
Pden_2825	1.46	0.13	0.90	0.09	1.62	Pden_2825	selB cysteine enlog.
Pden_2824	3.02	0.29	1.11	0.09	2.72	Pden_2824	aldo/keto reductase
Pden_2710	1.99	0.18	1.93	0.67	1.03	Pden_2710	SndhB
Pden_2709	3.65	0.53	1.91	0.18	1.91	Pden_2709	NAP (P)
Pden_2708	3.74	0.65	1.72	0.21	2.18	Pden_2708	
Pden_2707	3.41	0.41	1.79	0.17	1.90	Pden_2707	
Pden_2706	0.65	0.04	0.37	0.09	1.73	Pden_2706	aldose?
Pden_2705	4.86	0.60	2.75	0.61	1.76	Pden_2705	carbonic anhydrase
Pden_2670	9.06	1.29	2.19	0.39	4.15	Pden_2670	ubiH/F
Pden_2589	2.68	0.29	7.44	5.29	0.36	Pden_2589	ubiG
Pden_2563	3.29	0.72	1.84	0.39	1.79	Pden_2563	b561?
Pden_2551	31.90	4.11	21.42	4.43	1.49	Pden_2551	etfB β subunit
Pden_2550	29.78	4.07	20.84	3.30	1.43	Pden_2550	etfA α subunit
Pden_2545	3.57	0.34	5.70	1.03	0.63	Pden_2545	b561?
Pden_2495	3.74	0.32	2.90	0.23	1.29	Pden_2495	nirN
Pden_2494	4.61	0.71	4.21	0.78	1.10	Pden_2494	nirJ
Pden_2493	4.38	0.84	2.84	0.41	1.54	Pden_2493	nirH
Pden_2492	5.26	1.03	4.38	0.98	1.20	Pden_2492	nirG
Pden_2491	7.01	1.44	5.62	0.67	1.25	Pden_2491	nirD
Pden_2490	9.55	1.13	6.12	1.10	1.56	Pden_2490	nirF
Pden_2489	10.05	3.58	5.11	1.12	1.97	Pden_2489	nirC
Pden_2488	15.34	1.82	6.51	0.84	2.36	Pden_2488	nirE
Pden_2487	60.27	14.43	35.52	3.69	1.70	Pden_2487	nirS
Pden_2486	7.06	0.68	3.62	0.33	1.95	Pden_2486	nirI
Pden_2485	15.66	2.95	3.64	0.34	4.30	Pden_2485	nirX (apbE)

Pden_2484	67.79	23.18	42.95	12.83	1.58	Pden_2484	norC
Pden_2483	44.38	4.51	28.33	3.24	1.57	Pden_2483	norB
Pden_2482	66.42	8.55	40.16	6.30	1.65	Pden_2482	norQ
Pden_2481	50.93	6.81	20.23	2.44	2.52	Pden_2481	norD
Pden_2480	19.65	2.93	8.97	1.41	2.19	Pden_2480	norE
Pden_2479	5.06	1.08	3.03	0.39	1.67	Pden_2479	norF
Pden_2478	5.07	0.76	4.13	1.46	1.23	Pden_2478	nnrR
Pden_2475	2.80	0.40	2.41	0.36	1.16	Pden_2475	ubiC (GntR)
Pden_2363	6.03	0.82	4.18	1.28	1.44	Pden_2363	ppqA
Pden_2362	2.58	0.49	12.59	2.55	0.20	Pden_2362	ppqB
Pden_2361	1.42	0.19	6.96	3.08	0.20	Pden_2361	ppqC
Pden_2360	1.09	0.29	7.26	2.11	0.15	Pden_2360	ppqD
Pden_2359	0.87	0.19	4.84	1.77	0.18	Pden_2359	ppqE
Pden_2358	0.69	0.14	3.12	0.62	0.22	Pden_2358	hypothetical soxZ-like
Pden_2357	0.60	0.06	0.93	0.14	0.64	Pden_2357	abcC
Pden_2356	0.77	0.05	1.25	0.12	0.61	Pden_2356	abcB
Pden_2355	1.86	0.21	2.82	0.46	0.66	Pden_2355	abcA
Pden_2354	19.98	3.06	34.49	5.67	0.58	Pden_2354	flhR luxR 2 comp reg
Pden_2353	10.98	1.38	12.68	1.25	0.87	Pden_2353	hypothetical
Pden_2352	2.92	0.31	3.90	0.88	0.75	Pden_2352	flhS histidine kinase se
Pden_2351	2.43	0.36	5.52	1.27	0.44	Pden_2351	hypothetical
Pden_2350	1.75	0.33	4.70	0.99	0.37	Pden_2350	hypothetical
Pden_2349	5.30	0.67	5.18	1.09	1.02	Pden_2349	SDR cofactor vitamin
Pden_2307	42.94	5.44	31.37	3.82	1.37	Pden_2307	fbcC cyt c1 heme
Pden_2306	27.76	2.93	16.37	1.61	1.70	Pden_2306	fbcB cyt bL/bH heme
Pden_2305	40.32	20.77	30.69	7.58	1.31	Pden_2305	fbcF Rieske 2Fe2S
Pden_2272	0.82	0.06	1.06	0.12	0.77	Pden_2272	p451
Pden_2250	22.08	6.55	7.05	2.06	3.13	Pden_2250	nuoA
Pden_2249	20.32	1.84	10.14	2.44	2.00	Pden_2249	nuoB
Pden_2248	16.05	2.17	9.86	2.06	1.63	Pden_2248	nuoC
Pden_2247	14.78	1.63	10.36	1.49	1.43	Pden_2247	nuoD
Pden_2246	12.74	1.80	12.69	1.88	1.00	Pden_2246	nuoE
Pden_2245	9.07	1.08	8.63	0.97	1.05	Pden_2245	hypothetical

Pden_2244	9.31	1.68	8.69	1.98	1.07	Pden_2244	hypothetical
Pden_2243	9.02	0.95	8.10	0.65	1.11	Pden_2243	nuoF
Pden_2242	8.17	0.74	7.59	0.65	1.08	Pden_2242	hypothetical
Pden_2241	10.82	0.95	12.10	1.07	0.89	Pden_2241	nuoG
Pden_2240	8.41	1.07	7.83	0.96	1.07	Pden_2240	hypothetical
Pden_2239	7.98	0.95	6.07	0.77	1.31	Pden_2239	nuoH
Pden_2238	6.64	1.17	5.73	1.00	1.16	Pden_2238	nuoI
Pden_2237	7.20	1.29	9.16	3.89	0.79	Pden_2237	hypothetical
Pden_2236	5.80	1.09	5.82	1.15	1.00	Pden_2236	Hypothetical
Pden_2235	7.03	0.93	6.52	1.18	1.08	Pden_2235	nuoJ
Pden_2234	7.89	1.60	5.63	1.51	1.40	Pden_2234	nuoK
Pden_2233	11.33	1.29	8.83	1.05	1.28	Pden_2233	nuoL
Pden_2232	7.63	0.85	5.03	0.79	1.52	Pden_2232	nuoM
Pden_2231	12.63	1.31	7.99	1.00	1.58	Pden_2231	nuoN
Pden_2187	2.90	0.38	1.98	0.40	1.46	Pden_2187	D-Lactate dh cyt c
Pden_1954	1.63	0.23	1.14	0.13	1.43	Pden_1954	methyltransferase
Pden_1953	1.64	0.29	1.04	0.19	1.57	Pden_1953	
Pden_1952	4.25	0.78	4.90	1.61	0.87	Pden_1952	G-6-P-1 dh
Pden_1951	2.99	0.94	3.47	0.61	0.86	Pden_1951	G-6-Lactonate
Pden_1950	2.46	0.78	2.64	0.25	0.93	Pden_1950	G-6-P isoenzyme
Pden_1949	3.11	0.39	2.70	0.32	1.15	Pden_1949	L-sorbosone dh
Pden_1948	6.84	1.10	1.95	0.28	3.51	Pden_1948	
Pden_1938	10.17	1.22	14.46	1.66	0.70	Pden_1938	ctaDII
Pden_1937	61.62	10.70	23.85	6.67	2.58	Pden_1937	cycA c550
Pden_1850	1.84	0.40	9.91	1.17	0.19	Pden_1850	FnrP
Pden_1849	4.74	0.59	48.56	19.70	0.10	Pden_1849	UspA
Pden_1848	5.28	0.81	13.18	3.56	0.40	Pden_1848	ccoN subunit I
Pden_1847	5.51	0.67	12.42	2.50	0.44	Pden_1847	ccoO subunit II
Pden_1846	6.37	2.24	18.54	6.76	0.34	Pden_1846	ccoQ subunit IV
Pden_1845	7.84	1.01	19.90	2.48	0.39	Pden_1845	ccoP subunit III
Pden_1844	11.98	2.01	7.70	1.58	1.56	Pden_1844	ccoG 4Fe-4S
Pden_1843	5.53	0.83	5.98	0.93	0.92	Pden_1843	ccoH/FixH
Pden_1842	6.00	0.50	5.56	0.48	1.08	Pden_1842	ccoI cu transp ATPase

Pden_1841	2.69	0.23	1.15	0.09	2.34	Pden_1841	ccoS cbb3 maturation
Pden_1808	29.19	3.69	14.65	3.20	1.99	Pden_1808	cycM
Pden_1807	2.32	0.23	2.05	0.22	1.13	Pden_1807	abc transporter
Pden_1806	1.24	0.15	1.05	0.12	1.19	Pden_1806	abc transporter
Pden_1805	1.52	0.15	1.59	0.25	0.95	Pden_1805	abc transporter
Pden_1804	1.65	0.25	2.07	0.14	0.79	Pden_1804	abc transporter
Pden_1803	1.59	0.16	2.08	0.55	0.77	Pden_1803	Glycosil trnasferase
Pden_1745	2.56	0.36	1.36	0.11	1.88	Pden_1745	b561?
Pden_1415	4.12	0.44	4.65	0.63	0.89	Pden_1415	secF
Pden_1414	1.81	0.40	2.33	0.44	0.78	Pden_1414	
Pden_1413	2.07	0.32	2.66	0.31	0.78	Pden_1413	ccmA
Pden_1412	1.07	0.08	1.52	0.14	0.70	Pden_1412	ccmB
Pden_1411	7.58	1.19	4.02	0.69	1.88	Pden_1411	ccmC
Pden_1410	5.66	0.87	4.14	0.62	1.37	Pden_1410	ccmG
Pden_1409	3.55	0.36	2.42	0.66	1.47	Pden_1409	hisH
Pden_1359	0.98	0.17	0.87	0.16	1.12	Pden_1359	Copper binding
Pden_1189	0.35	0.06	0.31	0.04	1.13	Pden_1189	Rieske 2Fe2S
Pden_1188	0.39	0.06	0.61	0.13	0.65	Pden_1188	ferredoxin NADH
Pden_1187	0.28	0.04	0.37	0.04	0.77	Pden_1187	mandelate racemase
Pden_1186	0.25	0.03	0.74	0.09	0.34	Pden_1186	fdhA
Pden_1161	0.42	0.07	0.37	0.07	1.15	Pden_1161	assimilaory nad-formate dh?
Pden_0893	1.03	0.08	11.37	3.88	0.09	Pden_0893	ccpA cyt c peroxidase
Pden_0625	4.58	0.57	2.47	0.34	1.86	Pden_0625	ubiA
Pden_0572	15.55	1.70	5.27	0.63	2.95	Pden_0572	sdhB (Fe-S)
Pden_0571	41.36	16.80	14.46	5.25	2.86	Pden_0571	hypothetical
Pden_0570	57.52	15.06	17.07	4.06	3.37	Pden_0570	hypothetical
Pden_0569	20.21	1.61	10.21	1.09	1.98	Pden_0569	sdhA
Pden_0568	11.94	3.31	7.42	1.73	1.61	Pden_0568	sdhD
Pden_0567	11.96	2.14	7.66	1.57	1.56	Pden_0567	sdhC
Pden_0566	2.77	0.26	1.87	0.16	1.48	Pden_0566	Sdh cyt b552
Pden_0511	41.30	5.39	5.25	0.84	7.86	Pden_0511	cycH
Pden_0432	33.31	6.53	10.91	4.59	3.05	Pden_0432	ctaIV
Pden_0425	13.73	1.12	5.27	0.75	2.60	Pden_0425	etfD

Pden_0023	0.59	0.09	2.71	0.41	0.22	Pden_0023	xoxI rhodanese
Pden_0022	0.78	0.12	4.68	1.10	0.17	Pden_0022	xoxJ quinole membr.
Pden_0021	1.22	0.31	12.30	4.22	0.10	Pden_0021	cycB c553i putative
Pden_0020	1.86	0.47	12.27	2.42	0.15	Pden_0020	xoxF PPQ
Pden_0019	1.72	0.20	3.56	0.71	0.48	Pden_0019	fghA
Pden_0018	1.91	0.36	3.77	0.76	0.51	Pden_0018	N-acetyltransferase
Pden_0017	3.14	0.38	6.03	0.69	0.52	Pden_0017	clpP
Pden_0016	1.15	0.26	11.06	3.43	0.10	Pden_0016	flhA
Pden_0015	2.39	0.95	45.28	16.53	0.05	Pden_0015	gfa activation factor
Pden_0014	0.63	0.07	2.04	0.50	0.31	Pden_0014	hypothetical
Pden_0013	0.50	0.05	1.08	0.12	0.46	Pden_0013	coproporphyrinogen ox
Pden_0012	1.12	0.17	1.53	0.37	0.73	Pden_0012	endoribonuclease
Pden_0011	2.30	0.27	2.57	0.46	0.90	Pden_0011	pyrophosphatase
Pden_0010	2.46	0.35	2.86	0.61	0.86	Pden_0010	rph ribonuclease PH

Pden_4448	4.94	1.23	3.10	0.70	1.59	Pden_4448	ABC
Pden_4449	1.54	0.14	2.03	1.40	0.76	Pden_4449	nasC
Pden_4450	0.43	0.05	0.22	0.05	1.91	Pden_4450	nasH
Pden_4451	0.38	0.06	0.21	0.03	1.80	Pden_4451	nasG
Pden_4452	0.38	0.07	0.39	0.11	0.98	Pden_4452	nasB
Pden_4453	0.48	0.08	0.97	0.34	0.49	Pden_4453	nasA
Pden_4454	0.51	0.05	0.52	0.14	0.98	Pden_4454	nasS
Pden_4455	0.62	0.12	0.46	0.07	1.35	Pden_4455	nasT

3.4.2 Microarray gene expression dataset for the Δf*nrP* strain

Note: The microarray dataset for the Δ*fnrP* strain is enclosed in the attached CD-ROM

3.4.3 Respirome gene expression dataset for the Δ*nnrR* strain

Georgios Giannopoulos

Respirome Relative Expression WT *vs* . Δ*nnrR*
20140214_nnrR_wt

Gene ID	Δ*nnrR*		WT		Ratio	Gene ID	Annotation
	Average	SE Norm	Average	SE Norm	Δ*nnrR* /WT		
Pden_5108	7.17	0.69	1.58	0.58	4.53	Pden_5108	qoxA ba3 subunit II
Pden_5107	5.64	0.47	1.32	0.16	4.27	Pden_5107	qoxB ba3 subunit I
Pden_5106	4.52	0.45	1.07	0.26	4.23	Pden_5106	qoxC ba3 subunit III
Pden_5105	3.13	0.31	1.05	0.21	2.97	Pden_5105	qoxD ba3 subunit IV
Pden_5104	3.90	0.62	2.52	0.38	1.55	Pden_5104	surF1 surfeit family
Pden_5063	0.79	0.11	1.23	0.31	0.64	Pden_5063	Alcohol dh
Pden_5062	0.30	0.03	0.41	0.08	0.73	Pden_5062	L-Lactate dh
Pden_5013	0.54	0.06	0.34	0.03	1.59	Pden_5013	peroxidase
Pden_4938	0.49	0.07	0.54	0.14	0.90	Pden_4938	ubiX
Pden_4877	0.51	0.08	0.51	0.09	1.00	Pden_4877	L-lactate dh
Pden_4866	0.36	0.03	0.64	0.19	0.56	Pden_4866	Malate/lactate dh
Pden_4855	0.44	0.07	0.42	0.04	1.04	Pden_4855	Malate/lactate dh
Pden_4738	0.39	0.05	0.44	0.07	0.89	Pden_4738	mauN ferrodoxin nap
Pden_4737	1.25	0.22	0.47	0.07	2.63	Pden_4737	mauM ferrodoxin nap
Pden_4736	0.27	0.03	0.35	0.16	0.76	Pden_4736	mauG diheme c perox
Pden_4735	0.64	0.15	0.33	0.05	1.93	Pden_4735	mauJ
Pden_4734	0.26	0.03	0.23	0.03	1.15	Pden_4734	mauC amicyamin
Pden_4733	0.25	0.03	0.33	0.09	0.77	Pden_4733	mauA small subnit
Pden_4732	0.70	0.11	0.58	0.37	1.20	Pden_4732	mauD accessory prot
Pden_4731	0.23	0.03	0.19	0.09	1.20	Pden_4731	mauE ma utilization
Pden_4730	0.45	0.08	0.31	0.04	1.48	Pden_4730	mauB MADH heavy ch
Pden_4729	0.46	0.07	0.40	0.06	1.15	Pden_4729	mauF big subunit
Pden_4728	0.46	0.06	0.30	0.07	1.50	Pden_4728	lysR
Pden_4727	2.35	0.20	1.68	0.17	1.40	Pden_4727	sndhA
Pden_4726	0.45	0.09	0.87	0.27	0.52	Pden_4726	mscS-aldose dh
Pden_4724	1.38	0.29	8.37	6.94	0.16	Pden_4724	GreA kinase regulat

Pden_4723	0.91	0.10	1.69	0.12	0.54	Pden_4723	napC
Pden_4722	1.21	0.19	3.20	0.57	0.38	Pden_4722	napB cyt c
Pden_4721	1.06	0.08	2.47	0.17	0.43	Pden_4721	napA catalytic
Pden_4720	1.00	0.20	1.69	0.40	0.59	Pden_4720	napD
Pden_4719	3.05	0.17	3.46	0.36	0.88	Pden_4719	napE
Pden_4718	0.75	0.15	0.71	0.26	1.06	Pden_4718	Hypotherical
Pden_4700	0.71	0.14	0.49	0.06	1.46	Pden_4700	CytCP
Pden_4699	0.73	0.10	0.26	0.06	2.81	Pden_4699	B651
Pden_4511	3.68	0.56	3.92	3.21	0.94	Pden_4511	ubiE
Pden_4510	3.61	0.65	1.55	0.13	2.33	Pden_4510	ubiB
Pden_4397	1.15	0.14	2.67	0.37	0.43	Pden_4397	hypothetical
Pden_4396	7.43	0.64	2.69	0.34	2.76	Pden_4396	cysN/cysC
Pden_4395	8.54	1.04	2.11	0.63	4.05	Pden_4395	cysD
Pden_4394	0.98	0.26	0.35	0.07	2.80	Pden_4394	hypothetical protein
Pden_4393	0.64	0.07	1.03	0.26	0.63	Pden_4393	glpD homodimeric quin
Pden_4392	0.53	0.05	0.96	0.13	0.55	Pden_4392	ABC transporter ATP
Pden_4391	0.60	0.06	0.86	0.14	0.70	Pden_4391	ABC transporter ATP
Pden_4390	0.80	0.12	0.69	0.18	1.15	Pden_4390	ABC transporter
Pden_4389	1.38	0.27	0.72	0.11	1.92	Pden_4389	ABC transporter
Pden_4388	1.24	0.24	1.68	0.60	0.74	Pden_4388	hypothetical
Pden_4387	5.08	0.67	6.18	0.49	0.82	Pden_4387	ABC transporter
Pden_4386	1.02	0.10	1.43	0.09	0.72	Pden_4386	glycerol kinase
Pden_4356	1.00	0.15	1.96	0.54	0.51	Pden_4356	b561?
Pden_4323	0.37	0.05	0.49	0.04	0.75	Pden_4323	DprA
Pden_4322	3.34	0.44	4.48	0.75	0.75	Pden_4322	TldD
Pden_4321	19.84	2.29	23.27	4.32	0.85	Pden_4321	ctaC subunit II
Pden_4320	6.99	1.18	9.20	1.67	0.76	Pden_4320	ctaB
Pden_4319	9.70	1.89	11.26	2.13	0.86	Pden_4319	hypothetical
Pden_4318	7.05	1.15	6.87	0.99	1.03	Pden_4318	ctaG assembly protein
Pden_4317	11.21	2.08	7.76	1.57	1.45	Pden_4317	ctaE subunit III
Pden_4316	2.77	0.19	2.81	0.27	0.99	Pden_4316	surF1
Pden_4315	3.76	0.38	5.19	0.67	0.72	Pden_4315	thrC
Pden_4238	1.14	0.12	1.00	0.13	1.14	Pden_4238	narR

Pden_4237	7.70	0.58	7.62	1.02	1.01	Pden_4237	narK
Pden_4236	18.22	0.95	16.36	1.30	1.11	Pden_4236	narI
Pden_4235	18.58	1.64	15.64	1.65	1.19	Pden_4235	narH
Pden_4234	31.20	5.72	30.10	3.99	1.04	Pden_4234	narJ
Pden_4233	18.61	2.30	14.28	2.53	1.30	Pden_4233	narG
Pden_4232	18.24	3.89	21.46	3.12	0.85	Pden_4232	
Pden_4231	7.66	1.97	16.02	2.80	0.48	Pden_4231	
Pden_4230	1.31	0.19	6.06	1.20	0.22	Pden_4230	nnrS
Pden_4226	1.30	0.17	8.98	4.18	0.14	Pden_4226	ubiD
Pden_4225	0.40	0.03	6.66	1.34	0.06	Pden_4225	ubiD
Pden_4222	4.16	0.89	36.79	29.56	0.11	Pden_4222	pasZ
Pden_4221	3.28	0.72	11.79	5.70	0.28	Pden_4221	nosC
Pden_4220	3.17	0.29	8.24	1.96	0.38	Pden_4220	nosR
Pden_4219	23.99	2.07	24.30	1.89	0.99	Pden_4219	nosZ
Pden_4218	7.67	1.62	12.45	4.95	0.62	Pden_4218	nosD
Pden_4217	2.40	0.32	5.50	0.88	0.44	Pden_4217	nosF
Pden_4216	3.59	0.51	6.89	0.85	0.52	Pden_4216	nosY
Pden_4215	3.77	0.51	5.37	0.58	0.70	Pden_4215	nosL
Pden_4214	3.37	0.47	6.15	0.87	0.55	Pden_4214	nosX
Pden_4161	0.58	0.09	2.96	2.70	0.20	Pden_4161	hypothetical
Pden_4160	0.78	0.10	1.03	0.32	0.76	Pden_4160	soxH
Pden_4159	0.81	0.11	0.94	0.09	0.86	Pden_4159	soxG β-lactamase
Pden_4158	0.76	0.12	0.87	0.13	0.87	Pden_4158	SoxF FAD disulfide ox
Pden_4157	0.47	0.03	0.57	0.11	0.83	Pden_4157	SoxE cyt c-I
Pden_4156	0.34	0.03	0.71	0.17	0.47	Pden_4156	soxD cyt c551
Pden_4155	0.81	0.15	0.47	0.03	1.71	Pden_4155	soxC Mo-oxidase
Pden_4154	0.29	0.02	0.43	0.04	0.67	Pden_4154	soxB Rden
Pden_4153	1.30	0.19	2.24	0.38	0.58	Pden_4153	socA di-heme cyt c
Pden_4152	2.41	0.55	1.75	0.43	1.38	Pden_4152	soxZ sulfur oxidase
Pden_4151	2.63	0.57	2.78	0.47	0.95	Pden_4151	soxY sulfur oxidase
Pden_4150	0.86	0.09	1.32	0.37	0.65	Pden_4150	soxX cyt c
Pden_4149	0.29	0.05	0.42	0.06	0.68	Pden_4149	soxW thioredoxin
Pden_4148	0.23	0.02	0.77	0.12	0.31	Pden_4148	soxV cyt c

Pden_4147	0.50	0.07	0.65	0.22	0.78	Pden_4147	soxS cyt c biogenesis
Pden_4146	1.33	0.30	2.06	0.50	0.65	Pden_4146	ArsR regulatory
Pden_4145	1.55	0.12	2.31	0.25	0.67	Pden_4145	Hypothetical (YeeD)
Pden_4075	9.98	2.25	3.41	0.84	2.93	Pden_4075	L-Lactate dh cyt c
Pden_4012	0.40	0.03	0.63	0.04	0.63	Pden_4012	ATPase
Pden_4011	0.35	0.03	0.25	0.05	1.43	Pden_4011	d subunit II
Pden_4010	0.46	0.08	0.37	0.07	1.24	Pden_4010	bd subunit I
Pden_4009	0.43	0.06	0.47	0.06	0.93	Pden_4009	Mo-pterin α subunit
Pden_4008	0.30	0.02	0.43	0.04	0.70	Pden_4008	σ54 Fis transcript reg
Pden_4007	0.47	0.04	0.54	0.11	0.86	Pden_4007	Membrane sensor kina
Pden_3985	0.50	0.06	0.70	0.08	0.71	Pden_3985	p450
Pden_3978	5.33	0.86	3.73	0.55	1.43	Pden_3978	ccmH
Pden_3977	6.69	0.57	5.93	0.53	1.13	Pden_3977	ccmF
Pden_3974	4.65	0.76	4.60	0.84	1.01	Pden_3974	cycJ
Pden_3942	8.35	1.06	7.47	1.22	1.12	Pden_3942	ubiH/F
Pden_3543	0.42	0.04	0.49	0.04	0.85	Pden_3543	Short Chain Reductase
Pden_3286	0.56	0.10	0.48	0.07	1.16	Pden_3286	b561?
Pden_3113	0.56	0.06	0.36	0.08	1.54	Pden_3113	hypothetical
Pden_3112	1.78	0.57	0.70	0.28	2.56	Pden_3112	hypE
Pden_3111	0.61	0.06	0.79	0.09	0.78	Pden_3111	hypD
Pden_3110	0.42	0.11	0.57	0.15	0.74	Pden_3110	hypC
Pden_3109	0.65	0.08	0.44	0.09	1.47	Pden_3109	hypothetical
Pden_3108	0.71	0.04	0.74	0.13	0.96	Pden_3108	hypB
Pden_3107	0.35	0.05	0.86	0.08	0.41	Pden_3107	hypA
Pden_3106	0.33	0.05	1.07	0.35	0.31	Pden_3106	HupK
Pden_3105	0.56	0.07	0.39	0.04	1.46	Pden_3105	HupJ Rubredoxin
Pden_3104	0.70	0.15	0.62	0.08	1.12	Pden_3104	HupH
Pden_3103	0.56	0.11	0.51	0.08	1.09	Pden_3103	HupG
Pden_3102	0.56	0.07	1.20	0.20	0.46	Pden_3102	hupF
Pden_3101	0.71	0.07	0.44	0.05	1.59	Pden_3101	HupD
Pden_3100	0.53	0.10	0.21	0.04	2.50	Pden_3100	hupC cyt b
Pden_3099	0.45	0.05	0.32	0.13	1.38	Pden_3099	hupE
Pden_3098	0.32	0.03	0.23	0.02	1.41	Pden_3098	hupL large subunit

Pden_3097	0.29	0.03	0.19	0.02	1.50	Pden_3097	hupA/S small subunit
Pden_3096	0.57	0.04	0.74	0.08	0.78	Pden_3096	hupF maturation
Pden_3095	1.04	0.07	1.08	0.09	0.96	Pden_3095	hupV
Pden_3094	1.28	0.14	1.18	0.14	1.09	Pden_3094	hupU
Pden_3093	1.18	0.08	1.27	0.13	0.93	Pden_3093	hupT hist-kinase sensor
Pden_3028	6.74	0.82	4.07	0.47	1.66	Pden_3028	ctaDI
Pden_3027	2.34	0.24	4.56	3.27	0.51	Pden_3027	ahpD Alkylhydroperoxidase
Pden_3026	4.71	1.05	10.61	8.68	0.44	Pden_3026	Hypothetical
Pden_3025	11.08	2.20	13.13	9.88	0.84	Pden_3025	NO & morphol reg
Pden_3024	2.42	0.66	6.38	3.92	0.38	Pden_3024	nsrR NO repressor
Pden_3023	1.09	0.16	5.21	4.96	0.21	Pden_3023	hypothetical
Pden_3022	1.41	0.27	1.93	1.18	0.73	Pden_3022	sdhB
Pden_3021	1.45	0.22	1.34	0.49	1.08	Pden_3021	sdhC
Pden_3020	0.98	0.15	1.07	0.28	0.92	Pden_3020	sdhD
Pden_3019	1.14	0.17	1.27	0.33	0.90	Pden_3019	Signal protein
Pden_3003	11.09	2.01	3.22	0.53	3.44	Pden_3003	mxaD
Pden_3002	5.86	0.71	1.42	0.19	4.12	Pden_3002	mxaL
Pden_3001	8.79	1.51	2.26	0.43	3.89	Pden_3001	mxaK
Pden_3000	12.20	2.16	2.83	0.63	4.32	Pden_3000	mxaC von Willebr.
Pden_2999	9.17	1.84	2.53	0.40	3.62	Pden_2999	mxaA
Pden_2998	8.55	1.32	2.82	0.55	3.03	Pden_2998	mxaS unknown
Pden_2997	16.99	2.86	5.26	0.97	3.23	Pden_2997	mxaR unknown
Pden_2996	165.38	37.37	35.87	9.81	4.61	Pden_2996	mxaI β subunit
Pden_2995	43.56	7.10	12.32	2.73	3.54	Pden_2995	mxaG cyt C-L c551i
Pden_2994	30.00	4.27	12.91	4.11	2.32	Pden_2994	mxaJ binding prot.
Pden_2993	64.97	7.30	26.06	9.43	2.49	Pden_2993	mxaF α subunit
Pden_2929	2.43	0.32	2.89	0.66	0.84	Pden_2929	lctR Lactate Regulator
Pden_2928	1.18	0.24	1.24	0.09	0.96	Pden_2928	Dld D-Lactate dh
Pden_2927	2.24	0.19	3.80	0.57	0.59	Pden_2927	lctP L-Lactate permeas
Pden_2859	1.81	0.13	1.60	0.30	1.13	Pden_2859	LysR family
Pden_2858	11.74	2.22	4.53	1.36	2.59	Pden_2858	Fdh γ subunit
Pden_2857	13.04	1.18	6.24	1.56	2.09	Pden_2857	NADH dh (quinone)
Pden_2856	22.35	2.00	6.61	0.80	3.38	Pden_2856	Fdh α subunit

Pden_2855	13.59	2.23	4.18	0.71	3.26	Pden_2855	FdhD family
Pden_2854	11.37	0.90	2.14	0.30	5.31	Pden_2854	NAD-fdh δ subunit
Pden_2853	2.14	0.20	2.49	0.23	0.86	Pden_2853	ribonuclease R
Pden_2830	4.82	0.81	9.47	2.05	0.51	Pden_2830	4Fe-4S
Pden_2829	1.72	0.11	0.96	0.12	1.79	Pden_2829	fdnG α subunit
Pden_2828	1.85	0.19	1.13	0.26	1.64	Pden_2828	fdnH β subunit
Pden_2827	1.53	0.15	1.23	0.23	1.25	Pden_2827	fdnI γ subunit
Pden_2826	2.62	0.39	2.59	0.36	1.01	Pden_2826	fdhE
Pden_2825	0.74	0.06	0.89	0.08	0.83	Pden_2825	selB cysteine enlog.
Pden_2824	1.80	0.14	1.06	0.09	1.69	Pden_2824	aldo/keto reductase
Pden_2710	0.91	0.09	1.85	0.63	0.49	Pden_2710	SndhB
Pden_2709	1.98	0.22	1.80	0.16	1.10	Pden_2709	NAP (P)
Pden_2708	1.47	0.18	1.60	0.19	0.92	Pden_2708	
Pden_2707	1.70	0.15	1.68	0.15	1.01	Pden_2707	
Pden_2706	0.49	0.04	0.39	0.09	1.28	Pden_2706	aldose?
Pden_2705	3.61	0.40	2.55	0.56	1.42	Pden_2705	carbonic anhydrase
Pden_2670	1.94	0.28	1.98	0.36	0.98	Pden_2670	ubiH/F
Pden_2589	2.95	0.55	6.85	4.71	0.43	Pden_2589	ubiG
Pden_2563	2.94	0.71	1.73	0.35	1.70	Pden_2563	b561?
Pden_2551	13.96	1.70	18.85	4.00	0.74	Pden_2551	etfB β subunit
Pden_2550	16.42	2.25	18.61	3.03	0.88	Pden_2550	etfA α subunit
Pden_2545	5.71	0.50	5.31	0.90	1.08	Pden_2545	b561?
Pden_2495	0.58	0.06	2.64	0.19	0.22	Pden_2495	nirN
Pden_2494	0.29	0.05	3.74	0.55	0.08	Pden_2494	nirJ
Pden_2493	0.16	0.02	2.55	0.33	0.06	Pden_2493	nirH
Pden_2492	1.11	0.28	3.93	0.79	0.28	Pden_2492	nirG
Pden_2491	0.19	0.02	4.87	0.56	0.04	Pden_2491	nirD
Pden_2490	0.30	0.04	5.27	0.85	0.06	Pden_2490	nirF
Pden_2489	0.14	0.04	4.45	0.88	0.03	Pden_2489	nirC
Pden_2488	0.52	0.09	5.58	0.76	0.09	Pden_2488	nirE
Pden_2487	0.86	0.12	33.09	3.69	0.03	Pden_2487	nirS
Pden_2486	0.59	0.08	3.17	0.37	0.19	Pden_2486	nirI
Pden_2485	0.32	0.05	3.16	0.38	0.10	Pden_2485	nirX (apbE)

Pden_2484	4.29	0.49	38.76	11.58	0.11	Pden_2484	norC
Pden_2483	2.95	0.31	25.00	2.89	0.12	Pden_2483	norB
Pden_2482	3.72	0.42	35.09	5.71	0.11	Pden_2482	norQ
Pden_2481	2.05	0.21	17.46	2.10	0.12	Pden_2481	norD
Pden_2480	1.89	0.60	7.77	1.40	0.24	Pden_2480	norE
Pden_2479	1.32	0.38	2.74	0.32	0.48	Pden_2479	norF
Pden_2478	2.32	0.41	3.75	1.33	0.62	Pden_2478	nnrR
Pden_2475	1.22	0.19	2.24	0.29	0.55	Pden_2475	ubiC (GntR)
Pden_2363	2.57	0.48	3.78	1.15	0.68	Pden_2363	ppqA
Pden_2362	6.81	1.01	11.71	2.17	0.58	Pden_2362	ppqB
Pden_2361	4.92	0.66	6.69	2.68	0.73	Pden_2361	ppqC
Pden_2360	4.40	1.61	7.00	1.97	0.63	Pden_2360	ppqD
Pden_2359	2.43	0.35	4.71	1.56	0.52	Pden_2359	ppqE
Pden_2358	1.43	0.20	3.05	0.54	0.47	Pden_2358	hypothetical soxZ-like
Pden_2357	1.24	0.11	0.95	0.13	1.31	Pden_2357	abcC
Pden_2356	1.03	0.09	1.26	0.12	0.82	Pden_2356	abcB
Pden_2355	2.18	0.27	2.70	0.41	0.81	Pden_2355	abcA
Pden_2354	15.40	2.87	30.47	4.97	0.51	Pden_2354	flhR luxR 2 comp reg
Pden_2353	6.97	0.95	11.34	1.09	0.61	Pden_2353	hypothetical
Pden_2352	2.12	0.19	3.63	0.80	0.58	Pden_2352	flhS histidine kinase se
Pden_2351	3.76	0.54	5.17	1.13	0.73	Pden_2351	hypothetical
Pden_2350	3.15	0.19	4.47	0.90	0.70	Pden_2350	hypothetical
Pden_2349	3.10	0.42	4.73	1.00	0.65	Pden_2349	SDR cofactor vitamin
Pden_2307	44.15	5.17	28.44	3.54	1.55	Pden_2307	fbcC cyt c1 heme
Pden_2306	32.69	3.90	14.62	1.35	2.24	Pden_2306	fbcB cyt bL/bH heme
Pden_2305	63.31	9.91	28.36	7.05	2.23	Pden_2305	fbcF Rieske 2Fe2S
Pden_2272	0.81	0.09	1.06	0.12	0.76	Pden_2272	p451
Pden_2250	13.81	2.22	6.29	1.82	2.20	Pden_2250	nuoA
Pden_2249	16.52	1.07	9.06	2.18	1.82	Pden_2249	nuoB
Pden_2248	18.02	2.38	8.85	1.79	2.04	Pden_2248	nuoC
Pden_2247	16.01	2.04	9.30	1.30	1.72	Pden_2247	nuoD
Pden_2246	18.53	3.40	11.39	1.66	1.63	Pden_2246	nuoE
Pden_2245	7.35	0.76	7.80	0.85	0.94	Pden_2245	hypothetical

Pden_2244	6.94	1.91	7.80	1.75	0.89	Pden_2244	hypothetical
Pden_2243	8.17	0.91	7.32	0.57	1.12	Pden_2243	nuoF
Pden_2242	10.47	0.95	6.90	0.57	1.52	Pden_2242	hypothetical
Pden_2241	11.76	0.97	10.87	0.95	1.08	Pden_2241	nuoG
Pden_2240	11.43	1.63	7.12	0.86	1.61	Pden_2240	hypothetical
Pden_2239	11.94	1.59	5.53	0.68	2.16	Pden_2239	nuoH
Pden_2238	10.35	1.77	5.25	0.89	1.97	Pden_2238	nuoI
Pden_2237	5.72	1.03	8.25	3.42	0.69	Pden_2237	hypothetical
Pden_2236	6.42	1.04	5.32	1.01	1.21	Pden_2236	Hypothetical
Pden_2235	13.30	2.38	5.96	1.05	2.23	Pden_2235	nuoJ
Pden_2234	8.90	1.39	5.12	1.34	1.74	Pden_2234	nuoK
Pden_2233	14.00	1.28	7.96	0.89	1.76	Pden_2233	nuoL
Pden_2232	8.16	0.68	4.60	0.71	1.77	Pden_2232	nuoM
Pden_2231	6.71	0.67	7.16	0.86	0.94	Pden_2231	nuoN
Pden_2187	2.30	0.24	1.88	0.37	1.22	Pden_2187	D-Lactate dh cyt c
Pden_1954	0.58	0.08	1.12	0.11	0.52	Pden_1954	methyltransferase
Pden_1953	0.48	0.09	1.02	0.16	0.47	Pden_1953	
Pden_1952	2.03	0.20	4.45	1.40	0.46	Pden_1952	G-6-P-1 dh
Pden_1951	2.12	0.35	3.22	0.54	0.66	Pden_1951	G-6-Lactonate
Pden_1950	1.61	0.14	2.49	0.23	0.65	Pden_1950	G-6-P isoenzyme
Pden_1949	3.71	0.37	2.54	0.28	1.46	Pden_1949	L-sorbosone dh
Pden_1948	7.07	0.84	1.82	0.25	3.89	Pden_1948	
Pden_1938	20.32	1.68	12.97	1.39	1.57	Pden_1938	ctaDII
Pden_1937	146.18	31.82	24.84	7.60	5.88	Pden_1937	cycA c550
Pden_1850	6.72	0.65	9.54	1.03	0.70	Pden_1850	FnrP
Pden_1849	13.81	1.79	43.41	18.26	0.32	Pden_1849	UspA
Pden_1848	16.19	1.42	12.04	3.21	1.34	Pden_1848	ccoN subunit I
Pden_1847	20.66	3.47	11.36	2.18	1.82	Pden_1847	ccoO subunit II
Pden_1846	31.21	10.62	16.85	6.00	1.85	Pden_1846	ccoQ subunit IV
Pden_1845	22.00	2.19	17.96	2.19	1.23	Pden_1845	ccoP subunit III
Pden_1844	15.45	2.37	6.99	1.42	2.21	Pden_1844	ccoG 4Fe-4S
Pden_1843	6.05	0.89	5.45	0.82	1.11	Pden_1843	ccoH/FixH
Pden_1842	4.51	0.37	5.09	0.44	0.89	Pden_1842	ccoI cu transp ATPase

Pden_1841	3.07	0.13	1.13	0.08	2.72	Pden_1841	ccoS cbb3 maturation
Pden_1808	23.97	3.03	12.96	2.80	1.85	Pden_1808	cycM
Pden_1807	3.04	0.30	1.96	0.20	1.55	Pden_1807	abc transporter
Pden_1806	2.06	0.28	1.04	0.11	1.98	Pden_1806	abc transporter
Pden_1805	2.16	0.28	1.56	0.26	1.38	Pden_1805	abc transporter
Pden_1804	1.81	0.10	2.00	0.13	0.90	Pden_1804	abc transporter
Pden_1803	1.12	0.13	1.98	0.50	0.57	Pden_1803	Glycosil trnasferase
Pden_1745	1.37	0.11	1.30	0.10	1.05	Pden_1745	b561?
Pden_1415	5.64	0.73	4.29	0.56	1.31	Pden_1415	secF
Pden_1414	1.98	0.31	2.24	0.40	0.88	Pden_1414	
Pden_1413	1.52	0.19	2.52	0.27	0.60	Pden_1413	ccmA
Pden_1412	1.16	0.17	1.50	0.14	0.77	Pden_1412	ccmB
Pden_1411	6.57	1.02	3.68	0.62	1.79	Pden_1411	ccmC
Pden_1410	5.44	0.54	3.81	0.54	1.43	Pden_1410	ccmG
Pden_1409	3.17	0.36	2.27	0.60	1.40	Pden_1409	hisH
Pden_1359	0.91	0.20	0.87	0.16	1.05	Pden_1359	Copper binding
Pden_1189	0.63	0.12	0.32	0.04	1.99	Pden_1189	Rieske 2Fe2S
Pden_1188	0.26	0.03	0.61	0.12	0.43	Pden_1188	ferredoxin NADH
Pden_1187	0.35	0.06	0.37	0.04	0.93	Pden_1187	mandelate racemase
Pden_1186	0.59	0.07	0.75	0.09	0.79	Pden_1186	fdhA
Pden_1161	0.49	0.09	0.38	0.08	1.30	Pden_1161	assimilaory nad-formate dh?
Pden_0893	9.03	0.90	10.92	3.69	0.83	Pden_0893	ccpA cyt c peroxidase
Pden_0625	2.37	0.28	2.27	0.30	1.04	Pden_0625	ubiA
Pden_0572	14.17	1.73	4.74	0.56	2.99	Pden_0572	sdhB (Fe-S)
Pden_0571	14.01	4.51	12.73	4.57	1.10	Pden_0571	hypothetical
Pden_0570	11.77	2.64	14.96	3.52	0.79	Pden_0570	hypothetical
Pden_0569	15.32	1.28	9.11	0.96	1.68	Pden_0569	sdhA
Pden_0568	9.99	2.94	6.68	1.53	1.50	Pden_0568	sdhD
Pden_0567	9.39	1.89	6.88	1.39	1.37	Pden_0567	sdhC
Pden_0566	1.90	0.13	1.78	0.14	1.07	Pden_0566	Sdh cyt b552
Pden_0511	6.92	0.78	4.63	0.78	1.50	Pden_0511	cycH
Pden_0432	15.47	0.85	9.65	4.08	1.60	Pden_0432	ctaIV
Pden_0425	8.19	0.68	4.75	0.68	1.73	Pden_0425	etfD

Pden_0023	2.52	0.22	2.77	0.36	0.91	Pden_0023	xoxI rhodanese
Pden_0022	4.65	0.59	4.62	0.93	1.01	Pden_0022	xoxJ quinole membr.
Pden_0021	14.97	2.19	11.80	3.53	1.27	Pden_0021	cycB c553i putative
Pden_0020	7.39	0.73	11.51	2.08	0.64	Pden_0020	xoxF PPQ
Pden_0019	4.50	0.53	3.43	0.62	1.31	Pden_0019	fghA
Pden_0018	3.22	0.38	3.56	0.70	0.90	Pden_0018	N-acetyltransferase
Pden_0017	6.37	1.03	5.63	0.61	1.13	Pden_0017	clpP
Pden_0016	9.22	0.78	10.66	2.93	0.86	Pden_0016	flhA
Pden_0015	30.50	5.32	41.41	14.00	0.74	Pden_0015	gfa activation factor
Pden_0014	1.17	0.10	2.05	0.50	0.57	Pden_0014	hypothetical
Pden_0013	0.80	0.06	1.10	0.11	0.73	Pden_0013	coproporphyrinogen ox
Pden_0012	2.10	0.34	1.52	0.34	1.38	Pden_0012	endoribonuclease
Pden_0011	3.17	0.37	2.46	0.41	1.29	Pden_0011	pyrophosphatase
Pden_0010	2.83	0.45	2.70	0.55	1.05	Pden_0010	rph ribonuclease PH
Pden_4448	1.07	0.19	2.79	0.68	0.38	Pden_4448	ABC
Pden_4449	0.66	0.12	1.87	1.25	0.35	Pden_4449	nasC
Pden_4450	0.36	0.07	0.23	0.05	1.55	Pden_4450	nasH
Pden_4451	0.53	0.20	0.22	0.03	2.43	Pden_4451	nasG
Pden_4452	0.39	0.05	0.40	0.11	0.96	Pden_4452	nasB
Pden_4453	0.97	0.14	0.97	0.31	1.00	Pden_4453	nasA
Pden_4454	0.41	0.06	0.53	0.14	0.77	Pden_4454	nasS
Pden_4455	0.29	0.04	0.47	0.07	0.61	Pden_4455	nasT

3.4.4 Microarray gene expression dataset for the Δ*nnrR* strain

Note: The microarray dataset for the Δ*nnrR* strain is enclosed in the attached CD-ROM

References

Bergaust, L., Y. Mao, L. R. Bakken and A. Frostegard (2010). "Denitrification response patterns during the transition to anoxic respiration and posttranscriptional effects of suboptimal pH on nitrogen oxide reductase in *Paracoccus denitrificans*." Appl. Environ. Microbiol. **76**(19): 6387-6396.

Bueno, E., D. J. Richardson, E. J. Bedmar and M. J. Delgado (2009). "Expression of *Bradyrhizobium japonicum cbb$_3$* terminal oxidase under denitrifying conditions is subjected to redox control." FEMS Microbiology Letters **298**(1): 20-28.

Crack, J. C., A. J. Jervis, A. A. Gaskell, G. F. White, J. Green, A. J. Thomson and N. E. Le Brun (2008). "Signal perception by FNR: the role of the iron-sulfur cluster." Biochem Soc Trans **36**(Pt 6): 1144-1148.

Crack, J. C., M. R. Stapleton, J. Green, A. J. Thomson and N. E. Le Brun (2013). "Mechanism of [4Fe-4S](Cys)4 cluster nitrosylation is conserved among NO-responsive regulators." J Biol Chem **288**(16): 11492-11502.

Cruz-Ramos, H., J. Crack, G. Wu, M. N. Hughes, C. Scott, A. J. Thomson, J. Green and R. K. Poole (2002). NO sensing by FNR: regulation of the Escherichia coli NO-detoxifying flavohaemoglobin, Hmp.

de Gier, J. W. L., M. Lubben, W. N. M. Reijnders, C. A. Tipker, D. J. Slotboom, R. J. M. van Spanning, A. H. Stouthamer and J. van der Oost (1994). "The terminal oxidases of *Paracoccus denitrificans*." Molecular Microbiology **13**(2): 183-196.

Felgate, H., G. Giannopoulos, M. J. Sullivan, A. J. Gates, T. A. Clarke, E. Baggs, G. Rowley and D. J. Richardson (2012). "The impact of copper, nitrate and carbon status on the emission of nitrous oxide by two species of bacteria with biochemically distinct denitrification pathways." Environ Microbiol **14**(7): 1788-1800.

Hutchings, M. I., N. Shearer, S. Wastell, R. J. M. van Spanning and S. Spiro (2000). "Heterologous NNR-mediated nitric oxide signaling in *Escherichia coli*." Journal of Bacteriology **182**(22): 6434-6439.

Hutchings, M. I. and S. Spiro (2000). "The nitric oxide regulated nor promoter of *Paracoccus denitrificans*." Microbiology **146**(10): 2635-2641.

Jervis, A. J., J. C. Crack, G. White, P. J. Artymiuk, M. R. Cheesman, A. J. Thomson, N. E. Le Brun and J. Green (2009). "The O_2 sensitivity of the transcription factor FNR is controlled by Ser24 modulating the kinetics of [4Fe-4S] to [2Fe-2S] conversion." Proceedings of the National Academy of Sciences **106**(12): 4659-4664.

Kolesov, G., Z. Wunderlich, O. N. Laikova, M. S. Gelfand and L. A. Mirny (2007). "How gene order is influenced by the biophysics of transcription regulation." Proceedings of the National Academy of Sciences **104**(35): 13948-13953.

Preisig, O., R. Zufferey, L. Thöny-Meyer, C. A. Appleby and H. Hennecke (1996). "A high-affinity *cbb*$_3$-type cytochrome oxidase terminates the symbiosis-specific respiratory chain of *Bradyrhizobium japonicum*." Journal of Bacteriology **178**(6): 1532-1538.

Saunders, N. F. W., J. J. Hornberg, W. N. M. Reijnders, H. V. Westerhoff, S. de Vries and R. J. M. van Spanning (2000). "The NosX and NirX Proteins of *Paracoccus denitrificans* are functional homologues: their role in maturation of nitrous oxide reductase." Journal of Bacteriology **182**(18): 5211-5217.

Sullivan, M. J., A. J. Gates, C. Appia-Ayme, G. Rowley and D. J. Richardson (2013). "Copper control of bacterial nitrous oxide emission and its impact on vitamin B12-dependent metabolism." Proceedings of the National Academy of Sciences.

van Spanning, R. J. M., A. P. N. de Boer, W. N. M. Reijnders, H. V. Westerhoff, A. H. Stouthamer and J. van der Oost (1997). "FnrP and NNR of *Paracoccus denitrificans* are both members of the FNR family of transcriptional activators but have distinct roles in respiratory adaptation in response to oxygen limitation." Molecular Microbiology **23**(5): 893-907.

Van Spanning, R. J. M., E. Houben, W. N. M. Reijnders, S. Spiro, H. V. Westerhoff and N. Saunders (1999). "Nitric oxide is a signal for NNR-mediated transcription activation in *Paracoccus denitrificans*." Journal of Bacteriology **181**(13): 4129-4132.

Veldman, R., W. N. M. Reijnders and R. J. M. van Spanning (2006). "Specificity of FNR-type regulators in *Paracoccus denitrificans*." Biochemical Society Transactions **34**(1): 94-96.

Wood, N. J., T. Alizadeh, S. Bennett, J. Pearce, S. J. Ferguson, D. J. Richardson and J. W. Moir (2001). "Maximal expression of membrane-bound nitrate reductase in *Paracoccus* is induced by nitrate via a third FNR-like regulator named NarR." J Bacteriol **183**(12): 3606-3613.

Wood, N. J., T. Alizadeh, D. J. Richardson, S. J. Ferguson and J. W. Moir (2002). "Two domains of a dual-function NarK protein are required for nitrate uptake, the first step of denitrification in *Paracoccus pantotrophus*." Mol Microbiol **44**(1): 157-170.

4. The metabolic and transcriptional profiles of the narR mutant of P. denitrificans in anaerobic CSTR cultures.

A possible role of *narR* in the transcriptional regulation of denitrification in *P. denitrificans*. Investigations of metabolic and transcriptional profiles in steady state cultures (CSTR) of a mutant strain (PD2345) having a non-functional *narR* gene (pden_4238).

Contents

4.1 Introduction

Previously, the anaerobic denitrification metabolic and transcriptional profiles of a strain having a non-functional copy of *fnrP* (Δ*fnrP*) of *P. denitrificans* and one having a non-functional copy of *nnrR* (Δ*nnrR*) were established in continuous cultures using CSTR and analysed with metabolic and transcriptional analysis.

Firstly, it was observed that during continuous culture of the Δ*fnrP* strain of *P. denitrificans* (PD2921), 5 mM succinate was consumed and ~4 mM nitrate was reduced to di-nitrogen anaerobically in the steady state phase of growth. The consumption quotient for nitrate during continuous culture of the Δ*fnrP* strain was ~700 $\mu mol.g^{-1}.h^{-1}$ $N\text{-}NO_3^-$, which was 500 $\mu mol.g^{-1}.h^{-1}$ lower that the control treatment of the wild type strain of *P. denitrificans* (PD1222). The continuous culture had a steady state biomass density of 0.31 $g.L^{-1}$, towards the end of the incubation. Results show that the Δ*fnrP* mutant was able to reduce nitrate to di-nitrogen at a lower rate than that of the wild type strain (PD1222). Additionally, it was found that genes expressing the nitrate reductase (*narG*; pden_4233) were repressed and genes encoding nitrite (*nirS*; pden_2487), nitric oxide (*norB*; pden_2483) and nitrous oxide reductase (*nosZ*; pden_4219) were induced in the Δ*fnrP* strain when compared to the control strain. The above transcriptional observation confirms that FnrP acts an activator for *narG.* Additionally, a novel role of FnrP was demonstrated, whereby FnrP acts as a repressor by preventing the activation of the genes encoding nitrite (*nirS*; pden_2487), nitric oxide (*norB*; pden_2483) and nitrous oxide reductase (*nosZ*; pden_4219).

Secondly, it was observed that, towards the end of the continuous culture incubation of the Δ*nnrR* stain of *P. denitrificans* (PD7771), 5 mM succinate was consumed and ~18 mM nitrate was reduced to nitrite, which accumulated upon the depletion of the remaining dissolved oxygen till the end of the incubation. The consumption quotient of nitrate was 4500 $N\text{-}NO_3^-$ $\mu mol.g^{-1}.h^{-1}$ which was 3.7 times higher than the control treatment (PD1222). The biomass density towards the end of the incubation (steady-state phase) was 0.21 $g.L^{-1}$ or 16% lower that the control treatment. The Δ*nnrR* strain balanced the excess electron supply from the oxidation of succinate (~48 mM electron equivalents) by enhancing the activity of nitrate reductase (~40 mM electron equivalents for the reduction of 20 mM nitrate). The complete reduction of two moles of nitrate to one mole of di-nitrogen is a 10 electron reduction;

however the reduction of nitrate to nitrite is a 2 electron process. The relatively increased reduction of nitrate, compensated for the lack of nitrite, nitric oxide and nitrous oxide reduction when compared to the wild type strain treatment. Therefore, the Δ*nnrR* strain was unable to fully denitrify and nitrite accumulated in the reaction vessel with a noticeable decrease in the biomass of the continuous culture. Furthermore, transcriptional analysis revealed that the expression of the gene encoding nitrate reductase was highly induced (*narG*; pden_4233), consistent with the increased nitrate consumption. The target genes for nitrite (*nirS*; pden_2487), nitric oxide (*norB*; pden_2483) were highly repressed and for nitrous oxide reductase (*nosZ*; pden_4219) 3 fold repression was observed when compared to the control treatment. The above results confirm that NnrR acts as a transcriptional activator for the *nir* and *nor* gene cluster. However, the above results also demonstrate a novel role of NnrR repressing gene expression by preventing (competition for the same binding site) the activation of genes expressing nitrate and nitrous oxide reductase (*narG,* pden_4233; *nosZ*, pden_4219).

During denitrification, the metabolic products nitrite, nitric oxide and nitrous oxide could potentially accumulate to concentrations that may act as a cytotoxin if not reduced efficiently to di-nitrogen and subsequently exported from the cell. *P. denitrificans* is able to respire on nitrate anaerobically and effectively reduce nitrogen oxyanions to di-nitrogen utilising specific oxidoreductases. The kinetic and intracellular concentration differences of the denitrification reductases could be transcriptionally overcome by precisely regulating the respective gene expression (see Chapter 1 and 3). This hypothesis is possible because the TF involved in the regulation of denitrification have a similar helix-turn-helix DNA binding domain and could potentially recognise similar motifs and so compete against each other in positive and negative fashions depending on the gene being regulated.

Another transcription factor with a highly similar C terminal domain is NarR. The NarR C terminal domain contains a helix-turn-helix (HTH) motif with 70% similarity to NNR helix-turn-helix motif. An amino-acid sequence alignment of NarR showed similarity with other homologues of the CRP/ FNR family, FnrP and NnrR. The TF FNR which senses oxygen is transcriptionally active when oxygen levels are low and NNR is proposed to sense nitric oxide and activate the *nir* and *nor* gene cluster however little is known about the TF NnrR. Wood *et al.* (2001) demonstrated using a *narR* mutant in *Paracoccus pantotrophus* and *lacZ*

fusions that *narR* is instrumental for the expression of *nark*, which encodes a nitrate/nitrite transporter. Additionally it was demonstrated that *narR* is located upstream of the *narKGHJI operon* and that NarR binds to the promoter region of *narK*. Further promoter investigations indicate that NarR negatively regulates its own expression and is repressed under anaerobic conditions. The mechanism of the nitrate/nitrite response is not clear, but NarR can also be activated by azide indicating the possibility that NarR could be a metalloprotein (Wood *et al.* 2001, Wood *et al.* 2002). *P. denitrificans* is closely related to *P. pantotrophus* and contains a NarR homologue also found in the genome. Analysis of the *P. denitrificans* and *P. pantotrophus* NarR has shown that they lack the four cysteines that anchor an [4Fe-4S] cluster in the N terminal region of FnrP that responds to oxygen. Additionally the N terminal region of NarR is different to the region of FnrP (see 1. Introduction). The last observation may indicate a different mode of RNA polymerase binding other than the one involved in the FnrP-RNA polymerase interaction.

To conclude it is therefore possible that small concentrations of nitrate or nitrite formed by existing *nar* or *nap* operon activity will induce *narR* activity and subsequently enhance *nar* operon expression. This could only occur when oxygen levels are low to avoid the deleterious reaction of nitrogen oxyanions with oxygen radicals (see Introduction chapter). In this chapter, a mutant strain of *P. denitrificans* was constructed by deleting the intragenic region of *narR*. The metabolic and transcriptional profile of Δ*narR* (PD2345) cultures in anaerobicity was analysed using the well-established continuous culture technique (CSTR).

4.2 Results

4.2.1 Construction of a *narR* deficient strain of *P. denitrificans.*

To investigate the mode of action of the TF NarR, a strain having a non-functional disrupted *narR* gene in *P. denitrificans* was designed and constructed (Figure 1). The flanking regions of the 5' and 3' end of *narR* (pden_4238) were PCR amplified with specifically designed primers containing a restriction site (Table 1) and cloned to the suicide plasmid vector pK18mob*SacB*. Subsequently, this vector was transformed into competent *E. coli* 808 cells and mobilised to *P. denitrificans* with the helper strain *E. coli* pRK2013 by tri-parental mating. An unmarked region of *narR* was deleted by allelic replacement using

pK18mobS*acB*. A single cross-over recombination event was selected using rifampicin. Trans-conjugants were screened for double cross-over events by sucrose resistance (6% w/v) as explained in the Materials and Methods. Several random isolates were picked and the deletion event was verified by PCR amplification and DNA gel electrophoresis (Figure 2) and plasmid digestion (Figure 3). Four of those isolates were confirmed by sequencing. Isolate PD2345 had a 559 bp unmarked deletion with 600 and 826 bp remaining in the 5' and 3' flanking region. This isolate (PD2345) was used for further metabolic and transcriptional studies.

Table 1 Oligonucleotide primers used for the construction and verification of PD2345 mutation in *narR* (pden_4238).

Primer ID	Direction	Sequence[1]	Purpose
narR_5flnF1	Forward	GAGAATTCgtccagacacccaggatcag	Cloning 5' flanking region of pden_4238
narR_5flnR1	Reverse	GATCTAGAgggaaagacctggtcatagg	
narR_3flnF1	Forward	GATCTAGAcccaacaccctgctggatac	Cloning 3' flanking region of pden_4238
narR_3flnR1	Reverse	GACTGCAgaaagcggtcctggaagtc	
narR_ChkF1	Forward	gcatcgggggaaaggaact	Verification of PD2345 mutation in pden_4238
narR_ChkR1	Reverse	gaaagtggaacgggctcag	

[1] Capitalized nucleotide bases indicate restriction sites

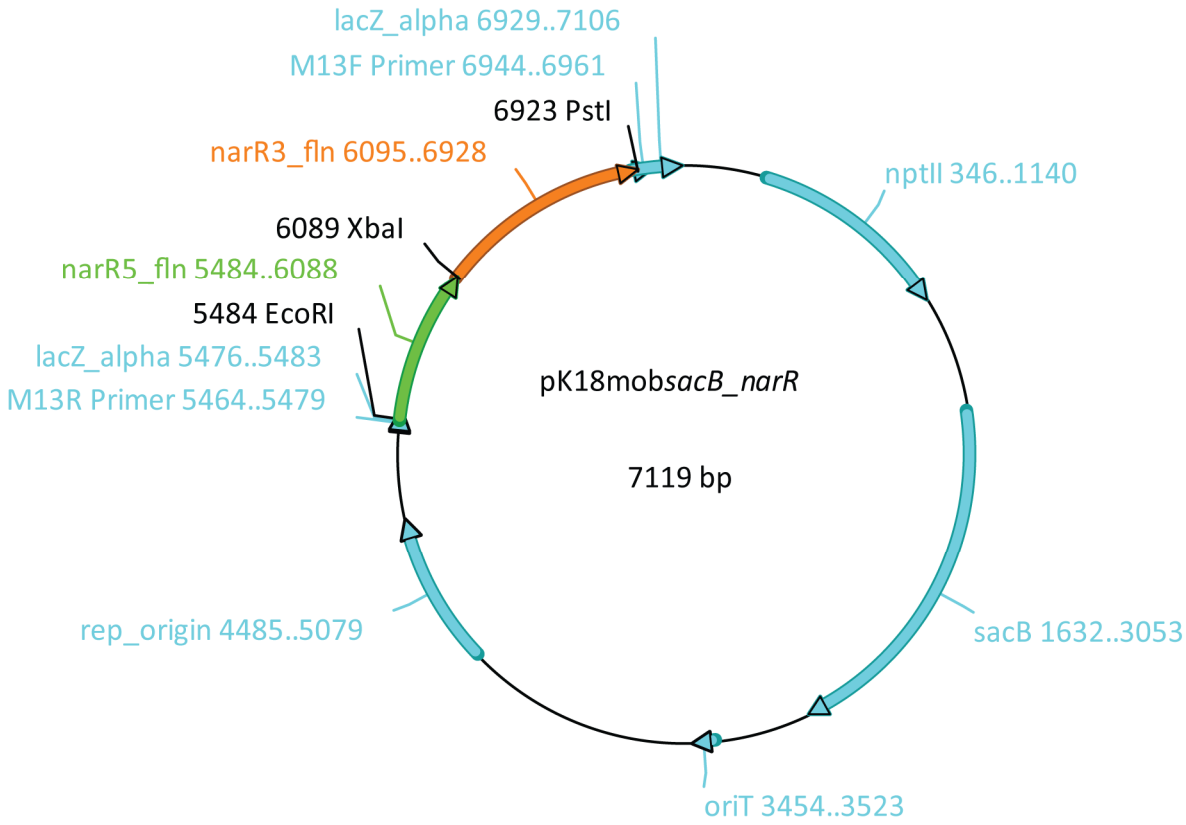

Figure 1 Graphical map of the pK18mob*sacB_narR* used to delete the intragenic region of *narR* (pden_4238) by allelic gene exchange. Features of the vector are indicated; *ntp*II denotes gene for kanamycin resistance, *sacB* levansucrase, oriT mobility site, rep-origin replication of origin site, M13F (M13 Forward) and M13R (M13 Reverse) universal primer sites, *LacZ* β-galactosidase and the restriction sites for the 5' and 3' flanking regions of *narR* are also indicated with *Eco*RI, *Xba*I and *Pst*I.

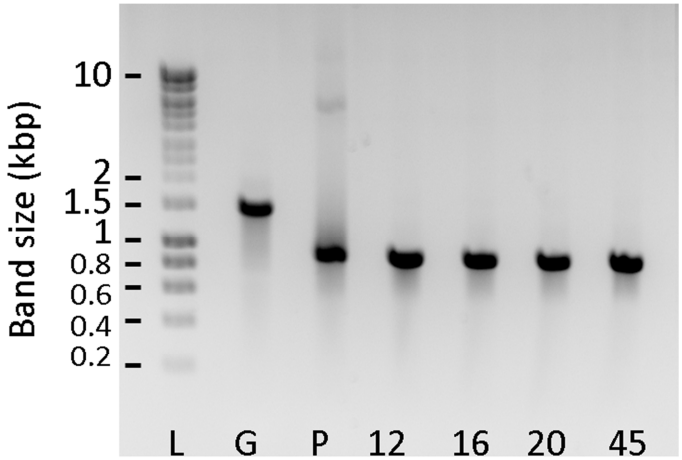

Figure 2 Agarose gel confirming the deletion of the intragenic region (~800 bp) of *narR*. L denotes the DNA ladder, G the genomic DNA standard (PD1222), P the pK18mob*SacB-narR* and 12, 16, 20 and 45 four isolates positive for an unmarked deletion.

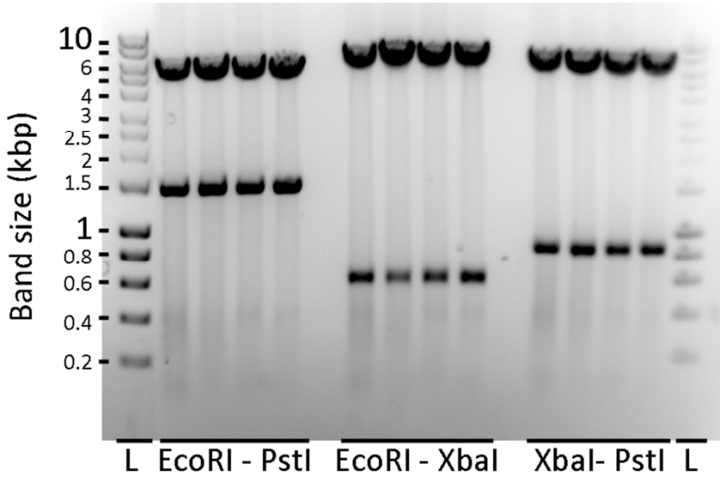

Figure 3 Agarose gel showing the digestion products of pK18mob*SacB-narR* with *Eco*RI and *Pst*I, *Eco*RI and *Xba*I and with *Xba*I and *Pst*I. L denotes the DNA ladder in kbp. Digestion with restriction endonucleases is denoted with the respective restriction site below the gel lane.

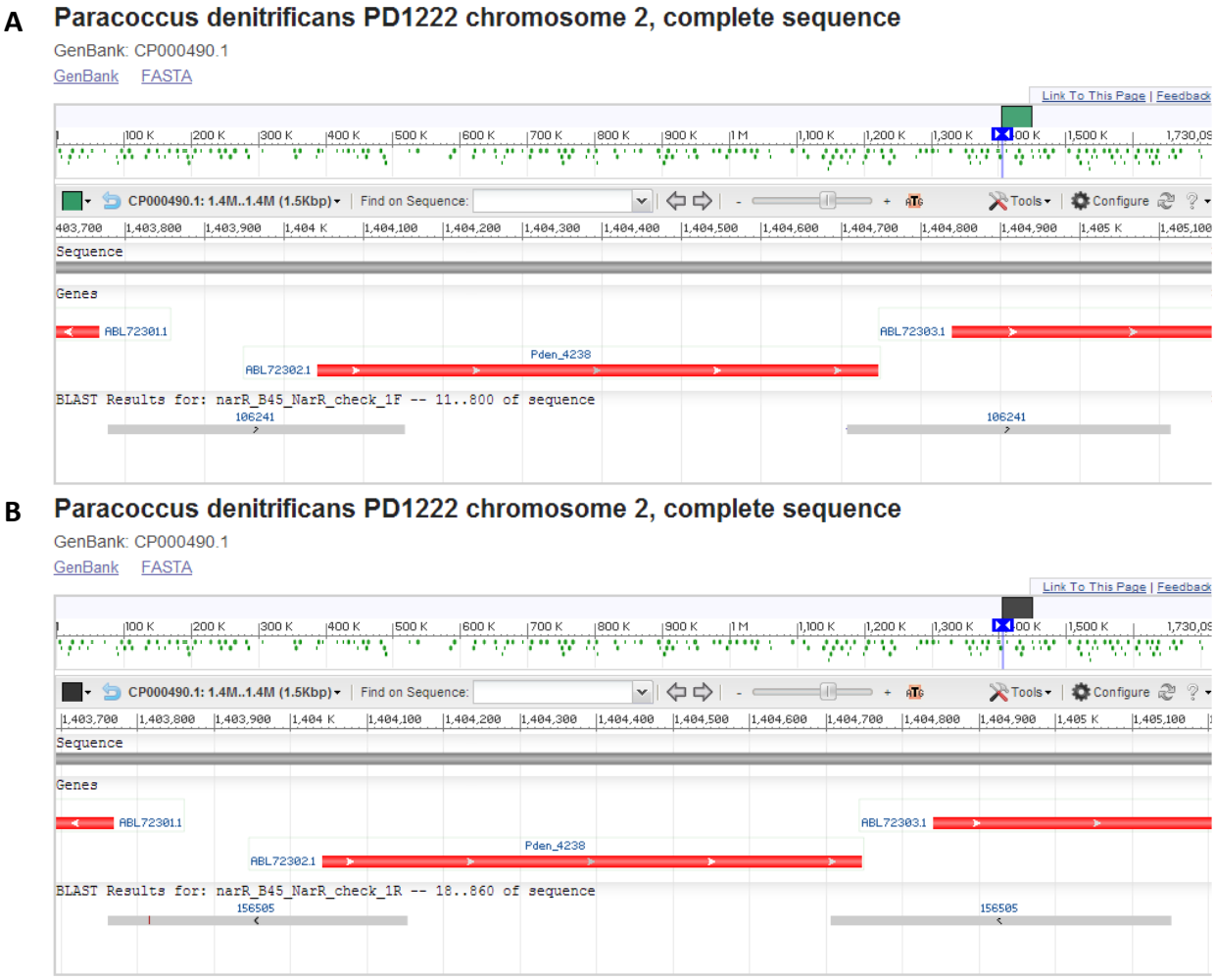

Figure 4 Nucleotide alignment of the sequenced isolate of Δ*narR* (PD2345). Panel A shows the sequence alingment in forward direction with 97% sequence identity to the *narR* gene (pden_4238; accession: 4582788) of *P. denitrificans* with 559 bp missing from the intragenic region (grey bar, 106241); Panel B shows reverse direction sequencing alignment with 98% sequence identity to the *narR* gene of *P. denitrificans* with 559 bp missing from the intragenic region (grey bar, 156505). The sequencing results of each isolate are attached at the end of this chapter.

4.2.2 Investigating the denitrification profiles of the *narR* mutant of *P. denitrificans.*

Following the successful construction and validation of a Δ*narR* strain of *P. denitrificans* by sequencing, a set of batch experiments was carried out to determine the growth phenotype of the Δ*narR* strain. The Δ*narR* isolates were tested for aerobic growth in minimal medium containing either nitrate or nitrite. The Δ*narR* isolates had a comparable productivity (Y) to the wild type strain (PD1222) $Y_{succinate}^{max}$ of 0.14 OD.mM^{-1} after 24 hours. However, the anaerobic growth of the Δ*narR* strain was hindered when nitrate was present as an alternative terminal electron acceptor during 24 hours of incubation (Figure 6 A). Contrary to this, the anaerobic growth was unaffected in the Δ*narR* strains when cells were cultured in a nitrite containing medium (Figure 6 A and B). Anaerobic batch cultures of Δ*narR* isolates containing nitrate were further incubated for an extended period of 44 h (Figure 6 B). Interestingly, at the end of this period, it was observed that the Δ*narR* batch cultures reached an OD of ~0.6 AU which is comparable to the wild type strain cultures (PD1222).

After a prolonged lag phase of adaptation lasting approximately 20 hours, bubbles accumulated on the surface of the medium indicating that the Δ*narR* isolates were able to denitrify during anaerobic growth. This observation suggests other possible mechanisms of nitrate reduction are expressed in the Δ*narR* strain not controlled by the TF NarR or perhaps not involving the membrane bound nitrate reductase (*nar* gene cluster). An alternative nitrate reductase which is found in the *P. denitrificans* genome is the periplasmic nitrate reductase (*nap* operon). The hypothesis, that the periplasmic nitrate reductase could be induced and initiate the first step of nitrate reduction will also be tested in this chapter.

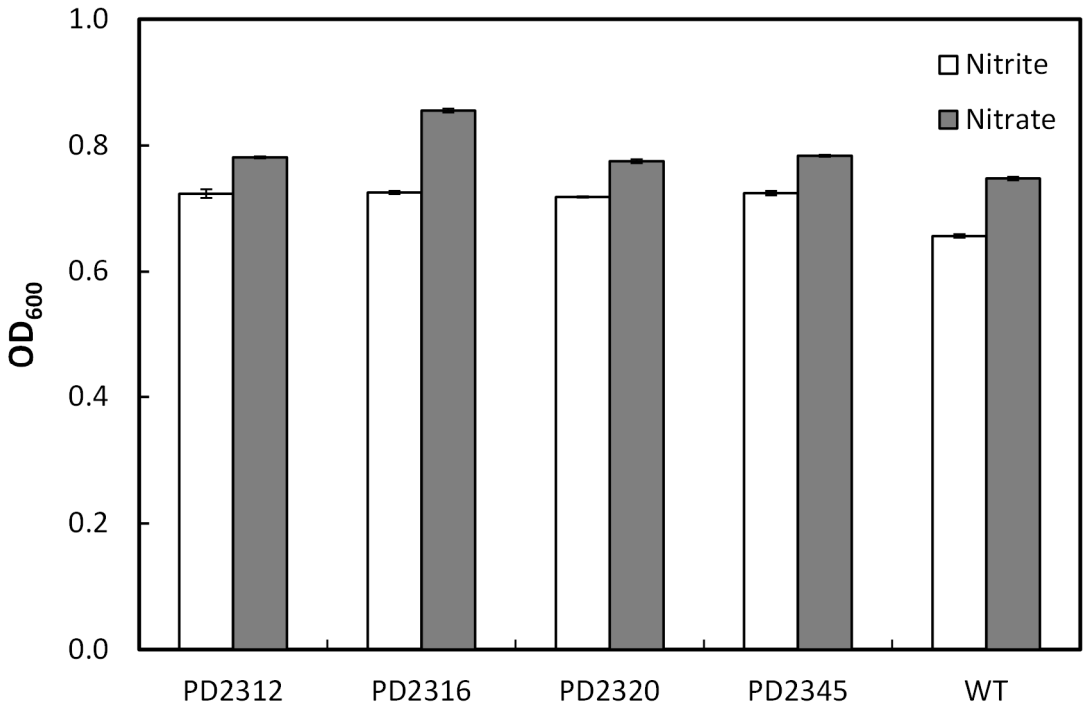

Figure 5 Final OD (600 nm) readings of the Δ*narR* (PD2312, PD2316, PD2320 and PD2345) and wild type (WT) strains of *P. denitrificans* (PD1222) in aerobic batch incubation (15 hours) with nitrate (shaded) and nitrite (clear) (n=3 error bars denote ±SEM).

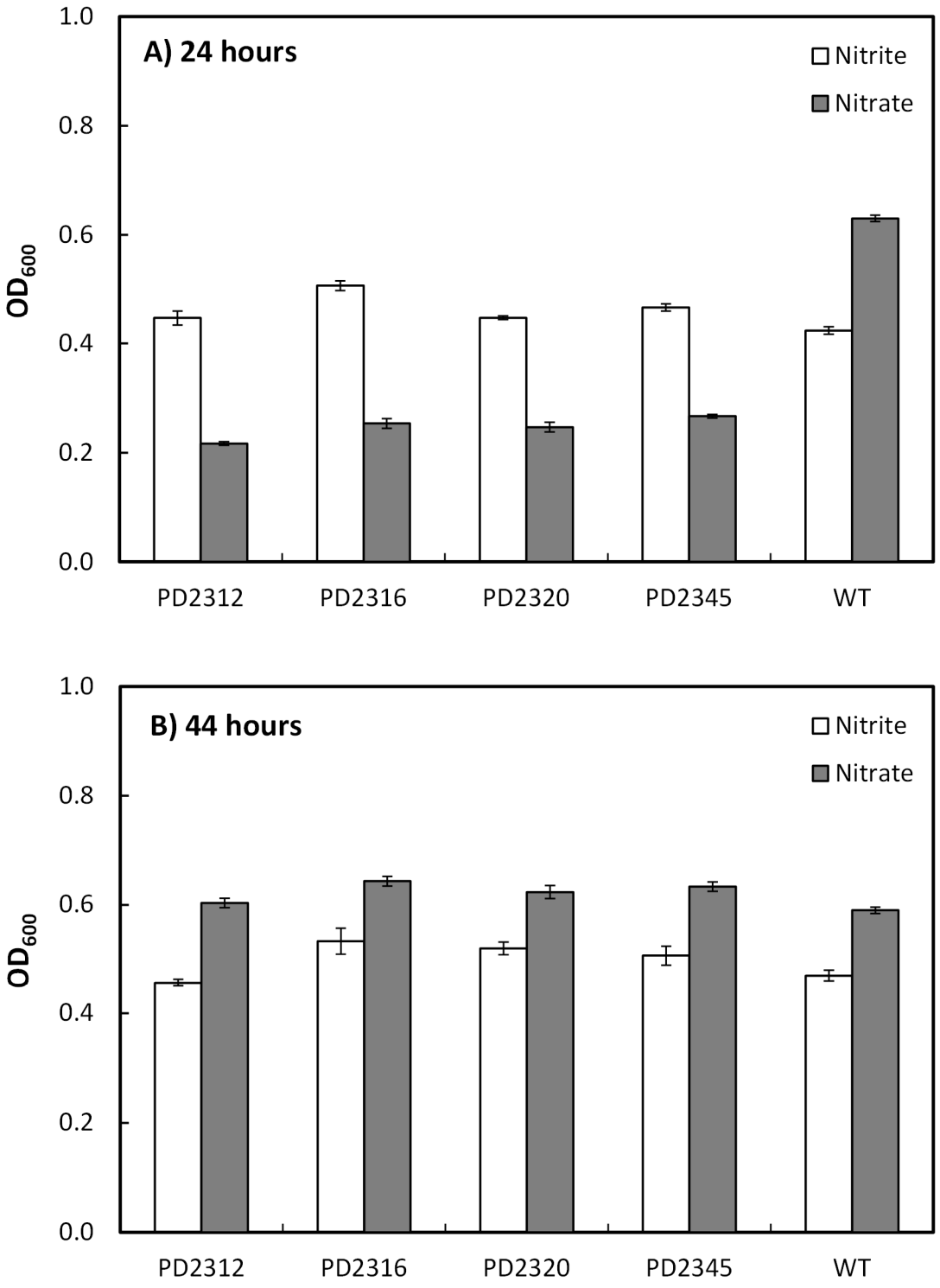

Figure 6 Average OD measurements (600 nm) of the Δ*narR* (PD2312, PD2316, PD2320 and PD2345) and wild type (WT) strains of *P. denitrificans* (PD1222) in anaerobic batch incubations with nitrate (shaded) and nitrite (clear box). Panel A illustrates the OD readings taken after 24 hours and panel B illustrates the final OD readings taken after 44 hours (n=3 error bars denote ±SEM).

To further elucidate the nitrate reduction pathway CTSR experiments with the Δ*narR* strain were performed. As for previous experiments, the temperature and the pH were 30 ^{o}C and 7.5, respectively, throughout the 120 h incubation. The biomass density reached its maximum during the initial aerobic batch phase of the incubation in the CSTR system. Upon the initiation of continuous feed at 20 hours, the oxygen supply was restricted and the remaining dissolved oxygen was consumed by basal respiration (Figure 7 B). After ~80 hours of continuous culture incubation the biomass of the Δ*narR* treatment remained at comparable levels until the end of the experiment (120 hours). At steady state the biomass of this culture was ~0.3 mg.ml^{-1} (Figure 7 A). This last phase of continuous culture in the CSTR system is defined as steady state based on the unchanged biomass. The extracellular nitrate concentration was ~22 mM at the beginning of the incubation and was reduced to ~16 mM in the steady-state (80-120 hours of incubation). It is interesting to point out that the reduction of nitrate did not coincide with the oxygen depletion (~20 hours) but it was observed at a later stage ~40 hours (Figure 7 C). The concentration of nitrite and nitrous oxide concentration in the reaction vessel was below detection limits.

The Δ*narR* culture had a biomass quotient of 0.16 g.L^{-1}.h^{-1} which was 0.04 g.L^{-1}.h^{-1} higher than that of the control strain (PD1222), towards the end of the incubation. The nitrate, nitrite and nitrous oxide consumption quotients were comparable to the control treatment; ~1190 µmol.g^{-1}.h^{-1}. However, the nitrate reduction in the Δ*narR* treatment was relatively delayed by ~20 hours when compared to the control (Figure 7 C). During that period (between the 20 and 40 hour time point) the rate of nitrate reduction was 0 µmol.g^{-1}.h^{-1} as the extracellular nitrate concentration remained at 22 mM. This indicates a phenotype that is unable to respire on nitrate and required a prolonged period of anaerobicity to adapt and alter the regulatory network to respond to the external stimulus. This biochemical adaptation will be further investigated with a whole genome transcriptional approach in the 4.3 Discussion section of this chapter.

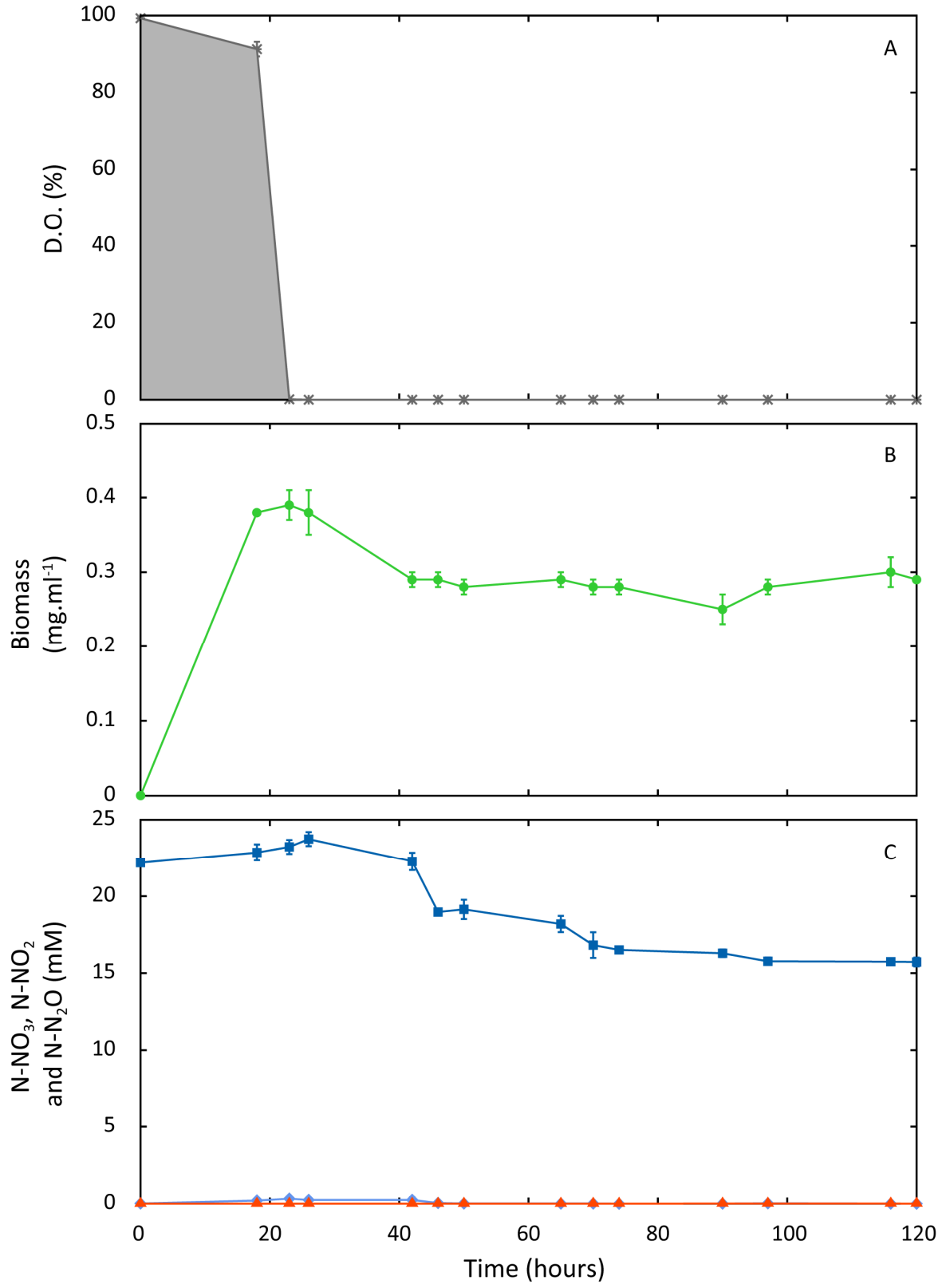

Figure 7 Anaerobic continuous culture of *P. denitrificans* (PD2345) lacking a functional copy of *narR* (Pden_4238) at 30 °C in CSTR. A) Average dissolved oxygen (D.O.) concentration of the culture, B) Average biomass (●) of the culture and C) Average nitrate (■), nitrite (◆) and nitrous oxide (▲) concentration of the culture (n=3; error bars denote standard error).

Table 2 The consumption and production quotient rates of the Δ*narR* continuous culture treatment in CSTR*.

#	Strain	Temp. °C	pH	D h^{-1}	OD	±SE	X $g.L^{-1}$	±SE	D/X $L.g^{-1}.h^{-1}$	±SE	qX $g.L^{-1}.h^{-1}$	±SE
1	PD1222	30	7.5	0.05	0.52	0.02	0.25	0.01	0.22	0.01	0.12	0.01
2	PD2345	30	7.5	0.05	0.52	0.01	0.29	0.01	0.18	0.01	0.16	0.01

Table continues below.

#	Strain	Temp. °C	$[NO_3]_0$ µM	±SE	$[NO_3]_t$ µM	±SE	$[NO_2]_t$ µM	±SE	$[N_2O]_t$ µM	±SE	$[N_2]_t$ µM	±SE
1	PD1222	30	20723	1096	15159	115	4745	44	0.3	0.11	5475	1078
2	PD2345	30	22240	174	15723	289	6.67	3.33	1.19	1.19	6509	405

Table continues below.

#	Strain	Temp. °C	$[NO_3]_c$ $\mu mol.g^{-1}.h^{-1}$	±SE	$[NO_2]_p$ $\mu mol.g^{-1}.h^{-1}$	±SE	$[NO_2]_c$ $\mu mol.g^{-1}.h^{-1}$	±SE	$[N_2O]_p$ $\mu mol.g^{-1}.h^{-1}$	±SE	$[N_2]_p$ $\mu mol.g^{-1}.h^{-1}$	±SE
1	PD1222	30	1215	274	18	9.2	1196	283	0.2	0.03	1196	283
2	PD2345	30	1188	66	1.23	0.6	1187	66	0.2	0.22	1187	67

* The quotient rates were calculated based on the average value of the last three data points taken at the steady state phase of the incubation. The index number (#) in front of each row indicates the treatment; where 1 indicates the control treatment with the wild type strain of *P. denitrificans* (PD1222) and 2 the test treatment with the Δ*narR* strain of *P. denitrificans* (PD2345)

4.2.3 Transcriptional analyses with RT-PCR of the *narR* mutant of *P. denitrificans* in anaerobic CSTR cultures

At the end of the incubation period (120 hours) a sample was taken from each culture to assess if the CSTR cultures were contaminated. A sample was used to evaluate the culture purity by sub-culturing 10^{-4} 10^{-5} and 10^{-6} dilutions on LB agar or minimal media agar petri-dishes and incubating them aerobically and anaerobically in oxoid jars. The colonies formed appeared phenotypically identical to *P. denitrificans* and contaminant free. Besides this phenotypical confirmation, culture samples were taken from each Δ*narR* treatment and were assessed with colony PCR specific to the intragenic *narR* deletion to test for mutant purity in the culture. The resulting PCR product was amplified with the 5' and 3' flanking region *narR* primers. Samples A, B and C in figure 10 had a smaller product size (~900) when compared to genomic DNA (~1500), this indicates a Δ*narR* strain with a ~550 bp intragenic deletion.

At the end of the CSTR incubation and steady state phase (120 hours) samples were taken for total RNA extraction from each Δ*narR* continuous culture treatment. Total RNA was extracted as described in the Materials and Methods and DNA contamination was assessed with standard PCR. Figure 8 depicts the electrophoresis of the PCR products on an agarose gel stained with ethidium bromide. The lack of bands in lanes A and B indicates the absence of any DNA contamination. Lane S shows the PCR product with genomic DNA used as a positive control.

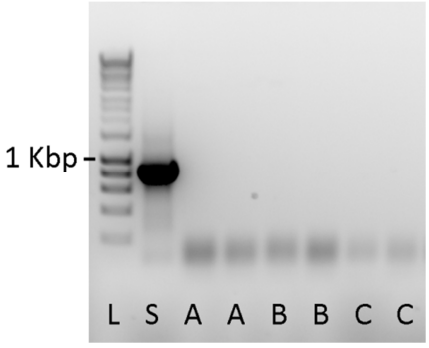

Figure 8 Electrophoresis gel presenting the products of DNA contamination quality check with standard PCR from Δ*narR* CSTR culture samples. L denotes DNA ladder, S standard genomic DNA (PD1222) and A, B and C the CSTR culture samples (PD2345)

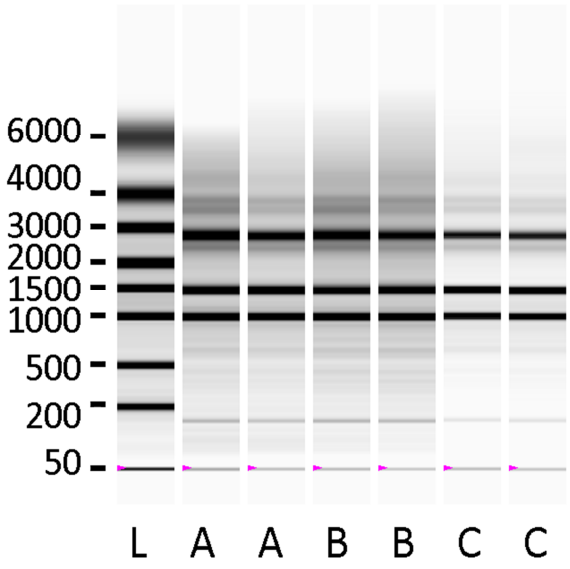

Figure 9 Experion electrophoresis gel of total RNA samples from CSTR cultures of Δ*narR* (PD1234). L denotes ladder in nt (DNA ladder) and A, B and C samples from Δ*narR* (PD2345).

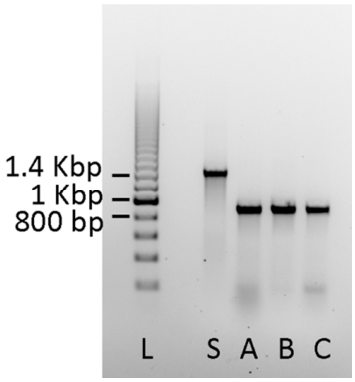

Figure 10 Electrophoresis gel of colony PCR amplification from CSTR culture samples. L denotes 200 bp step DNA ladder (Promega #G696A), S standard genomic DNA (PD1222) and A, B and C CSTR culture samples (PD2345).

The total RNA yield was on average 392.91 (SE ±24.69) ng.µl^{-1}. The samples from each culture were stored at -80^{o}C until further use. A 2 µg.µl^{-1} aliquot of RNA was reverse transcribed and was used to determine the expression of selected genes with qRT-PCR, as described in the Materials and Methods.

The expression of the respiratory genes *napA* (pden_4721) and *narG* (4233), in the Δ*narR* treatment, was 5 fold repressed when compared to the control treatment (Figure 11 A and B). Genes encoding nitrite (*nirS*; pden_2478) and nitrous oxide reductase (*nosZ*; pden_2478), cytochrome c_{550} (*cycA*; pden_1983) pseudoazurin (*pasZ*; pden_4222), and cytochrome ba_3 oxidase (*qoxB*; pden_5107) were relatively induced ~5, 3 7, 9, 1.4 fold respectively compared to the control (Figure 11 C, E, F, G, and H). The gene for nitric oxide reductase (*norB*; pden_2483) remained unchanged in the Δ*narR* strain (Figure 11 D). As expected, *narG* expression was down-regulated due to the mutation in the TF gene *narR* (pden_4238) but not completely repressed. This observation would suggest either basal levels of expression or other mechanisms of transcriptional activation of the *nar* gene cluster. However, besides the low expression of the membrane and periplasmic nitrate reductase target genes *narG* and *napA* respectively, other genes involved in nitrogen metabolism may be involved in transporting the extracellular nitrate to the cell and reducing it to nitrite.

The next set of qRT-PCR analyses examined the expression of the *nas* gene cluster that is involved in the nitrogen assimilation of *P. denitrificans* (Figure 12). This investigation could possibly reveal new putative roles of the target genes involved in nitrogen transport and reduction. The expression of *nasC* (pden_4449) which encodes an assimilatory nitrate reductase was found unchanged when compared to the control strain (PD1222). The gene for assimilatory nitrite transporter (*nasH*; pden_4450) and reductase (*nasB*; pden_4452) were ~3.5 and 2 fold induced (Figure 12 J and L). The regulatory genes *nasS* (pden_4454) and *nasT* (pden_4455) were induced ~3.2 and 2.2 fold, respectively (Figure 12 M and N). The gene expressing a putative ferredoxin, *nasG* (pden_4451), of the *nas* gene cluster was relatively repressed ~1.5 fold when compared to the control treatment (PD1222).

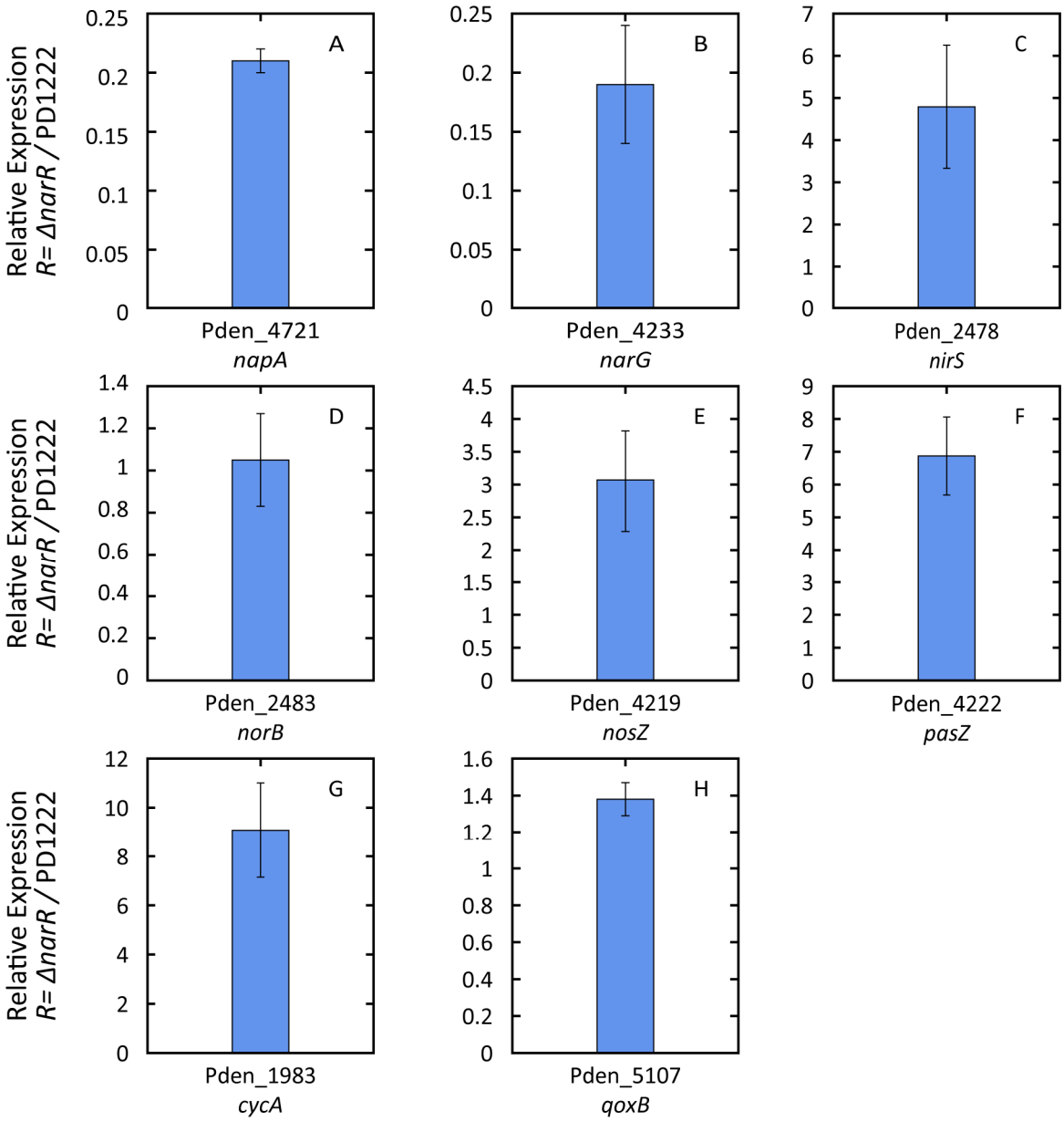

Figure 11 Average relative expression of genes in the Δ*narR* strain (PD2345) detected with RT-PCR. A) *napA* (pden_4721), B) *narG* (pden_4233), C) *nirS* (pden_2487), D) *norB* (pden_2483), E) *nosZ* (pden_4219), F) *pasZ* (pden_4222), G) *cycA* (pden_1937) and H) *qoxB* (pden_5107). Expression values were normalized on expression of *polB* and the relative ratio R is calculated using the anaerobic treatment of the PD1222 strain as a reference based on the Pfaffl method (n=3, error bars denote standard error).

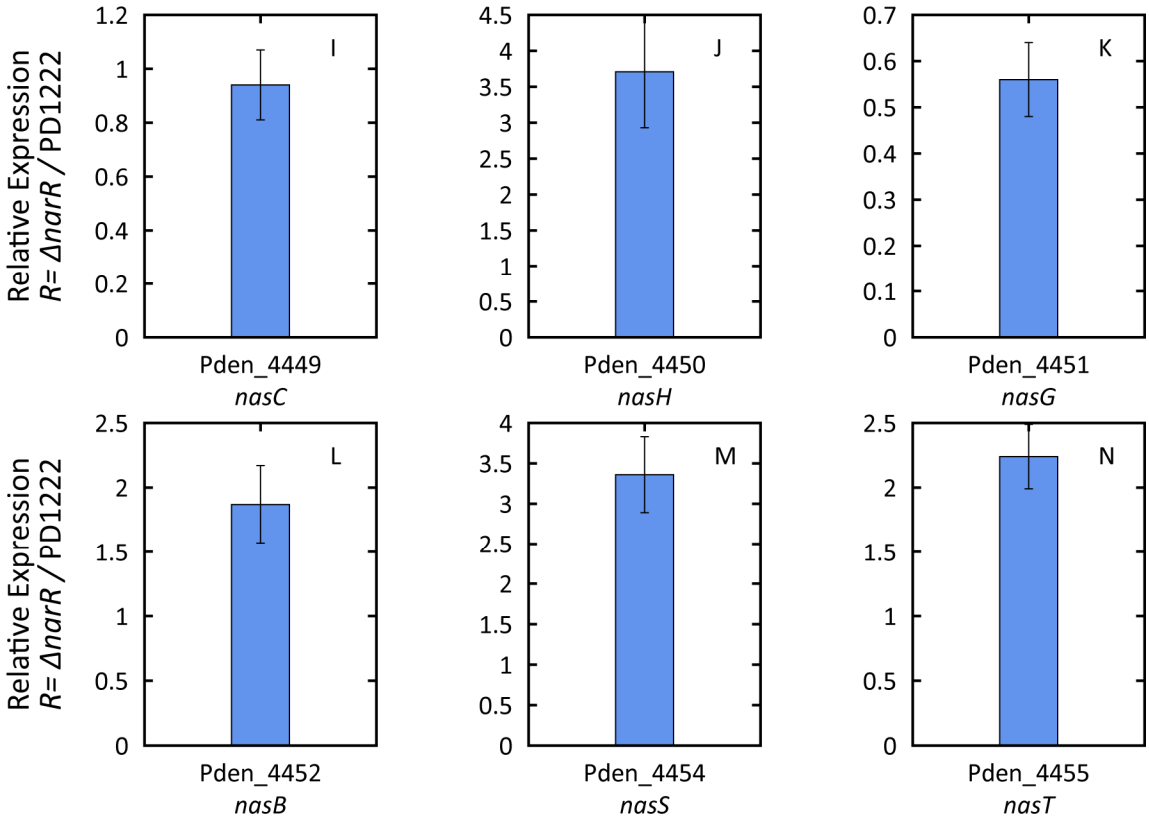

Figure 12 Average relative expression of genes in the Δ*narR* strain (PD2345) detected with RT-PCR. I) *nasC* (pden_4449), J) *nasH* (pden_4450), K) *nasG* (pden_4451), L) *nasB* (pden_4452), M) *nasS* (pden_4454) and N) *nasT* (pden_4455). Expression values were normalized on expression of *polB* and the relative ratio R is calculated using the anaerobic treatment of the PD1222 strain as a reference based on the Pfaffl method (n=3, error bars denote standard error).

4.2.3 Whole genome transcriptional analyses of *narR* mutant of *P. denitrificans* in anaerobic CSTR cultures

Total RNA from the Δ*narR* strain was extracted from each replicate, quantified and assessed as described in the Materials and Methods chapter of this study. A subsample of total RNA (10 µg) was used for whole genome transcriptional analysis with custom designed microarrays. The array data were normalized with the Babar algorithm (Alston *et al.* 2010) and enriched with volcano plot statistical analysis ($p \leq 0.005$). Microarray gene expression is calculated as the fluorescence ratio of the Δ*narR* cDNA over the control gDNA (PD1222). The enrichment analysis revealed 1649 genes, of which 1511 and 138 showed a significant up- and down-regulation respectively (Figure 13). Genes involved in the expression of cytochrome aa_3, ba_3 and cbb_3 oxidase, methylamine, methanol and sulphur oxidation as

well in the periplasmic and membrane bound nitrate reductase were significantly regulated (Volcano test, $p \leq 0.005$). The detailed expression dataset of the proposed respirome and whole genome of the Δ*narR* mutant of *P. denitrificans* are attached in the Appendix at the end of this chapter.

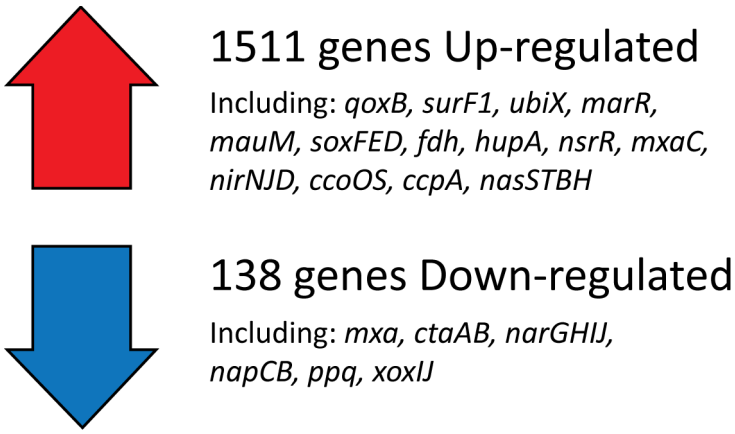

Figure 13 Schematic **r**epresentation of the enrichment analysis in the Δ*narR* treatment.

Note: The microarray and respirome gene expression dataset of the *ΔnarR* strain is presented in section 4.4 ΔnarR strain gene expression datasets.

The comparison of the Δ*narR* and wild type strain datasets showed that ~30% of the *P. denitrificans* genome was either relatively induced or repressed. The microarray datasets capture the snapshot of gene expression however the magnitude of gene expression should be considered carefully. Furthermore, the relative expression of selected target genes was additionally assessed with RT-PCR.

The *cta* operon (expressing the cytochrome aa_3 oxidase) was repressed ~2 fold, the *cco* (expressing the cytochrome cbb_3 oxidase), *qox* (expressing the cytochrome ba_3 oxidase) and *fbc* operon (expressing the cytochrome bc_1 oxidase) were induced ~9, 2 and 2 fold respectively. The gene for cytochrome *c* peroxidase, *ccpA* (pden_0893) was induced 10 fold when compared to the control strain (PD1222).

The gene cluster expressing the periplasmic nitrate reductase (*nap* operon) was repressed by ~2 fold; however the target gene for the catalytic subunit was induced 1.7 fold. The target operon encoding the membrane bound nitrate reductase was relatively repressed ~4 fold, apart from *narK* gene expressing a nitrate/nitrite transporter which was 2 fold induced when compared to the control strain. The expression of the nitrite reductase operon (*nir*), the nitric oxide reductase gene cluster (*nor*) and the nitrous oxide gene operon (*nos*) was induced ~6 fold, remained unchanged and was induced ~2 fold respectively.

The expression of the gene cluster for the assimilatory nitrate reductase (*nas*) was on average induced 30 fold, however genes expressing a nitrite transporter (*nasA*; pden_4453) a putative ferredoxin (*nasG*; pden_4451), and ABC type transporter (pden_4448) and the assimilatory nitrate reductase (*nasC*; pden_4449) were repressed by ~2 fold.

The expression of genes encoding pseudoazurin (pden_4219) and cytochrome c_{550} (pden_1938), that are involved in electron transport remained unchanged. Another notable gene cluster was that expressing *bd* ubiquinol oxidase that was induced by 30 fold. This cluster contains a target gene expressing a putative alpha molybdopterin oxidoreductase (pden_4009) upstream of a σ^{54} transcriptional regulator (pden_4007). The target gene for the NO sensitive repressor, *nsrR* (pden_3024), was induced by 6 fold. The *fdh* gene cluster expressing a NADH dependent formate dehydrogenase was ~50 fold induced.

A similar pattern of gene expression was confirmed with qRT-PCR. However, the expression of *napA* (pden_4721) appeared to be induced in the microarray data set (Table 3).

Table 3 Table presenting the average ratio of gene expression (Δ*narR* vs. wild type strain of *P. denitrificans*) detected with RT-PCR and Microarray.

		RT-PCR		Microarray	
Gene ID	**Annotation**	**R**	**±SE**	**R**	**±SE**
Pden_4721	*napA*	0.21	0.01	1.72	0.20
Pden_4452	*nasB*	1.87	0.30	46.19	25.37
Pden_4233	*narG*	0.19	0.10	0.66	0.12
Pden_2487	*nirS*	4.79	2.46	3.20	0.66
Pden_2483	*norB*	1.05	0.22	1.08	0.22
Pden_4219	*nosZ*	3.07	1.38	4.56	1.28
Pden_4222	*pasZ*	6.87	1.19	1.51	0.52
Pden_1938	*cycA*	9.08	1.93	1.44	0.23
Pden_5107	*qoxB*	1.38	0.09	9.50	3.83
pden_4455	*nasT*	2.24	0.25	20.56	6.25
pden_4454	*nasS*	3.36	0.47	27.02	5.57
pden_4451	*nasG*	0.56	0.08	0.67	0.06
pden_4450	*nasH*	3.71	0.78	43.01	15.25
pden_4449	*nasC*	0.94	0.13	0.44	0.20

4.3 Discussion

4.3.1 Towards the elucidation of the regulon of the transcription factor NarR of *P. denitrificans* in anaerobicity.

In this chapter a mutant of *narR* (PD2345) in *P. denitrificans* was constructed successfully by allelic exchange (4.5 ΔnarR sequencing dataset). All selected mutant isolates were unable to respire on nitrate in batch culture (Figure 6). These cultures had a noticeable optical density of 0.2 AU due to the initial respiration of the existing oxygen. However, after 44 hours of batch culture it was observed that the isolates could respire on nitrate. A similar pattern was observed when the mutant isolate PD2345 was cultured in CSTR. It was demonstrated in continuous culture that nitrate reduction was delayed by ~20 hours after the basal consumption of the dissolved oxygen when compared to the control treatment (PD1222). At a later stage of the anaerobic continuous culture incubation (> 40 hours) the Δ*narR* strain of *P. denitrificans* was able to reduce the extracellular nitrate to di-nitrogen and furthermore the concentration levels of the denitrification intermediate products were below the detection limit. It is rather interesting to test if the basal gene expression of the *nar* or *nap*

operons is adequate to support such phenotype of the Δ*narR* strain. One way to assess this would be to construct double mutants; Δ*narR*.Δ*narG* and Δ*narR*.Δ*napA* and monitor their phenotypes and gene expression levels. Additionally, the contribution of the putative molybdopterin reductase gene (pden_4009) to nitrate reduction should be further tested with disruptive mutational analysis.

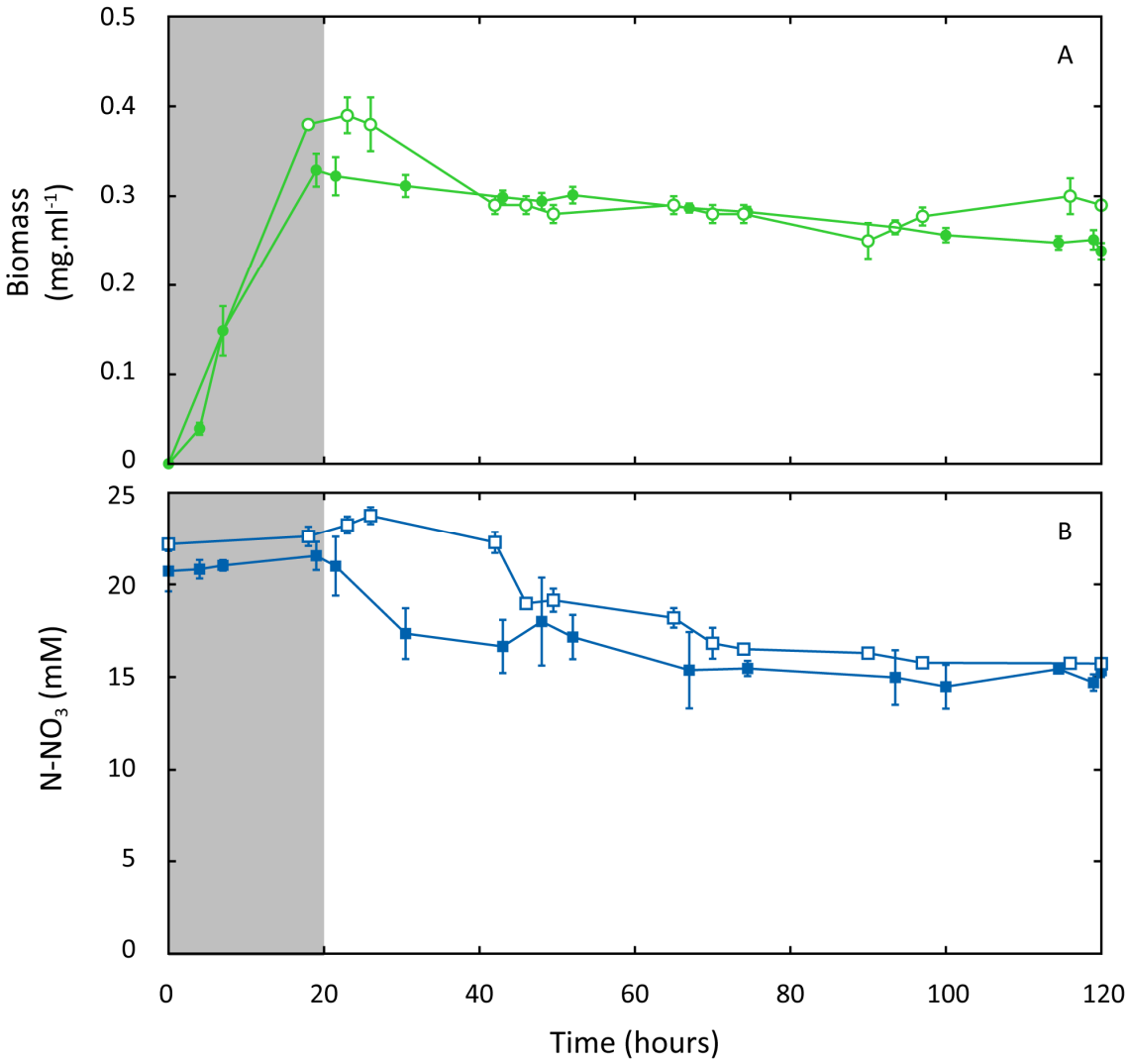

Figure 14 Comparison of the growth (biomass) and nitrate extracellular concentration of the wild type (solid symbols) and Δ*narR* (open symbols) strain of *P. denitrificans* in continuous cultures. Panel A illustrates the biomass density (circles) and panel B illustrates the nitrate concentration (squares) in the CSTR (n=3; error bars denote SEM).

A reduced expression of *narR* and *narG* genes was confirmed by RT-PCR transcriptional analysis. This finding is consistent with the observations of Wood et al. (2001) using *P. pantotrophus* and *P. denitrificans.* Transcriptionally, the expression of the nitrite, and nitrous oxide reductase were induced with the absence of the TF *narR*. Furthermore the expression of the nitric oxide reductase operon remained relatively unchanged when compared to the control treatment (PD1222). It appears that NarR is involved in the activation of the *nar* gene cluster in the early stage of the aerobic to anaerobic transition. This suggested mechanism could be possible if NarR is active at relatively higher oxygen levels than FnrP, which is deactivated by oxygen. However, the above hypothesis remains to be tested with a high resolution time series transcriptional analysis. Another point to consider is the relative abundance of *narR* transcripts in the cell. In Chapter 2 of this thesis it was demonstrated that the order of the relative expression of FnrP, NnrR and NarR was 9>3>1 based on the absolute fluorescence magnitude. These linear relationships are based on the assumption that the mRNA transcripts could reflect the protein abundance; however this requires further proteomic investigation. One could assume that the low level of NarR may have a localized effect on the whole genome expression and possibly substituted by the other two TF that have a similar HTH motif; FnrP or NnrR. It was also demonstrated that the absence of TF NarR induced the *nir* and *nos* gene cluster (Figure 15). This observation could suggest that TF NarR may repress gene expression by competing for the same binding motif recognized also by the other two TF. To elucidate this suggestion, it is crucial to investigate and understand the structure of NarR and its interaction with nitrate, RNA polymerase and the putative DNA binding motifs. Another point to consider is whether NarR is a global anaerobic regulator rather than a denitrification-specific regulator due to the greater number of genes affected by the *narR* mutation when compared to the wild type strain. However, this requires further additional investigations. A synthesis of the mutation studies on the regulation of denitrification in *P. denitrificans* is presented in the 6. Discussion.

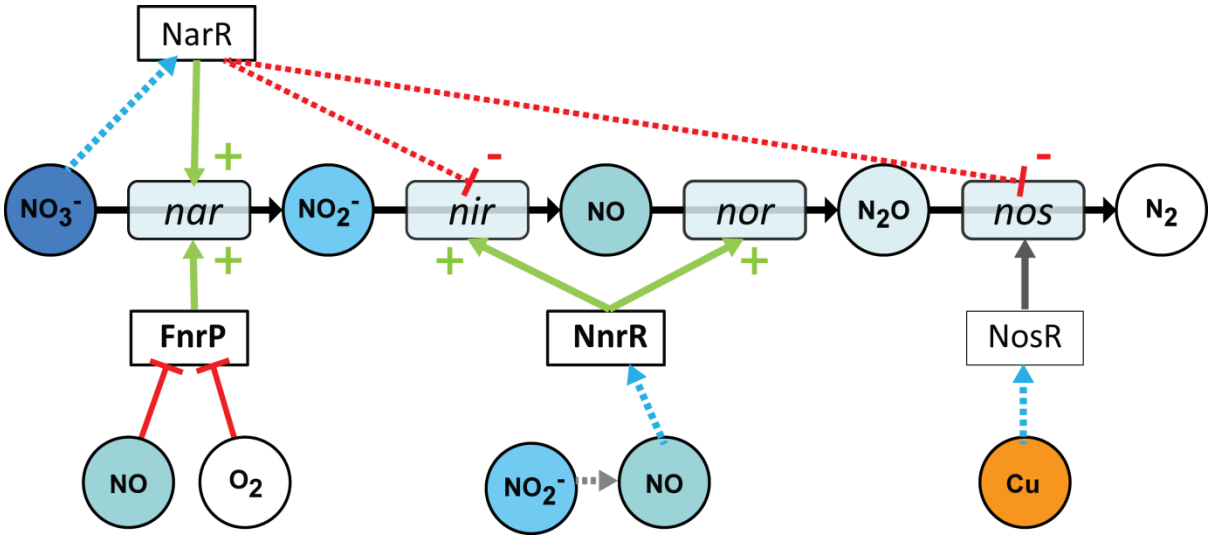

Figure 15 Updated version of the simplified illustration of the regulatory network controlling expression of denitrification genes in *P. denitrificans* with the newly proposed roles of TF *narR*. The solid arrows represent positive activating events between the TF and the target gene. Dashed arrows indicate positive signalling between the metabolites and the TF. The lines with a bar end indicate inhibition events between the TF and the signal metabolite. The dashed lines with a bar end indicate inhibition events between the TF and the target genes. The TF and subsequently the regulatory proteins are boxed by clear layers; those are the FNR (Fumarate and Nitrate Regulatory), NNR (Nitrite and Nitric Oxide Regulatory), NarR (Nitrate reductase Regulatory) and NosR (Nitrous oxide reductase Regulatory protein). The target genes clusters are boxed by a shaded layer; those are the membrane nitrate reductase (*nar*), the nitrite reductase (*nir*), the nitric oxide reductase (*nor*) and the nitrous oxide reductase gene operon (*nos*). The metabolites are represented in circles.

4.4 Δ*narR* strain gene expression datasets

4.4.1 Respirome gene expression dataset

Georgios Giannopoulos

Respirome Relative Expression WT *vs* . Δ*narR*
20140214_narR_wt

Gene ID	Δ*narR*		WT		Ratio	Gene ID	Annotation
	Average	SE Norm	Average	SE Norm	Δ*narR* /WT		
Pden_5108	1.98	0.31	1.55	0.62	1.27	Pden_5108	qoxA ba3 subunit II
Pden_5107	10.06	4.26	1.32	0.17	7.64	Pden_5107	qoxB ba3 subunit I
Pden_5106	1.26	0.20	1.05	0.23	1.20	Pden_5106	qoxC ba3 subunit III
Pden_5105	1.21	0.19	1.04	0.21	1.17	Pden_5105	qoxD ba3 subunit IV
Pden_5104	115.43	39.17	2.90	0.50	39.83	Pden_5104	surF1 surfeit family
Pden_5063	2.22	0.72	1.23	0.31	1.81	Pden_5063	Alcohol dh
Pden_5062	0.51	0.09	0.41	0.08	1.24	Pden_5062	L-Lactate dh
Pden_5013	1.63	0.55	0.34	0.03	4.78	Pden_5013	peroxidase
Pden_4938	58.38	35.94	0.57	0.16	102.63	Pden_4938	ubiX
Pden_4877	1.41	0.67	0.51	0.09	2.77	Pden_4877	L-lactate dh
Pden_4866	1.86	0.52	0.67	0.24	2.76	Pden_4866	Malate/lactate dh
Pden_4855	7.54	3.42	0.43	0.04	17.69	Pden_4855	Malate/lactate dh
Pden_4738	0.47	0.05	0.44	0.07	1.08	Pden_4738	mauN ferrodoxin nap
Pden_4737	5.40	2.60	0.48	0.07	11.23	Pden_4737	mauM ferrodoxin nap
Pden_4736	0.25	0.05	0.35	0.16	0.71	Pden_4736	mauG diheme c perox
Pden_4735	0.38	0.05	0.33	0.05	1.15	Pden_4735	mauJ
Pden_4734	0.20	0.03	0.23	0.03	0.87	Pden_4734	mauC amicyamin
Pden_4733	0.55	0.16	0.34	0.09	1.64	Pden_4733	mauA small subnit
Pden_4732	5.79	2.78	0.60	0.38	9.72	Pden_4732	mauD accessory prot
Pden_4731	0.59	0.30	0.19	0.09	3.12	Pden_4731	mauE ma utilization
Pden_4730	0.33	0.04	0.31	0.04	1.07	Pden_4730	mauB MADH heavy ch
Pden_4729	1.32	0.30	0.40	0.06	3.32	Pden_4729	mauF big subunit
Pden_4728	0.36	0.05	0.31	0.06	1.17	Pden_4728	lysR
Pden_4727	2.09	0.18	1.68	0.17	1.25	Pden_4727	sndhA
Pden_4726	0.59	0.09	0.87	0.28	0.68	Pden_4726	mscS-aldose dh
Pden_4724	3.64	1.13	8.78	7.58	0.41	Pden_4724	GreA kinase regulat

Pden_4723	0.50	0.04	1.67	0.14	0.30	Pden_4723	napC
Pden_4722	1.53	0.45	3.23	0.58	0.47	Pden_4722	napB cyt c
Pden_4721	4.20	0.88	2.48	0.17	1.70	Pden_4721	napA catalytic
Pden_4720	0.71	0.17	1.67	0.41	0.43	Pden_4720	napD
Pden_4719	1.59	0.08	3.43	0.41	0.46	Pden_4719	napE
Pden_4718	0.79	0.15	0.71	0.25	1.12	Pden_4718	Hypotherical
Pden_4700	2.33	0.53	0.49	0.06	4.77	Pden_4700	CytCP
Pden_4699	1.14	0.14	0.26	0.06	4.45	Pden_4699	B651
Pden_4511	4.23	0.68	3.98	3.21	1.06	Pden_4511	ubiE
Pden_4510	1.96	0.22	1.54	0.13	1.27	Pden_4510	ubiB
Pden_4397	1.82	0.22	2.71	0.36	0.67	Pden_4397	hypothetical
Pden_4396	5.42	0.80	2.75	0.36	1.97	Pden_4396	cysN/cysC
Pden_4395	14.26	3.72	2.19	0.67	6.50	Pden_4395	cysD
Pden_4394	0.50	0.14	0.35	0.07	1.43	Pden_4394	hypothetical protein
Pden_4393	12.52	3.38	1.04	0.25	12.07	Pden_4393	glpD homodimeric quin
Pden_4392	5.45	1.60	0.97	0.14	5.63	Pden_4392	ABC transporter ATP
Pden_4391	3.23	1.00	0.86	0.14	3.77	Pden_4391	ABC transporter ATP
Pden_4390	0.45	0.04	0.68	0.16	0.65	Pden_4390	ABC transporter
Pden_4389	0.83	0.20	0.72	0.11	1.15	Pden_4389	ABC transporter
Pden_4388	0.65	0.18	1.67	0.57	0.39	Pden_4388	hypothetical
Pden_4387	2.29	0.40	6.20	0.50	0.37	Pden_4387	ABC transporter
Pden_4386	0.95	0.09	1.42	0.08	0.67	Pden_4386	glycerol kinase
Pden_4356	0.84	0.10	1.95	0.54	0.43	Pden_4356	b561?
Pden_4323	0.30	0.03	0.49	0.04	0.62	Pden_4323	DprA
Pden_4322	6.09	1.08	4.66	0.77	1.31	Pden_4322	TldD
Pden_4321	19.27	1.95	28.63	5.56	0.67	Pden_4321	ctaC subunit II
Pden_4320	5.24	0.51	9.67	1.83	0.54	Pden_4320	ctaB
Pden_4319	5.01	0.39	11.71	2.24	0.43	Pden_4319	hypothetical
Pden_4318	4.88	0.53	7.14	1.05	0.68	Pden_4318	ctaG assembly protein
Pden_4317	27.07	7.96	9.53	2.19	2.84	Pden_4317	ctaE subunit III
Pden_4316	3.24	0.34	2.84	0.27	1.14	Pden_4316	surF1
Pden_4315	43.98	11.85	5.65	0.82	7.79	Pden_4315	thrC
Pden_4238	57.61	15.74	1.07	0.13	53.80	Pden_4238	narR

Pden_4237	15.59	3.31	7.60	1.19	2.05	Pden_4237	narK
Pden_4236	2.67	0.22	17.00	1.55	0.16	Pden_4236	narI
Pden_4235	2.72	0.30	16.26	1.77	0.17	Pden_4235	narH
Pden_4234	10.47	4.32	34.66	4.90	0.30	Pden_4234	narJ
Pden_4233	10.76	3.37	17.08	2.64	0.63	Pden_4233	narG
Pden_4232	3.03	0.45	22.31	3.40	0.14	Pden_4232	
Pden_4231	2.43	0.18	16.44	2.93	0.15	Pden_4231	
Pden_4230	11.50	1.84	6.79	1.37	1.69	Pden_4230	nnrS
Pden_4226	7.29	0.89	10.08	4.92	0.72	Pden_4226	ubiD
Pden_4225	58.31	30.94	7.76	1.60	7.51	Pden_4225	ubiD
Pden_4222	88.53	29.12	58.45	49.51	1.51	Pden_4222	pasZ
Pden_4221	17.74	4.66	14.60	7.27	1.22	Pden_4221	nosC
Pden_4220	13.24	1.39	9.66	2.37	1.37	Pden_4220	nosR
Pden_4219	152.37	47.12	36.88	3.30	4.13	Pden_4219	nosZ
Pden_4218	44.43	10.22	18.33	9.72	2.42	Pden_4218	nosD
Pden_4217	9.12	1.29	6.01	1.00	1.52	Pden_4217	nosF
Pden_4216	24.49	6.41	7.78	1.01	3.15	Pden_4216	nosY
Pden_4215	13.79	1.98	5.89	0.67	2.34	Pden_4215	nosL
Pden_4214	9.14	1.49	6.70	1.00	1.36	Pden_4214	nosX
Pden_4161	3.23	0.43	3.10	3.01	1.04	Pden_4161	hypothetical
Pden_4160	3.75	1.93	1.03	0.32	3.63	Pden_4160	soxH
Pden_4159	0.85	0.14	0.93	0.09	0.91	Pden_4159	soxG β-lactamase
Pden_4158	10.15	2.60	0.91	0.14	11.16	Pden_4158	SoxF FAD disulfide ox
Pden_4157	41.40	14.72	0.60	0.12	69.29	Pden_4157	SoxE cyt c-I
Pden_4156	9.37	3.32	0.72	0.17	12.96	Pden_4156	soxD cyt c551
Pden_4155	0.47	0.07	0.47	0.03	0.99	Pden_4155	soxC Mo-oxidase
Pden_4154	1.23	0.54	0.43	0.04	2.84	Pden_4154	soxB Rden
Pden_4153	0.73	0.15	2.22	0.41	0.33	Pden_4153	socA di-heme cyt c
Pden_4152	0.96	0.30	1.71	0.46	0.56	Pden_4152	soxZ sulfur oxidase
Pden_4151	4.47	1.22	2.85	0.48	1.57	Pden_4151	soxY sulfur oxidase
Pden_4150	0.54	0.14	1.31	0.38	0.41	Pden_4150	soxX cyt c
Pden_4149	0.27	0.04	0.43	0.06	0.63	Pden_4149	soxW thioredoxin
Pden_4148	2.45	0.62	0.76	0.16	3.22	Pden_4148	soxV cyt c

Pden_4147	0.70	0.21	0.65	0.22	1.08	Pden_4147	soxS cyt c biogenesis
Pden_4146	2.56	0.61	2.11	0.52	1.22	Pden_4146	ArsR regulatory
Pden_4145	1.81	0.18	2.33	0.26	0.78	Pden_4145	Hypothetical (YeeD)
Pden_4075	2.19	0.35	3.37	0.92	0.65	Pden_4075	L-Lactate dh cyt c
Pden_4012	3.68	1.07	0.63	0.05	5.80	Pden_4012	ATPase
Pden_4011	0.65	0.27	0.25	0.05	2.59	Pden_4011	d subunit II
Pden_4010	17.51	5.20	0.38	0.08	46.14	Pden_4010	bd subunit I
Pden_4009	11.02	2.63	0.49	0.06	22.29	Pden_4009	Mo-pterin α subunit
Pden_4008	0.31	0.02	0.43	0.04	0.72	Pden_4008	σ54 Fis transcript reg
Pden_4007	29.01	7.06	0.59	0.15	49.27	Pden_4007	Membrane sensor kina
Pden_3985	1.36	0.37	0.70	0.08	1.94	Pden_3985	p450
Pden_3978	9.61	1.69	3.92	0.60	2.45	Pden_3978	ccmH
Pden_3977	21.38	3.35	6.56	0.61	3.26	Pden_3977	ccmF
Pden_3974	7.25	1.49	4.86	0.92	1.49	Pden_3974	cycJ
Pden_3942	11.18	2.44	7.89	1.28	1.42	Pden_3942	ubiH/F
Pden_3543	0.61	0.10	0.49	0.04	1.25	Pden_3543	Short Chain Reductase
Pden_3286	0.59	0.11	0.48	0.07	1.23	Pden_3286	b561?
Pden_3113	0.52	0.08	0.36	0.08	1.42	Pden_3113	hypothetical
Pden_3112	3.48	1.77	0.71	0.32	4.88	Pden_3112	hypE
Pden_3111	0.97	0.11	0.78	0.09	1.23	Pden_3111	hypD
Pden_3110	1.52	0.65	0.57	0.15	2.64	Pden_3110	hypC
Pden_3109	17.13	5.04	0.45	0.09	37.89	Pden_3109	hypothetical
Pden_3108	0.70	0.06	0.74	0.13	0.95	Pden_3108	hypB
Pden_3107	0.87	0.10	0.85	0.08	1.02	Pden_3107	hypA
Pden_3106	1.03	0.19	1.08	0.38	0.96	Pden_3106	HupK
Pden_3105	0.58	0.12	0.39	0.04	1.48	Pden_3105	HupJ Rubredoxin
Pden_3104	0.61	0.10	0.61	0.08	1.00	Pden_3104	HupH
Pden_3103	0.37	0.06	0.51	0.08	0.73	Pden_3103	HupG
Pden_3102	4.08	1.20	1.23	0.18	3.32	Pden_3102	hupF
Pden_3101	0.55	0.04	0.44	0.05	1.25	Pden_3101	HupD
Pden_3100	0.25	0.03	0.22	0.04	1.13	Pden_3100	hupC cyt b
Pden_3099	0.42	0.06	0.33	0.14	1.28	Pden_3099	hupE
Pden_3098	0.36	0.03	0.23	0.02	1.57	Pden_3098	hupL large subunit

Pden_3097	4.57	1.92	0.20	0.02	22.97	Pden_3097	hupA/S small subunit
Pden_3096	1.23	0.18	0.74	0.09	1.65	Pden_3096	hupF maturation
Pden_3095	1.00	0.09	1.07	0.09	0.93	Pden_3095	hupV
Pden_3094	2.34	0.79	1.19	0.14	1.97	Pden_3094	hupU
Pden_3093	1.21	0.12	1.27	0.13	0.96	Pden_3093	hupT hist-kinase sensor
Pden_3028	9.88	1.10	4.42	0.54	2.24	Pden_3028	ctaDI
Pden_3027	3.01	0.57	4.65	3.41	0.65	Pden_3027	ahpD Alkylhydroperoxidase
Pden_3026	5.32	1.09	11.28	9.74	0.47	Pden_3026	Hypothetical
Pden_3025	9.65	2.42	14.98	11.93	0.64	Pden_3025	NO & morphol reg
Pden_3024	51.54	22.07	7.53	4.65	6.84	Pden_3024	nsrR NO repressor
Pden_3023	1.88	0.36	5.35	5.19	0.35	Pden_3023	hypothetical
Pden_3022	1.64	0.31	1.94	1.20	0.85	Pden_3022	sdhB
Pden_3021	1.14	0.14	1.34	0.49	0.85	Pden_3021	sdhC
Pden_3020	6.58	4.64	1.10	0.27	5.96	Pden_3020	sdhD
Pden_3019	1.21	0.20	1.27	0.34	0.96	Pden_3019	Signal protein
Pden_3003	1.33	6.36	3.09	0.50	0.43	Pden_3003	mxaD
Pden_3002	1.54	1.35	1.37	0.13	1.13	Pden_3002	mxaL
Pden_3001	0.95	0.90	2.15	0.40	0.44	Pden_3001	mxaK
Pden_3000	65.93	20.17	3.17	0.82	20.77	Pden_3000	mxaC von Willebr.
Pden_2999	8.44	2.26	2.56	0.39	3.30	Pden_2999	mxaA
Pden_2998	1.01	2.00	2.72	0.46	0.37	Pden_2998	mxaS unknown
Pden_2997	2.62	5.60	5.16	0.94	0.51	Pden_2997	mxaR unknown
Pden_2996	3.35	626.06	38.12	10.64	0.09	Pden_2996	mxaI β subunit
Pden_2995	2.12	116.07	12.33	2.83	0.17	Pden_2995	mxaG cyt C-L c551i
Pden_2994	4.85	30.94	13.04	4.31	0.37	Pden_2994	mxaJ binding prot.
Pden_2993	3.40	417.02	27.62	11.09	0.12	Pden_2993	mxaF α subunit
Pden_2929	1.57	0.22	2.88	0.68	0.55	Pden_2929	lctR Lactate Regulator
Pden_2928	0.87	0.11	1.22	0.09	0.71	Pden_2928	Dld D-Lactate dh
Pden_2927	1.91	0.23	3.82	0.58	0.50	Pden_2927	lctP L-Lactate permeas
Pden_2859	1.43	0.17	1.59	0.32	0.90	Pden_2859	LysR family
Pden_2858	1.56	0.34	4.37	1.46	0.36	Pden_2858	Fdh γ subunit
Pden_2857	13.04	3.40	6.09	1.71	2.14	Pden_2857	NADH dh (quinone)
Pden_2856	8.16	1.59	6.48	0.96	1.26	Pden_2856	Fdh α subunit

Pden_2855	1.40	0.24	4.03	0.75	0.35	Pden_2855	FdhD family
Pden_2854	1.12	0.14	2.04	0.24	0.55	Pden_2854	NAD-fdh δ subunit
Pden_2853	27.98	6.20	2.59	0.26	10.81	Pden_2853	ribonuclease R
Pden_2830	5.62	1.75	10.25	2.28	0.55	Pden_2830	4Fe-4S
Pden_2829	0.88	0.19	0.95	0.11	0.92	Pden_2829	fdnG α subunit
Pden_2828	9.29	2.69	1.15	0.26	8.08	Pden_2828	fdnH β subunit
Pden_2827	0.92	0.14	1.20	0.22	0.76	Pden_2827	fdnI γ subunit
Pden_2826	20.53	6.39	2.64	0.36	7.78	Pden_2826	fdhE
Pden_2825	1.20	0.19	0.89	0.08	1.36	Pden_2825	selB cysteine enlog.
Pden_2824	18.48	5.38	1.08	0.09	17.18	Pden_2824	aldo/keto reductase
Pden_2710	25.74	6.60	1.94	0.64	13.24	Pden_2710	SndhB
Pden_2709	12.83	4.44	1.88	0.18	6.82	Pden_2709	NAP (P)
Pden_2708	4.67	1.97	1.64	0.19	2.84	Pden_2708	
Pden_2707	11.08	2.88	1.71	0.16	6.47	Pden_2707	
Pden_2706	0.57	0.10	0.38	0.09	1.48	Pden_2706	aldose?
Pden_2705	6.45	0.72	2.62	0.56	2.46	Pden_2705	carbonic anhydrase
Pden_2670	2.50	0.25	2.00	0.36	1.25	Pden_2670	ubiH/F
Pden_2589	15.33	3.86	7.51	5.32	2.04	Pden_2589	ubiG
Pden_2563	1.71	0.26	1.72	0.35	0.99	Pden_2563	b561?
Pden_2551	21.28	2.86	23.51	4.51	0.91	Pden_2551	etfB β subunit
Pden_2550	25.67	3.37	22.93	3.45	1.12	Pden_2550	etfA α subunit
Pden_2545	6.61	0.68	5.49	0.94	1.20	Pden_2545	b561?
Pden_2495	26.74	6.90	2.82	0.21	9.49	Pden_2495	nirN
Pden_2494	64.43	15.98	4.73	1.21	13.64	Pden_2494	nirJ
Pden_2493	4.27	0.91	2.69	0.38	1.59	Pden_2493	nirH
Pden_2492	4.57	0.88	4.13	0.93	1.10	Pden_2492	nirG
Pden_2491	105.97	28.67	6.05	0.83	17.52	Pden_2491	nirD
Pden_2490	7.35	0.81	5.81	1.08	1.27	Pden_2490	nirF
Pden_2489	59.88	28.11	5.53	1.41	10.84	Pden_2489	nirC
Pden_2488	12.67	1.26	6.25	0.84	2.03	Pden_2488	nirE
Pden_2487	172.49	34.56	56.43	7.03	3.06	Pden_2487	nirS
Pden_2486	22.33	8.84	3.45	0.33	6.47	Pden_2486	nirI
Pden_2485	6.12	1.46	3.38	0.34	1.81	Pden_2485	nirX (apbE)

Pden_2484	60.14	9.45	55.84	15.44	1.08	Pden_2484	norC
Pden_2483	34.73	3.52	33.52	4.25	1.04	Pden_2483	norB
Pden_2482	33.33	4.44	47.85	7.71	0.70	Pden_2482	norQ
Pden_2481	13.09	1.91	21.38	2.86	0.61	Pden_2481	norD
Pden_2480	9.63	1.71	8.41	1.34	1.15	Pden_2480	norE
Pden_2479	2.82	0.97	2.80	0.35	1.01	Pden_2479	norF
Pden_2478	2.33	0.33	3.81	1.37	0.61	Pden_2478	nnrR
Pden_2475	1.62	0.34	2.25	0.31	0.72	Pden_2475	ubiC (GntR)
Pden_2363	33.41	10.22	3.89	1.19	8.60	Pden_2363	ppqA
Pden_2362	4.06	5.61	12.05	2.36	0.34	Pden_2362	ppqB
Pden_2361	1.58	2.07	6.56	2.84	0.24	Pden_2361	ppqC
Pden_2360	1.62	2.56	6.92	1.97	0.23	Pden_2360	ppqD
Pden_2359	3.66	1.06	4.74	1.62	0.77	Pden_2359	ppqE
Pden_2358	1.17	0.63	3.02	0.57	0.39	Pden_2358	hypothetical soxZ-like
Pden_2357	1.10	0.33	0.95	0.14	1.17	Pden_2357	abcC
Pden_2356	0.62	0.23	1.24	0.12	0.50	Pden_2356	abcB
Pden_2355	1.37	0.61	2.67	0.44	0.51	Pden_2355	abcA
Pden_2354	82.99	29.78	39.99	7.28	2.08	Pden_2354	flhR luxR 2 comp reg
Pden_2353	3.97	0.70	11.77	1.17	0.34	Pden_2353	hypothetical
Pden_2352	16.85	6.88	3.87	0.89	4.35	Pden_2352	flhS histidine kinase se
Pden_2351	1.92	2.24	5.13	1.19	0.37	Pden_2351	hypothetical
Pden_2350	1.22	0.84	4.37	0.88	0.28	Pden_2350	hypothetical
Pden_2349	2.01	0.19	4.74	1.03	0.42	Pden_2349	SDR cofactor vitamin
Pden_2307	69.34	8.43	40.78	5.67	1.70	Pden_2307	fbcC cyt c1 heme
Pden_2306	56.32	13.68	19.25	2.13	2.93	Pden_2306	fbcB cyt bL/bH heme
Pden_2305	90.78	15.30	40.76	9.98	2.23	Pden_2305	fbcF Rieske 2Fe2S
Pden_2272	17.77	4.90	1.08	0.13	16.53	Pden_2272	p451
Pden_2250	22.66	4.87	7.29	2.20	3.11	Pden_2250	nuoA
Pden_2249	19.30	1.94	10.21	2.38	1.89	Pden_2249	nuoB
Pden_2248	23.19	2.95	10.27	2.15	2.26	Pden_2248	nuoC
Pden_2247	17.14	1.92	10.54	1.46	1.63	Pden_2247	nuoD
Pden_2246	20.05	3.08	13.47	2.13	1.49	Pden_2246	nuoE
Pden_2245	10.62	0.99	8.36	0.96	1.27	Pden_2245	hypothetical

Pden_2244	9.24	2.44	8.34	1.91	1.11	Pden_2244	hypothetical
Pden_2243	64.01	14.27	8.54	0.75	7.49	Pden_2243	nuoF
Pden_2242	21.44	4.84	7.70	0.74	2.79	Pden_2242	hypothetical
Pden_2241	15.58	1.50	12.66	1.21	1.23	Pden_2241	nuoG
Pden_2240	14.14	1.89	7.81	1.00	1.81	Pden_2240	hypothetical
Pden_2239	14.34	1.50	6.09	0.80	2.35	Pden_2239	nuoH
Pden_2238	13.22	2.56	5.71	1.02	2.32	Pden_2238	nuoI
Pden_2237	172.65	74.32	11.34	5.81	15.22	Pden_2237	hypothetical
Pden_2236	9.46	1.59	5.67	1.11	1.67	Pden_2236	Hypothetical
Pden_2235	17.08	2.48	6.62	1.35	2.58	Pden_2235	nuoJ
Pden_2234	15.32	2.86	5.69	1.55	2.69	Pden_2234	nuoK
Pden_2233	16.99	1.82	9.16	1.15	1.86	Pden_2233	nuoL
Pden_2232	24.96	6.56	5.02	0.91	4.97	Pden_2232	nuoM
Pden_2231	16.56	2.77	8.03	1.18	2.06	Pden_2231	nuoN
Pden_2187	2.86	0.41	1.90	0.38	1.50	Pden_2187	D-Lactate dh cyt c
Pden_1954	0.88	0.08	1.11	0.12	0.79	Pden_1954	methyltransferase
Pden_1953	0.78	0.13	1.01	0.16	0.77	Pden_1953	
Pden_1952	23.87	5.40	5.15	1.99	4.64	Pden_1952	G-6-P-1 dh
Pden_1951	76.78	28.75	3.81	0.79	20.15	Pden_1951	G-6-Lactonate
Pden_1950	7.34	1.82	2.55	0.25	2.88	Pden_1950	G-6-P isoenzyme
Pden_1949	2.51	0.25	2.54	0.30	0.99	Pden_1949	L-sorbosone dh
Pden_1948	4.94	1.20	1.84	0.27	2.68	Pden_1948	
Pden_1938	21.97	2.18	15.63	1.70	1.41	Pden_1938	ctaDII
Pden_1937	198.13	52.36	37.95	10.29	5.22	Pden_1937	cycA c550
Pden_1850	17.77	4.60	10.66	1.14	1.67	Pden_1850	FnrP
Pden_1849	43.90	6.59	62.35	25.12	0.70	Pden_1849	UspA
Pden_1848	114.29	17.75	16.94	4.08	6.75	Pden_1848	ccoN subunit I
Pden_1847	193.45	45.77	16.31	2.75	11.86	Pden_1847	ccoO subunit II
Pden_1846	82.82	35.36	23.63	9.29	3.50	Pden_1846	ccoQ subunit IV
Pden_1845	77.38	9.84	24.63	3.38	3.14	Pden_1845	ccoP subunit III
Pden_1844	21.90	2.36	7.97	1.51	2.75	Pden_1844	ccoG 4Fe-4S
Pden_1843	11.57	2.02	5.88	0.94	1.97	Pden_1843	ccoH/FixH
Pden_1842	17.52	2.27	5.57	0.41	3.15	Pden_1842	ccoI cu transp ATPase

Pden_1841	15.98	5.56	1.19	0.10	13.41	Pden_1841	ccoS cbb3 maturation
Pden_1808	19.49	2.96	15.23	3.30	1.28	Pden_1808	cycM
Pden_1807	8.84	1.81	2.00	0.21	4.41	Pden_1807	abc transporter
Pden_1806	1.96	0.24	1.04	0.11	1.89	Pden_1806	abc transporter
Pden_1805	1.71	0.17	1.56	0.25	1.10	Pden_1805	abc transporter
Pden_1804	43.15	9.07	2.12	0.15	20.35	Pden_1804	abc transporter
Pden_1803	57.33	16.99	2.43	0.85	23.59	Pden_1803	Glycosil trnasferase
Pden_1745	1.14	0.09	1.29	0.09	0.88	Pden_1745	b561?
Pden_1415	6.64	0.76	4.49	0.60	1.48	Pden_1415	secF
Pden_1414	2.13	0.49	2.25	0.41	0.95	Pden_1414	
Pden_1413	5.01	1.46	2.59	0.28	1.94	Pden_1413	ccmA
Pden_1412	27.01	9.97	1.60	0.19	16.89	Pden_1412	ccmB
Pden_1411	10.37	2.41	3.92	0.69	2.64	Pden_1411	ccmC
Pden_1410	6.75	0.87	3.95	0.58	1.71	Pden_1410	ccmG
Pden_1409	3.30	0.36	2.30	0.62	1.44	Pden_1409	hisH
Pden_1359	75.20	30.29	0.91	0.18	82.39	Pden_1359	Copper binding
Pden_1189	1.10	0.68	0.32	0.04	3.45	Pden_1189	Rieske 2Fe2S
Pden_1188	17.63	5.24	0.63	0.14	28.12	Pden_1188	ferredoxin NADH
Pden_1187	0.23	0.04	0.38	0.04	0.61	Pden_1187	mandelate racemase
Pden_1186	13.42	4.13	0.76	0.09	17.64	Pden_1186	fdhA
Pden_1161	31.13	9.31	0.38	0.08	81.39	Pden_1161	assimilaory nad-formate dh?
Pden_0893	172.54	62.56	15.74	5.37	10.96	Pden_0893	ccpA cyt c peroxidase
Pden_0625	3.17	0.45	2.32	0.32	1.36	Pden_0625	ubiA
Pden_0572	15.77	2.17	5.17	0.63	3.05	Pden_0572	sdhB (Fe-S)
Pden_0571	15.89	6.14	15.07	5.74	1.05	Pden_0571	hypothetical
Pden_0570	13.20	3.26	17.38	4.40	0.76	Pden_0570	hypothetical
Pden_0569	17.88	2.24	10.37	1.03	1.72	Pden_0569	sdhA
Pden_0568	11.26	3.11	7.20	1.75	1.56	Pden_0568	sdhD
Pden_0567	69.38	26.52	8.51	1.87	8.16	Pden_0567	sdhC
Pden_0566	3.27	0.42	1.81	0.15	1.81	Pden_0566	Sdh cyt b552
Pden_0511	6.56	0.76	4.82	0.82	1.36	Pden_0511	cycH
Pden_0432	17.90	4.00	10.72	4.60	1.67	Pden_0432	ctaIV
Pden_0425	23.24	7.34	4.96	0.72	4.69	Pden_0425	etfD

Pden_0023	0.93	0.75	2.68	0.38	0.34	Pden_0023	xoxI rhodanese
Pden_0022	1.44	1.59	4.53	1.01	0.32	Pden_0022	xoxJ quinole membr.
Pden_0021	4.22	9.76	12.16	3.94	0.35	Pden_0021	cycB c553i putative
Pden_0020	14.17	2.68	12.32	2.24	1.15	Pden_0020	xoxF PPQ
Pden_0019	4.23	0.46	3.49	0.64	1.21	Pden_0019	fghA
Pden_0018	4.43	0.75	3.67	0.73	1.21	Pden_0018	N-acetyltransferase
Pden_0017	8.30	1.19	5.97	0.70	1.39	Pden_0017	clpP
Pden_0016	6.57	8.32	11.16	3.21	0.59	Pden_0016	flhA
Pden_0015	10.11	65.20	48.27	17.44	0.21	Pden_0015	gfa activation factor
Pden_0014	1.16	0.24	2.02	0.49	0.57	Pden_0014	hypothetical
Pden_0013	0.87	0.08	1.09	0.11	0.80	Pden_0013	coproporphyrinogen ox
Pden_0012	2.32	0.66	1.53	0.34	1.52	Pden_0012	endoribonuclease
Pden_0011	3.85	0.50	2.49	0.42	1.54	Pden_0011	pyrophosphatase
Pden_0010	3.45	0.50	2.75	0.56	1.25	Pden_0010	rph ribonuclease PH

Pden_4448	2.42		3.03		0.80	Pden_4448	ABC
Pden_4449	0.69		2.36		0.29	Pden_4449	nasC
Pden_4450	9.06		0.25		36.96	Pden_4450	nasH
Pden_4451	0.15		0.23		0.67	Pden_4451	nasG
Pden_4452	16.44		0.44		37.17	Pden_4452	nasB
Pden_4453	0.75		1.09		0.69	Pden_4453	nasA
Pden_4454	13.85		0.58		24.06	Pden_4454	nasS
Pden_4455	10.05		0.48		20.73	Pden_4455	nasT

4.4.2 Microarray gene expression dataset

Note: The microarray dataset of this chapter is supplied in the accompanying CD-ROM.

4.5 Δ*narR* sequencing dataset

Note: The Δ*narR* sequencing dataset of this chapter is supplied in the accompanying CD-ROM.

References

Alston, M., J. Seers, J. Hinton and S. Lucchini (2010). "BABAR: an R package to simplify the normalisation of common reference design microarray-based transcriptomic datasets." BMC Bioinformatics **11**(1): 73.

Wood, N. J., T. Alizadeh, S. Bennett, J. Pearce, S. J. Ferguson, D. J. Richardson and J. W. Moir (2001). "Maximal expression of membrane-bound nitrate reductase in *Paracoccus* is induced by nitrate via a third FNR-like regulator named NarR." J Bacteriol **183**(12): 3606-3613.

Wood, N. J., T. Alizadeh, D. J. Richardson, S. J. Ferguson and J. W. Moir (2002). "Two domains of a dual-function NarK protein are required for nitrate uptake, the first step of denitrification in *Paracoccus pantotrophus*." Mol Microbiol **44**(1): 157-170.

The regulation of denitrification in *P. denitrificans*

5. The effect of pH on denitrification

Georgios Giannopoulos

Contents

5.1 Introduction

5.1.1 pH

Bacteria sense and respond to extracellular environmental changes by adjusting their metabolic pathways and rates, this in turn affects their growth rates (White *et al.* 2012). Besides the electron acceptors (nitrate and oxygen), one of the many environmental signals that microbes respond to is the pH, which is a logarithmic measure of hydrogen ion concentration, in its simplified form (Equation 1 and 2; (Covington *et al.* 1985). Field data have shown that final product of denitrification is affected by the pH (Enwall *et al.* 2005, Cuhel *et al.* 2010).

$$pH = -log(\alpha_H) = -log\left(\frac{m_H * \lambda_H}{m^o}\right)$$

Equation 1 Calculation of the pH value, which equals to the decimal logarithm of the reciprocal of the hydrogen ion activity in a solution. Where $\boldsymbol{a_H}$ is the hydrogen ion activity, $\boldsymbol{m_H}$ molarity, $\boldsymbol{\lambda_H}$ molar activity coefficient and $\boldsymbol{m^o}$ standard molality of the hydrogen ions.

$$pH = -log([H^+])$$

Equation 2 Simplified calculation of the pH value, where pH is the negative decimal logarithm of the hydrogen ion concentration in a solution

Bacteria can be found growing in environments with varying external pH (pH_o) from pH 1 to in acid springs up to pH 11 in soda lakes. The genus *Paracoccus* has an optimal growth range between pH 6.5 and 8.5 for the different individual *Paracoccus* species, with the exception of *P. alcaliphilus*, which is able to grow over a pH range spanning from pH 7 to 9.5 with a growth optimum pH between 8 and 9. *P. denitrificans* is a member of the *Paracoccus* genus known to reduce nitrate to di-nitrogen in a ratio of 2:1 anaerobically and has a pH optimum around pH 7.6 (Kelly *et al.* 2006). However, during anaerobic denitrification it is often observed that the pH of the medium increases due to the consumption of the extracellular hydrogen ions (See 1. Introduction).

P. denitrificans is classified as a neutrophile and maintains an internal pH (pH_i) of around 7.5 – 8. Neutrophiles can maintain a pH gradient (ΔpH) of 0.5 – 1.5 units (Equation 3). The proton motive force (Δp) is a function of the membrane potential (ΔΨ) and the ΔpH (Equation 4). Thus, by lowering the pH_o of the growth medium, the ΔpH will increase, directly affecting the ΔΨ and changing the relative contribution of the ΔΨ to the Δp. In neutrophiles the ΔΨ and the ΔpH contributes ~80% and ~20% respectively to the Δp (White *et al.* 2012).

$$\Delta pH = pH_i - pH_o$$

Equation 3 Calculation of the bacterial pH gradient (*ΔpH*), where pH_i is the cytoplasmic pH and pH_o is the extracellular pH

$$\Delta p = \frac{\Delta \mu_{H^+}}{F} = \Delta\Psi - 60\Delta pH$$

Equation 4 Calculation of the proton motive force *Δp*, where $\boldsymbol{\Delta\mu_{H^+}}$ is the proton electrochemical energy, *F* the Faraday constant, *ΔΨ* the membrane potential and *ΔpH* the pH gradient.

5.1.2 pH induced metabolism in cells

Changes in the the external pH signals transcriptional and metabolic mechanisms to maintain the desired pH_i, in a process generally described as pH homeostasis, to control the continuous proton flow across the cell membrane (Booth 1985). Generally, the cytoplasmic membrane is highly impermeable to protons (H^+). ATP synthase brings ~3 H^+ from the periplasmic space to the cytoplasm to produce one ATP molecule. However the ion-to-ATP ratio depends firstly, on the number of *c*-subunits in the F_O unit; there are three catalytic sites on ATP synthase which driven by a rotary mechanism $\left(\frac{H^+}{ATP} = \frac{number\ of\ c\ subunits}{3}\right)$ and secondly, the physiological and redox conditions of the bacterial cell (Toei *et al.* 2007, von Ballmoos *et al.* 2008). These protons accumulate in the cyctoplam, lowering the H^+ gradient difference. Subsequently the imported protons are exported to the cell surface when used in the respiration pathway to reduce NADH and

oxygen or in other metabolic processes such as the decarboxylation of amino-acids (Figure 1). When the cytoplasmic pH (pH_i) becomes too acidic, protons are pumped outside and exchanged for K^+ to the cytoplasm. When the cytoplasm becomes alkaline protons are brought in by specific Na^+ and K^+ antiporters (Figure 2). Little is known about the pH induced genetic regulation. However, the pH induced effects on protein and metabolic functioning are well described in vivo and in vitro experiments (Kucera *et al.* 1986, Dermastia *et al.* 1991, Berks *et al.* 1993, Berks *et al.* 1994, Kucera 2005, Gates *et al.* 2008, Talley and Alexov 2010).

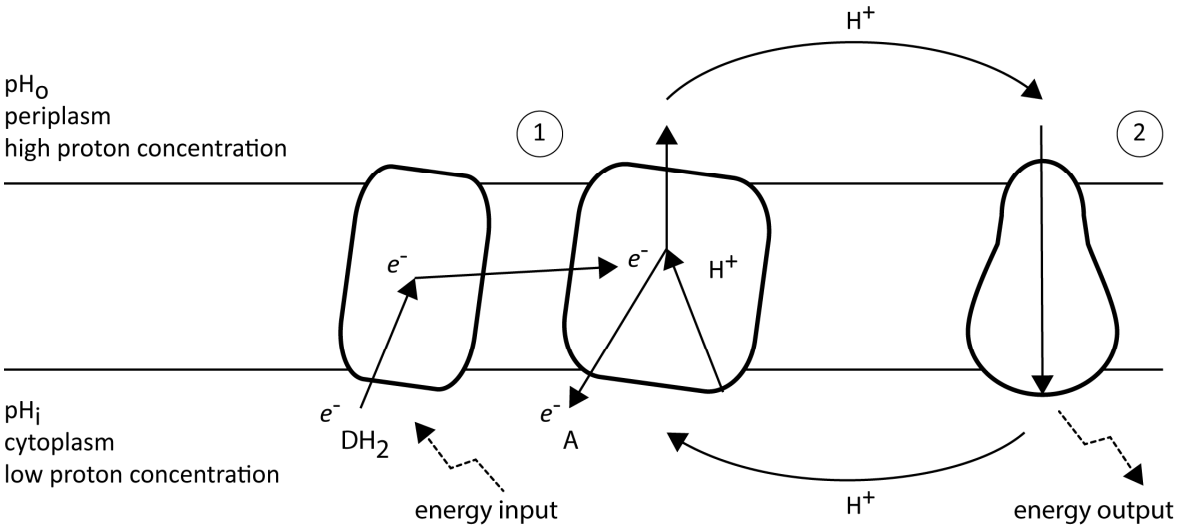

Figure 1 Simplified illustration of the proton and electron loop and gradient. Protons are translocated to the periplasm by a proton pump using chemical or light energy; electrons are transferred from the electron donor (DH_2) to the electron acceptor (A) via an electron transport chain to maintain electrical balance (1). Protons are then imported to the cytoplasm by specialized proton importers that produce energy. The accumulation of protons outside the membrane establishes a membrane potential, which is positive outside. The pH gradient is also established and is acidic outside (pH_o). For detailed respiration diagrams see Chapter 1.

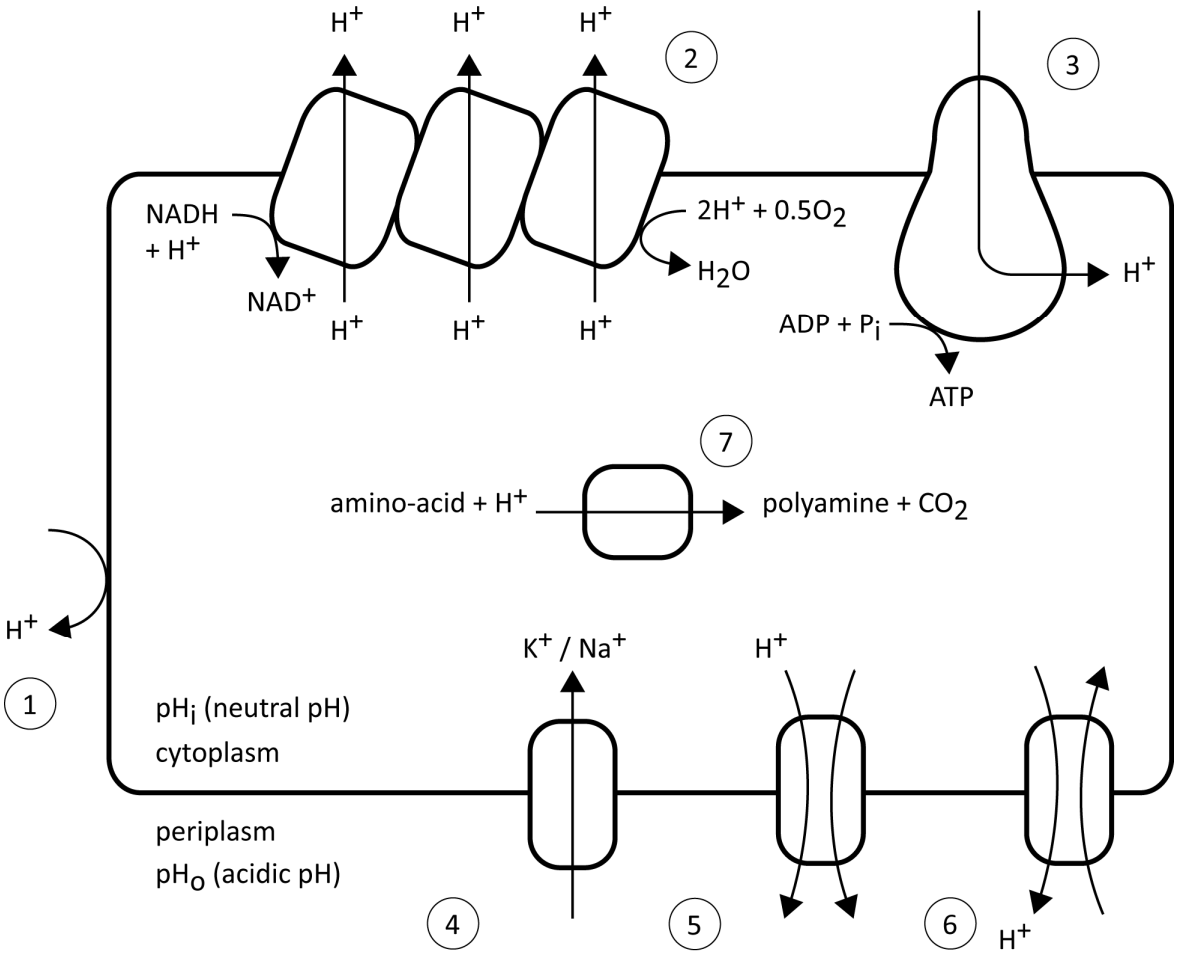

Figure 2 Schematic illustration presenting general mechanisms to respond in an external pH (pH_o) change and to maintain the internal pH (pH_i) homeostasis in bacteria. 1: Cytoplasmic membrane is impermeable to the influx of hydrogen ions (protons). 2: Respiration dependent proton pumps remove the cytoplasmic protons or use them to reduce oxygen and nitrogen oxyanions in aerobic and anaerobic respiration, respectively. 3: Protons renter the cytoplasm via the ATPase and ATP is generated. 4: The internal positive membrane potential (potentially generated by potassium or sodium uptake) creates a chemiosmotic gradient and protons have to be transported against to enter the cytoplasm. 5 and 6: Other secondary symporters and antiporters that can be used to remove excess cytoplasmic protons. 7: Adjustment of metabolic pathway to reduce the cytoplasmic [H^+]; for illustration purposes, decarboxylase converts an intracellular amino-acid to polyamine and subsequently the polyamine is exported via an antiporter in exchange of another amino-acid and effectively removing on proton.

The anaerobic respiratory system of *P. denitrificans* generates a ΔΨ of 150 mV at pH_o 7.3 (McCarthy *et al.* 1981). At this neutral pH the contribution of ΔpH to the overall Δp is relatively low (ΔpH < 0.5). Besides the obvious effect of the pH_o to the proton flow and subsequently to the Δp of the cell, the pH_o may affect the exposed periplasmic enzymes of the anaerobic respiratory electron transport chain. Two of the four respiratory enzymes involved in the anaerobic reduction of nitrate to di-nitrogen are located in the periplasmic compartment making them more susceptible to the environmental changes of the pH_o. Those enzymes are the nitrite (Nir) and nitrous oxide (Nos) reductase. Nitrite reductase reduces nitrite to nitric oxide with one proton and one electron and the nitrous oxide reductase converts nitrous oxide to di-nitrogen in a two proton and two electron processes. Studies have shown that purified enzymes show a pH optimum around pH 5.5 and 8 for the nitrite and nitrous oxide reductase using an artificial electron donor, N, N, N', N'-tetramethyl-p-phenylene-diamine (Kucera *et al.* 1986). It is therefore suggested that the rate of denitrification or the final denitrification product may be pH dependent.

Kucera *et al.* (1987) demonstrated that in a pH 6.4 batch culture of *P. denitrificans* nitrous oxide accumulated until nitrite was completely consumed; then nitrous oxide was slowly reduced. At pH 7.2, nitrite was consumed and reduced to di-nitrogen without any observation of nitrous oxide accumulation. Those experiments were performed in batch cultures supplied with nitrite and succinate as a physiological electron donor. Kucera *et al.* (1987) concluded that pH affects the redox state of cytochrome *c* oxidation and plays an important role in electron distribution between nitrite and nitrous oxide reductase (for a detailed electron flow diagram please see Chapter 1).

In another study using cells of *P. denitrificans* taken from nitrate limited continuous cultures, Thomsen *et al.* (1994) observed a similar pattern of denitrification intermediate products; at pH 5.5 nitrite and nitrous oxide could be detected whereas at pH 8.5 nitrate was converted directly to di-nitrogen. At pH 8.5 nitrate consumption rate was 0.23 and the di-nitrogen production rate was 0.23 $\mu mol.m^{-1}$.mg C cell. At a lower pH (5.5) the nitrate consumption, the nitrite consumption and production and the nitrous oxide production rates were equally 0.19 $\mu mol.m^{-1}$.mg C cell. However, the nitrous oxide consumption and di-nitrogen production rates were 10 fold lower than the nitrate consumption rate (0.02 $\mu mol.m^{-1}$.mg C cell).

Baumann *et al.* (1997) has observed that the denitrification activity in *P. denitrificans* is hindered at pH 6.8 with a corresponding nitrite accumulation in the continuous culture system. At pH 7.5 the cumulative production of nitrite and di-nitrogen was 11 and 21 mmole respectively, with a 2:1 denitrification ratio. At pH 6.8 nitrite and di-nitrogen cumulative concentration was 31 and 2 mmole respectively. Nitrous oxide could be detected but at that time point the biomass gradually decreased accompanied by a complete reduction of carbon dioxide production in the reaction vessel and thus microbial activity. It was assumed by the authors that this inhibition was due to the low pH and nitrite accumulation that resulted in the formation of free nitrous acid in the culture.

Several investigations that studied the total soil microbial community have shown that pH has a strong influence in the nitrous oxide to di-nitrogen ratio and an underlying effect in the structure of the microbial community. Parkin *et al.* (1985) demonstrated using the acetylene inhibition method that the potential denitrification rate of a neutral soil (pH 6) was 2.7 times higher that of an acidic soil (pH 3.9; 1800 N $ng.g^{-1}.d^{-1}$) in anaerobic soil slurries supplemented with 1 mM glucose. This study shows that microbial denitrification is occurring at low pH levels; however, the end product of denitrification (nitrous oxide or di-nitrogen) was not estimated. In another study using sequential batch reactor (SBR) culture systems van den Heuvel *et al.* (2010) indicated that at pH 4 a *Rhodanobacter* dominated community was able to reduce nitrate to nitrous oxide, which was the end product. There are more supporting data that illustrate the detrimental role of extracellular pH to the last step of denitrification, the reduction of nitrous oxide to di-nitrogen, using the denitrification product ratio $\left(\frac{N_2}{N_2O}\right)$ based on high resolution batch cultures (Bakken *et al.* 2012). The authors found that the pH dependent denitrification product ratio decreases with acidity. Further investigations of this broad phenomenon, indicated that pH has a post-transcriptional effect on the assembly of the nitrous oxide reductase. In batch cultures of *P. denitrificans* it was found that the relative transcription rate of *nosZ* was unchanged at pH 6, however the relative mRNA gene copies were noticeably low when compared with the pH 7 treatment (Bergaust *et al.* 2011). Generally, it has been demonstrated that the acidic pH in soil microbial communities resulted in high nitrous oxide emissions and that liming or increasing the pH resulted in lower nitrous

oxide emissions and favoured di-nitrogen production (Bååth and Arnebrant 1994). The same pattern has also been demonstrated in soil microbial populations and pure cultures. Clearly, the external pH has an overall effect on denitrification and metabolic rates. However, little is known about the pH induced transcriptional regulation of denitrification. In this chapter, *P. denitrificans* cultures were incubated in continuous mode (continuously stirred tank reactors; CSTR) and the denitrification by-products were monitored continually in three treatments; with sub-optimal (pH 6.5), optimal (pH 7.5) and above optimal pH (8.5). Furthermore, transcriptional investigations of the *P. denitrificans* genome were made in continuous culture treatments of sub-optimal (pH 6.5) and optimal pH (control; pH 7.5).

5.1.3 Practise of the pH determination

To investigate the pH effect on denitrification a defined mineral medium (based on Vishniac and Santer (1957)) was used. The medium was buffered with a mono and di-basic phosphate buffer (see Chapter 7. Materials and Methods). The pH of the medium was adjusted by adding sodium hydroxide or sulphuric acid. The addition of hydrochloric acid to lower the pH completely inhibited the growth of *P. denitrificans*. The pH of the medium was determined prior to autoclaving or continuously in the CSTR. The probes were calibrated as described in the Materials and Methods chapter and were found to have a response time of 5.74 (±0.36) seconds to achieve a stable reading to ±0.1 pH units. All pH probes used had an embedded reference probe to correct the pH measurements.

5.2 Results

5.2.1 Batch Results

The phenotype of *P. denitrificans* at below and above optimum pH was determined using anaerobic batch cultures. The pH 7.5 treatment was assigned as the control treatment of this experimental investigation. The control treatment (pH 7.5) has a short lag phase and reached its maximum growth at ~18 hours with an optical density of ~0.7. The pH 8.5 treatment has a similar pattern as the control with a short lag phase and the maximum

growth was achieved at ~18 hours. Contrary to the control and the pH 8.5 treatments, the pH 6.5 treatment had a long lag phase (48 hours) and gradually reached a maximum optical density of 0.6 after 100 hours (Figure 3). The pH had a notable effect on the maximum specific growth rate (μ_{max}) of the cultures. The μ_{max} was 0.23, 0.34 and 0.21 h^{-1} for the pH 6.5, 7.5 and 8.5 treatments respectively. At the end of the incubation period, the pH was determined for each treatment and was 6.8, 7.8 and 8.8 for the acidic, neutral and alkaline treatment respectively. Additionally, three more pH treatments were tested and no growth was observed anaerobically; these were the pH 4.5, 5.5 and 9.5 treatments.

At the end of the anaerobic incubation the nitrite and nitrous oxide concretions were determined. The extracellular nitrite concentration was ~56, 3 and 4 μM for the pH 6.5, 7.5 and 8.5 treatment, respectively. The nitrous oxide concentration was 184, 6 and 8 μM for the pH 6.5, 7.5 and 8.5 treatments respectively (Figure 4).

In summary, a single unit change in the extracellular pH (pH_o), which corresponds to a 10 fold change in the proton concentration, had an effect on the growth phenotype and the concentration of nitrite and nitrous oxide. Specifically the sub-optimal treatment (pH 6.5) had along lag phase and a lower μ_{max}. The concentration of nitrite and nitrous oxide was at similar levels for the pH 8.5 and pH 7.5 treatment; the detected concentration for the aforementioned metabolites was very close to the detection limit of 2 μM. However, a small but detectable accumulation of nitrite and nitrous oxide was observed in the acidic treatment. The last observation suggests that the denitrification pathway at sub-optimal pH_o may have nitrous oxide as the end product. The growth rates in all three treatments were greater than the dilution rate used in the CSTR systems. Therefore, incubating the pH 6.5, 7.5 and 8.5 treatments could be feasible with the continuous culture parameters previously used (see Chapters 2, 3 and 4).

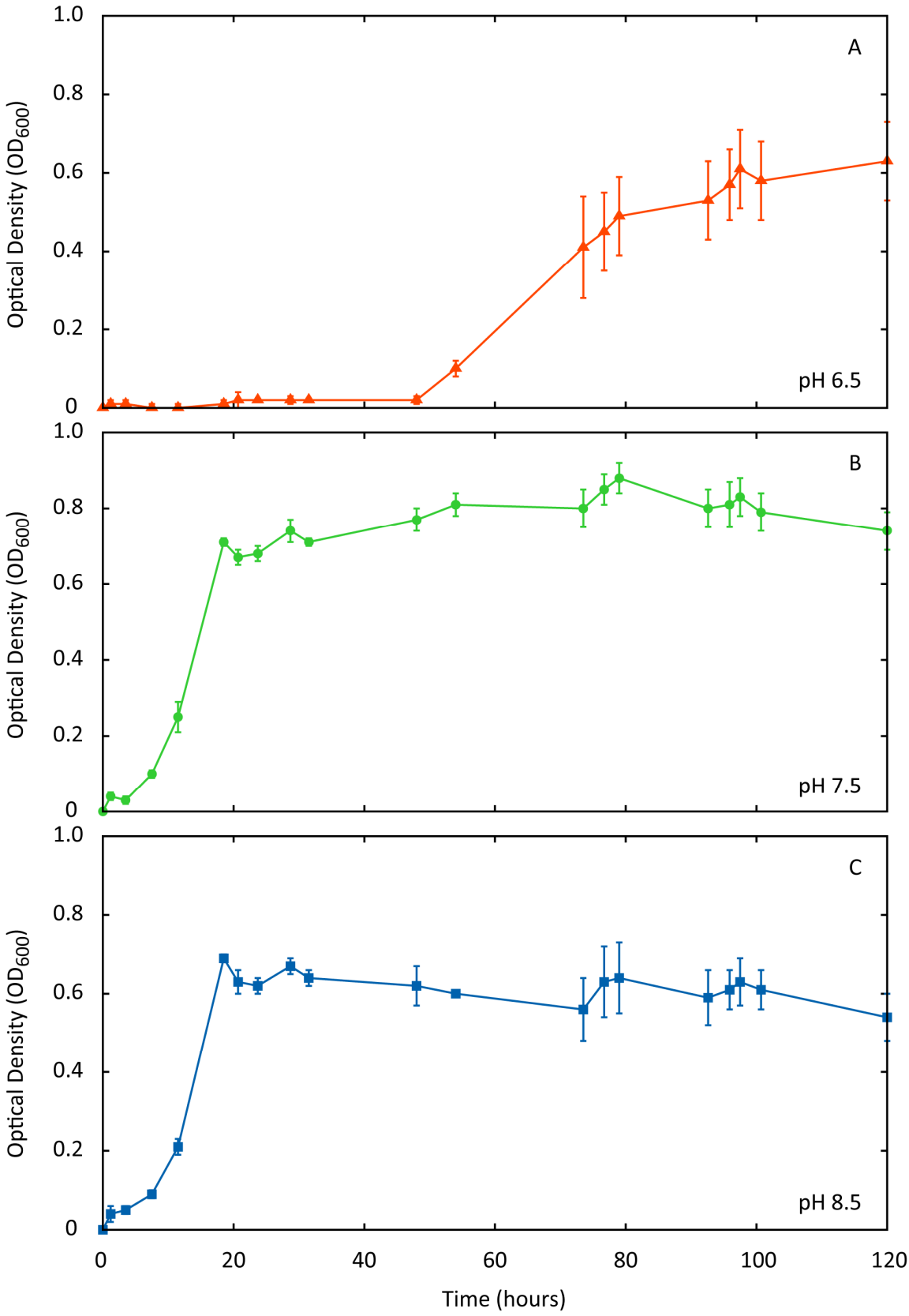

Figure 3 Anaerobic growth curves of *P. denitrificans* cultures in Hungate tubes. Panel A illustrates anaerobic growth at pH 6.5 (▲), B at pH 7.5 (●) and C at pH 8.5 (■). Error bars denote standard error of means (n=6).

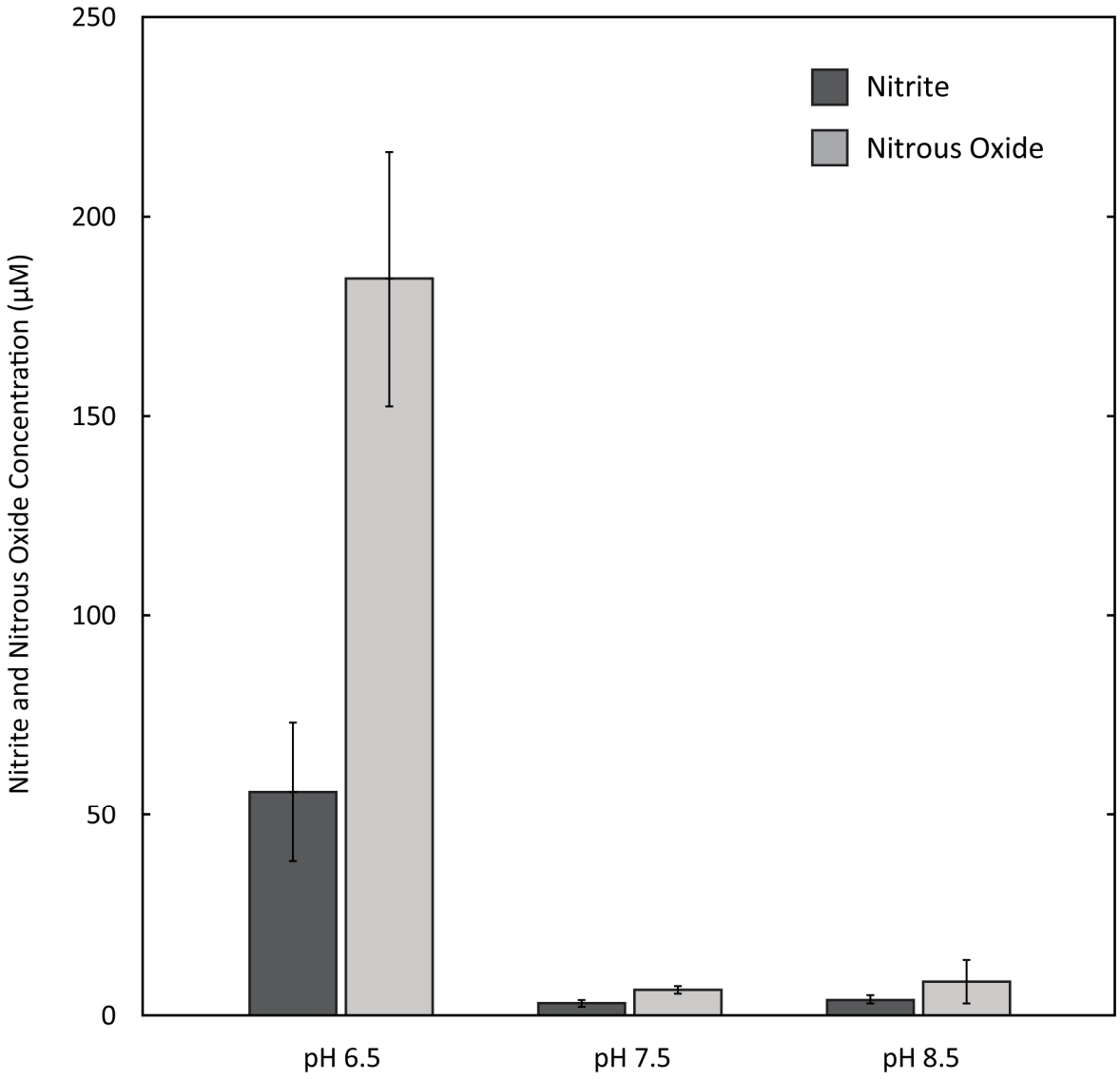

Figure 4 Average concentrations of nitrite and nitrous oxide in the anaerobic batch treatments of *P. denitrificans* with acidic (pH 6.5), neutral (pH 7.5) and alkaline pH (pH 8.5). Error bars denote standard error of means (n=6).

5.2.2 Chemostat results

A series of chemostat incubations were performed to investigate the effect of pH on denitrification in *P. denitrificans* continuous cultures. Previously, it was demonstrated that at low pH (6.5) *P. denitrificans* had a relatively long lag phase and a low specific growth when compared to the control pH (7.5) cultures. No differences were observed in the batch growth rate of *P. denitrificans* at higher pH (8.5) when compared with the control treatment.

In the first experimental approach, the pH_o was adjusted directly after the end of the batch phase of incubation which coincided with the complete consumption of the remaining dissolved oxygen in the tank reactor. Specifically, the cells were incubated aerobically for ~24 hours at pH 7.5. The biomass density reached its maximum observable value of ~0.45 $g.L^{-1}$ at 22 hours. At 20 hours, the air supply was switched off. The cells completely consumed the remaining dissolved oxygen and the dissolved oxygen concentration was ~0 µM at ~24-26 hours. At ~24 hours the pH was lowered to 6.5 with the automatic addition of small volumes of 0.1 M sulphuric acid (Figure 5 A). Instantly a gradual increase of the dissolved oxygen with a rate of ~1.5 $\mu M.h^{-1}$ was observed in the reactor. At the end of the incubation dissolved oxygen concentration was ~180 µM (Figure 5 B). The temperature of the incubation was stable at 37^oC throughout the incubation. The bacterial biomass decreased from 0.4 to 0.05 $mg.ml^{-1}$ during the continuous culture phase of the incubation from 20 to 120 hours (Figure 5 C). Therefore, in this experiment the CSTR system did not reach a steady-state in terms of biomass. It was assumed that the sudden change of the pH_o which coincided with the switch from aerobic batch to anaerobic continuous culture affected severely the viability of the cells. An increase in the dissolved oxygen in the culture vessel indicated that anaerobic respiration on nitrate was hindered. This experiment was discarded because the biomass slowly washed out and did not reach a steady-state, thus $\mu \ll D$ (see 2.1.2 Medium composition and mass balances in continuous stirred tank reactors for a detailed chemostat model).

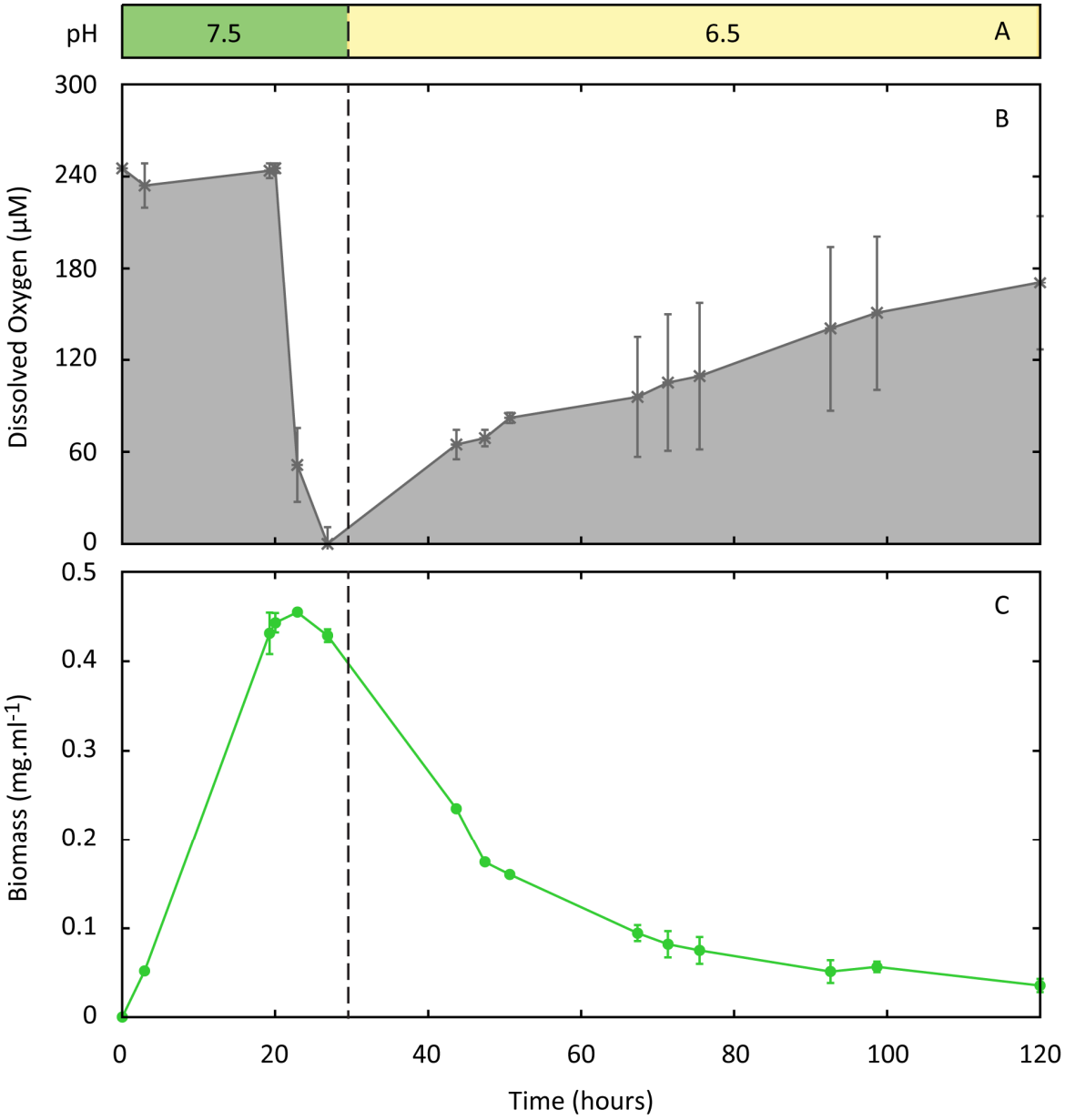

Figure 5 Continuous culture of *P. denitrificans* in the acidic treatment. Panel A illustrates the pH change from 7.5 to 6.5 units, B the concentration of dissolved oxygen (µM) in the culture medium and C the biomass density ($mg.ml^{-1}$) of the culture. The dashed line indicates the pH change in the culture. Error bars denote standard error of the means (n=2).

Based on the previous experience the second series of chemostat incubations were adjusted allowing a longer adaptation period for cells after the aerobic to anaerobic transition and prior to a pH change in the culture medium. In these series the pH was lowered at 64 hours, corresponding to two vessel volumes of continuous culture (Figure 6 A). The culture was incubated at 37^{o}C throughout the experiment. The biomass reached a maximum density of 0.35 mg.ml^{-1} at 20 hours (Figure 6 B). At this point the air supply was switched off and the feed supply was activated injecting fresh sterile medium at 80 ml.h^{-1}. This event initiated the incubation anaerobic continuous culture phase. The pH was constant at 7.5 units from the vessel inoculation until two vessel volumes of continuous culture. During this phase of continuous culture the biomass density stabilized to ~0.28 mg.ml^{-1}. Then, the pH was lowered to 6.5 with the addition of 0.1 M sulphuric acid, and was maintained at that level until the end of the incubation in CSTR systems (64 to 120 hours). This latter phase was annotated as anaerobic continuous culture at acidic pH. During this phase the biomass density dropped from ~0.28 (64 hours) to ~0.2 mg.ml^{-1} (~80 hours) and remained at similar levels after ~4 vessel volumes of continuous culture in CSTR (120 hours Figure 6 B). The culture reached a steady state biomass at the sub-optimal pH (6.5).

Nitrate, nitrite and nitrous oxide were continually sampled, and their concentrations were determined throughout the CSTR incubation (Figure 6 C). The initial concentration of nitrate in the culture medium was ~22 mM during the aerobic batch phase of incubation. Then, a constant reduction of the nitrate concentration in the vessel was observed from 22 mM to 16 mM between 20 and 70 hours of continous culture. During the third phase of sub-optimal pH (6.5) the nitrate concentration flactuated but remained on average at 16 mM. The nitrite concentration was on average below 300 µM during the 120 hour incubation. Nitrous oxide was detected during the steady state phase of the CSTR incubation, on average at 1200 µM. Nitrite and nitrous oxide has been also detected in batch incubations at pH 6.5.

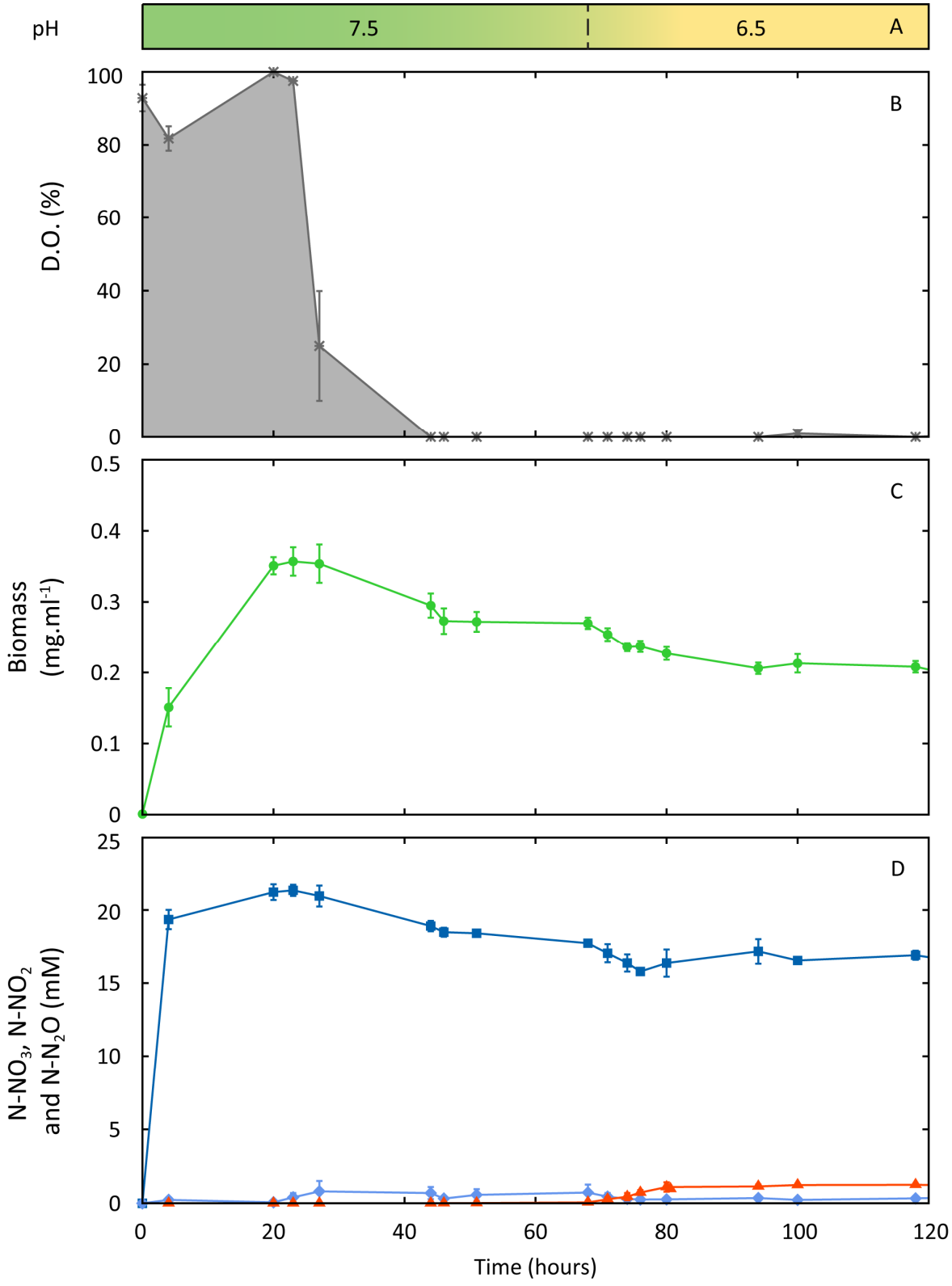

Figure 6 Anaerobic continuous culture of *P. denitrificans* (PD1222) at sub-optimal pH. The temperature was maintained at 37 °C in CSTR. A) pH in the culture vessel B) Average dissolved oxygen (D.O.) concentration of the culture, C) Average biomass (●) of the culture and D) Average nitrate (■), nitrite (◆) and nitrous oxide (▲) concentration of the culture (n=3; error bars denote SEM).

The third chemostat experiment was performed with a pH constant at 7.5 throughout the incubation (Figure 7 A). Cells of *P. denitrificans* were incubated in aerobic batch mode until ~20 hours; the biomass was ~0.32 $mg.ml^{-1}$ at that time point. Then the air supply was restricted and the incubation mode changed to continuous culture. The dissolved oxygen profile is illustrated in panel B of Figure 7. The grey filled curve indicates clearly the aerobic batch and the anaerobic continuous culture phase of the incubation. Soon after the air supply restriction, the cells removed any remaining dissolved air by basal respiration. During the continuous culture phase of this incubation the biomass decreased and reached a steady state after ~2 vessel volumes (~60 hours) and remained at ~0.25 $mg.ml^{-1}$ till the end of the continuous culture (Figure 7 C).

The concentrations of extracellular nitrate, nitrite and nitrous oxide were determined at frequent time points as indicated on panel D of Figure 7**.** It was observed that the extracellular nitrate concentration remained unchanged during the aerobic batch phase of the incubation; the nitrate concentration was ~22 mM in the culture vessel. A decline in the nitrate concentration corresponded with switch from aerobic to anaerobic incubation. During the anaerobic continuous culture mode, cells reduced ~22 mM of nitrate initially available in culture vessel to ~16 mM. Samples were also analysed for nitrite and nitrous oxide. The concentration of nitrite was on average 880 µM. The levels on nitrous oxide in the culture vessel were below detection limit. Therefore, at pH 7.5 the cell-consumed nitrate was reduced efficiently to di-nitrogen in anaerobic continuous culture.

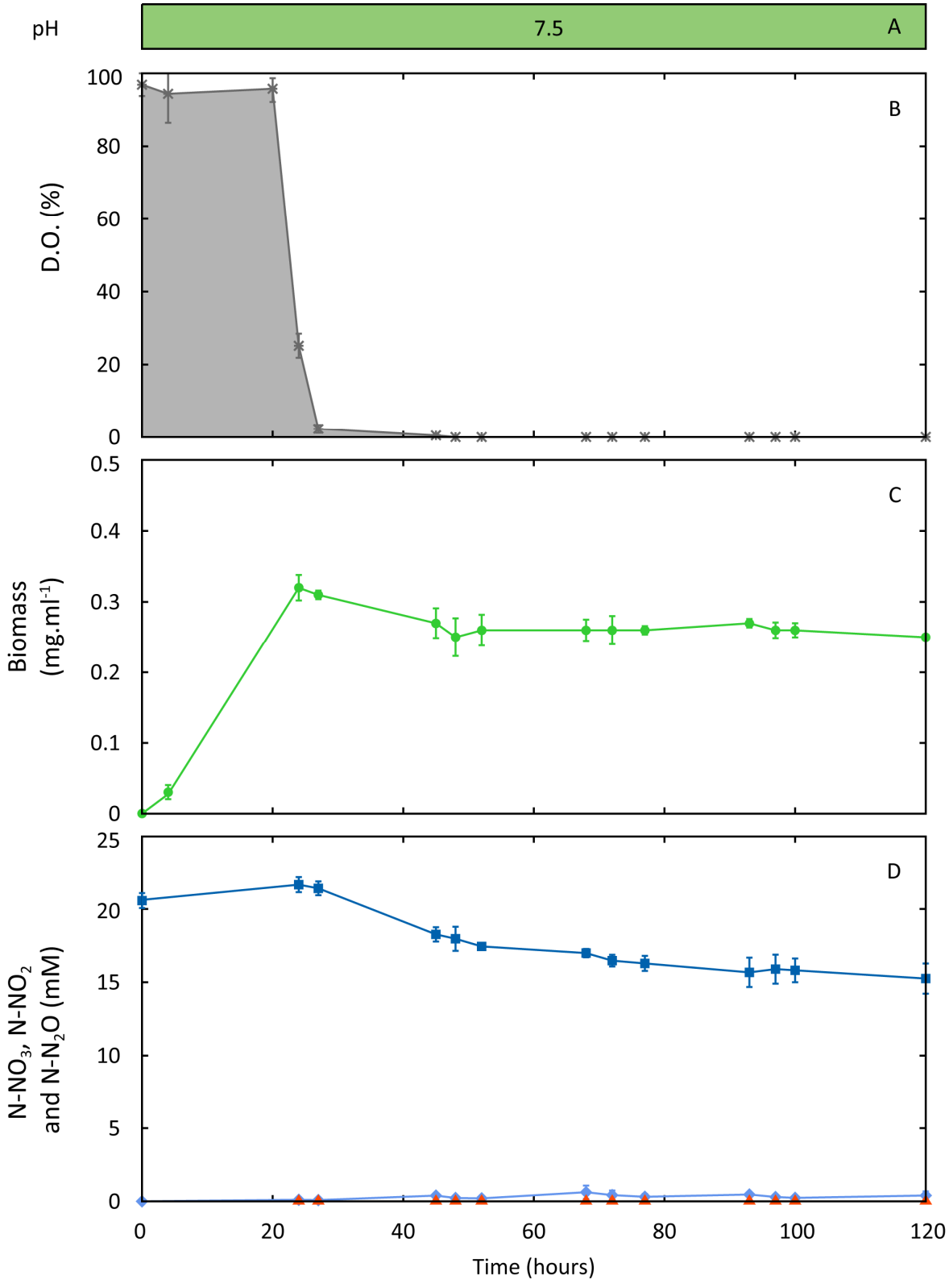

Figure 7 Anaerobic continuous culture of *P. denitrificans* (PD1222) at optimal pH. The temperature was maintained at 37 ^{o}C in CSTR. A) pH in the culture vessel B) Average dissolved oxygen (D.O.) concentration of the culture, C) Average biomass (●) of the culture and D) Average nitrate (■), nitrite (◆) and nitrous oxide (▲) concentration of the culture (n=3; error bars denote SEM).

The effects of above-optimal pH (8.5) on the denitrification rates were studied in the fourth chemostat experiment. As previously performed, cells of *P. denitrificans* were cultured initially in aerobic batch mode and then anaerobically in continuous culture mode at pH 7.5. The temperature in the culture vessel remained at 37^{o}C throughout the incubation (120 hours). During the anaerobic continuous culture phase and after ~2 vessel volumes of hydraulic retention time the pH in the culture medium was adjusted to 8.5 with the addition of 1 M of sodium hydroxide and remained until the end of the incubation. The time point of the pH increase is indicated with a dashed line in panel A of figure 8 at ~68 hours. Initially, cells were grown in aerobic conditions for ~24 hours and reached a biomass density of ~0.35 mg.ml^{-1} in the culture vessel. At that moment, the air supply was restricted and the bacterial culture consumed the remaining dissolved oxygen; the dissolved oxygen consumption profile of the culture is illustrated in figure 8 B. During the continuous culture phase of the incubation the cell biomass declined from 0.35 to 0.2 mg.ml^{-1} and remained to this level at the steady state phase (Figure 8 C; ~100 to 120 hours). A clear effect of the above-optimal pH was observed in the biomass density of the culture corresponding to a further decline of the biomass density in the culture (68 hours).

The denitrification metabolic profile of the pH 8.5 CSTR treatment was similar to the control (pH 7.5 CSTR treatment). During the aerobic batch culture the nitrate concentration levels remained unchanged to ~21 mM. Then, during the anaerobic continuous culture, the extracellular nitrate concentration levels declined to a steady state nitrate concentration of ~16 mM. The nitrite concentration was on average > 200 μM throughout the incubation and the nitrous oxide concentration was below detection level. Thus the consumed nitrate was effectively reduced to di-nitrogen in the anaerobic continuous culture at pH 8.5.

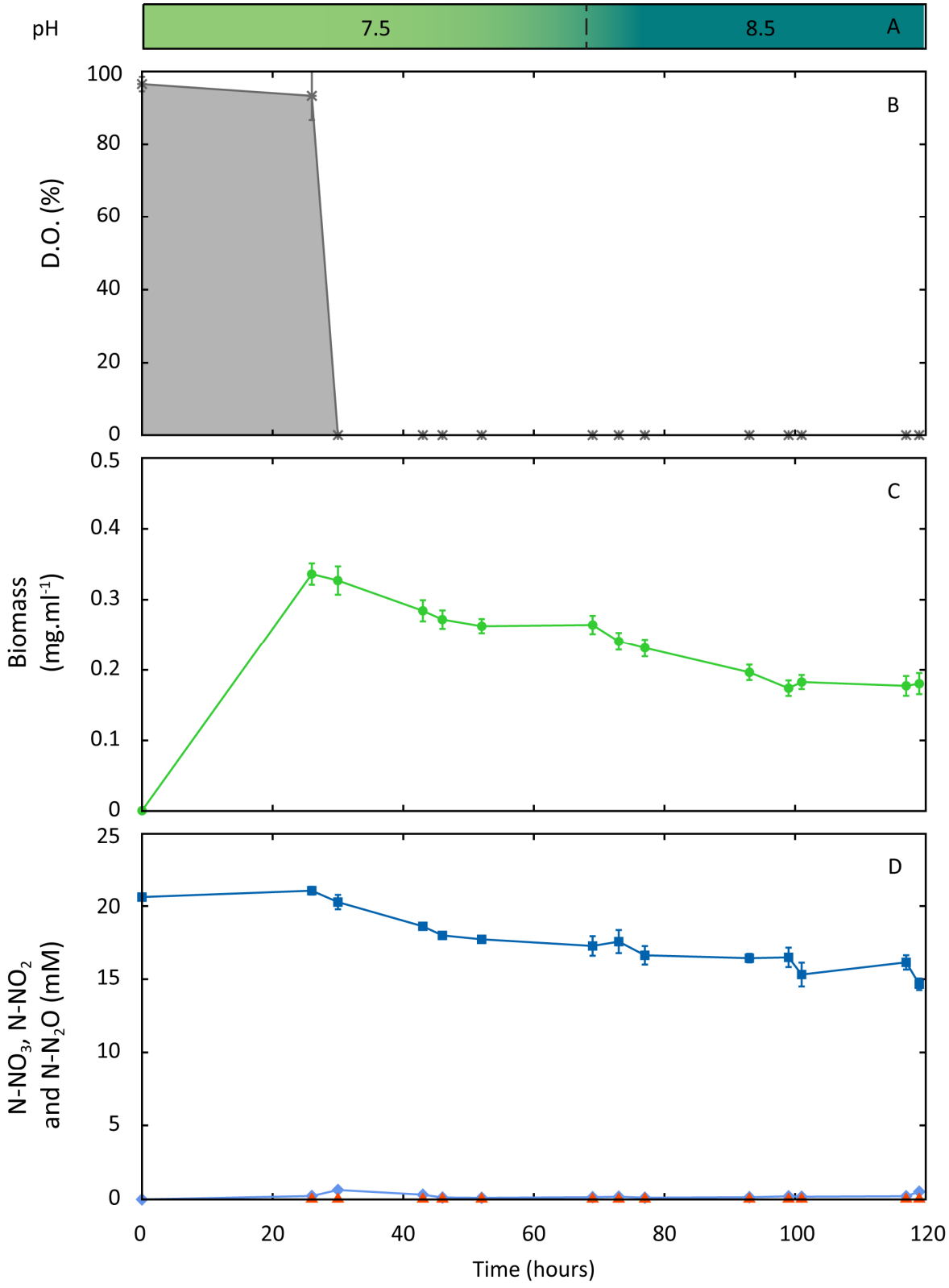

Figure 8 Anaerobic continuous culture of *P. denitrificans* (PD1222) at above-optimal pH. The temperature was maintained at 37 °C in CSTR. A) pH in the culture vessel B) Average dissolved oxygen (D.O.) concentration of the culture, C) Average biomass (●) of the culture and D) Average nitrate (■), nitrite (◆) and nitrous oxide (▲) concentration of the culture (n=3; error bars denote ±SEM).

Table 1 The consumption and production quotient rates of the pH continuous culture treatment in CSTR.

#	Strain	pH	Temp. ^{o}C	D h^{-1}	OD	±SE	X $g.L^{-1}$	±SE	D/X L.g-1.h-1	±SE	qX $g.L^{-1}.h^{-1}$	±SE
1	PD1222	7.5	30	0.053	0.52	0.02	0.25	0.01	0.22	0.01	0.12	0.01
2	PD1222	6.5	30	0.017	0.39	0.02	0.20	0.01	0.08	0.00	0.08	0.01
3	PD1222	8.5	30	0.053	0.35	0.02	0.18	0.01	0.30	0.02	0.06	0.01

Table continues below.

#	Strain	pH	$[NO_3]_0$ µM	±SE	$[NO_3]_t$ µM	±SE	$[NO_2]_t$ µM	±SE	$[N_2O]_t$ µM	±SE	$[N_2]_t$ µM	±SE
1	PD1222	7.5	20723	1095	15159	115	89	44	0.7	0.1	5475	1078
2	PD1222	6.5	20533	352	15783	577	323	46	1238	25	3289	458
3	PD1222	8.5	20767	145	15376	72	307	60	7	1.7	5076	145

Table continues below.

#	Strain	pH	$[NO_3]_c$ $\mu mol.g^{-1}.h^{-1}$	±SE	$[NO_2]_p$ $\mu mol.g^{-1}.h^{-1}$	±SE	$[NO_2]_c$ $\mu mol.g^{-1}.h^{-1}$	±SE	$[N_{2O}]_p$ $\mu mol.g^{-1}.h^{-1}$	±SE	$[N_2]_p$ $\mu mol.g^{-1}.h^{-1}$	±SE
1	PD1222	7.5	1215	274	18	9	1197	283	0.2	0.0	1196	283
2	PD1222	6.5	406	43	27	3	379	38	104	6.4	275	57
3	PD1222	8.5	1597	79	92	21	1505	72	2	0.6	1503	72

The quotient rates were calculated based on the average value of the last three data points taken at the steady state phase of the incubation. The index number (#) in front of each row indicates the treatment, where 1 indicates the control treatment (pH 7.5), 2 the pH 6.5 and 3 the pH 8.5 treatment. All treatments used the wild type strain of *P. denitrificans* (PD1222) (n=3, standard errors (±SE) were calculated as SEM).

The production and consumption rates were calculated and summarised with the accompanying culture parameters of each treatment in **Table 1**. The above optimum pH treatment of 8.5 was comparable to the control treatment of pH 7.5. Specifically, the consumption rates for nitrate and nitrite were on average at 1400 N $\mu mol.g^{-1}.h^{-1}$. A 6 and a 10 fold difference was observed in the nitrite and nitrous oxide production quotient rate between the pH 8.5 and the control treatment (pH 7.5). However, the absolute magnitude is quite low <100 and <2 N $\mu mol.g^{-1}.h^{-1}$ for the nitrite and nitrous oxide production quotient respectively. The di-nitrogen production quotient rate was ~1200 and ~1500 N $\mu mol.g^{-1}.h^{-1}$ for the control (pH 7.5) and the alkaline (pH 8.5) treatment.

The sub-optimal pH treatment had generally low quotient rates. In detail, the nitrate consumption quotient rate was 3 times lower than the control at 406 N $\mu mol.g^{-1}.h^{-1}$. Approximately, 6% of the nitrate consumption quotient rate was recovered as the nitrite production quotient rate at 27 N $\mu mol.g^{-1}.h^{-1}$, 26% as the nitrous oxide production quotient rate at 27 N $\mu mol.g^{-1}.h^{-1}$ and 69% as the di-nitrogen production quotient rate at 275 N $\mu mol.g^{-1}.h^{-1}$. Clearly, the normalized lower production and consumption rates in the acidic pH treatment correspond with the low growth rates observed in the batch and continuous culture incubation mentioned above.

Out of the four chemostat experiments studying the effect of pH on denitrification rates described previously in this chapter, the sub-optimal pH (6.5) treatment indicated lower growth and nitrate consumption rates for *P. denitrificans*. These pH effects could be reversible once the pH_o is adjusted to neutral levels (pH 7.5). The following long term experiment in continuous culture investigated the denitrification rates when alternating the pH_o from neutral to acidic and finally to neutral again. The pH_o values are illustrated in Figure 9 A, where the dashed line indicates the event of adjusting the pH with the addition of sulphuric acid and sodium hydroxide to lower and increase the pH in the culture vessel respectively. This CSTR experimental followed the same experimental chemostat procedure for the pH 6.5 treatment as previously performed up to 120 hours, after that the continuous culture was extended to 380 hours. A second pH change was introduced at ~280 hours that increased the pH_o from 6.5 to 7.5 units.

Cells of *P. denitrificans* were growth aerobically in batch mode for the first ~20 hours, then then the air supply was switched of and the anaerobic culture mode was initiated, allowing the cells to consume the remaining dissolved oxygen by basal respiration. However, during the pH 6.5 phase of this treatment the oxygen probe recorded a relative small increase of the dissolved oxygen in the culture vessel from 150 to 280 hours (Figure 9 B). This observation is unique and rather interesting because the previous CSTR experiments were performed only up to 120 hours. When the cells entered the second neutral phase of the continuous culture the dissolved oxygen in the culture decreased to zero and the conditions in the culture vessel were anaerobic again.

The biomass dynamics in the reaction vessel are depicted in Figure 9 C. During the aerobic batch phase the cell density reached it maximum recorded value of ~0.38 $mg.ml^{-1}$. Then at the first pH neutral phase of this continuous culture experiment the biomass gradually declined and reached a steady state level of ~0.2 $mg.ml^{-1}$ (~90 to 120 hours). Throughout the acidic phase of this incubation the biomass remained at the same levels as previously, however at the end of this phase a notable drop) in the biomass density was recorded (~0.15 $mg.ml^{-1}$ at ~240 hours in Figure 9 C). During the final phase of this incubation (~260 till 380 hours) the biomass density increased to a steady state level of ~0.2 $mg.ml^{-1}$.

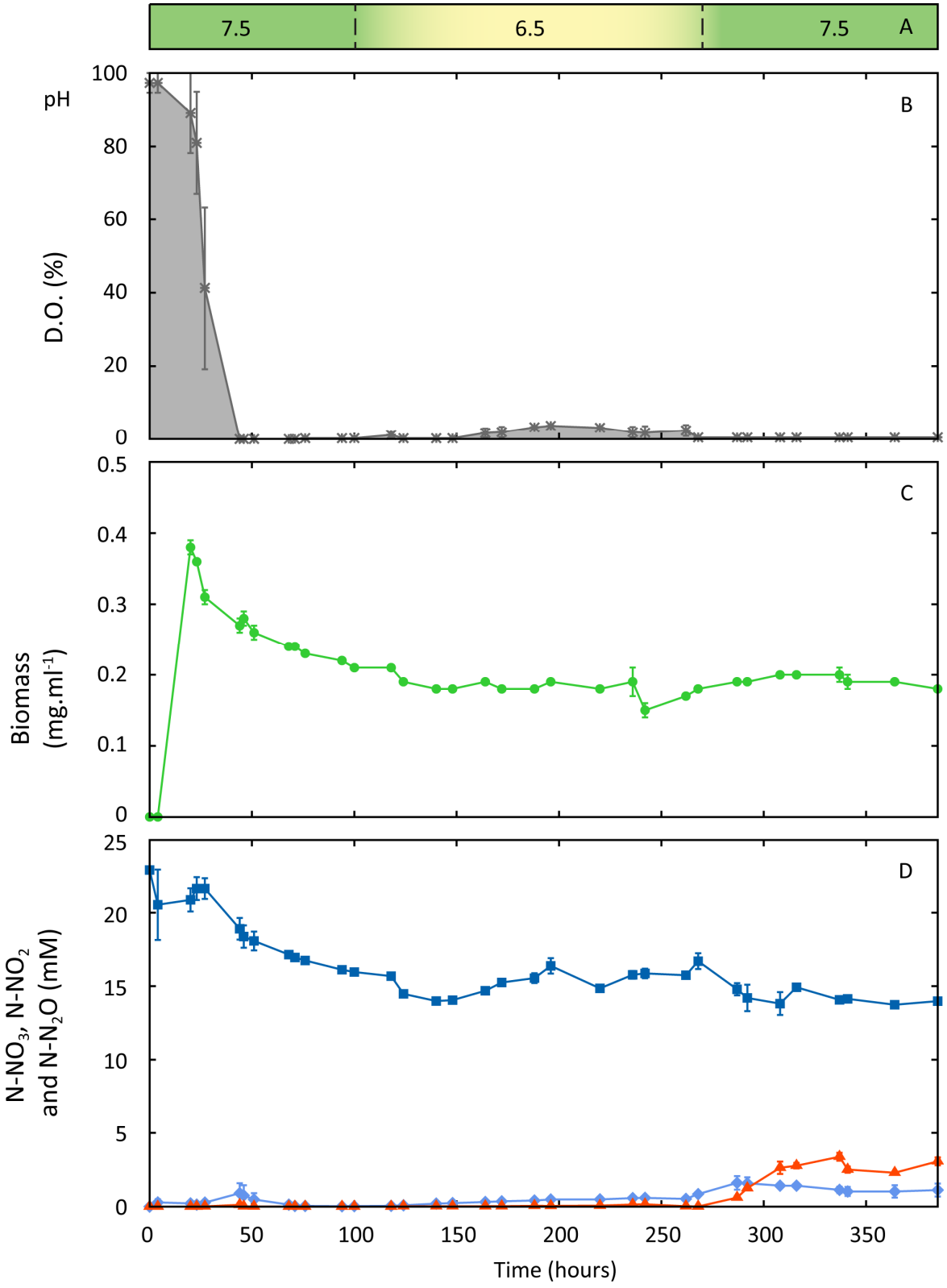

Figure 9 Long term anaerobic continuous culture of *P. denitrificans* (PD1222), the culture was subjected to a dual pH change. The temperature was maintained at 37 ^{o}C in CSTR. A) pH in the culture vessel B) Average dissolved oxygen (D.O.) concentration of the culture, C) Average biomass (●) of the culture and D) Average nitrate (■), nitrite (◆) and nitrous oxide (▲) concentration of the culture (n=3; error bars denote SEM).

The denitrification profile of this treatment revealed some interesting observations for each phase of this long term incubation (Figure 9). During the aerobic batch phase the nitrate levels remained unchanged to ~22 mM. Towards the end of the aerobic phase no nitrite and nitrous oxide were detected. During the first anaerobic phase with a pH of 7.5 the nitrate levels were reduced from 22 to ~15 mM, at ~20 and 120 hours, respectively. There were transient amounts of nitrite (<250 μM) at the early stage of this phase, ~50 hours, that were non detectable later on. Additionally, no nitrous oxide was detected in the reaction vessel of the CSTR system. Then, during the acidic pH phase of the incubation a gradual increase of the nitrate levels was observed, from ~15 mM to ~18 mM at 120 to 280 hours respectively. A gradual increase in the extracellular nitrite concentration to ~1 mM was observed, however the nitrous oxide levels in the reaction vessel were below the detection limit (<2 μM). At ~280 hours the cell culture entered the third anaerobic phase with a neutral pH of 7.5. From this point and onwards a gradual decline in the nitrate concentration from ~18 to 14 mM was observed. The chemostat culture reached a nitrate steady state concentration of ~14 mM from 350 hours and onwards. The nitrite levels remained at ~1mM during this phase and a corresponding increase in the nitrous oxide emissions from this culture was detected. The concentration of nitrous oxide reached ~2mM at the end of this phase and the end of the CSTR incubation (380 hours).

During the acidic phase of the first and last prolonged chemostat experiment small amounts of dissolved oxygen were observed at sub-optimum pH. In the first case, this observation was accompanied by a strong effect on the biomass. The growth rate of the bacterial biomass was relatively lower than the dilution rate of the CSTR system and resulted in a "wash-out". The synchronous pH change with the aerobic to anaerobic switch negatively affected the physiological parameters of the culture. A similar observation was made in the second case, during the prolonged continuous culture incubation. Amounts of dissolved oxygen were recorded with a corresponding decline in the biomass. Both observations may suggest that besides the observed pH effect on bacterial growth and physiology an underlying masking effect could be the limiting substrate. The following batch experiment tested the effect of succinate on the anaerobic bacterial growth in stepwise increasing concentrations.

Succinate was added at 5, 10, 20, 30, 40, 50, 60, 80 and 100 mM in a culture medium of pH 6.5. Figure 10 shows the average growth curves at sub-optimal pH. Furthermore, an additional neutral pH treatment was included as a control; the apparent specific growth rate μ_{app} was 0.27 h^{-1} and the culture reached its maximum optical density at ~14 hours. The test subjects with a sub-optimal pH had a longer lag phase when compared to the control and in the 60, 80 and 100 mM succinate treatments no growth was observed. The addition of succinate in the medium did not enhance the μ_{app} to the magnitude of the control treatment (μ_{app}= 0.27 h^{-1}). However, the 10 mM succinate treatment had μ_{app}= 0.15 h^{-1} slightly higher than the 5 mM succinate treatment (μ_{app}= 0.13 h^{-1}). The 20, 30, 40, 50 mM succinate treatment had a μ_{app} of 0.11, 0.08, 0.05 and 0.02 h^{-1} respectively. Additionally, the end point concentration of nitrate and nitrite in this batch experiment was investigated; the results are depicted in figure 11 . All treatments received an initial amount of 20 mM nitrate. After 48 hours of anaerobic incubation the control treatment and the 5 mM succinate acidic treatment had ~13 mM nitrate remaining. The 10 mM succinate treatment had consumed 15 mM of nitrate, and in the following treatments of 20, 30, 40 and 50 mM the final end point of the nitrate concentration was ~0 mM. This observation indicated that nitrate was the limiting factor in excess of succinate for the sub-optimal pH treatments. In all treatments the extracellular nitrite concentration was ~0 mM.

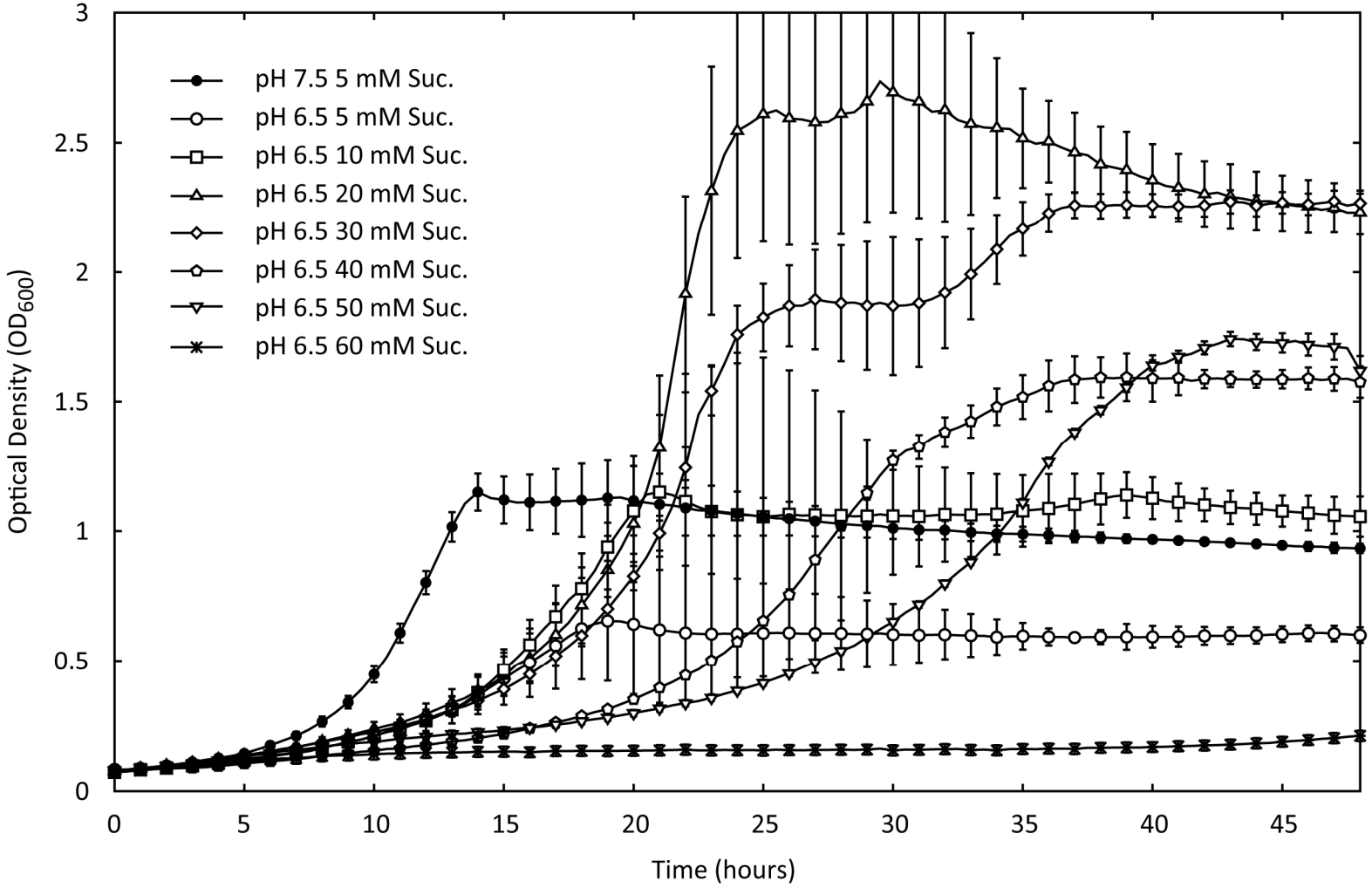

Figure 10 Average anaerobic growth curves at pH 6.5 with varying amounts of succinate (see key legend for treatment annotation). An additional treatment of pH 7.5 with 5 mM succinate has been included to serve as control (n=6, error bars denote SEM).

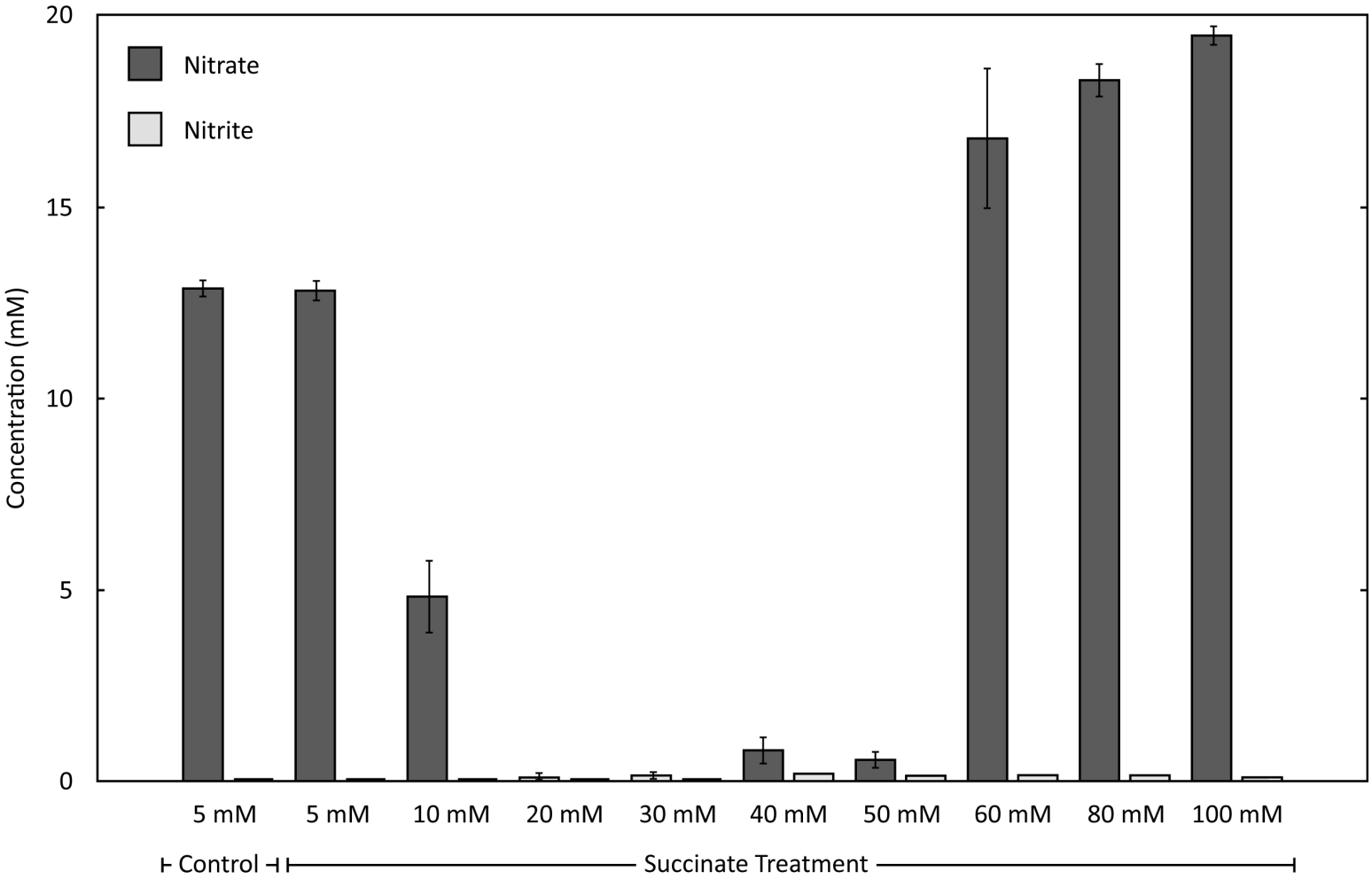

Figure 11 Average end point (48 hours) concentration of nitrate and nitrite in anaerobic batch culture of sub-optimal pH. Cells of *P. denitrificans* were incubated in pH 6.5 with varying amounts of succinate ranging from 5 to 100 mM, additionally a control treatment of pH 7.5 and 5 mM succinate was included, as indicated in the figure respectively. All treatments received 20 mM nitrate (n=4, error bars indicate SEM).

5.2.3 Transcriptional analysis with RT-PCR

Total RNA was extracted after 120 hours of continuous culture in CSTR systems for the sub-optimal and optimal pH (control) treatment. Approximately 127 and 123 $ng.\mu l^{-1}$ of DNA free total RNA were extracted and purified from the pH 7.5 and the pH 6.5 treatment, respectively. The purity of total RNA samples was tested with qPCR and analysed with agarose gel electrophoresis and was found to be contaminant free from DNA fragments (Figure 12). Figure 13 illustrates the results from the total RNA quality check. The results show clear distinct RNA fragments that lack any degradation. Based on the above quality investigations the RNA samples were subjected to qRT-PCR analysis to investigate the expression of selected genes and the type II microarray analysis to investigate the whole genome expression of *P. denitrificans*.

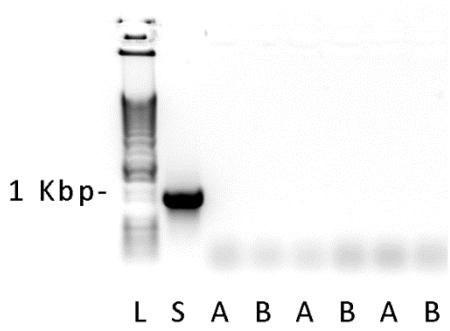

Figure 12 Agarose gel testing residual DNA contamination in total RNA samples. L denotes ladder, A pH 6.5 and B pH 7.5 continuous culture treatment. Marker indicates the 1 Kbp weight on DNA ladder.

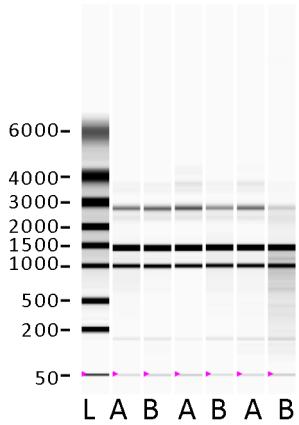

Figure 13 Total RNA electrophoresis gel with Experion. L denotes ladder, A pH 6.5 and B pH 7.5 continuous culture treatment. The ladder weights are expressed in nt.

The expression of genes involved in the denitrification pathway of *P. denitrificans* was tested with qRT-PCR (See Material and Methods for further details). The relative expression was calculated using the Pfaffl method. The expression of the gene expressing the membrane bound nitrate reductase (*narG*, pden_4233), was induced ~1.7 fold at sub-optimal pH (Figure 14 A). The expression of genes for the nitrite reductase (*nirS*, pden_2487), the nitric oxide reductase (*norB,* pden_2483) and the nitrous oxide reductase (*nosZ*, pden_4219) in the sub-optimal pH treatment (pH 6.5) were inhibited ~100, 33 and 3 fold, respectively (Figure 14 B, C and D), when compared to the neutral pH (7.5) CSTR treatment. Relatively high standard errors were observed due to the very low absolute expression levels occurring at lower range of sub-optimal pH growth of *P. denitrificans*.

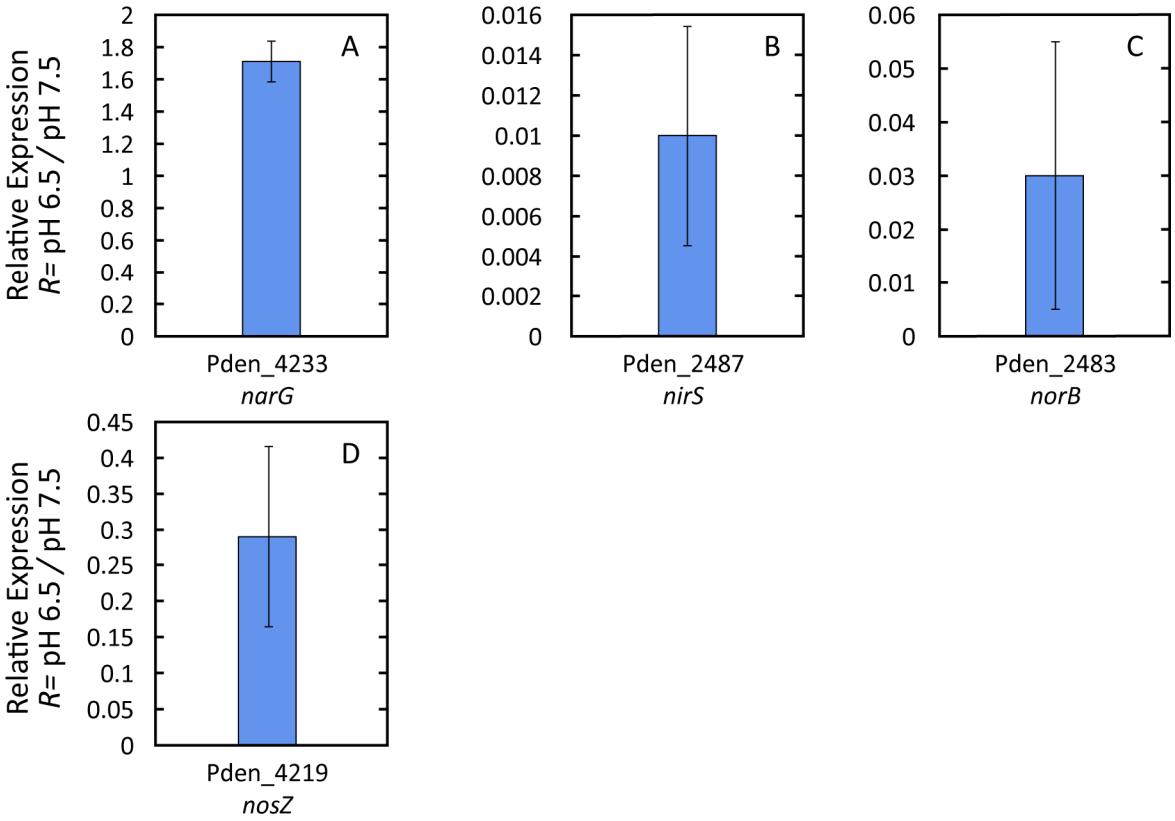

Figure 14 Average relative expression of selected genes; A) *narG* (pden_4233), B) *nirS* (pden_2487), C) *norB* (pden_2483) and D) *nosZ* (pden_4219) detected with RT-PCR. Expression values were normalized on the expression of *gapdh* and the relative ratio R was calculated using the optimal pH treatment of pH 7.5 as a referenced based on the Pfaffl method (n=3, error bars denote SEM).

5.2.4 Whole genome transcriptional analysis

Whole genome transcriptional analysis of *P. denitrificans* with type II microarray and gene enrichment with volcano test (*fold change*≥2, *p*=0.05) showed that 75 genes of the sub-optimal pH treatment had significant changes in expression when compared to the control treatment (pH 7.5; Figure 15). This enrichment list included genes involved in amino acid transport (ABC type transporters), outer membrane protein (*omp*), cytochrome cbb_3 oxidase, cytochrome *c*, nitrite reductase, nitric oxide reductase, nitrous oxide reductase, formate dehydrogenase and ATP synthase expression.

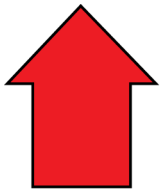

35 genes Up-regulated

Including: *marR*, *fdh, tolA, araC, lysR*

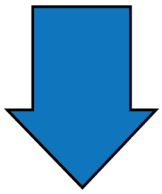

40 genes Down-regulated

Including: *nirS*, *norCB*, *ompW*, *asnC*, *nosZ*, *ccoN*, *tetR*

Figure 15 Schematic illustration summarizing the volcano statistical filtering (≥2 fold, $p \leq 0.05$) of the microarray dataset.

Note: The microarray and respirome gene expression dataset is presented in 5.4 Gene expression datasets

Gene clusters involved in the denitrification pathway were repressed apart from the gene cluster of the periplasmic nitrate reductase that was induced ~1.6 fold when compared the control treatment of the neutral pH. The nitrate reductase gene cluster (*nar*) was repressed 1.4 fold and the gene expressing a nitrate nitrite transporter (*nirK*) was repressed 2.5 fold. The gene clusters expressing the nitrite, nitric oxide and nitrous oxide reductase were repressed on average 5 times in the sub-optimal pH treatment. Interestingly, the periplasmic nitrate reductase operon (*nap*) was induced by 63% when compared to the control.

Genes involved in aerobic respiration, cytochrome bc_1, cytochrome ccb_3, cytochrome ba_3 and cytochrome aa_3 were relatively repressed in the acidic treatment when compared to the control treatment. Specifically, the *cta* (expressing the cytochrome aa_3 oxidase) and *qox* gene cluster (cytochrome ba_3 oxidase) were repressed 1.2 fold when compared to the control. The *fbc* (expressing the cytochrome bc_1 oxidase) and *cco* gene cluster (expressing the cytochrome cbb_3 oxidase) were repressed ~2 fold on average, when compared to the control. The cytochrome *c* peroxidase gene (*ccpA*, pden_0893) was relatively repressed by ~5 fold at acidic conditions (pH 6.5).

The expression of gene clusters involved in methanol (*mxa*) and sulphite oxidation (*sox*) was relatively repressed by 1.2 and 2.7 fold when compared to the control. On the contrary, the relative expression of the methylamine gene cluster (*mau*) remained unchanged, when compared to the control treatment (pH 6.5).

The gene cluster of NADH dehydrogenase (*nuo*) was slightly induced by the sub-optimal pH condition and was found to have a relative induction of 1.2 fold. The expression levels of succinate dehydrogenase (*sdh*) and hydrogenase operons (*hyp* and *hup*) were approximately unchanged. However the expression of the formate dehydrogenase gene cluster (*fdh*) was notably induced by ~3.3 fold when compared to the control. Additionally the relative expression of the ATP synthase operon was ~3 fold repressed when compared to the control treatment of pH 7.5.

The various ABC transporters had a mixed expression profile. A gene annotated as putative outer membrane protein was highly induced in the acidic conditions. The relative expression of the *ompW* (pden_3636) gene was 11 fold repressed at pH 6.5. Another interesting observation was the expression of cytochrome B_{561} that was ~9 fold induced at pH 6.5

Pseudoazurin and cytochrome c_{550} genes (*pasZ*, pden_4222 and *cycA*, pden_1937) involved in electron transport were relatively repressed by 14 and 2.8 fold respectively. Genes involved in cytochrome *c* biosynthesis and maturation (*cyc*) were relatively repressed by 60% when compared to the control. The gene cluster involved in ubiquinone biosynthesis (*ppq*) was respectively induced by 50% when compared to the control treatment.

The relative expression of genes involved in the regulation of denitrification *fnrP* (pden_1850), *nnrR* (pden_2478) and *narR* (pden_4238) remained unchanged and ranged from 0.88-0.98. The expression of *nsrR* (pden_3024) expressing a NO repressor was also unchanged. The assimilatory nitrate reductase cluster (*nas*) was relatively repressed 2 fold when compared to the control treatment.

5.3 Discussion

5.3.1 Physiological comparison of the pH induced effects in batch and continuous culture

In this chapter the growth of *P. denitrificans* over a pH range was tested and three pH treatments were selected; a sub-optimal (pH 6.5), a neutral (pH 7.5) and an above-optimal pH (pH 8.5) treatment. Those three treatments were used to investigate the pH effect on denitrification. Cells of *P. denitrificans* were incubated in the aforementioned treatments and their denitrification dynamics were investigated. Furthermore, the transcriptional profile of the acidic treatment was investigated and compared to the neutral treatment. Nitrous oxide and di-nitrogen co-production was observed in two of the four treatments investigated. These treatments were the sub-optimal pH and the long term continuous culture treatment (Figure 6 and 9 respectively). This was in contrast with the control (pH 7.5) and alkali (above-optimal of pH 8.5) treatment which showed di-nitrogen as the only end product of denitrification.

The anaerobic incubation of *P. denitrificans* in a pH 6.5 batch culture showed a notable extended lag phase and a μ_{max} of 0.23 h^{-1}. The specific growth rate of the acidic culture is 4 times greater than the selected dilution rate in the chemostats (CSTR). It was assumed that *P. denitrificans* cells could be easily cultured in a CSTR without adjusting the dilution rate previously used. However, the first continuous culture incubation (pH 6.5) with a dilution rate of 0.05 h^{-1} showed that the bacterial biomass slowly diluted to very low levels (>0.05 $mg.ml^{-1}$; Figure 5) towards the end of the incubation. A screen of chemostat incubations testing the dilution rates of 0.05, 0.025 and 0.017 h^{-1} showed that a prolonged anaerobic incubation at optimal pH (pH 7.5) and a 30% reduction of the dilution rate were required to maintain the sub-optimal pH culture in steady state (Figure 5 and 6). Prolonged lag phases or low growth rates in sub-optimum pH cultures have been previously observed in anaerobic incubations of denitrifying bacteria (Bakken *et al.* 2012). This is a clear indication that at sub-optimal pH range the metabolic function of the cells is affected resulting in lower physiological and bio-chemical rates (Booth 1985, White *et al.* 2012). The increased addition of carbon source was used to further explore the inhibitory effect of sub-optimal pH on the growth of *P. denitrificans*. Cells were grown

anaerobically in batch culture at pH 6.5 and succinate was added to the medium at a 5-100 mM range. The growth rates from these batch culture conditions were recorded and compared. The addition of succinate did not increase the growth rate at pH 6.5 and it remained below that of optimal pH and therefore unable to maintain steady state in CSTR systems with the same dilution rate (D=0.05 h^{-1}) The 10 mM succinate addition had a minor stimulation of the growth rate, however the growth rate recorded was still below the rates observed in cell cultures incubated at optimum pH (pH 7.5) with 5 mM succinate (Figure 10 and 11). All subsequent experiments were therefore conducted with 5 mM succinate and 20 mM nitrate as previously done, with a decreased dilution rate of 0.017 h^{-1}.

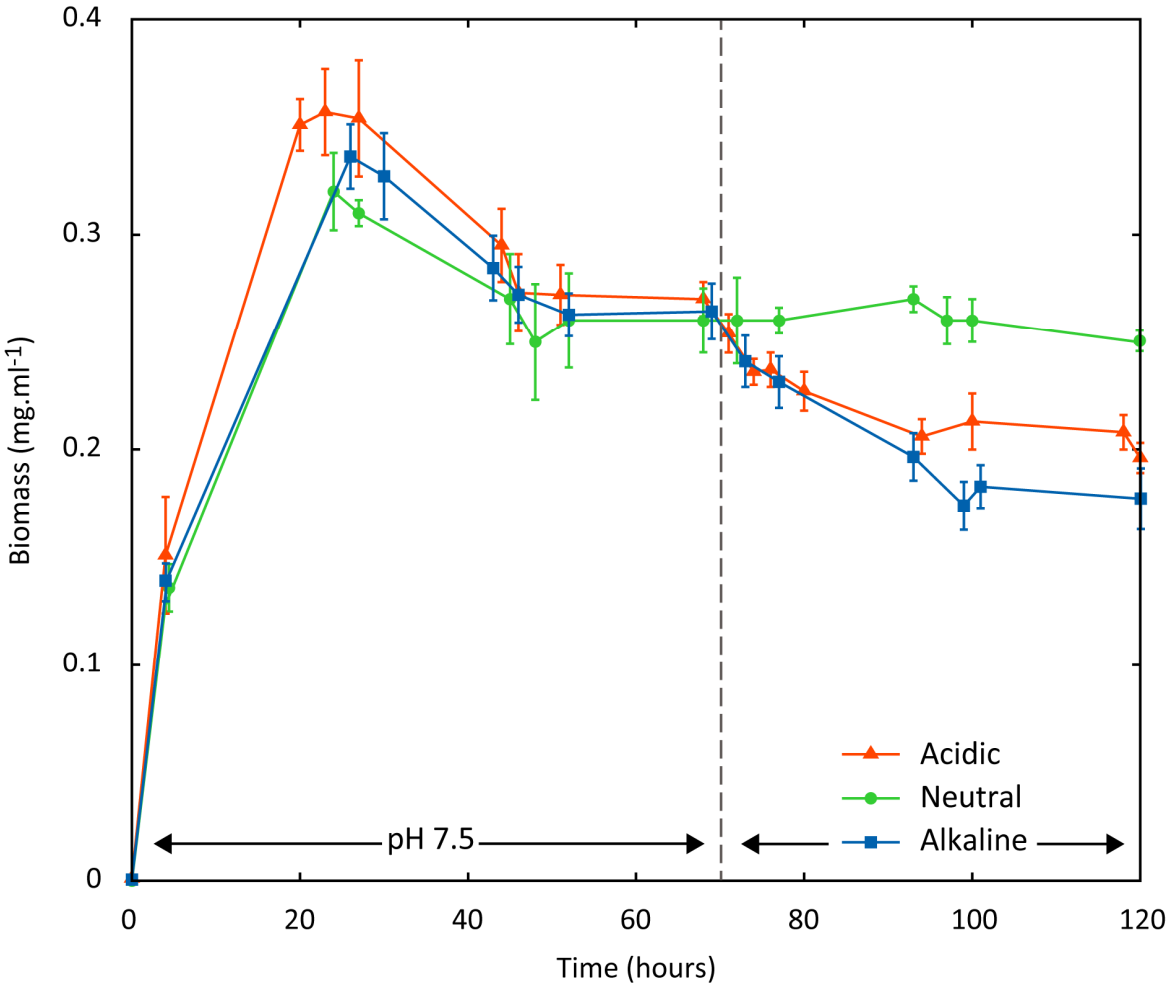

Figure 16 Average comparative biomass density of the three CSTR treatments of *P. denitrificans*; the sub-optimal acidic pH treatment (pH 6.5) is illustrated with a filled triangle, the neutral (pH=7.5) with a filled circle and the above-optimal alkaline (pH 8.5) with a filled square (n=3, error bars denote SEM).

The following continuous culture incubations (sub-, optimal and above-optimal) reached a steady biomass towards the end of the incubation (90 to 120 hours) and the biomass levels were ~0.2 $mg.ml^{-1}$ for the pH 6.5 and 7.5 treatment and 0.25 $mg.ml^{-1}$ for the control treatment (Figure 16).

At the steady state phase of the alkaline and neutral continuous culture treatments nitrite and nitrous oxide did not accumulate in the culture vessel (~0 mM). The consumption of nitrate was also comparable at an average rate of 1400 N $\mu mol.g^{-1}.h^{-1}$ (Table 1). Thus, it was assumed that the end product of denitrification at pH 7.5 and 8.5 was di-nitrogen. This observation confirms other experimental evidence that indicate di-nitrogen as the end product of denitrification at optimal or above optimal pH conditions in batch cultures (Bergaust *et al.* 2011, Bakken *et al.* 2012).

Interestingly, at a lower sub-optimal pH the rate of nitrate consumption was 3 fold lower than that of the control. This observation was accompanied by transient accumulation of low amounts of nitrite and nitrous oxide in the reaction vessel of the CSTR system (Figure 6). The quotient rate of nitrite and nitrous oxide production was 27 and 104 N $\mu mol.g^{-1}.h^{-1}$, respectively (Table 1). Calculated quotient rates are independent of dilution rate. However, direct comparison of chemostat cultures at different dilution rates is not possible due to the dilution rate determining the state of cellular growth: i.e. the cells growth at a dilution rate of 0.017 hr^{-1} are at a later stage of exponential growth to that of those grown at a faster dilution rate and are therefore physiologically not comparable. In this instance, it has to be noted that the dilution rate of the continuous culture was lowered 3 fold to achieve a steady state towards the end of the acidic treatment. Direct comparisons between chemostat incubations with different dilution rates are only indicative of the potential biochemical rates and transcriptional profiles and caution should be taken when extrapolating those results (Doran 2013). Previous studies (Bergaust *et al.* 2011, Bakken *et al.* 2012) utilizing batch culture techniques have shown that at below optimal pH the end product of denitrification is nitrous oxide; the same trend was also indicated when *P. denitrificans* was cultured in anaerobic Hungate tubes. However, in continuous culture systems the concentration of nitrite and nitrous oxide was detectable at low amounts (<500 µM), and accompanied by a relative lower growth rate (D=0.017).

5.3.2 Transcriptional investigation in continuous culture

The average relative expression of the genes involved in the denitrification pathway was compared between the qRT-PCR and the microarray dataset. The expression pattern of *nirS* (pden_2487), *norB* (pden_2483) and *nosZ* (pden_4219) in the microarray dataset showed gene repression in the sub-optimal conditions (pH 6.5) and this was confirmed using qRT-PCR (Table 2). Furthermore, the absolute expression of *nirS* (pden_2487), *norB* (pden_2483) and *nosZ* (pden_4219) was notably low and may affect the magnitude of the standard error of the mean value.

However, the microarray analysis for *narG* (pden_4233) revealed a relative gene repression of 0.76 and the qRT-PCR analysis showed the opposite of 1.71 fold induction in the pH 6.5 condition when compared to the control (Table 2). This discrepancy of the relative expression of the *narG* (pden_4233) gene between the microarray and qRT-PCR data could be due to technical limitations of the method applied. The cycle threshold value (C_T) for the housekeeping gene was on average 23.88 (±0.15 SEM) and 25.18 (±0.15 SEM) for the control and the pH 6.5 treatment, respectively. Although the Pfaffl method takes into account the different PCR efficiencies of the target genes, the difference of the threshold value (C_T) in the housekeeping gene of the target and control condition still affects the overall normalization of the relative expression value. However, the physiological data (biomass and nitrate consumption quotient) should be used additionally to interpret the transcriptional datasets. The sub-optimal pH treatment had a 3 fold lower nitrate consumption quotient at ~400 N µmol.g^{-1}.h^{-1} than the control, which is indicative of a lower nitrate reduction rate. Subsequently, two assumptions are possible; firstly the qRT-PCR relative expression is realistic and there could be post-transcriptional pH effects on nitrate reductase (NarG) lowering its rate or secondly there are less *narG* transcripts as indicated in the microarray dataset, which result in a lower nitrate reduction rate. The latter assumption is more probable because the general transcriptional pattern of the rest of the denitrification genes harmonizes with the rest of the qRT-PCR and chemostat rates. And even more when the C_T difference of the housekeeping gene was submitted to sensitivity analysis it showed that the relative expression of *narG* decreased to 0.81 when an average C_T value of 24 was used.

Therefore it appears that *narG* is repressed and nitrate is reduced jointly by the Nap enzyme since the *nap* operon was induced by 1.63 fold in the acidic treatment.

Table 2 Average relative expression values of selected genes of interest from the microarray and RT-PCR datasets (n=3, ±SEM).

Gene_ID	Annotation	Microarray		qRT-PCR	
		Average	±SEM	Average	±SEM
Pden_4233	*narG*	0.76	0.15	1.71	0.13
Pden_2487	*nirS*	0.02	0.00	0.01	0.01
Pden_2483	*norB*	0.11	0.01	0.03	0.02
Pden_4219	*nosZ*	0.14	0.01	0.29	0.13

The sub-optimal pH (6.5) had negative effects on the total biomass of the continuous culture treatments. In addition the sub-optimal pH repressed the expression of denitrification operons, which showed reduced nitrate reduction rate and reduced production of nitrite, nitrous oxide and di-nitrogen. Nitrite, nitric oxide and nitrous oxide reductase receive their electrons from the cytochrome bc_1 complex via cytochrome *c* or pseudoazurin. The relative expression of the transcription activators FnrP, NarR and NnnR was found unchanged. Therefore, assuming no pH-induced post-transcriptional effects on the transcriptional factors, as they are relatively protected by the cytoplasmic membrane, the electron flow could be restricted by the low turnover activity of the Q_o site of the cytochrome bc_1 complex at pH 6.5 (Lhee *et al.* 2010). Subsequently, Nap and Nar will receive any electrons via the ubiquinone pool (Q-pool). The periplasmic nitrate reductase was seen to be up-regulated 1.7 fold in acidic growth conditions. Nap is induced by the destabilization of the Q-pool (Sears *et al.* 1992, Watmough and Frerman 2010). This was firstly demonstrated on the growth of *P. denitrificans* using a reduced carbon source. Specifically, the reduced fatty acid metabolism passes through β-oxidation in which the fatty acid is broken down to form acetyl Co-A molecules to feed directly into the citric acid cycle (TCA). This is additional process to that of the relatively oxidised succinate molecule, which feeds directly into the TCA cycle. A by-product of β-oxidation is the

production of NADH equivalents which feed into the Q-pool via NADH dehydrogenase and imitates an excessive production of ubiquinol and reduced presence of ubiquinone. This causes the stalling of the cytochrome bc_1 complex, because the oxidation of two ubiquinol molecules is coupled to a reduction of one ubiquinone molecule. An absence of ubiquinone prevents oxidation of ubiquinol. Therefore, *napAB* is induced and NapAB removes the excessive electrons via NapC from the Q-pool. Those electrons are used to reduce nitrate to nitrite and subsequently, the Q-pool is rebalanced in favour of ubiquinone allowing the continuation of the cytochrome bc_1 function. In acidic conditions the Q-pool is suggested to be destabilized, so the NapAB complex may be induced. Our data suggest a new role for Nap in anaerobic nitrate respiration at sub-optimum pH.

The pH affects bacterial growth in a multivariate fashion. A direct and well-studied effect of pH is the direct interaction of protein with a high proton concentration resulting in the denaturation and reduced function of proteins. In this chapter the effect of pH was investigated by physiological, metabolic and transcriptional techniques, however to improve our understanding a more holistic approach is recommended. Additional to the datasets presented in this chapter, datasets investigating the combined determination of concentration and functional rate of protein as well as the gene expression at a range of sub-optimal pH values would be highly valuable to better understand bacterial growth at sub-optimal pH.

In summary, it is therefore suggested that pH has an overall effect on bacterial physiology, lowering the bio-chemical rates and subsequently the rates of anaerobic respiration. The cells may adjust their metabolism to overcome such pH induced effects as explained in the 5.1 Introduction and by utilizing an alternative nitrate reductase (Nap).

5.4 Gene expression datasets

5.4.1 Volcano enrichment and respirome gene expression dataset

Georgios Giannopoulos

Microarray expression at pH 6.5 and 7.5 of *P. denitrificans*
Volcano Enrichment (2 fold cut-off, p=<0.005)

Gene ID	pH 6.5				pH 7.5				Ratio
	1		2		1		2		
	Average	SE Norm	Average	SE Raw	Average	SE Norm	Average	SE Norm	pH 6.5 / pH 7.5
Pden_0050	6.64	1.28	6.76	1.26	0.67	0.09	0.67	0.10	9.94
Pden_0051	1.92	0.23	1.92	0.24	0.69	0.06	0.69	0.06	2.80
Pden_0380	0.57	0.11	0.57	0.12	1.37	0.26	1.37	0.26	0.42
Pden_0522	21.19	5.49	21.19	6.29	8.24	1.83	8.24	2.02	2.57
Pden_0523	3.97	0.38	3.97	0.39	1.69	0.14	1.69	0.15	2.35
Pden_0685	7.26	1.14	7.27	1.32	2.17	0.23	2.17	0.25	3.34
Pden_0688	19.56	3.36	19.67	3.77	6.97	1.15	7.01	1.33	2.81
Pden_0753	7.92	1.79	7.94	1.91	15.85	3.90	15.88	4.16	0.50
Pden_0849	31.61	9.65	31.64	11.50	5.12	0.92	5.13	1.01	6.17
Pden_0893	1.75	0.41	1.79	0.40	9.84	2.54	10.15	2.49	0.18
Pden_1804	3.60	0.29	3.60	0.31	1.79	0.14	1.80	0.15	2.00
Pden_1844	1.51	0.13	1.51	0.14	3.99	0.42	4.00	0.44	0.38
Pden_1845	5.69	0.90	5.70	1.01	15.04	2.18	15.08	2.41	0.38
Pden_1846	4.29	1.42	4.29	1.50	12.58	4.75	12.60	5.14	0.34
Pden_1952	2.00	0.20	2.00	0.21	6.54	0.93	6.54	1.06	0.31
Pden_1990	0.88	0.13	0.89	0.14	2.25	0.46	2.27	0.51	0.39
Pden_2033	6.06	0.55	6.06	0.59	3.03	0.26	3.03	0.28	2.00
Pden_2367	11.31	1.26	11.31	1.32	5.61	0.55	5.62	0.58	2.01
Pden_2368	9.34	0.81	9.37	0.80	4.37	0.54	4.40	0.54	2.14
Pden_2403	0.27	0.14	0.27	0.16	0.58	0.33	0.58	0.38	0.46
Pden_2433	2.73	0.19	2.73	0.19	6.91	0.85	6.92	0.83	0.39
Pden_2482	4.34	0.42	4.34	0.43	24.78	4.30	24.99	4.59	0.17
Pden_2483	2.16	0.24	2.18	0.25	20.52	2.63	20.56	2.83	0.11
Pden_2484	1.93	0.33	1.93	0.35	31.07	8.91	32.26	8.68	0.06
Pden_2485	0.84	0.16	0.84	0.20	2.73	0.28	2.74	0.32	0.31

Pden_2486	0.60	0.06	0.60	0.07	2.49	0.22	2.49	0.23	0.24
Pden_2487	0.55	0.06	0.55	0.06	24.53	3.15	24.61	3.64	0.02
Pden_2488	0.43	0.06	0.43	0.06	5.30	0.92	5.38	0.91	0.08
Pden_2489	0.69	0.11	0.69	0.11	4.16	1.25	4.16	1.34	0.17
Pden_2490	0.64	0.06	0.64	0.06	5.61	0.70	5.66	0.70	0.11
Pden_2491	0.55	0.07	0.55	0.07	4.29	0.55	4.29	0.58	0.13
Pden_2493	0.26	0.03	0.26	0.03	2.24	0.32	2.24	0.33	0.12
Pden_2494	0.67	0.10	0.68	0.12	3.43	0.87	3.54	0.85	0.20
Pden_2623	2.22	0.43	2.22	0.46	4.59	0.91	4.59	0.96	0.48
Pden_2624	0.67	0.07	0.67	0.07	1.54	0.19	1.54	0.20	0.43
Pden_2661	3.29	0.34	3.31	0.35	1.53	0.13	1.53	0.13	2.16
Pden_2827	3.41	0.40	3.43	0.42	1.33	0.17	1.33	0.18	2.57
Pden_2828	3.14	0.30	3.16	0.30	1.32	0.13	1.33	0.13	2.38
Pden_2829	2.85	0.19	2.85	0.20	1.25	0.11	1.25	0.12	2.29
Pden_2854	6.72	1.02	6.80	1.01	2.39	0.27	2.41	0.27	2.81
Pden_2855	16.53	2.32	16.68	2.53	3.66	0.87	3.76	0.85	4.52
Pden_2928	2.84	0.22	2.84	0.23	1.24	0.11	1.24	0.12	2.30
Pden_2945	4.85	2.00	4.86	3.08	2.13	0.83	2.13	1.21	2.28
Pden_3086	0.20	0.03	0.20	0.03	0.50	0.12	0.50	0.15	0.40
Pden_3137	0.62	0.25	0.62	0.31	0.22	0.07	0.22	0.08	2.78
Pden_3491	1.79	0.20	1.79	0.21	12.22	1.71	12.32	1.85	0.15
Pden_3492	1.86	0.58	1.87	0.65	9.78	1.61	9.80	1.70	0.19
Pden_3493	1.39	0.12	1.39	0.12	5.87	0.97	5.88	1.06	0.24
Pden_3512	2.05	0.63	2.05	0.74	1.02	0.25	1.02	0.28	2.01
Pden_3636	0.87	0.10	0.87	0.10	9.75	2.56	9.78	2.93	0.09
Pden_3783	0.85	0.25	0.85	0.26	2.26	0.62	2.26	0.65	0.38
Pden_3815	4.15	0.62	4.15	0.65	10.92	1.25	10.92	1.28	0.38
Pden_3904	3.19	0.43	3.19	0.46	1.58	0.17	1.58	0.17	2.02
Pden_3905	4.74	0.50	4.74	0.54	2.15	0.20	2.15	0.22	2.21
Pden_3942	2.32	0.27	2.34	0.27	4.88	0.70	4.89	0.77	0.48
Pden_4217	1.46	0.28	1.47	0.32	5.84	1.33	5.94	1.71	0.25
Pden_4219	3.14	0.39	3.16	0.38	21.78	4.16	22.17	4.11	0.14
Pden_4227	0.89	0.13	0.89	0.14	7.55	1.54	7.60	1.72	0.12

Pden_4228	0.72	0.12	0.73	0.12	7.65	1.50	7.79	1.48	0.09
Pden_4376	1.20	0.31	1.20	0.33	2.90	0.80	2.90	0.90	0.41
Pden_4465	5.27	0.81	5.30	0.90	10.85	1.74	10.88	1.94	0.49
Pden_4481	8.98	1.72	8.99	1.96	2.73	0.50	2.73	0.57	3.29
Pden_4483	1.87	0.15	1.88	0.15	0.93	0.15	0.93	0.16	2.02
Pden_4494	7.38	0.84	7.41	0.91	3.53	0.36	3.54	0.39	2.09
Pden_4658	0.55	0.05	0.55	0.06	4.47	0.64	4.49	0.75	0.12
Pden_4660	0.55	0.07	0.55	0.08	1.30	0.10	1.30	0.10	0.42
Pden_4661	0.46	0.05	0.46	0.05	1.13	0.11	1.13	0.11	0.41
Pden_5068	2.35	0.45	2.36	0.51	0.71	0.11	0.72	0.12	3.31
Pden_5069	23.54	3.06	23.55	3.31	1.01	0.11	1.01	0.12	23.33
Pden_5070	3.36	0.63	3.36	0.71	0.97	0.13	0.97	0.13	3.47

Georgios Giannopoulos

Respirome at pH 6.5 and pH 7.5 of *P. denitrificans*

Gene ID	pH 7.5	pH 7.5	pH 6.5	pH 6.5	Average	SEM	Annotation
Pden_0010	1.66	1.40	0.95	1.14	0.69	0.12	rph ribonuclease PH
Pden_0011	1.75	1.38	1.07	1.05	0.69	0.07	pyrophosphatase
Pden_0012	1.07	0.67	0.73	0.66	0.84	0.15	endoribonuclease
Pden_0013	1.03	0.75	0.91	0.86	1.02	0.13	coproporphyrinogen ox
Pden_0014	1.92	1.62	2.33	1.48	1.07	0.15	hypothetical
Pden_0015	17.83	26.40	28.91	26.67	1.32	0.31	gfa activation factor
Pden_0016	5.83	6.67	7.31	7.16	1.16	0.09	flhA
Pden_0017	3.90	4.26	3.47	3.80	0.89	0.00	clpP
Pden_0018	3.16	2.26	2.36	2.25	0.87	0.12	N-acetyltransferase
Pden_0019	2.28	2.15	2.12	2.38	1.02	0.09	fghA
Pden_0020	6.59	14.43	20.06	24.13	2.36	0.69	xoxF **PPQ**
Pden_0021	5.63	7.36	9.61	14.35	1.83	0.12	cycB c553i putative
Pden_0022	2.79	2.77	4.72	5.24	1.79	0.10	xoxJ quinole membr.
Pden_0023	2.18	2.16	2.93	3.02	1.37	0.03	xoxI rhodanese
Pden_0425	3.26	3.01	3.38	2.99	1.02	0.02	etfD
Pden_0432	3.62	5.21	3.13	3.43	0.76	0.10	*ctaIV*
Pden_0511	2.81	3.04	2.82	2.64	0.94	0.07	cycH
Pden_0566	1.68	1.45	2.16	2.01	1.33	0.05	Sdh cyt b552
Pden_0567	4.89	3.21	2.27	2.43	0.61	0.15	*sdhC*
Pden_0568	4.05	3.38	1.76	2.68	0.61	0.18	*sdhD*
Pden_0569	6.14	5.95	5.23	5.40	0.88	0.03	*sdhA*
Pden_0570	8.55	14.53	16.74	14.69	1.48	0.47	*hypothetical*
Pden_0571	8.16	8.85	11.64	8.71	1.21	0.22	*hypothetical*
Pden_0572	4.34	3.38	5.10	4.70	1.28	0.11	*sdhB* (Fe-S)
Pden_0625	2.09	1.90	1.48	1.72	0.81	0.10	ubiA
Pden_0893	7.66	12.63	1.39	2.19	0.18	0.00	ccpA cyt c peroxidase
Pden_1161	0.51	0.67	0.66	0.69	1.16	0.13	assimilaory nad-formate dh?

Pden_1186	0.72	0.86	0.98	0.80	1.15	0.22	fdhA
Pden_1187	0.51	0.55	0.52	0.52	0.98	0.03	mandelate racemase
Pden_1188	0.93	0.78	0.52	0.66	0.70	0.14	ferredoxin NADH
Pden_1189	0.44	0.40	0.54	0.47	1.19	0.03	Rieske 2Fe2S
Pden_1359	1.15	0.58	0.47	0.57	0.69	0.29	Copper binding
Pden_1409	1.27	1.30	1.15	1.04	0.85	0.05	hisH
Pden_1410	2.93	2.13	2.74	3.24	1.23	0.29	ccmG
Pden_1411	2.44	2.27	2.01	2.25	0.91	0.08	ccmC
Pden_1412	1.66	1.35	1.72	1.49	1.07	0.03	ccmB
Pden_1413	2.24	1.58	2.82	2.76	1.50	0.24	ccmA
Pden_1414	2.05	1.35	2.25	2.65	1.53	0.43	
Pden_1415	3.66	2.04	2.56	2.92	1.07	0.37	secF
Pden_1745	1.31	1.13	1.49	1.63	1.29	0.16	*b561?*
Pden_1803	2.79	1.89	2.48	2.37	1.07	0.18	Glycosil trnasferase
Pden_1804	1.88	1.72	3.46	3.74	2.01	0.17	abc transporter
Pden_1805	1.90	1.16	2.32	2.63	1.75	0.52	abc transporter
Pden_1806	0.90	0.79	1.12	1.32	1.46	0.21	abc transporter
Pden_1807	1.53	1.67	2.19	3.14	1.65	0.22	abc transporter
Pden_1808	7.16	5.17	3.39	3.44	0.57	0.10	cycM
Pden_1841	1.04	1.25	0.86	0.63	0.66	0.16	ccoS cbb_3 maturation
Pden_1842	3.62	4.20	2.28	2.39	0.60	0.03	ccoI cu transp ATPase
Pden_1843	4.24	3.94	1.82	2.71	0.56	0.13	ccoH/FixH
Pden_1844	3.75	4.25	1.46	1.56	0.38	0.01	ccoG 4Fe-4S
Pden_1845	14.02	16.13	6.05	5.36	0.38	0.05	ccoP subunit III
Pden_1846	11.89	13.32	4.36	4.23	0.34	0.02	ccoQ subunit IV
Pden_1847	6.17	9.01	2.26	2.06	0.30	0.07	ccoO subunit II
Pden_1848	6.37	10.51	1.93	2.17	0.25	0.05	ccoN subunit I
Pden_1849	26.90	85.40	15.94	22.47	0.43	0.16	UspA
Pden_1850	6.90	9.03	6.07	6.40	0.79	0.09	FnrP
Pden_1937	10.78	17.41	4.22	5.41	0.35	0.04	*cycA c550*
Pden_1938	8.53	8.97	4.77	5.09	0.56	0.00	*cycA c550*

Pden_1948	1.34	1.36	0.94	0.98	0.71	0.01	*ctaDII*
Pden_1949	1.88	2.33	2.24	2.31	1.09	0.10	
Pden_1950	2.65	2.46	2.80	2.70	1.08	0.02	L-sorbosone dh
Pden_1951	3.07	3.27	2.65	2.66	0.84	0.03	G-6-P isoenzyme
Pden_1952	6.65	6.43	1.90	2.10	0.31	0.02	G-6-Lactonate
Pden_1953	1.36	1.71	1.04	1.09	0.70	0.06	G-6-P-1 dh
Pden_1954	1.37	1.92	1.31	1.13	0.78	0.19	methyltransferase
Pden_2187	1.19	1.63	1.09	1.27	0.84	0.07	D-Lactate dh cyt c
Pden_2231	7.01	4.82	7.08	7.13	1.24	0.24	*nuoN*
Pden_2232	5.00	3.64	5.51	5.43	1.30	0.19	*nuoM*
Pden_2233	6.25	4.38	6.69	6.44	1.27	0.20	*nuoL*
Pden_2234	4.31	3.02	4.09	3.65	1.08	0.13	*nuoK*
Pden_2235	5.84	3.49	6.02	5.46	1.30	0.27	*nuoJ*
Pden_2236	4.82	3.58	5.64	6.24	1.46	0.28	*Hypothetical*
Pden_2237	4.86	3.79	6.48	6.50	1.52	0.19	*hypothetical*
Pden_2238	4.14	2.92	4.80	4.96	1.43	0.27	*nuoI*
Pden_2239	4.72	3.20	4.72	4.70	1.24	0.24	*nuoH*
Pden_2240	5.42	4.65	7.59	7.10	1.46	0.06	*hypothetical*
Pden_2241	7.99	7.26	11.25	11.19	1.47	0.07	*nuoG*
Pden_2242	5.63	4.33	7.58	8.41	1.64	0.30	*hypothetical*
Pden_2243	5.69	5.25	6.12	6.10	1.12	0.04	*nuoF*
Pden_2244	5.22	5.80	7.28	6.97	1.30	0.10	*hypothetical*
Pden_2245	5.84	7.31	9.27	9.30	1.43	0.16	*hypothetical*
Pden_2246	8.39	7.19	7.22	7.80	0.97	0.11	*nuoE*
Pden_2247	6.05	5.39	4.72	5.25	0.88	0.10	*nuoD*
Pden_2248	5.27	4.11	2.94	3.90	0.75	0.20	*nuoC*
Pden_2249	4.52	4.03	2.50	3.75	0.74	0.19	*nuoB*
Pden_2250	2.94	2.65	1.58	2.17	0.68	0.14	*nuoA*
Pden_2272	1.25	0.88	1.00	1.03	0.98	0.18	*p451*
Pden_2305	14.09	12.11	7.97	6.90	0.57	0.00	*fbcF* Rieske 2Fe2S
Pden_2306	10.61	7.22	5.03	4.96	0.58	0.11	*fbcB* cyt b_L/b_H heme

Pden_2307	21.70	18.33	15.54	14.40	0.75	0.03	*fbcC* cyt c_1 heme
Pden_2349	2.95	3.90	3.37	3.49	1.02	0.12	SDR cofactor vitamin
Pden_2350	3.12	2.94	4.17	4.30	1.40	0.06	hypothetical
Pden_2351	3.13	3.66	5.30	5.85	1.64	0.05	hypothetical
Pden_2352	2.30	2.52	4.01	3.81	1.63	0.11	flhS histidine kinase se
Pden_2353	8.10	8.99	12.26	12.21	1.44	0.08	hypothetical
Pden_2354	18.67	27.17	25.80	26.21	1.17	0.21	flhR luxR 2 comp reg
Pden_2355	1.82	2.14	1.94	2.58	1.13	0.07	abcA
Pden_2356	1.14	1.08	1.32	1.52	1.28	0.12	abcB
Pden_2357	0.80	0.92	1.28	1.25	1.48	0.12	abcC
Pden_2358	2.03	3.21	4.32	3.95	1.68	0.45	hypothetical soxZ-like
Pden_2359	2.29	4.58	6.35	5.75	2.01	0.76	ppqE
Pden_2360	3.78	6.05	7.87	7.43	1.65	0.43	ppqD
Pden_2361	2.76	5.29	5.78	5.48	1.57	0.53	ppqC
Pden_2362	6.71	10.04	11.33	10.31	1.36	0.33	ppqB
Pden_2363	2.86	2.14	2.44	2.94	1.11	0.26	ppqA
Pden_2475	2.60	3.18	5.61	3.95	1.70	0.46	ubiC (GntR)
Pden_2478	2.42	2.73	2.38	2.68	0.98	0.00	*nnrR*
Pden_2479	2.76	2.30	1.75	1.37	0.61	0.02	*norF*
Pden_2480	4.72	4.88	2.58	1.85	0.46	0.08	*norE*
Pden_2481	11.55	18.12	4.63	4.02	0.31	0.09	*norD*
Pden_2482	21.78	28.21	4.43	4.25	0.18	0.03	*norQ*
Pden_2483	19.25	21.88	1.93	2.42	0.11	0.01	*norB*
Pden_2484	23.57	40.94	1.80	2.07	0.06	0.01	*norC*
Pden_2485	2.49	2.99	0.90	0.77	0.31	0.05	*nirX* (apbE)
Pden_2486	2.48	2.51	0.60	0.59	0.24	0.00	*nirI*
Pden_2487	26.64	22.59	0.61	0.49	0.02	0.00	*nirS*
Pden_2488	4.47	6.29	0.49	0.38	0.08	0.02	*nirE*
Pden_2489	4.21	4.10	0.72	0.66	0.17	0.01	*nirC*
Pden_2490	4.96	6.35	0.64	0.64	0.11	0.01	*nirF*
Pden_2491	4.27	4.31	0.51	0.59	0.13	0.01	*nirD*

Pden_2492	4.96	3.99	2.16	1.60	0.42	0.02	*nirG*
Pden_2493	2.38	2.11	0.27	0.25	0.12	0.00	*nirH*
Pden_2494	4.39	2.68	0.59	0.77	0.21	0.08	*nirJ*
Pden_2495	2.49	1.92	0.88	0.87	0.41	0.05	*nirN*
Pden_2545	3.49	4.01	3.66	4.29	1.06	0.01	*b561?*
Pden_2550	10.62	10.39	7.73	8.45	0.77	0.04	etfA α subunit
Pden_2551	10.47	12.15	9.43	10.12	0.87	0.03	etfB β subunit
Pden_2563	1.59	2.16	1.93	2.14	1.10	0.11	*b561?*
Pden_2589	2.11	1.62	2.07	2.41	1.23	0.25	ubiG
Pden_2670	1.49	1.65	1.25	1.59	0.90	0.06	ubiH/F
Pden_2705	1.45	1.26	1.11	1.17	0.85	0.08	carbonic anhydrase
Pden_2706	0.29	0.28	0.22	0.32	0.97	0.21	aldose?
Pden_2707	1.63	1.65	1.60	2.09	1.12	0.14	
Pden_2708	1.51	1.67	1.69	1.98	1.15	0.04	
Pden_2709	1.58	2.35	1.77	2.09	1.01	0.12	NAP (P)
Pden_2710	1.48	1.22	0.98	1.10	0.78	0.12	SndhB
Pden_2824	0.91	1.02	1.23	1.17	1.25	0.10	*aldo/keto reductase*
Pden_2825	0.95	1.22	1.60	1.35	1.39	0.28	*selB cysteine enlog.*
Pden_2826	2.49	2.76	3.83	3.34	1.37	0.16	*fdhE*
Pden_2827	1.41	1.25	3.77	3.09	2.57	0.10	*fdnI* γ subunit
Pden_2828	1.46	1.20	3.46	2.85	2.38	0.00	*fdnH* β subunit
Pden_2829	1.16	1.34	2.98	2.72	2.30	0.27	*fdnG* α subunit
Pden_2830	7.99	13.86	11.79	12.04	1.17	0.30	4Fe-4S
Pden_2853	2.53	2.75	3.69	3.87	1.43	0.02	ribonuclease R
Pden_2854	2.14	2.68	7.81	5.79	2.91	0.75	NAD-fdh δ subunit
Pden_2855	2.91	4.61	18.92	14.45	4.82	1.68	*FdhD* family
Pden_2856	4.37	6.96	34.45	30.16	6.11	1.78	Fdh α subunit
Pden_2857	3.16	5.81	25.46	26.02	6.27	1.79	NADH dh (quinone)
Pden_2858	2.30	5.33	17.56	17.64	5.47	2.16	Fdh γ subunit
Pden_2859	1.03	1.07	1.62	1.65	1.56	0.01	LysR family
Pden_2927	3.10	3.35	8.45	3.85	1.94	0.79	lctP L-Lactate permeas
Pden_2928	1.14	1.34	2.99	2.69	2.32	0.31	Dld D-Lactate dh

Pden_2929	2.03	2.69	3.33	3.54	1.48	0.16	lctR Lactate Regulator
Pden_2993	19.75	9.22	3.05	1.50	0.16	0.00	*mxaF* α subunit
Pden_2994	11.68	5.41	1.92	0.80	0.16	0.01	*mxaJ* binding prot.
Pden_2995	11.10	5.89	2.39	1.19	0.21	0.01	*mxaG* cyt $_{C\text{-}L}$ c551i
Pden_2996	24.93	15.62	4.97	2.00	0.16	0.04	*mxaI* β subunit
Pden_2997	4.89	2.98	1.79	0.83	0.32	0.04	*mxaR* unknown
Pden_2998	3.28	2.63	1.82	1.39	0.54	0.01	*mxaS* unknown
Pden_2999	2.86	2.92	1.59	1.40	0.52	0.04	*mxaA*
Pden_3000	3.07	2.36	1.66	1.30	0.55	0.01	mxaC von Willebr.
Pden_3001	2.21	1.96	1.05	0.76	0.43	0.04	*mxaK*
Pden_3002	1.60	1.41	0.98	0.61	0.52	0.09	*mxaL*
Pden_3003	3.10	2.27	1.22	0.71	0.35	0.04	*mxaD*
Pden_3019	0.92	1.10	0.64	0.67	0.66	0.04	Signal protein
Pden_3020	0.82	0.92	0.71	0.92	0.93	0.06	sdhD
Pden_3021	0.96	1.00	0.69	0.72	0.72	0.00	sdhC
Pden_3022	1.19	1.31	0.69	0.84	0.61	0.03	sdhB
Pden_3023	2.63	3.21	1.94	2.11	0.70	0.04	hypothetical
Pden_3024	3.87	6.08	4.47	4.69	0.96	0.19	nsrR NO repressor
Pden_3025	7.66	9.69	3.88	5.98	0.56	0.06	NO & morphol reg
Pden_3026	6.15	8.48	3.56	5.02	0.59	0.01	Hypothetical
Pden_3027	3.09	4.36	1.65	2.39	0.54	0.01	Alkylhydroperoxidase
Pden_3028	2.77	3.11	1.78	1.96	0.64	0.01	Cytochrome C
Pden_3093	1.22	1.42	1.67	1.66	1.27	0.10	hupT hist-kinase sensor
Pden_3094	0.97	1.02	1.64	1.64	1.66	0.04	hupU
Pden_3095	1.05	1.06	1.37	1.38	1.30	0.00	hupV
Pden_3096	0.81	0.90	1.05	0.84	1.11	0.18	hupF maturation
Pden_3097	0.19	0.24	0.19	0.24	1.02	0.01	hupA/S small subunit
Pden_3098	0.23	0.25	0.26	0.27	1.10	0.04	hupL large subunit
Pden_3099	0.75	0.47	0.44	0.55	0.88	0.29	hupE
Pden_3100	0.22	0.20	0.22	0.22	1.05	0.03	hupC cyt b
Pden_3101	0.41	0.46	0.47	0.51	1.13	0.02	HupD

Pden_3102	0.97	1.06	0.76	1.10	0.91	0.13	hupF
Pden_3103	0.62	0.47	0.57	0.60	1.09	0.17	HupG
Pden_3104	0.58	0.45	0.58	0.54	1.10	0.09	HupH
Pden_3105	0.45	0.51	0.51	0.50	1.06	0.07	HupJ Rubredoxin
Pden_3106	1.71	2.28	1.48	1.84	0.84	0.03	HupK
Pden_3107	0.91	0.54	0.84	1.25	1.62	0.70	*hypA*
Pden_3108	1.08	0.97	1.00	0.85	0.90	0.03	*hypB*
Pden_3109	0.61	0.63	0.61	0.68	1.04	0.04	*hypothetical*
Pden_3110	0.69	0.64	1.23	0.82	1.54	0.25	*hypC*
Pden_3111	0.80	0.70	0.75	0.76	1.01	0.07	*hypD*
Pden_3112	1.45	0.97	1.19	1.12	0.99	0.17	*hypE*
Pden_3113	0.37	0.31	0.58	0.48	1.57	0.01	*hypothetical*
Pden_3286	0.47	0.82	2.84	10.52	9.41	3.36	*B561*
Pden_3543	0.57	0.54	0.61	0.57	1.06	0.01	Short Chain Reductase
Pden_3942	4.57	5.22	2.07	2.61	0.48	0.02	ubiH/F
Pden_3974	3.07	3.85	1.53	2.12	0.52	0.03	cycJ
Pden_3977	4.78	5.07	4.00	4.83	0.90	0.06	ccmF
Pden_3978	3.18	3.19	3.22	3.61	1.07	0.06	ccmH
Pden_3985	0.68	0.68	0.60	0.48	0.80	0.08	*p450*
Pden_4007	0.68	0.58	0.80	0.90	1.36	0.17	Membrane sensor kina
Pden_4008	0.52	0.61	0.63	0.66	1.15	0.08	σ54 Fis transcript reg
Pden_4009	0.54	0.57	0.32	0.36	0.61	0.02	Mo-pterin α subunit
Pden_4010	0.59	0.48	0.42	0.54	0.92	0.20	bd subunit I
Pden_4011	0.41	0.36	0.37	0.40	1.02	0.11	d subunit II
Pden_4012	0.70	0.77	0.67	0.84	1.03	0.07	ATPase
Pden_4075	1.78	1.43	1.42	1.38	0.88	0.08	L-Lactate dh cyt c
Pden_4145	2.27	1.83	1.83	2.10	0.97	0.17	Hypothetical (*YeeD*)
Pden_4146	1.96	1.84	1.39	1.52	0.77	0.06	*ArsR* regulatory
Pden_4147	0.55	0.93	0.78	0.66	1.05	0.35	*soxS c* yt c biogenesis
Pden_4148	1.11	0.75	0.79	0.70	0.82	0.11	*soxV* cyt c
Pden_4149	0.40	0.69	0.48	0.36	0.87	0.35	*soxW* thioredoxin

Pden_4150	0.80	1.49	0.84	0.78	0.78	0.27	*soxX* cyt c
Pden_4151	2.01	2.53	1.53	1.26	0.63	0.13	*soxY* sulfur oxidase
Pden_4152	1.03	1.54	0.92	0.85	0.73	0.17	*soxZ* sulfur oxidase
Pden_4153	1.58	1.96	1.34	1.11	0.71	0.14	*socA* di-heme cyt c
Pden_4154	0.58	0.48	0.44	0.43	0.82	0.07	*soxB* Rden
Pden_4155	0.58	0.69	0.66	0.38	0.85	0.29	*soxC* Mo-oxidase
Pden_4156	0.73	0.65	0.64	0.68	0.96	0.09	*soxD* cyt c_{551}
Pden_4157	0.88	0.86	0.89	0.70	0.92	0.10	*SoxE* cyt c-I
Pden_4158	1.10	1.00	1.13	1.00	1.02	0.02	*SoxF* FAD disulfide ox
Pden_4159	0.99	1.07	0.99	0.93	0.93	0.07	*soxG* β-lactamase
Pden_4160	1.03	1.37	0.73	0.86	0.67	0.04	*soxH*
Pden_4161	2.94	5.27	0.89	1.52	0.30	0.01	hypothetical
Pden_4214	4.47	7.93	1.67	1.87	0.30	0.07	*nosX*
Pden_4215	4.21	5.71	1.40	1.28	0.28	0.06	*nosL*
Pden_4216	5.30	6.90	1.66	1.75	0.28	0.03	*nosY*
Pden_4217	4.89	6.98	1.31	1.62	0.25	0.02	*nosF*
Pden_4218	5.00	17.49	2.29	2.89	0.31	0.15	*nosD*
Pden_4219	18.06	26.27	2.78	3.55	0.14	0.01	*nosZ*
Pden_4220	5.83	9.53	1.20	1.47	0.18	0.03	*nosR*
Pden_4221	6.38	10.24	1.35	1.39	0.17	0.04	*nosC*
Pden_4222	25.84	48.31	2.20	2.42	0.07	0.02	*pasZ*
Pden_4225	5.54	9.58	1.58	1.72	0.23	0.05	ubiD
Pden_4226	5.94	12.96	0.79	0.99	0.11	0.03	ubiD
Pden_4230	4.87	6.72	1.61	1.45	0.27	0.06	nnrS
Pden_4231	9.57	16.46	16.72	11.16	1.21	0.53	
Pden_4232	12.61	26.10	19.57	15.91	1.08	0.47	
Pden_4233	12.23	13.56	11.16	8.39	0.77	0.15	narG
Pden_4234	25.58	24.90	21.45	17.18	0.76	0.07	narJ
Pden_4235	13.79	16.05	12.51	9.77	0.76	0.15	narH
Pden_4236	13.75	15.81	11.52	9.66	0.72	0.11	narI
Pden_4237	4.94	6.54	2.54	2.60	0.46	0.06	narK

Pden_4238	1.01	1.00	1.00	0.78	0.88	0.11	narR
Pden_4315	3.86	2.68	3.83	3.34	1.12	0.13	thrC
Pden_4316	2.28	2.01	2.09	2.00	0.96	0.04	surF1
Pden_4317	5.20	4.66	4.47	3.99	0.86	0.00	ctaE subunit III
Pden_4318	4.83	3.30	3.88	3.45	0.92	0.12	ctaG assembly protein
Pden_4319	8.58	6.81	7.95	6.57	0.95	0.02	hypothetical
Pden_4320	6.48	4.46	4.91	4.57	0.89	0.13	ctaB
Pden_4321	13.94	12.40	9.73	9.52	0.73	0.04	ctaC subunit II
Pden_4322	2.85	2.75	2.60	2.31	0.88	0.04	TldD
Pden_4323	0.57	0.57	0.52	0.50	0.89	0.02	DprA
Pden_4356	1.78	4.62	3.82	3.46	1.45	0.70	*b561?*
Pden_4386	1.41	1.92	1.97	1.40	1.07	0.33	glycerol kinase
Pden_4387	5.19	7.83	7.43	4.93	1.03	0.40	ABC transporter
Pden_4388	2.93	2.58	2.58	1.91	0.81	0.07	hypothetical
Pden_4389	0.76	1.02	0.89	0.59	0.87	0.30	ABC transporter
Pden_4390	0.93	1.26	1.08	0.77	0.88	0.27	ABC transporter
Pden_4391	0.98	1.83	1.25	0.94	0.89	0.38	ABC transporter ATP
Pden_4392	1.13	1.62	1.16	0.77	0.75	0.28	ABC transporter ATP
Pden_4393	1.41	1.96	1.05	0.76	0.57	0.18	**glpD** homodimeric quin
Pden_4394	0.34	0.37	0.20	0.24	0.61	0.03	hypothetical protein
Pden_4395	1.21	0.88	0.78	0.70	0.72	0.07	*cysD*
Pden_4396	2.00	1.40	1.50	1.43	0.89	0.14	*cysN/cysC*
Pden_4397	1.89	3.26	2.70	2.57	1.11	0.32	*hypothetical*
Pden_4510	1.40	1.18	1.20	1.17	0.92	0.06	ubiB
Pden_4511	1.05	0.94	0.88	0.80	0.84	0.00	ubiE
Pden_4699	0.44	0.39	0.36	0.44	0.97	0.14	B651
Pden_4700	0.46	0.51	0.45	0.28	0.77	0.22	CytCP
Pden_4718	0.66	2.19	1.74	1.54	1.67	0.97	*Hypotherical*
Pden_4719	2.48	4.05	4.42	4.70	1.47	0.31	*napE*
Pden_4720	1.14	2.36	2.64	2.21	1.63	0.69	*napD*
Pden_4721	2.25	3.02	3.58	3.33	1.35	0.24	*napA catalytic*

Pden_4722	2.99	4.13	5.95	5.09	1.61	0.38	*napB cyt c*
Pden_4723	1.46	2.45	4.05	3.31	2.06	0.71	*napC*
Pden_4724	6.61	12.44	3.90	4.03	0.46	0.13	*GreA kinase regulat*
Pden_4726	1.28	0.82	1.27	1.47	1.39	0.40	*mscS-aldose dh*
Pden_4727	1.56	1.67	1.71	1.82	1.10	0.00	*sndhA*
Pden_4728	0.49	0.42	0.44	0.43	0.96	0.07	mauR lysR family reg.
Pden_4729	0.58	0.59	0.51	0.46	0.83	0.05	mauF big subunit
Pden_4730	0.32	0.26	0.40	0.34	1.28	0.01	mauB MADH heavy ch
Pden_4731	0.53	0.52	0.49	0.35	0.80	0.12	mauE ma utilization
Pden_4732	1.22	0.70	0.97	0.61	0.83	0.03	mauD accessory prot
Pden_4733	0.50	0.29	0.33	0.34	0.91	0.25	mauA small subnit
Pden_4734	0.28	0.42	0.64	0.55	1.81	0.50	mauC **amicyamin**
Pden_4735	0.44	0.64	0.42	0.35	0.75	0.20	mauJ
Pden_4736	0.82	0.61	0.51	0.68	0.87	0.25	**mauG** diheme c perox
Pden_4737	0.63	0.58	0.55	0.59	0.94	0.07	mauM ferrodoxin nap
Pden_4738	0.54	0.65	0.72	0.69	1.18	0.13	mauN ferrodoxin nap
Pden_4855	0.48	0.48	0.47	0.52	1.03	0.06	Malate/lactate dh
Pden_4866	1.14	0.92	1.04	0.99	1.00	0.09	Malate/lactate dh
Pden_4877	0.74	0.61	0.78	0.61	1.03	0.03	L-lactate dh
Pden_4938	0.67	0.63	0.74	0.69	1.10	0.00	ubiX
Pden_5013	0.42	0.51	0.58	0.79	1.45	0.08	peroxidase
Pden_5062	0.66	0.63	0.81	0.66	1.14	0.09	L-Lactate dh
Pden_5063	1.84	1.64	1.62	1.95	1.04	0.15	Alcohol dh
Pden_5104	1.83	1.96	1.85	1.85	0.98	0.03	surF1 surfeit family
Pden_5105	1.10	1.17	1.08	1.02	0.93	0.05	qoxD ba_3 subunit IV
Pden_5106	1.49	0.95	0.68	0.79	0.65	0.19	qoxC ba_3 subunit III
Pden_5107	1.18	0.80	0.74	0.81	0.83	0.19	qoxB ba_3 subunit I
Pden_5108	0.77	0.55	0.39	0.42	0.63	0.13	qoxA ba_3 subunit II

5.4.2 Microarray gene expression dataset

Note: This dataset is supplied with the accompanying CD-ROM

References

Bååth, E. and K. Arnebrant (1994). "Growth rate and response of bacterial communities to pH in limed and ash treated forest soils." Soil Biology and Biochemistry **26**(8): 995-1001.

Bakken, L. R., L. Bergaust, B. Liu and Å. Frostegård (2012). "Regulation of denitrification at the cellular level: a clue to the understanding of N2O emissions from soils." Philosophical Transactions of the Royal Society B: Biological Sciences **367**(1593): 1226-1234.

Baumann, B., J. R. Van Der Meer, M. Snozzi and A. J. B. Zehnder (1997). "Inhibition of denitrification activity but not of mRNA induction in *Paracoccus dentrificans* by nitrite at a suboptimal pH." Antonie van Leeuwenhoek, International Journal of General and Molecular Microbiology **72**(3): 183-189.

Bergaust, L., Lars R. Bakken and Å. Frostegård (2011). "Denitrification regulatory phenotype, a new term for the characterization of denitrifying bacteria." Biochemical Society Transactions **39**(1): 207-212.

Bergaust, L., R. R. J. M. van Spanning, Å. Frostegård and L. R. Bakken (2011). "Expression of nitrous oxide reductase in *Paracoccus denitrificans* is regulated by oxygen and nitric oxide through FnrP and NNR." Microbiology.

Berks, B. C., D. Baratta, D. J. Richardson and S. J. Ferguson (1993). "Purification and characterization of a nitrous oxide reductase from *Thiosphaera pantotropha*." European Journal of Biochemistry **212**(2): 467-476.

Berks, B. C., D. J. Richardson, C. Robinson, A. Reilly, R. T. Aplin and S. J. Ferguson (1994). "Purification and characterization of the periplasmic nitrate reductase from Thiosphaera pantotropha." European Journal of Biochemistry **220**(1): 117-124.

Booth, I. R. (1985). "Regulation of cytoplasmic pH in bacteria." Microbiol Rev **49**(4): 359-378.

Covington, A. K., R. G. Bates and R. A. Durst (1985). "Definition of pH scales, standard reference values, measurement of pH and related terminology." Pure and Applied Chemistry **57**(3): 531-542.

Cuhel, J., M. Simek, R. J. Laughlin, D. Bru, D. Cheneby, C. J. Watson and L. Philippot (2010). "Insights into the Effect of Soil pH on N2O and N2 Emissions and Denitrifier Community Size and Activity." Appl. Environ. Microbiol. **76**(6): 1870-1878.

Dermastia, M., T. Turk and T. C. Hollocher (1991). "Nitric oxide reductase. Purification from *Paracoccus denitrificans* with use of a single column and some characteristics." Journal of Biological Chemistry **266**(17): 10899-10905.

Doran, P. (2013). Bioprocess Engineering Priciples. MA, USA, Academic Press.

Enwall, K., L. Philippot and S. Hallin (2005). "Activity and composition of the denitrifying bacterial community respond differently to long-term fertilization." Applied and Environmental Microbiology **71**(12): 8335-8343.

Gates, Andrew J., David J. Richardson and Julea N. Butt (2008). "Voltammetric characterization of the aerobic energy-dissipating nitrate reductase of *Paracoccus pantotrophus*: exploring the activity of a redox-balancing enzyme as a function of electrochemical potential." Biochemical Journal **409**(1): 159.

Kelly, D., F. Rainey and A. Wood (2006). The Genus: *Paracoccus*. The Prokaryotes. M. Dworkin, S. Falkow, E. Rosenberg, K.-H. Schleifer and E. Stackebrandt, Springer New York**:** 232-249.

Kucera, I. (2005). "Energy coupling to nitrate uptake into the denitrifying cells of *Paracoccus denitrificans*." Biochimica et Biophysica Acta (BBA) - Bioenergetics **1709**(2): 113-118.

Kucera, I., L. Lampardova and V. Dadak (1987). "Control of respiration rate in non-growing cells of *Paracoccus denitrificans*." Biochem J **246**(3): 779-782.

Kucera, I., R. Matyasek and V. Dadak (1986). "The influence of pH on the kinetics of dissimilatory nitrite reduction in *Paracoccus denitrificans*." Biochimica et Biophysica Acta **848**(1986): 1-7.

Lhee, S., D. R. J. Kolling, S. K. Nair, S. A. Dikanov and A. R. Crofts (2010). "Modifications of protein environment of the [2Fe-2S] Cluster of the bc_1 complex: Effects on the biophysical properties of the rieske iron-sulfur protein and on the kinetics of the complex." Journal of Biological Chemistry **285**(12): 9233-9248.

Parkin, T. B., A. J. Sexstone and J. M. Tiedje (1985). "Adaptation of Denitrifying Populations to Low Soil pH." Appl Environ Microbiol **49**(5): 1053-1056.

Sears, H. J., S. Spiro and D. J. Richardson (1992). "Effect of carbon substrate and aeration on nitrate reduction and expression of the periplasmic and membrane-boundnitrate reductases in carbon-limited continuous cultures of *Paracoccus denitrificans* Pdl222." Microbiology **9971**: 3767-3774.

Talley, K. and E. Alexov (2010). "On the pH-optimum of activity and stability of proteins." Proteins: Structure, Function, and Bioinformatics **78**(12): 2699-2706.

Thomsen, J. K., T. Geest and R. P. Cox (1994). "Mass spectrometric studies of the effect of pH on the accumulation of intermediates in denitrification by *Paracoccus denitrificans*." Applied and Environmental Microbiology **60**(2): 536-541.

Toei, M., C. Gerle, M. Nakano, K. Tani, N. Gyobu, M. Tamakoshi, N. Sone, M. Yoshida, Y. Fujiyoshi, K. Mitsuoka and K. Yokoyama (2007). "Dodecamer rotor ring defines H+/ATP ratio for ATP synthesis of prokaryotic V-ATPase from Thermus thermophilus." Proceedings of the National Academy of Sciences **104**(51): 20256-20261.

van den Heuvel, R. N., E. van der Biezen, M. S. M. Jetten, M. M. Hefting and B. Kartal (2010). "Denitrification at pH 4 by a soil-derived *Rhodanobacter*-dominated community." Environmental Microbiology **12**(12): 3264-3271.

Vishniac, W. and M. Santer (1957). "The *Thiobacilli*." Bacteriological Reviews **21**(3): 195-213.

von Ballmoos, C., G. M. Cook and P. Dimroth (2008). "Unique Rotary ATP Synthase and Its Biological Diversity." Annual Review of Biophysics **37**(1): 43-64.

Watmough, N. J. and F. E. Frerman (2010). "The electron transfer flavoprotein: ubiquinone oxidoreductases." Biochim Biophys Acta **1797**(12): 1910-1916.

White, D., J. Drummond and C. Fuqua (2012). The physiology and biochemistry of prokaryates. New York, Oxford University Press.

The regulation of denitrification in *P. denitrificans*

6. Discussion

General discussion; a synthesis of transcriptional expression investigations to form a new model of regulation for denitrification in *P. denitrificans.*

Georgios Giannopoulos

Contents

6. Discussion

As exemplified previously in 1. Introduction of this thesis, bacterial respiration utilises an electron transport system which conveys electrons from the primary dehydrogenases to the terminal electron acceptor (Chen and Strous 2013). Respiration under anaerobic conditions on an alternative electron acceptor such as nitrate has vital implications due its principal role in the nitrogen cycle (Richardson 2008). Nitrate reduction or denitrification is the step-wise process that reduces inorganic nitrate to di-nitrogen and is possible due to the comparatively similar oxidative potential that nitrate has to oxygen. Denitrification is the major contributing pathway besides anammox that releases nitrogen back to the atmosphere (see 1.3.2 Significance of anaerobic respiration on nitrate)**.** However, there is only one enzyme known at the moment, the nitrous oxide reductase, which catalyses the last reduction of denitrification (Richardson *et al.* 2008, Richardson *et al.* 2009).

Denitrification is mainly regarded as an anaerobic process, however there is evidence of aerobic denitrification or nitrate oxyanion reduction (Berks *et al.* 1993). In this study the model organism *Paracoccus denitrificans* (PD1222) was employed to investigate the regulation of the denitrification pathway at the transcriptional level. These investigations were underpinned by a set of well-defined and replicated continuous cultures allowing high resolution monitoring of culture parameters such as physiological state, temperature, pH, dissolved oxygen and substrate concentration. The effect of oxygen on the regulatory pathways of nitrate respiration was investigated using *P. denitrificans*. This initial investigation suggested a pleiotropic system of regulation under anaerobic nitrate respiration for *P. denitrificans* (Chapter 2). Based on this observation, several mutant strains lacking a functional gene-copy of the three major FNR-type transcriptional regulators, *fnrP* (pden_1850) *nnrR* (Pden_2478) (Chapter 3) and *narR* (pden_4238) (Chapter 4), were used to investigate the potential transcriptional and physiological effects of such mutations. Lastly, the effect of pH on growth and denitrification was investigated (Chapter 5).

6.1 *P. denitrificans* as a model organism

P. denitrificans is a widely used model organism to study denitrification, baring comparison among other such well-studied denitrifying organisms as *Pseudomonas stutzeri, Ps. aeruginosa, Achromobacter xylosoxidans, Rhodobacter sphaeroides* and the non-denitrifier *Escherichia coli.* The latter bacterium, *E. coli*, is incapable of complete nitrate reduction to di-nitrogen (Unden and Bongaerts 1997, Constantinidou *et al.* 2006). Denitrification in *E. coli* is truncated and ends in the accumulation of nitric oxide, that in turn is degraded by a nitric oxide stress induced mechanism (Hutchings *et al.* 2002), however the nitrate reductase of *E. coli* is one of the most well studied nitrate reductases (Bertero *et al.* 2003) and features in a vast wealth of studies investigating host nitric oxide host defence mechanisms due to the presence nitric oxide detoxification proteins such as the flavohemoglobin *Hmp* (Poole *et al.* 1996, Kim *et al.* 1999). Additionally, previous investigations of anaerobic growth in *E. coli* provided insights in the regulation of anaerobic respiration of *P. denitrificans*. The genomes for aforementioned bacteria are available through various research collaborations enabling transcriptional analysis of complex networks and pathways. The genome of *P. denitrificans* is available through the Joint Genome Institute of the US Department of Energy and has been used extensively in this study to construct microarrays or to investigate the existence of transcriptional motifs. As illustrated in Chapter 1 and 2 of this study, *P. denitrificans* grows aerobically and anaerobically using specific oxidoreductases in a branched electron transfer network. The majority of the oxidoreductases involved in the respiratory network of *P. denitrificans* have been characterized providing additional insight into the kinetics and regulation of denitrification (Chapter 3). Furthermore the relative ease of culturing *P. denitrificans* in defined continuous culture systems proved *P. denitrificans* as a successful denitrifying model organism.

6.2 Growth of *P. denitrificans* in continuous cultures with minimal medium.

Continuous culture systems have been employed previously in physiological studies and have recently gained more recognition when combined with transcriptional or proteomic studies. Chemostats are continuously stirred tank reactor systems in which bacteria grow in continuous culture mode limited by a selected factor. In this study the limiting factor was the supply of succinate. In the extreme situation of the organism being constrained to the single step of nitrate reduction to nitrite, as observed in the continuous culture of the Δ*nnrR* strain, the medium used provided effectively the required electron acceptors and the system reached a steady state biomass (Chapter 3). This technique successfully controlled the physiological stage of the bacterium and was highly reproducible. The latter fact was not only supported by the low standard error for the mean values in the continuous detection of bacterial biomass and concentrations of nitrate, nitrite and nitrous oxide, but also by the low variation in the microarray genome datasets.

The minimal medium used for the experiments contained nitrate, succinate, a phosphate buffer, ammonia and trace elements (see Materials and Methods for details). The 10 mM of mono and di-basic phosphate buffer was found weak and additional titrations of diluted sulphuric acids were required to maintain the pH in the CSTR at the desired levels. This was expected in a proton consuming process that reduces nitrate to di-nitrogen (1. Introduction). The 10 mM of ammonium chloride was found enough to suppress the expression of the nitrate assimilatory reductase, however there were detectable mRNA transcripts. In the case of the *narR* mutant strain several genes of the *nas* cluster were up-regulated when compared to the control. This indication may suggest competition of the *nar* and *nas* nitrate reductase systems in the acquisition of inorganic nitrogen in the form of nitrate and nitrite for nitrate respiration and assimilation respectively. The regulation of the *nas* gene cluster in *P. denitrificans* is not clearly elucidated; however it is suspected that is regulated at RNA level and the presence of ammonia holds a primary regulatory role (Gates *et al.* 2011). The ammonium concentration range required for effective *nas* suppression has not been defined yet.

The minimal medium was supplemented with an adjusted microelement solution based on Vishniac and Santer (1957). This solution contains the majority of metal ions required for the

assembly and functioning of various metalloenzymes or cofactors. Previous studies have indicated that the concentration of copper, molybdenum and sulphur were crucial for the functioning of nitrous oxide, nitrate and nitrite reductase and depletion of these micronutrients could lead to reduced function of these enzymes (Zumft 1997). This study found that total copper concentrations lower than 2 µM affected the assembly and function of the nitrous oxide reductase. It has also been found that at 18 µM copper nitrous oxide was detected in batch cultures. In those two cases high nitrous oxide emissions were detected in batch cultures that suggested di-nitrogen formation was not occurring in these conditions. A recent study of Hahnke *et al.* (2014) has assessed the role of medium composition on the growth of *P. denitrificans* in aerobic and anaerobic conditions. It was found that highest generation times were achieved with a medium containing iron, manganese, molybdenum, copper and zinc at a concentration ranging between 0.01 and 9 µM. Physiological processes are therefore strongly influenced by media composition and culturing technique and subsequently the effect of the growth medium and especially the effect of the availability of metal ions on transcriptional regulation has not been clearly defined and may mask previous observations.

6.3 Gene expression techniques

Traditionally gene expression has been measured by qRT-PCR. According to this methodology mRNA is reverse transcribed to cDNA and amplified using dye-labelled specific primers. For each cycle of amplification the analogue fluorescent signal is converted to quantitative data, allowing real-time acquisition and monitoring of the amplification process. This technique is widely available and has been used in many studies examining the transcription or regulation of specific genes of interest (Pfaffl 2001). Its applicability to selected genes of interest may limit further insight into the bacterial regulation beyond the selected gene targets.

Type II microarrays were used to capture the whole genome expression at the steady state phase of continuous growth in CSTR at a set time point providing an insight into the gene

expressions levels at that point of RNA extraction. The microarray slides used in this study were custom designed and produced by Oxford Gene Technology (UK). The oligo sequences of the microarray were based on a successful microarray study of *P. denitrificans* (Sullivan *et al.* 2013). The microarray gene expression technique is based on the semi-quantitative detection of the fluorescent ratio between the sample (mRNA-cDNA) and the control (genomic DNA). The datasets were subjected to principal component analysis and variation within the dataset was plotted in two principal axes. Generally the datasets were closely grouped and the strain or culture mode (aerobic vs anaerobic) explained the variation.

Direct RNA sequencing (next generation sequencing) would accurately detect the mRNA transcripts avoiding the error of a semi-quantitative technique, however the microarray techniques used in this study generated reliable information for whole genome transcriptional profile in addition to the RT-PCR investigations.

6.4 Transcription factor binding motif searches

Three approaches are available to search for putative or significant binding motifs in prokaryotic genomes, the first one considers similar motifs according to a sample sequence 'supervised motif searching', the second identifies similar sequences in the upstream regions of groups of transcriptionally regulated genes 'unsupervised motif searching' and the last search approach analyses the distance distribution of dispersed motif sequences combined with additional experimental data known as 'exploratory motif searching' (Mrazek 2009). In this study the first two motif search techniques were applied as the third one is highly dependent on r-scan marker statistics and it is usually meaningless without any experimental determinations. In this study position weighted matrices were constructed with co-regulated gene groups based on previous experimental data (van Spanning *et al.* 1997, Hutchings *et al.* 2000, Hutchings and Spiro 2000, Mazoch and Kučera 2002). The logos of those matrixes (Chapter 2, 3 and 4) were compared to those resulting from a genome wide analysis of FNR and DNR regulators (Dufour *et al.* 2010) and a highly conserved logo

was identified. Subsequently, the selected motif was used in a supervised motif search and several genes having the selected motif upstream were identified (Chapter 2). This gene list was indicative as it contained a majority of genes with unknown function; however the list also contained target genes known to be regulated by FnrP, NnrR or NarR. The latter observation indicates that this search strategy was optimal for the purposes of this study.

6.5 Evidence of a dynamic transcriptional regulation

The environmental signal that commonly influences the expression of genes involved in denitrification and other core bacterial processes is the gradient of oxygen. Bacterial denitrification is an anaerobic process and two conditions were compared; an oxic environment with 100 % dissolved oxygen in the tank reactor and an anoxic environment with 0% dissolved oxygen sensed by an oxygen probe. Oxygen has a reduction potential E_o of 820 mV and nitrogen, nitrate, nitric oxide and nitrous oxide of 420, 374, 1175 and 1355 mV suggesting that denitrification is a favourable process in the absence of oxygen (Richardson 2008).

In this study, aerobic conditions completely inhibited the reduction of nitrate and subsequently denitrification in continuous cultures of *P. denitrificans*. During the aerobic continuous culture the extracellular nitrate concentration remained unchanged at ~ 22 mM throughout the 120 h incubation. This finding indicates the primary role of oxygen as a signalling molecule for denitrification (Baumann *et al.* 1996, Mazoch *et al.* 2003, Lee *et al.* 2006, Bergaust *et al.* 2011), however this does not imply that all denitrifiers react in the same way to those two oxygen signals used in this study. The first nitrate reduction step of denitrification has been previously observed in aerobic cultures of denitrifying organisms that may be utilised as a nitrate detoxification or redox balancing strategy (Sears *et al.* 1992, Ellington *et al.* 2003).

DNA sequence pattern searches for conserved binding motifs in the upstream region of highly expressed genes in anaerobic conditions indicated various oxygen dependent

transcriptional regulators including several belonging to the CRP family. FnrP of *P. denitrificans,* a homologue of *E. coli* FNR, is thought to respond to oxygen and form a transcriptionally active dimer in anaerobic conditions (Hutchings *et al.* 2002, Jervis *et al.* 2009). FNR could be regarded as the major oxygen sensing transcriptional factor, however continuous culture studies showed that it is not required to initiate denitrification in the anaerobic cultivation of the Δ*fnrP* strain (Chapter 3). This is perhaps possible when an alternative transcription factor activates the denitrification genes by recognizing FNR motifs. A homologue of FnrP is NnrR in *P. denitrificans* and it has been demonstrated that absence of *fnrP* and *nnrR* prohibits anaerobic nitrate respiration (van Spanning *et al.* 1997, Van Spanning *et al.* 1999). FNR is known to induce the expression of *narK*, *narGHJI*, *napFDAGHBC* and *nirBDC* in *E. coli* K12 with a consensus sequence of TTGAT-NNNN-ATCAA (Constantinidou *et al.* 2006). In another model organism, *Bacillus subtilis* the FNR regulon included *narK*, *narGHIJ*, *fnr, cydABCD* and *nasDEF* with a FNR binding box of NNN-TGTGA-NN-TA-NN-TCAC-NN (Reents *et al.* 2006). The genome of *B. subtilis* contains 10 identified sigma factors including a σ^{54} enhancer-dependent sigma factor (Haldenwang 1995). The FnrA and Anr transcriptional regulators induced the expression of *ccp, hemN* and *ccoN* but not *narG*, *nirS* and *norCB* that were under the regulation of Dnr in *B. subtilis*. The aforementioned genes have binding motifs with a TTGAT-NNNN-GTCAA FNR-box pattern (Vollack *et al.* 1999). The *FnrL* regulon of *Rhodobacter sphaeroids* 2.4.1 included *ompW*, *ccpA, hemA, hemN, ccoNOQP* and *uspA* with a putative FNR box TTGA-NNNNNNN-TCAA, based on a chromatin immuno-precipitation study using σ^{70} antibodies (Dufour *et al.* 2010). In this study it was shown that *hemN*, *uspA*, *fnrP*, *cco*, *nar*, *nor* and *nap* are under the positive control of FnrP under anaerobic conditions with a binding consensus motif of TTG-NNNNNNNN-CAA as shown in earlier findings (van Spanning *et al.* 1997, Hutchings *et al.* 2002, Mazoch and Kučera 2002). Interestingly it was demonstrated that the expression of the *nos* operon was induced in the absence of FnrP suggesting a new transcriptional role for FNR (Chapter 3).

The NnrR transcriptional factor is homologue of FnrP and it has previously been demonstrated that NnrR is involved in the transcriptional regulation of *nir* and *nor* operons of *P. denitrificans* (van Spanning *et al.* 1997, Van Spanning *et al.* 1999, Hutchings and Spiro 2000) binding in a TT-N-A-NNNNN-GTCAA consensus. In a closely related bacterium to *P.*

denitrificans Rhodobacter sphaeroides 2.4.1*,* that lacks a membrane bound nitrate, nitrite and nitrous oxide reductase it was shown that only *norCB* is positively regulated by NNR (Arai *et al.* 2013). Additionally a TTG-NNNNNNNN-CAA motif was found upstream of the *norCB*, *nnrR* and *nnrS* genes of *R. sphaeroides,* which is very similar to the previously found FNR motif. Specifically, there is an indication that FnrL and NnrR bind to the promoter sequence upstream of *nnrS* (Bartnikas *et al.* 2002). Another striking point in the study of Arai *et al.* (2013) was the regulation of *fnrL*, *cco* and *cox* operons by FnrL in anoxic conditions in the presence of exogenous NO originating from sodium nitroprusside and S-nitrosoglutathione. This evidence could indicate a dual role of FNR as oxygen and nitric oxide sensor. In this study it was demonstrated that NnrR positively regulated the *nir*, *nor* operons which confirms earlier studies. It was also observed that the *nos* operon was repressed in the Δ*nnrR* strain however this is primarily due to the unavailability of a suitable substrate to activate the nitrous oxide reduction. The *narG* expression was induced by the absence of the NnrR suggesting a new transcriptional role.

Nitrate in the absence of oxygen acts as an external stimulus to initiate denitrification. The molecular mechanisms for *nar* activation are not clearly defined in *P. denitrificans*. A FNR-like transcriptional factor exists in *P. denitrificans* (Wood *et al.* 2001, Wood *et al.* 2002) which enhances the expression of the *nar* operon. *P. stutzeri*, another denitrifying organism, as well as *E. coli* utilize a two component nitrate responsive system *narXL* to regulate the expression of the *nar* operon. However, their deletion did not affect denitrification in *P. stutzeri* (Hartig *et al.* 1999). A similar observation was made at the steady state continuous culture of a strain lacking a functional copy of the nitrate responsive system strain *narR*. Interestingly though the reduction of nitrate did not coincide with the initiation of anaerobic conditions in the Δ*narR* strain and had a distinct phenotype as shown in Chapter 4. The expression of *nir,* and *nos* operons was repressed in the Δ*narR* strain suggesting that NarR may compete for the promoter binding sites and possibly repress the expression of those genes.

6.6 A novel transcriptional regulation model - Concluding remarks

In this study nitrate and anaerobic conditions combined were the main stimuli for the expression of the denitrification pathway. Nitrate reduction leads to the production of other nitrogen oxyanions that may also subsequently also act as stimuli; those are nitrite, nitric oxide and nitrous oxide. Batch cultures have shown that *P. denitrificans* is able to grow on nitrite with resulting lower yields and slower growth rates than nitrate. Other experimental data have shown the primary role of nitric oxide as a stimulus for the expression of the *nir* and *nor* gene clusters (Zumft 2002, Spiro 2007). Batch cultures of *P. denitrificans* saturated with nitrous oxide were unable to produce biomass due to the deleterious effect of nitrous oxide in the methionine biosynthesis pathway (Sullivan *et al.* 2013). Some of genes that were highly induced in denitrifying conditions (Chapter 2) have been previously reported to be regulated by and have binding motifs for the transcription regulators FnrP, NnrR and NarR that respond to gradients of oxygen, nitric oxide and nitrate-nitrite respectively (Van Spanning *et al.* 1999, Hutchings and Spiro 2000, Saunders *et al.* 2000, Wood *et al.* 2001, Spiro 2007, Spiro 2012).

Those transcriptional regulators belong to the cyclic-AMP-responsive protein (CRP) family of regulators and contain a highly conserved helix-turn-helix domain. This suggests and it has been experimentally confirmed that these regulators bind to very similar binding sites upstream of or overlapping gene promoters (Chapter 2). The FnrP, NnrR and NarR proteins interact with RNA polymerase and subsequently influence transcription competing for the same binding site by either repressing or activating gene expression (Chapter 1). To summarize, the findings of this study demonstrate that the transcriptional factor:

1. FnrP positively regulated the transcription of *nar*, *nor* and *nap* and repressed the expression of the *nos* operon by prohibiting the other transcriptional factors to bind on the promoter motif (Chapter 3).
2. NnrR positively regulated the *nir* and *nor* operons and inhibited the expression of the *nar* and *nos* operon, in the latter case due to substrate unavailability (Chapter 3).
3. NarR positively enhanced the expression of the *nar* operon at the initial stage of anaerobicity. Additionally the expression of *nir* and *nos* operons was repressed in the

Δ*narR* strain suggesting that NarR may compete for the promoter binding sites and possibly repress the expression of those genes (Chapter 4).

It is evident that the transcription factors FnrP, NnrR and NarR compete for the binding sites upstream of the denitrification operons in a way that optimizes the metabolic rates of denitrification and subsequently eliminates the accumulation of toxic denitrification intermediates. The latter was demonstrated in the continuous culture of *P. denitrificans* under nitrate respiration. Therefore a new model of the regulation of denitrification is proposed, see figure 1.

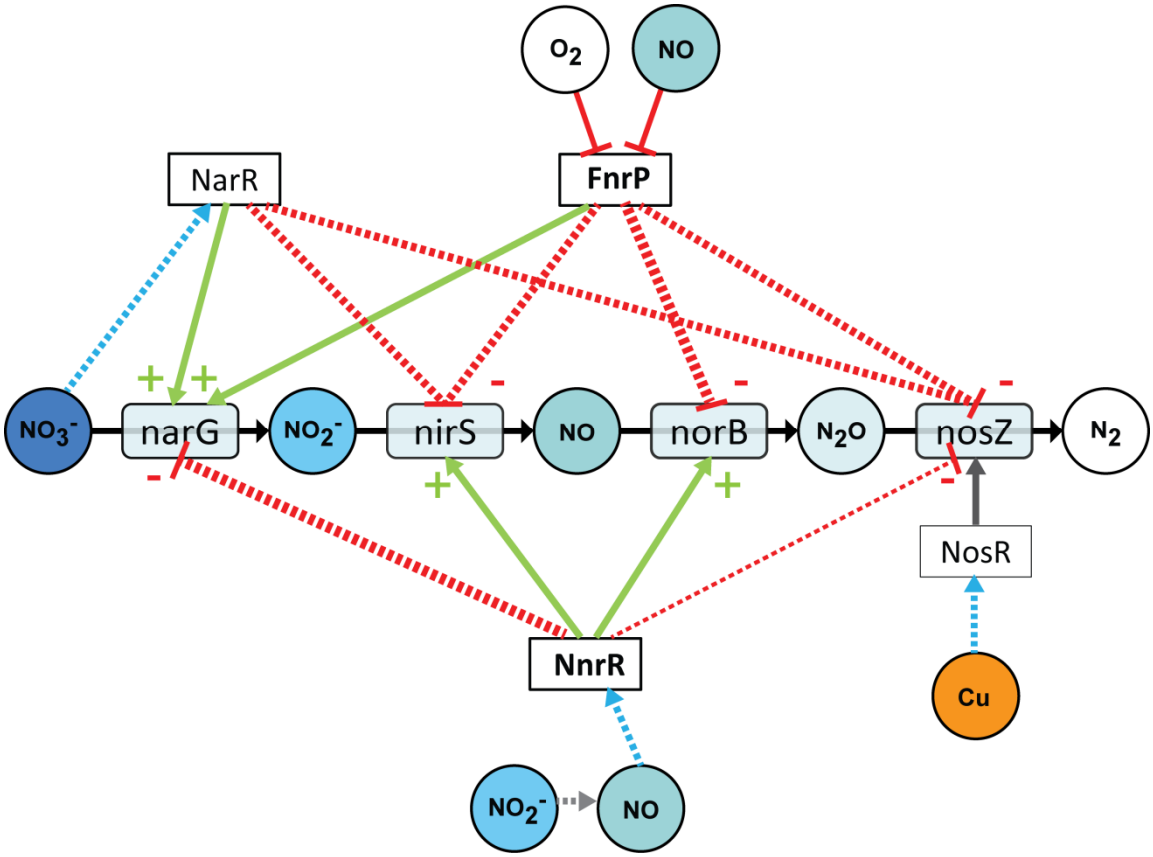

Figure 1 Proposed model of the regulatory network controlling expression of denitrification genes in *P. denitrificans* with the newly proposed roles of each denitrification transcription regulator. The solid arrows represent positive activating events between the transcription factor and the target gene. Dashed arrows indicate positive signalling between the metabolites and the transcription factor. The lines with a bar end indicate inhibition events between the transcription factor and the signal metabolite. The dashed lines with a bar end indicate inhibition events between the transcription factor and the target genes. The transcription factor and subsequently the regulatory proteins are boxed by clear layers; those are the FnrP (Fumarate and Nitrate Regulatory), NnrR (Nitrite and Nitric Oxide Regulatory), NarR (Nitrate reductase Regulatory) and NosR (Nitrous oxide reductase Regulatory protein). The target genes clusters are boxed by a shaded layer; those are the membrane nitrate reductase (*nar*), the nitrite reductase (*nir*), the nitric oxide reductase (*nor*) and the nitrous oxide reductase gene operon (*nos*). The metabolites are represented in circles.

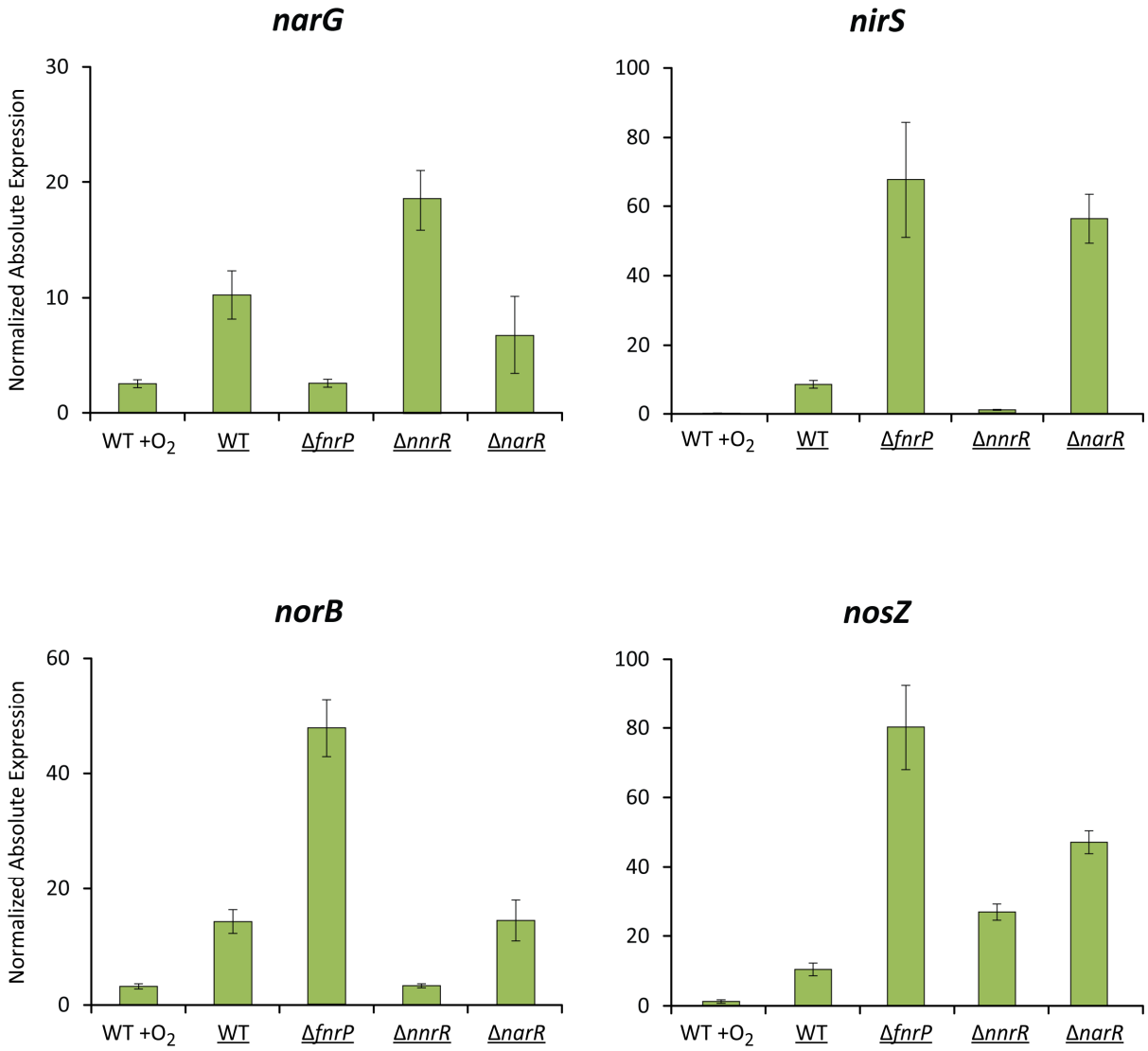

Figure 2 Normalized absolute expression profiles of the wild type PD1222 (WT), Δ*fnrP*, Δ*nnrR* and Δ*narR* strain of *P. denitrificans* for the functional denitrification genes *narG* (pden_4233), *nirS* (pden_2487), *norB* (pden_2483) and *nosZ* (pden_pden_4219) based on microarray analysis, underlined column labels indicate anaerobic continuous cultures, error bars denote ±SEM (n=3).

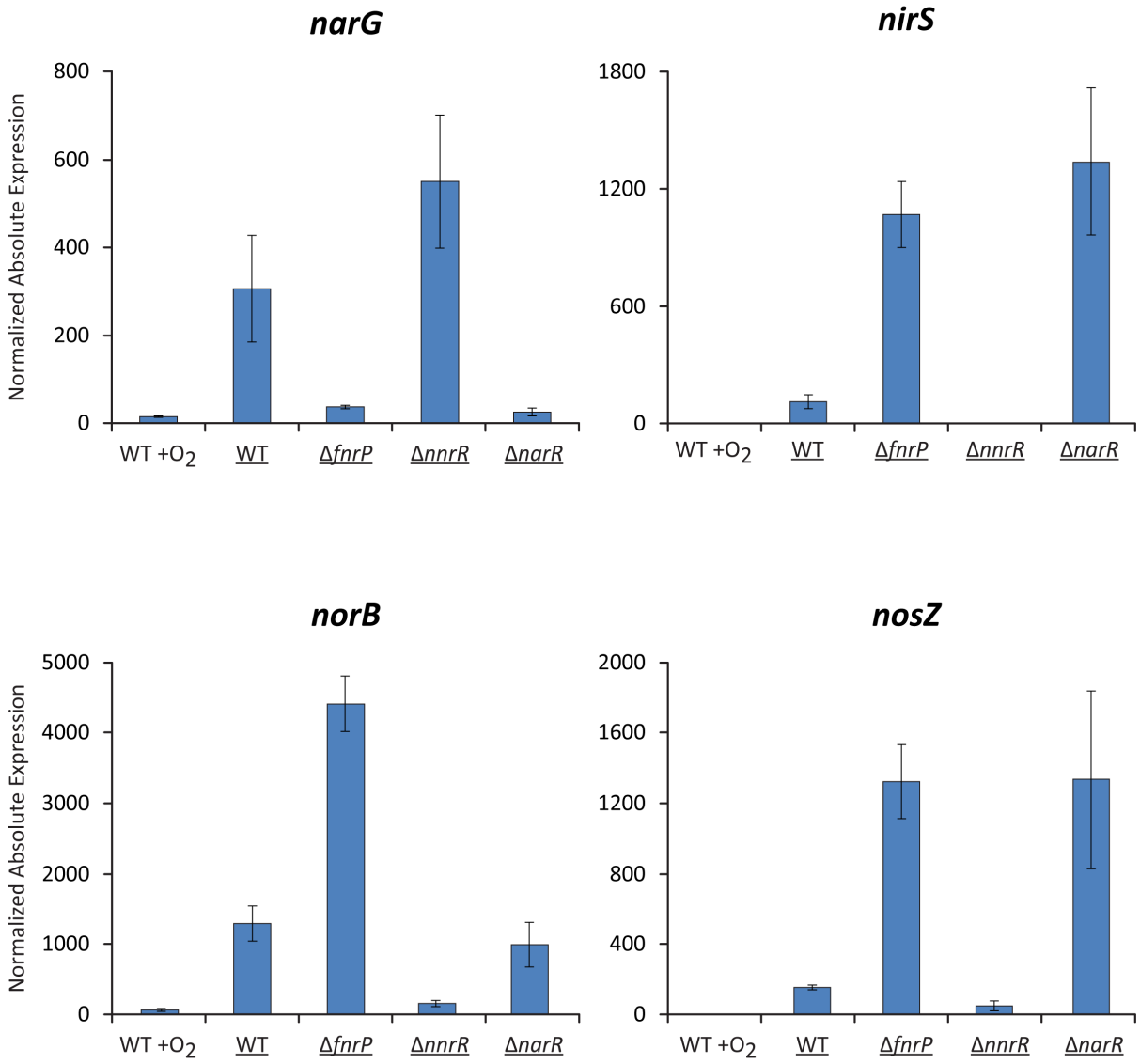

Figure 3 Normalized absolute expression profiles of the wild type PD1222 (WT), Δ*fnrP*, Δ*nnrR* and Δ*narR* strain of *P. denitrificans* for the functional denitrification genes *narG* (pden_4233), *nirS* (pden_2487), *norB* (pden_2483) and *nosZ* (pden_pden_4219) based on RT-PCR analysis, underlined column labels indicate anaerobic continuous cultures, error bars denote ±SEM (n=3).

The principles of kinesis of a transcriptional factor in search of a cognate site have been previously explained in 1.3.5 Background processes involved in transcriptional regulation. In summary, those involve diffusion dynamics, binding dynamics, spacial orientation, information dynamics and transcription factors concentration dynamics, that all interact pleiotropically in an oscillating system. The latter three dynamics were investigated in this thesis to elucidate the transcriptional regulation of denitrification. It is evident that the transcriptional regulators FnrP, NnrR and NarR recognise a similar binding motif pattern, based on the information content, and their binding inhibits or enhances the activity of RNA polymerase. Additionally the functional genes of the transcriptional regulators are in close proximity to the denitrification operons, apart from *fnrP*, suggesting a fast response and regulation upon signal reception which is supported by the simultaneous nitrate reduction to di-nitrogen upon dissolved oxygen elimination without any detection of extracellular nitrite or nitrous oxide in the continuous cultures. The Δ*fnrP* strain has a distinct dissolved oxygen phenotype confirming its regulatory role in the expression of the cbb_3 oxidase. Furthermore, it was observed that the quantity of mRNA transcripts and subsequently the concentration of the transcriptional regulators in the cell was ordered as *fnrP* > *nnrR* > *narR* in a ratio of 9:3:1 respectively. Firstly, assuming a linear relationship between the abundance of mRNA transcripts and the proteins expressed, more FnrP may be required to overcome intoxication by nitric oxide in anaerobic environments under nitrate respiration (Cruz-Ramos *et al.* 2002). Secondly, according to the motif search theory fast cognate site recognition can be achieved for low copy transcriptional regulators such as NnrR and NarR by colocalization which is actually true for the *nor-nir* and *nar* operon respectively. In the case of *fnrP* which is located distant to the *nar*, *nir*, *nor* or *nos* operons fast cognate site search and binding is achieved by having multiple copies of the transcriptional factor. To conclude, fast searching and binding to a cognate site of a transcriptional factor is possible for *fnrP*, *nnrR* and *narR* by having multiple copies or being co-localised. Fast successful searches and binding to the cognate site decreases the relative time required for transcriptional regulation than the duplication time, providing significant advantages in bacteria such as *P. denitrificans* to sense environmental changes and to survive in anaerobic environments.

6.9 Denitrification various pH levels

The average biomass at steady state in continuous cultures at pH 6.5 and 8.5 was comparable and lower than at pH 7.5. However the dilution rate and thus the growth rate at pH 7.5 and 8.5 remain unchanged (=0.05). The end product of nitrate respiration at steady state for pH 7.5 and 8.5 cultures was di-nitrogen with an average rate of 1350 µmol.g^{-1}.h^{-1} N-N_2. Interestingly, at pH 6.5 the end product of nitrate respiration was nitrous oxide and di-nitrogen with a dilution rate of 0.017 h^{-1}. Although it is not directly applicable to compare the sub-optimal pH with the control continuous culture due to the different physiological state of the culture the chemostat quotient rates clearly indicated a relatively lower growth rate of *P. denitrificans* at low pH and a subsequent absolute lower rate of nitrate, nitrite and nitrous oxide reduction. The nitrous oxide production rate was found 500 times higher than the control. In another chemostat study at sub-optimal pH it was found that nitrate reduction terminated to the accumulation of nitrite (Baumann *et al.* 1997). In this study, the transcriptional analysis of *nirS*, *norB* and *nosZ* gene showed significant down-regulation when compared to pH 7.5. The *narG* was on average unchanged. Therefore, the above data indicate that at low pH the reduction rates of nitrate to nitric oxide are relatively greater than the reduction rate of nitrous oxide to di-nitrogen whereas at pH 7.5 the reduction rates of nitrate to nitric oxide are relatively equal or smaller than the reduction rate of nitrous oxide to di-nitrogen. It appears that the lower pH induces the activity of *narG* and *napA* by restricting the electron turnover of the Q_o site of the cytochrome bc_1 (Lhee *et al.* 2010) which is further supported by the observation that the relative expression of the *fnrP*, *nnrR* and *narR* was unchanged assuming no pH induced post transcriptional effects. The latter could be further investigated by in vitro denitrification enzyme activity or proteomics analysis.

6.10 Practical implications

Flooded soils occur in nature due to seasonal flooding or anthropogenic activities. In flooded soils the air enclosed in the soil pore space is replaced by water leaving little oxygen for bacterial survival. Anaerobic zones are commonly found in flooded soils or through the soil profile below the water table. However, anaerobicity in non-flooded soils is even more common due to the basal bacterial activity in the soil aggregates where oxygen is not able to diffuse due to the physical protection of the clay particles. The stability of the soil particle depends on a number of factors including the concentration of clay and organic matter. Therefore an oxygen gradient may exist with anoxic conditions towards the centre of the soil particle, see figure 4 (Sexstone *et al.* 1985). In such micro-environments bacteria access carbon and nitrogen containing compounds, through the degradation of organic matter, and as well other oxidizing agents including manganese oxide, sulphate and iron hydroxide based on the mineral composition of the soil. Most importantly, nitrate could be used as an alternative electron acceptor to oxygen initiating denitrification in such anaerobic conditions.

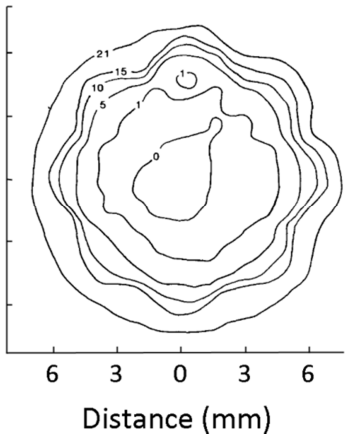

Figure 4 Contour mapping of O_2 concentration in a soil aggregate. Figure taken from Sexstone *et al.* (1985). Contour lines indicate oxygen percentage as shown on the graph.

Currently the metal ion gradient concentration for optimal denitrification rates in *P. denitrificans* or the soil denitrifiers community is unknown with practical implications and extensions arising from this knowledge gap. The efficiency of denitrifying bacteria to reduce nitrous oxide to di-nitrogen depends on the copper concentration as previously shown for *P.*

denitrificans (Granger and Ward 2003, Felgate *et al.* 2012, Wang *et al.* 2013). These observations are of particular interest in the agricultural industry. Nitrogen fertilisation creates hotspots of nitrate abundance and in an anaerobic event after irrigation or rainfall the much needed copper for the assembly of nitrous oxide reductase may not be in sufficiently close proximity of the fertiliser aggregate to allow the process of nitrous oxide reduction to occur. Nitrous oxide emission originating from soil agro-ecosystems are not only potent to ozone depletion and global warming, but may increase the carbon equivalents footprint which may unexpectedly unbalance the dynamic link between food security and carbon rights related economic costs of such systems. Therefore is it of great importance to establish those thresholds because standard medium solutions with excess of compounds unfortunately rarely exist in nature.

Denitrification is widely used in bio-processes including waste water treatment and water purification. In this study the competition for the cognate binding sites among the denitrification transcription regulators FnrP, NnrR and NarR was demonstrated by evaluating the respirome expression in the respective mutant strains. Each denitrification enzyme has unique kinetic properties that would stall the denitrification pathway if expressed constituently without any regulation. Therefore, by competing for the same cognate site expression may be fine-tuned in way that seamless reduction of nitrate to di-nitrogen is achieved without the accumulation of the denitrification by-products. This new role in negative regulation of the cognate sites for *nar*, *nir*, *nor* and *nos* operons was demonstrated by eliminating the expression of one of the three respective transcriptional factors. From a bio-process perspective it is rather interesting to maximize the efficiency and reduce the turnover times of this process. One approach would be to use a mixed continuous culture system containing a Δ*nnrR* strain and a Δ*narG*-Δ*fnrP* strain that could enhance the overall quotient rates of the system. The quotient rate of nitrogen reduction was ~3 fold greater in the Δ*nnrR* strain when compared to the wild type strain. The nitrite, nitric oxide and nitrous oxide reductase functional genes (*nirS, norB* and *nosZ*) were highly expressed in in the Δ*fnrP* strain that could imply a higher enzyme concentration and thus total activity. However, it remains to test such mixed strain or two stage continuous culture system. Also, the transcriptional regulation of the *nos* operon is still unknown and that requires further investigations to tackle such optimization.

6.11 Future questions

The technologies involved in high-throughput analysis and transcription-related processes on a genome-wide scale are rapidly developing. Although microarray based technologies are widely used, new sequencing based technologies have emerged and have been successfully applied in transcriptional studies. RNA sequencing could be one promising approach to process accurately a large number of samples. However, a fundamental question remains how do several transcriptional factors discriminate a cognate site among millions of sequence combinations? Unfortunately high resolution crystal structures of FnrP, NnrR or NarR are still unavailable to construct such binding modelling systems. Furthermore, the relative binding affinity between the transcriptional factor and a cognate site could be estimated by various empirical and mechanistic models. However, an in vitro micro-scale approach such as the one successfully applied by Leith *et al.* (2012) to track and determine the binding potential of a single molecule of the p53 transcriptional factor on a short string of DNA would enhance our knowledge about denitrification transcriptional factor binding specificity and affinity. The competition of FnrP, NnrR and NarR for binding could be tracked simultaneously with various distinct fluorescent tags on each transcriptional regulator. Another approach would be mutating the binding sites and detecting the level of gene expression of the respective target genes with *lacZ* fusions. Additionally to the total internal reflection fluorescence microscopy tracking and the mutation *lacZ* promoter approach a ChIP approach would also be applicable to address the above question.

The regulation of denitrification in this thesis was investigated at the transcription level supported by physiological evidence in continuous cultures. The flow of biological information passes through various stages the replication, the transcription and the expression. In this multi-disciplinary approach, the proteome of *P. denitrificans* under nitrate respiration is now being analysed by two dimensional gel electrophoresis by collaborators in the University of Cordoba (Figure 5), which will provide the basis for a future combined transcriptomics and proteomic analysis.

In this thesis the regulation of denitrification was studied using a relatively low dilution rate and thus a low substrate flow. The physiological state and enzyme production of a cell in a

continuous culture system is largely dictated by such parameters. Therefore a resolution of wide range of dilution rates would perhaps assist in understanding the relative contribution of each denitrification transcription factor to the overall denitrification rates. The resulting information is not only critical to elucidate the transcriptional regulation of denitrification at various physiological states but also to effectively model denitrification (Woolfenden *et al.* 2013).

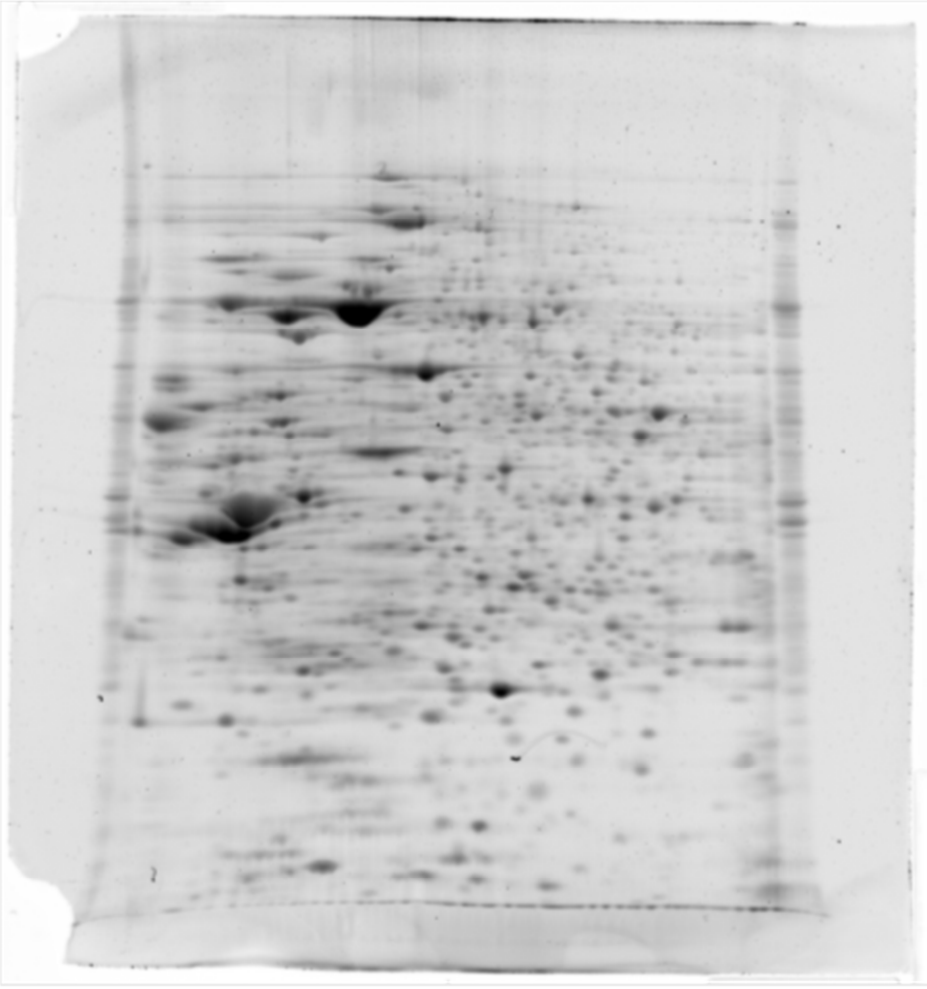

Figure 5 2D gel protein electrophoresis image from aerobic continuous culture of *P. denitrificans*.

References

Arai, H., J. H. Roh, J. M. Eraso and S. Kaplan (2013). "Transcriptome response to nitrosative stress in *Rhodobacter sphaeroides* 2.4.1." Bioscience, Biotechnology, and Biochemistry **77**(1): 111-118.

Bartnikas, T. B., Y. Wang, T. Bobo, A. Veselov, C. P. Scholes and J. P. Shapleigh (2002). "Characterization of a member of the NnrR regulon in *Rhodobacter sphaeroides 2.4.3* encoding a haem–copper protein." Microbiology **148**(3): 825-833.

Baumann, B., M. Snozzi, A. J. B. Zehnder and J. R. D. Van Meer (1996). "Dynamics of denitrification activity of *Paracoccus denitrificans* in continuous culture during aerobic-anaerobic changes." Journal of Bacteriology **178**(15): 4367-4374.

Baumann, B., J. R. Van Der Meer, M. Snozzi and A. J. B. Zehnder (1997). "Inhibition of denitrification activity but not of mRNA induction in *Paracoccus dentrificans* by nitrite at a suboptimal pH." Antonie van Leeuwenhoek, International Journal of General and Molecular Microbiology **72**(3): 183-189.

Bergaust, L., R. R. J. M. van Spanning, Å. Frostegård and L. R. Bakken (2011). "Expression of nitrous oxide reductase in *Paracoccus denitrificans* is regulated by oxygen and nitric oxide through FnrP and NNR." Microbiology.

Berks, B. C., D. Baratta, D. J. Richardson and S. J. Ferguson (1993). "Purification and characterization of a nitrous oxide reductase from *Thiosphaera pantotropha*." European Journal of Biochemistry **212**(2): 467-476.

Bertero, M. G., R. A. Rothery, M. Palak, C. Hou, D. Lim, F. Blasco, J. H. Weiner and N. C. J. Strynadka (2003). "Insights into the respiratory electron transfer pathway from the structure of nitrate reductase A." Nature Structural Biology **10**(9): 681-687.

Chen, J. and M. Strous (2013). "Denitrification and aerobic respiration, hybrid electron transport chains and co-evolution." Biochimica et Biophysica Acta (BBA) - Bioenergetics **1827**(2): 136-144.

Constantinidou, C., J. L. Hobman, L. Griffiths, M. D. Patel, C. W. Penn, J. A. Cole and T. W. Overton (2006). "A reassessment of the FNR regulon and transcriptomic analysis of the effects of nitrate, nitrite, NarXL, and NarQP as *Escherichia coli* K12 adapts from aerobic to anaerobic growth." J Biol Chem **281**(8): 4802-4815.

Cruz-Ramos, H., J. Crack, G. Wu, M. N. Hughes, C. Scott, A. J. Thomson, J. Green and R. K. Poole (2002). NO sensing by FNR: regulation of the Escherichia coli NO-detoxifying flavohaemoglobin, Hmp.

Dufour, Y. S., P. J. Kiley and T. J. Donohue (2010). "Reconstruction of the Core and Extended Regulons of Global Transcription Factors." Plos Genetics **6**(7).

Ellington, M. J. K., G. Sawers, H. J. Sears, S. Spiro, D. J. Richardson and S. J. Ferguson (2003). "Characterization of the expression and activity of the periplasmic nitrate reductase of Paracoccus pantotrophus in chemostat cultures." Microbiology **149**(6): 1533-1540.

Felgate, H., G. Giannopoulos, M. J. Sullivan, A. J. Gates, T. A. Clarke, E. Baggs, G. Rowley and D. J. Richardson (2012). "The impact of copper, nitrate and carbon status on the emission of nitrous oxide by two species of bacteria with biochemically distinct denitrification pathways." Environ Microbiol **14**(7): 1788-1800.

Gates, A. J., V. M. Luque-Almagro, A. D. Goddard, S. J. Ferguson, M. D. Roldan and D. J. Richardson (2011). "A composite biochemical system for bacterial nitrate and nitrite assimilation as exemplified by *Paracoccus denitrificans*." Biochem J **435**(3): 743-753.

Granger, J. and B. B. Ward (2003). "Accumulation of Nitrogen Oxides in Copper-Limited Cultures of Denitrifying Bacteria." Limnology and Oceanography **48**(1): 313-318.

Hahnke, S. M., P. Moosmann, T. J. Erb and M. Strous (2014). "An improved medium for the anaerobic growth of *Paracoccus denitrificans* Pd1222." Frontiers in Microbiology **5**.

Haldenwang, W. G. (1995). "The sigma factors of Bacillus subtilis." Microbiological Reviews **59**(1): 1-30.

Hartig, E., U. Schiek, K. U. Vollack and W. G. Zumft (1999). "Nitrate and nitrite control of respiratory nitrate reduction in denitrifying *Pseudomonas stutzeri* by a two-component regulatory system homologous to NarXL of *Escherichia coli*." J Bacteriol **181**(12): 3658-3665.

Hutchings, M. I., J. C. Crack, N. Shearer, B. J. Thompson, A. J. Thomson and S. Spiro (2002). "Transcription factor FnrP from *Paracoccus denitrificans* contains an Iron-Sulfur cluster and is activated by anoxia: Identification of essential cysteine residues." Journal of Bacteriology **184**(2): 503-508.

Hutchings, M. I., N. Mandhana and S. Spiro (2002). "The NorR Protein of Escherichia coli Activates Expression of the Flavorubredoxin Gene norV in Response to Reactive Nitrogen Species." Journal of Bacteriology **184**(16): 4640-4643.

Hutchings, M. I., N. Shearer, S. Wastell, R. J. M. van Spanning and S. Spiro (2000). "Heterologous NNR-mediated nitric oxide signaling in *Escherichia coli*." Journal of Bacteriology **182**(22): 6434-6439.

Hutchings, M. I. and S. Spiro (2000). "The nitric oxide regulated nor promoter of *Paracoccus denitrificans*." Microbiology **146**(10): 2635-2641.

Jervis, A. J., J. C. Crack, G. White, P. J. Artymiuk, M. R. Cheesman, A. J. Thomson, N. E. Le Brun and J. Green (2009). "The O_2 sensitivity of the transcription factor FNR is controlled by Ser24 modulating the kinetics of [4Fe-4S] to [2Fe-2S] conversion." Proceedings of the National Academy of Sciences **106**(12): 4659-4664.

Kim, S. O., Y. Orii, D. Lloyd, M. N. Hughes and R. K. Poole (1999). "Anoxic function for the *Escherichia coli* flavohaemoglobin (Hmp): reversible binding of nitric oxide and reduction to nitrous oxide." FEBS Letters **445**(2–3): 389-394.

Lee, Y.-Y., N. Shearer and S. Spiro (2006). "Transcription factor NNR from *Paracoccus denitrificans* is a sensor of both nitric oxide and oxygen: isolation of nnr* alleles encoding effector-independent proteins and evidence for a haem-based sensing mechanism." Microbiology **152**(5): 1461-1470.

Leith, J. S., A. Tafvizi, F. Huang, W. E. Uspal, P. S. Doyle, A. R. Fersht, L. A. Mirny and A. M. v. Oijenf (2012). "Sequence-dependent sliding kinetics of p53." PNAS **109**(41): 16552.

Lhee, S., D. R. J. Kolling, S. K. Nair, S. A. Dikanov and A. R. Crofts (2010). "Modifications of protein environment of the [2Fe-2S] Cluster of the bc_1 complex: Effects on the biophysical properties of the rieske iron-sulfur protein and on the kinetics of the complex." Journal of Biological Chemistry **285**(12): 9233-9248.

Mazoch, J. and I. Kučera (2002). "Control of gene expression by FNR-like proteins in facultatively anaerobic bacteria." Folia Microbiologica **47**(2): 95-103.

Mazoch, J., M. Kuňák, I. Kučera and R. J. M. van Spanning (2003). "Fine-tuned regulation by oxygen and nitric oxide of the activity of a semi-synthetic FNR-dependent promoter and expression of denitrification enzymes in *Paracoccus denitrificans*." Microbiology **149**(12): 3405-3412.

Mrazek, J. (2009). "Finding sequence motifs in prokaryotic genomes - a brief practical guide for a microbiologist." Brief Bioinform **10**(5): 525-536.

Pfaffl, M. W. (2001). "A new mathematical model for relative quantification in real-time RT–PCR." Nucleic Acids Research **29**(9): e45.

Poole, R. K., M. F. Anjum, J. Membrillo-Hernandez, S. O. Kim, M. N. Hughes and V. Stewart (1996). "Nitric oxide, nitrite, and Fnr regulation of *hmp* (flavohemoglobin) gene expression in *Escherichia coli* K-12." Journal of Bacteriology **178**(18): 5487-5492.

Reents, H., R. Munch, T. Dammeyer, D. Jahn and E. Hartig (2006). "The Fnr regulon of *Bacillus subtilis*." J Bacteriol **188**(3): 1103-1112.

Richardson, D. J. (2008). Structural and functional flexibilty of bacterial respirome. Bacterial Physiology: A molecular approach. W. El-Sharoud. Berlin Heidelberg, Springer-Verlag**:** 97-128.

Richardson, D. J., H. Felgate, N. Watmough, A. Thomson and E. Baggs (2009). "Mitigating release of the potent greenhouse gas N_2O from the nitrogen cycle – could enzymic regulation hold the key?" Trends in Biotechnology **27**(7): 388-397.

Richardson, D. J., A. J. Thomson and N. J. Watmough (2008). "NO laughing matter: The toxic gases of the nitrogen cycle." Microbiology Today **08**(3): 105-156.

Saunders, N. F. W., J. J. Hornberg, W. N. M. Reijnders, H. V. Westerhoff, S. de Vries and R. J. M. van Spanning (2000). "The NosX and NirX Proteins of *Paracoccus denitrificans* are functional homologues: their role in maturation of nitrous oxide reductase." Journal of Bacteriology **182**(18): 5211-5217.

Sears, H. J., S. Spiro and D. J. Richardson (1992). "Effect of carbon substrate and aeration on nitrate reduction and expression of the periplasmic and membrane-boundnitrate reductases in carbon-limited continuous cultures of *Paracoccus denitrificans* Pdl222." Microbiology **9971**: 3767-3774.

Sexstone, A. J., N. P. Revsbech, T. B. Parkin and J. M. Tiedje (1985). "Direct measurement of oxygen profiles and denitrification rates in soil aggregates." Soil Sci. Soc. Am. J. **49**(3): 645-651.

Spiro, S. (2007). "Regulators of bacterial responses to nitric oxide." FEMS Microbiology Reviews **31**(2): 193-211.

Spiro, S. (2012). "Nitrous oxide production and consumption: regulation of gene expression by gas-sensitive transcription factors." Philos Trans R Soc Lond B Biol Sci **367**(1593): 1213-1225.

Sullivan, M. J., A. J. Gates, C. Appia-Ayme, G. Rowley and D. J. Richardson (2013). "Copper control of bacterial nitrous oxide emission and its impact on vitamin B12-dependent metabolism." Proceedings of the National Academy of Sciences.

Unden, G. and J. Bongaerts (1997). "Alternative respiratory pathways of Escherichia coli: energetics and transcriptional regulation in response to electron acceptors." Biochimica et Biophysica Acta (BBA) - Bioenergetics **1320**(3): 217-234.

van Spanning, R. J. M., A. P. N. de Boer, W. N. M. Reijnders, H. V. Westerhoff, A. H. Stouthamer and J. van der Oost (1997). "FnrP and NNR of *Paracoccus denitrificans* are both members of the FNR family of transcriptional activators but have distinct roles in respiratory adaptation in response to oxygen limitation." Molecular Microbiology **23**(5): 893-907.

Van Spanning, R. J. M., E. Houben, W. N. M. Reijnders, S. Spiro, H. V. Westerhoff and N. Saunders (1999). "Nitric oxide is a signal for NNR-mediated transcription activation in *Paracoccus denitrificans*." Journal of Bacteriology **181**(13): 4129-4132.

Vishniac, W. and M. Santer (1957). "The *Thiobacilli*." Bacteriological Reviews **21**(3): 195-213.

Vollack, K.-U., E. Härtig, H. Körner and W. G. Zumft (1999). "Multiple transcription factors of the FNR family in denitrifying Pseudomonas stutzeri : characterization of four fnr-like genes, regulatory responses and cognate metabolic processes." Molecular Microbiology **31**(6): 1681-1694.

Wang, Q., M. Burger, T. A. Doane, W. R. Horwath, A. R. Castillo and F. M. Mitloehner (2013). "Effects of inorganic v. organic copper on denitrification in agricultural soil." Advances in Animal Biosciences **4**(Supplements1): 42-49.

Wood, N. J., T. Alizadeh, S. Bennett, J. Pearce, S. J. Ferguson, D. J. Richardson and J. W. Moir (2001). "Maximal expression of membrane-bound nitrate reductase in *Paracoccus* is induced by nitrate via a third FNR-like regulator named NarR." J Bacteriol **183**(12): 3606-3613.

Wood, N. J., T. Alizadeh, D. J. Richardson, S. J. Ferguson and J. W. Moir (2002). "Two domains of a dual-function NarK protein are required for nitrate uptake, the first step of denitrification in *Paracoccus pantotrophus*." Mol Microbiol **44**(1): 157-170.

Woolfenden, H. C., A. J. Gates, C. Bocking, M. G. Blyth, D. J. Richardson and V. Moulton (2013). "Modeling the effect of copper availability on bacterial denitrification." MicrobiologyOpen **2**(5): 756-765.

Zumft, W. G. (1997). "Cell Biology and Molecular Basis of Denitrification." Microbiology and Molecular Biology Reviews **61**(4): 533-616.

Zumft, W. G. (2002). "Nitric oxide signaling and NO dependent transcriptional control in bacterial denitrification by members of the FNR-CRP regulator family." J Mol Microbiol Biotechnol **4**(3): 277-286.

7. Materials and Methods

Contents

7.1 Culture Techniques

7.1.1 Media

Mineral Medium for *P. denitrificans*

Stock solutions (100x) were made up for potassium di-hydrogen orthophosphate (KH_2PO_4), ammonium chloride (NH_4Cl), magnesium sulfate ($MgSO_4$), sodium nitrate ($NaNO_3$) and sodium succinate ($Na_2C_4H_6O_4$) for use in mineral media preparation. Di-sodium orthophosphate (Na_2HPO_4) was added from the stock solution and made up to volume with demi-water for each medium batch required. The pH was adjusted to the desired level with the addition of sulfuric acid or sodium hydroxide. The medium was sterilized by autoclaving and 2 $ml.L^{-1}$ of filter sterilized trace element solution (based on Vishniac and Santer (1957)) was added post-autoclave. The copper content of the trace element solution was adjusted as required by the experimental conditions examined. When solid medum was required, 1.5 % w/v agar was added prior to autoclaving.

Table 1 The *Paracoccus denitrificans* mineral medium formula used in this study

Compound	MW	Concentration	
		mM	$g.L^{-1}$
Na_2HPO_4	**142**	29	4.12

KH_2PO_4	**136**	11	1.50
NH_4Cl	**53.5**	10	0.54
$MgSO_4$	**246.5**	0.4	0.10
$NaNO_3$	**85**	20	1.70
$Na_2C_4H_6O_4$	**270**	5	1.35

Table 2 The trace element solution* content for supplementing the *Paracoccus denitrificans* mineral medium.

Compound	MW	Stock Concentration		Final Concentration
		mM	g/L	µM
EDTA	292.24	171.09	50	342.2
$ZnSO_4.7H_2O$	287.55	7.65	2.2	15.3
$MnCl_{2.4}H_2O$	197.91	25.57	5.06	51.1
$FeSO_4.7H2O$	278.01	17.95	4.99	35.9
$(NH_4)_6Mo_7O_{24.4}H2O$	1235.9	0.89	1.1	1.8
$CuSO_4.5H_2O$	249.68	6.29	1.57	12.6
$CoCl_2.6H_2O$	237.93	6.77	1.61	13.5
$CaCl_2.2H_2O$	147.02	49.92	7.3391	99.8

*Adjusted to pH 6.6, and filter sterilized (0.22 µm).

LB media

LB medium was made by dissolving the premixed medium (Formedium, UK) in demi-water (25 $g.L^{-1}$). The final medium contained the following compounds: 10 $g.L^{-1}$ tryptone, 5 $g.L^{-1}$ yeast extract and 5 $g.L^{-1}$ of NaCl. When solid medium was required 1.5 % w/v was added prior to autoclaving.

7.1.2 Antibiotics

Antibiotics and their working concentrations used in this study are listed in Table 3. Stock solutions were dissolved in the appropriate solvent, filter sterilized and kept at 4°C for not longer than 8 weeks.

Table 3 Stock and working concentrations of the antibiotic compounds used in this study

Antibiotic		**Stock Concentration $mg.ml^{-1}$**	**Solvent**	**Working Concentration $\mu g.ml^{-1}$**
Rifampicin	Rif	50	Methanol	50
Kanamycin	Kan	50	H_2O	25
Streptomycin	Step	100	H_2O	100
Gentamicin	Gent	20	H_2O	20
Carbenicillin	Carb	60	H_2O	60

7.1.3 Bacterial Strains

The bacterial strains used within this study (Table 4) were kept frozen at -80°C in 25% v/v glycerol stocks. A loop full of the selected strains was streaked out on LB perti dishes with the appropriate antibiotic and incubated at 37°C overnight for the wild-type strain or for 48 hours for the mutant strains. LB and mineral media starter

cultures were made fresh prior to each experiment, by picking a single colony from the LB petri dish and inoculating a bottle containing 10 ml of LB with the appropriate antibiotic. These bottles were incubated overnight at 37^{o}C with 200 RPM orbital shacking. Subsequently, 1% of fresh LB culture was used to inoculate 10 or 100 ml mineral medium, which was later incubated overnight at 37^{o}C with orbital shacking. All bacterial or molecular handling was done aseptically.

Table 4 Strains of *Paracoccus denitrificans* used in this study

Strain	**Antibiotic Resistance**	**Description**	**Reference**
PD1222	Rif	DSM413 derivative; enhanced conjugation frequencies	de Vries et al. (1989) Baker et al. (1998)
PD10221	Rif/Kan	PD1222 derivative; Δ*nosZ*	Saunders et al. (2000)
PD29.21	Rif/Kan	PD1222 derivative; ΔfnrP	van Spanning et al. (1997)
PD77.21	Rif/Kan	Pd1222 derivative; Δ*nnrR*	van Spanning et al. (1997)
PD2345	Rif	PD1222 derivative; *ΔnarR*	This study
PD29.21: pGG002F01	Rif/Gent	PD29.21 *fnrP* compliment	This study
PD77.21: pGG001N10	Rif/Gent	PD77.21 *nnrR* compliment	This study
PD2345: pGG003NR1	Rif/Gent	PD2345 *narR* compliment	This study

7.1.4 Aerobic batch culture in flasks

Cultures of *P. denitrificans* were incubated aerobically in 250 ml conical flasks at 30^{o}C with 400 RPM orbital rotation. The conical flasks were filled with 50 ml of medium to ensure maximum air mixing and diffusion within the medium as previously demonstrated (Sears *et al.* 1992). A 500 µL sample was taken at regular intervals for optical density determination and further nitrate and nitrite ion analysis.

7.1.5 Anaerobic batch cultures in Hungate tubes or Duran bottles

Anaerobic cultures of *P. denitrificans* were either incubated in Hungate tubes (Hungate 1969) or in 500 ml Duran bottles with self-made silica septa. Both containers were equipped with a special screw cap and a septum to allow gas and liquid sampling. The Hungate tubes and the appropriate sized screw caps and rubber-buttyl septa were supplied from Chemglass Life Sciences, USA. The Duran bottles and the appropriate sized screw caps were supplied from Fischer Scientific, UK. The septa for the Duran bottles were self-made by piercing a 43 mm diameter bore through a 3 mm thick medical quality silica sheet supplied from Silicone Engineering Ltd, UK. Hungate tubes that were previously sterilized by autoclaving were aseptically filled with 10 ml of a mixture containing sterile medium, trace elements and inoculum (1%). Duran bottles were filled with 350 ml of medium and sterilized by autoclaving. The inoculum (1%) and trace elements were added after autoclaving. The tubes and the bottles were incubated at 30^{o}C without shaking. Samples to determine optical density, nitrous oxide, nitrate and nitrite concentration from the Duran bottles were taken at regular intervals using a sterile syringe. The optical density of the cultures enclosed in Hungate tubes was taken by a specialized colorimeter (Fischer Scientific, UK).

7.1.6 High resolution growth curves in anaerobic environment using the plate-reader

Anaerobic growth curves were monitored in high resolution following an adapted method of Koutny and Zaoralkova (2005). A 200 µL aliquot of sterile medium, trace elements and inoculum (1%) was aseptically added to each well of a 96-well plate. The lid was treated with an antifog solution and non-toxic silicon glue was applied to the rim of the lid. The 96-well plate containing the treatments was sealed in an anaerobic glove box and incubated for 48 h without shacking at 30^{o}C. An average optical density of six readings at 600 nm was taken per well every 30 minutes (Omega, UK). A negative control sample was included containing medium without any alternative electron acceptor and a blank sample containing only medium.

7.1.7 Continuous cultures in bio-reactors

Continuous cultures of *P. denitrificans* were used to study metabolic fluxes and transcriptional regulation under aerobic and anaerobic conditions (Hoskisson and Hobbs 2005). These cultures were performed in 2.5 L bio-reactors (BioFlo 310, New Brunswick Scientific, USA). Each bioreactor consisted of the reaction vessel, the main control unit (MCU) and the sensors. The vessel contained 1.5 L of minimal medium and the remaining headspace was 1 L. Gas and liquid samples were taken throughout the incubation period from specialized sampling ports to allow aseptic sample handling. The pH, dissolved oxygen tension, agitation, temperature and feeding rate were automatically controlled and adjusted to the desired levels via the MCU. The MCU consists of a power supply, relays, sensors, microcontrollers and a touch screen for user communication with the embedded reactor software (New Brunswick Scientific, USA). Typically, continuous cultures were incubated for 120 h at 30^{o}C with agitation; 500 RPM and 200 RPM for aerobic and anaerobic cultures respectively.

The 120 h incubation period consisted of two phases, the first phase included the inoculation (T=0 h) of the reactor vessel with 10 ml of fresh LB culture and the growth of the bacterial culture in batch mode aerobically for approximately 24 h. The second phase was initiated when the air supply was switched off or maintained for anaerobic and aerobic incubations respectively coupled with a simultaneous activation of the dilution rate (feed pump). After approximately 3 vessel volumes, steady biomass levels were observed (D=0.05 h^{-1}).

The pH in the reaction vessel was monitored with an InGold pH electrode (Mettler Toledo, UK) adjusted automatically with the addition of 1M NaOH and 0.1M H_2SO_4. The pH electrode was calibrated previously at pH 4 and pH 9.2 with calibration solutions supplied by Fisher Scientific, UK.

Dissolved air in the reaction vessel was monitored with an InPro polarographic electrode (Mettler Toledo, UK) that was previously calibrated in air saturated (100%) or nitrogen saturated (0%) medium. The % readings were converted to µM of dissolved O_2 using equation 3 which is derived from Henry's law and van't Hoff's equation (Equation 1and 2). Air and gas mixture supply (3 SLPM) was controlled by the MCU through specific electromechanical gas valves.

$$\boldsymbol{c = \frac{PO_2}{K_H}}$$

Equation 1 Solubility of oxygen in a solvent, where *c*= solubility, PO_2= partial pressure or oxygen (21%) and K_H=proportionality constant (769.23 atm.L.mol^{-1}).

$$K'_H = K_H * \exp\left[-C * \left(\frac{1}{T'} - \frac{1}{T}\right)\right]$$

Equation 2 van't Hoff equation to adjust the proportionality constant (K_H) to the required temperature, where K'_H= adjusted the proportionality constant, *C*= gas constant (1700K) *T*= temperature in Kelvin, *T'*= adjusted temperature.

$$[O_2] = \frac{248.5 * DO\%}{100}$$

Equation 3 Conversion of dissolved oxygen percentage readings (DO%) to micro molar concentration.

Temperature was monitored with a resistance temperature sensor (RTD) and was maintained by a water jacket intergrated in the reaction vessel. Water was circulated through the water jacket from a temperature controlled tank maintained in the main control unit.

Agitation was also monitored and controlled by the MCU. The agitator consisted of two parts: a shaft and a motor. There are two Rushton type impellers attached to the shaft. The impellers were submerged in the medium to avoid any surface disturbance, foam formation or excessive gas diffusion.

Data acquisitionwas carried out automatically at 1 minute intervals via the MCU reactor process controller (RPC) to PCs running the BioCommand software.

Table 5 Dilution rates (D) used to maintain a steady biomass rates after a pH change. These dilution rates are calculated based on the feed pump rate (F).

pH	**F** $ml.h^{-1}$	**D** h^{-1}
6.0	2.5	0.002
6.5	70	0.047
7.0	80	0.053
7.5	80	0.053
8.0	80	0.053
8.5	70	0.047
9.0	2.5	0.002

7.1.8 Calculations of productivity and consumption quotients for chemostats

Table 6 Calculations of productivity and consumption quotients in chemostat continuous cultures

Symbol	Description	Calculation formula	Units
X	Biomass	$X = OD * 0.518$	$g.L^{-1}$
D	Dilution rate	$D = \frac{F}{V} = \frac{80}{1500} = 0.053$	h^{-1}
*q*X	Biomass quotient	$qX = OD * 0.518 * D$	$g.L^{-1}.h^{-1}$
$[NO_3^-]_0$	Nitrate concentration in feed medium		
$[NO_3^-]_t$	Nitrate concentration in reactor vessel		
$[NO_2^-]_t$	Nitrite concentration in reactor vessel		
$[N_2O]_t$	Nitrous oxide concentration in reactor vessel, corrected to one nitrogen molecule	$[N_2O]_t = 2 * [N_2O]$	µM
$[N_2]_t$	Nitrogen concentration in reactor vessel, corrected to one nitrogen molecule	$[N_2]_t = 2 * ([NO_3]_0 - [NO_3]_t - [NO_2]_t - [N_2O]_t)$	
$qc[NO_3^-]$	Nitrate consumption	$qc[NO_3^-] = ([NO_3^-]_0 - [NO_3^-]_t) * \frac{D}{X}$	
$qp[NO_2^-]$	Nitrite production	$qp[NO_2^-] = [NO_2^-]_t * \frac{D}{X}$	
$qc[NO_2^-]$	Nitrite consumption	$qc[NO_2^-] = qc[NO_3^-] - qp[NO_2^-]$	$\mu mol.g^{-1}.h^{-1}$
$qp[N_2O]$	Nitrous oxide production	$qp[N_2O] = [N_2O]_t * \frac{D}{X}$	
$qp[N_2]$	Nitrogen production	$qp[N_2] = [N_2]_t * \frac{D}{X}$	

7.2 Analytical Techniques

7.2.1 Optical density or spectrophotometric readings

The optical density (OD) or spectrophotometric readings were taken in polystyrene cuvettes (Sarstedt, DE). The pathlength was 1 cm and volume of the sample was 1 ml. Optical density for growth determination was measured at 600 nm using a spectrophotometer (WPA, UK). The conversion of optical density to biomass was done with the following formula (Equation 4)(Felgate *et al.* 2012).

$$[\text{Biomass}] = OD_{600} * 0.518$$

Equation 4 Conversion of optical density readings to biomass concentration ($g.L^{-1}$).

7.2.2 Protein concentration determination

Protein content in solution was determined with a modified microplate BCA assay with BSA protein as standard (Olson and Markwell 2001). A 10µL sample or standard was mixed with 200 µL of reagent (1:50, 4% copper sulphate:bicinchonic acid). The plate was incubated at 37^{o}C for 30 minutes. Then, absorbance readings were taken with a microplate reader at 562 nm (Molecular Devices, USA) and converted to total protein concentration according to equation 5.

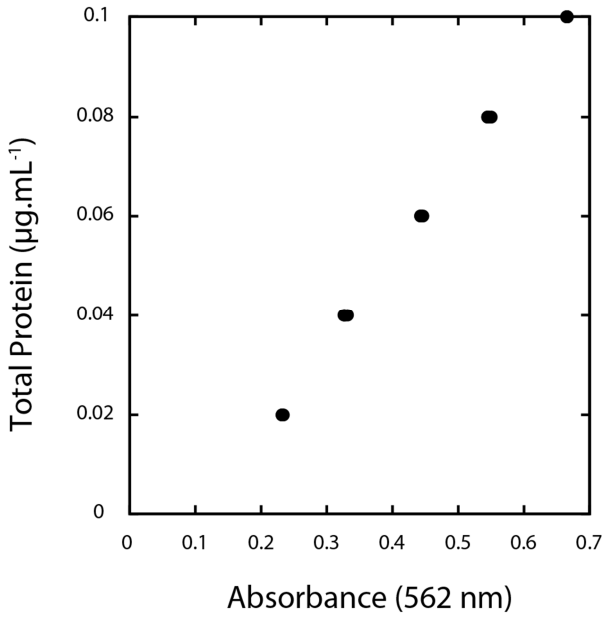

Figure 1 Total protein BSA standard curve in microplate assay format.

$$[\text{Protein}] = 0.178 * Absorbance_{562} - 0.018\,; R^2 = 0.998$$

Equation 5 Conversion of absorbance to protein concentration in µg.ml^{-1}.

7.2.3 NO_3^- and NO_2^- determination

The concentrations of NO_3^- and NO_2^- were determined with a high pressure liquid chromatography (HPLC) system (ICS-900, IonPac AS22 2mm column, Dionex). A 1.5 ml sample was spun at 13000 RPM and subsequently 0.5 ml of the supernatant was mixed with 4.5 ml of analytical water and passed through a 0.2 µm filter (Millipore). The HPLC was equipped with a conductivity detector that detected the anions after separation through the column and cation exchange via an ion specific membrane. The retention time for NO_3^- and NO_2^- was 7.5 and 4.7 minutes respectively. The eluent solution consisted of 1.8 mM sodium carbonate (Na_2CO_3) and 1.7 mM sodium bicarbonate ($NaHCO_3$). A sulfuric acid solution (0.1% v/v) was used as a regenerant. Standards of 0.1 – 30 mM NO_3^- and NO_2^- and were determined and the concentrations were calculated with linear regression (Equations 6 & 7). Pure analytical grade water (Fischer Scientific, UK) was used as a blank.

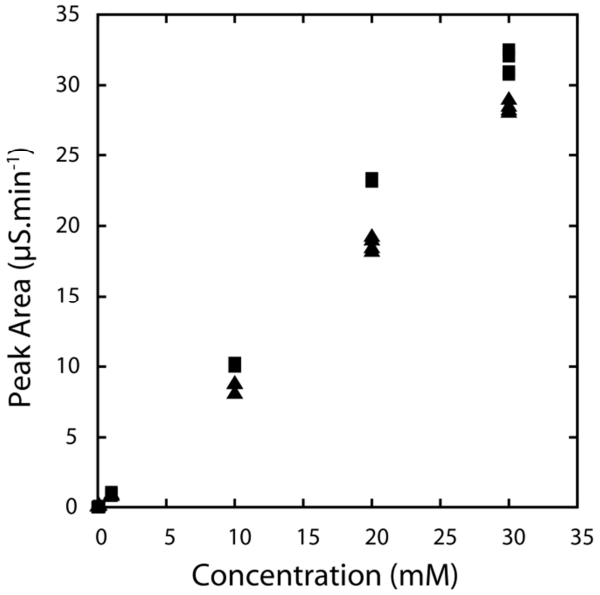

Figure 2 Calibration graph for nitrate (■) and nitrite (▲) analysis with Dionex HPLC.

$$[\text{nitrate}] = (peak\ area_{7.5\ mins}) * 0.919 + 0.080;\ R^2 = 0.995$$

Equation 6 Conversion of peak area to nitrate concentration in mM.

$$[\text{nitrite}] = (peak\ area_{4.7\ mins}) * 1.055 + 0.286;\ R^2 = 0.998$$

Equation 7 Conversion of peak area to nitrite concentration in mM.

7.2.4 N_2O determination

N_2O emissions were determined with gas chromatography (Clarus 500, Perkin Elmer). The gas molecules were non-destructively separated through a 30 m elite-Plot Q column with an inner diameter of 0.53 mm. The column was heated constantly at 90 ^oC. N_2O gas molecules were detected on a ^{63}Ni electron capture detector (ECD) heated constantly at 350 ^oC. The carrier gas was zero-grade nitrogen and the make-up gas a 5% methane argon mixture supplied by (BOC, UK). The retention time for N_2O was 5.2 minutes. N_2O gas standards were used and N_2O concentrations were determined with linear regression (figure 3 and equation 8). The total concentration of N_2O in culture

was calculated with the Henry and van't Hoff equations (similarly as in equation 1 and 2) and resulted in a conversion factor of 0.055 ($\mu M.ppm^{-1}$) at 30°C.

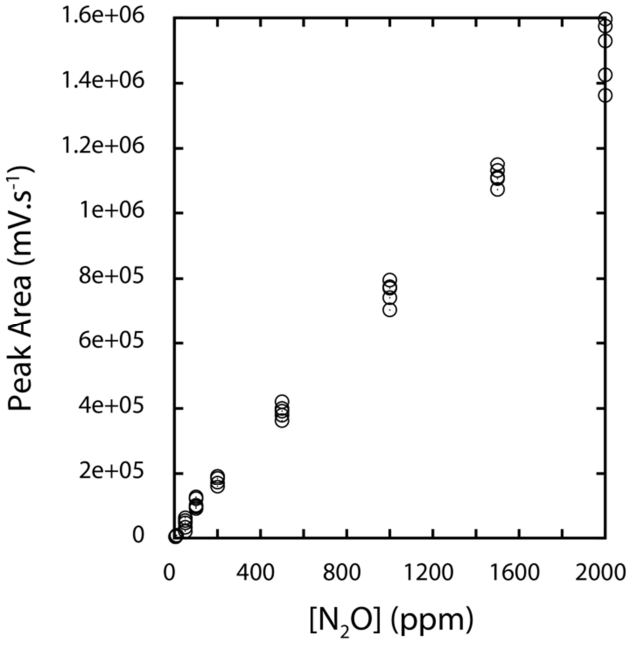

Figure 3 N_2O calibration curve with Perkin-Elmer Clarus 500 gas chromatograph

$$[\text{nitrous oxide}] = (peak\ area) * 0.0013 - 17.845\ ;\ R^2 = 0.999$$

Equation 8 Conversion of peak area to nitrous oxide concentration in ppm.

7.2.5 NO_3^- and NO_2^- Reductase assays

The relative activity of nitrate and nitrite reductase in cell cultures was assayed spectro-photometricaly using reduced methyl viologen (MV) dye as an electron donor. Samples of 10ml were collected from chemostat cultures at pH 6, 6.5, 7.2, 7.5, 8 and 8,5 and spun down at 6000 RPM for 10 minutes. The cell pellet was washed twice with phosphate saline buffer and carefully diluted to a concentration factor of 10x. The assay was carried out anaerobically in glass cuvettes sealed with butyl rubber septa. All materials were sparged with oxygen free N_2 (BOC, UK) for 15 minutes. A Hitachi U3310

spectrophotometer was used to record the change in absorbance at 600 nm. The activity was calculated using the Beer-Lambert law (Equation 9).

$$\mathbf{Absorbance}_{600\,nm} = \boldsymbol{C} * \boldsymbol{\varepsilon} * \boldsymbol{L}$$

Equation 9 Beer-Lambert law equation; where C= solute concentration, ε= extinction coefficient (MV: 13 $mM^{-1}.cm^{-1}$) and L= light path length (1 cm).

7.2.6 Agarose gel electrophoresis

Horizontal gel slabs of approx. 11 x 16 cm (W x L) dimensions consisting of 1% or 2% w/v agarose in 150 ml of Tris-Acetate-EDTA buffer (TAE), stained with ethidium bromide ($C_{21}H_{20}BrN_3$) as a fluorescent nucleic acid tag were used routinely for PCR product and restriction analysis. Gels images were taken and analysed using a UV imager (Biorad, UK) and QuantityOne imaging software (Biorad, UK).

Table 7 Formula of TAE buffer (50 x concentrated)

Component	Amount (L^{-1})
Tris base	242 g
Glacial acetic acid	57.1 ml
Na_2EDTA 0.5M – pH 8.0	100 ml

7.2.7 Western Blot and Immunoprobing

Gel electrophoresis, western blotting and immumoprobing was used to detect the expression of NosZ in batch cultures. Cells were lysed in a sonicator and spun down to

collect the soluble fraction (supernatant). Samples were diluted to equal amounts of total protein and were separated by molecular weight on a 12% SDS gel.

For western blotting and immune detection samples were electrobloted onto a PVDF membrane as described in (Felgate 2010). In short, the membrane was blocked with 5% skimmed milk powder in PBS. The primary antibody against NosZ raised in sheep and secondary antibody (IgG, Sigma Aldrich, UK) were used for detection. The membrane was exposed to a film (Bio max XAR, Kodak) in dark and developed using an x-ray film developer.

7.3 Molecular Techniques

7.3.1 Plasmids

The plasmids used in this study are listed in table 8. Plasmids were stored in RNA free H_2O at -20^{o}C or in glycerol stocks at -80^{o}C in their bacterial hosts.

Table 8 DNA vectors used in this study

Plasmid	Antibiotic Resistance	Accession number	Use
pLMB509	Gentamycin	JQ895027	Low copy complementation.
pJET2.1	Ampicillin	EF694056	General cloning (blunt end) and digestion.
pK19*mob*	Kanamycin	Schafer et al. (1994)	General cloning.
pK18*mobSacB*	Kanamycin	FJ437239	Mutations via homologous recombination; suicide vector.
pRK2013	Kanamycin	Figurski and Helinski (1979)	Helper plasmid for tri-parental mattings.

7.3.2 RNA extraction (RNA preps)

The RNA extraction process was done in two phases; firstly, the cells were harvested and killed instantly to stop transcription using a 5% phenol/ethanol solution. Secondly, the RNA was extracted and purified using a modified version of the supplier's protocol (SV Total RNA Isolation System, Promega, UK).

Bacterias were harvested at the mid-exponential growth stage (OD 0.3) and RNA was extracted following the phenol-ethanol extraction method. Cells (30 ml culture) were immediately incubated on ice for at least 30 minutes in tubes containing 12 ml ice-cold phenol/ethanol solution. After that the pellets were collected by a two-step centrifugation process to eliminate any residual phenol/ethanol contamination. The first step was done at 6000 RPM for 10 minutes at 4^{o}C and the second step at 12000 RPM for 2 minutes at 4^{o}C. Immediately after that the pellets were snap-frozen and stored at -80^{o}C until further use.

The frozen pellet was thawed in room temperature and lysed with 100 µL of 100 mg.ml^{-1} lysozyme in Tris-EDTA buffer. To assist the lysis, the samples were incubated at 37^{o}C for 10 minutes. Then, 75 µL of lysis buffer supplied with the kit was added. Additionally 350 µL of RNA dilution buffer was added and the samples were heated for 3 minutes at 70^{o}C. Following that, the samples were centrifuged for 10 minutes at 12000 RPM and the supernatant was transferred to clean 1.5 ml tubes. Then, the RNA was purified by centrifugation following the supplier's protocol.

7.3.3 DNA contamination removal

Any residual DNA contamination from RNA preparations was removed with Turbo DNAse treatment (Ambion, USA). RNA samples were diluted to 500 ng.µL^{-1} in 100 µL total volume. Then 11 µL of 10x TurboDNase buffer and 1 µL of TurboDNase enzyme were added and gently mixed. The sample was incubated at 37^{o}C for 30 minutes. The DNA digestion was stopped by adding 11.5 µL of DNase inactivation reagent. The

sample was mixed well and incubated for 5 minutes at room temperature. After incubation the sample was spun at 10000 RPM and the supernatant was carefully transferred to clean 1.5 ml tubes. Two aliquots of 5 and 95 µL were frozen in liquid nitrogen for further use to reduce contamination and degradation of RNA samples. The 5 µL was used for PCR and DNA gel electrophoresis to ensure DNA contamination was removed.

7.3.4 RNA quantity and quality check

The total RNA yield was determined spectrophotometricaly at 260 nm (NanoDrop, Thermo). Pure RNA-free water was used to blank the spectrophotometer. Purity of total RNA was determined as the absorbance ratio of $\frac{260}{280}$ with expected values between 1.8 - 2.00 indicating no protein contamination. The ration of $\frac{260}{230}$ is helpful in evaluating any carryover of phenol.

Additionally and prior to microarray analysis, the total RNA integrity was confirmed by gel electrophoresis on a chip following the manufacturer's protocol for RNA StdSens, Experion kit (Biorad, UK). A clear appearance of the 28S, 18S and 5S rRNA bands was the quality criterion for RNA integrity. Smearing below the bands would indicate degraded RNA and samples would be discarded from further analysis.

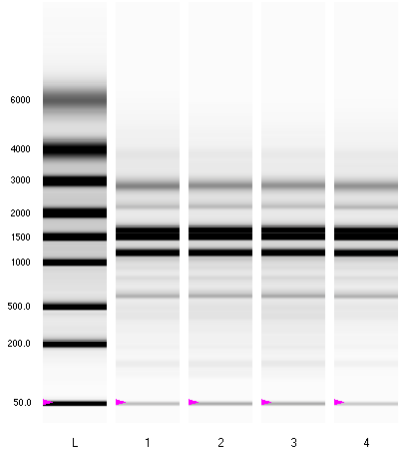

Figure 4 A typical gel-like image of Experion total RNA electrophoresis (Biorad, UK). The RNA was isolated from *P. denitrificans* culture according to the phenol-ethanol extraction method and was run on a RNA StdSens chip (Biorad, UK). Lane L depicts the ladder and lanes 1, 2, 3 and 4 the samples analysed.

7.3.5 DNA quantification and quality check

The total DNA yield was determined spectrophotometricaly at 260 nm (NanoDrop, Thermo) and the quality (purity) of total DNA was assessed similarly as total RNA quality check (spectrophotometricaly).

7.3.6 Reverse transcription

A sample containing 2 µg of total RNA in 11 µL total volume was prepared. Then 1 µL of 10 mM dNTPs and 1 µL of Random Primers 300 ng.µL^{-1} were added, and the sample was incubated for 5 minutes at 65^{o}C. Then the sample was chilled on ice for 1 minute and spun briefly to concentrate. To each sample 6 µL of pre-made Reverse Transcriptase (RT) master mix were added and briefly mixed by flicking the tubes. The RT master mix contained 4 µL of 5x First Strand buffer (Table 9) and 2 µL of 0.1 M DTT. The sample was incubated in the PCR Thermal Cycler for 2 minutes at 25^{o}C, and then 1µL of Super Script II Reverse Transcriptase was added to each sample and mixed well

by pipetting. This resulted in a total reaction volume of 20 µL. The samples were incubated using the PCR program as described in table 10 from step 2 and onwards. After the incubation, the sample was chilled for 2 minutes on ice and was transferred in new 1.5 ml tubes. The sample was diluted 10 fold with the addition of 180 µL of RNA-free H_2O.

Table 9 Contents of the 5x First-Strand buffer (Invitrogen, UK)

Compound	Concentration (mM)
Tris-HCl, pH 8.3	250
KCl	375
$MgCl_2$	15

Table 10 PCR program for First-Strand cDNA synthesis using SuperScript II Reverse Transcriptase

Fragment	Temperature	Duration (minutes)
Initial incubation (step 1)	25	2
Incubation (step 2)	25	10
Reaction Incubation	42	50
Heat inactivation	70	15

7.3.7 Primer design and validation

Primer oligonucleotides for colony PCR and RTPCR were designed using the Primer 3 Plus online software that can be accessed from http://www.bioinformatics.nl/cgi-bin/primer3plus/primer3plus.cgi/. Product size was set between 100-150 bp and primer oligo length was set at a range of 18-27 bp with an optimum of 20 bp, primer melting temperature (Tm) was set at a range of 58-62 ^{o}C with an optimum Tm of 60 ^{o}C and the Guanine and Thymine percentage content was set at an optimum of 50 %.
The DNA sequence of the target gene was selected as FASTA data, and reverse and forward primers were picked from the middle region of the sequence if possible.

The selected primer oligonucleotide sequences were ordered from Eurofins / MWG Operon (Germany). Upon arrival the oligonucleotides were rehydrated with RNA free H_2O to 100 µM and diluted to 20 µM aliquots for PCR. Each pair of forward and reverse primers was validated and quality checked with PCR with genomic DNA (gDNA) from *P. denitrificans* PD1222. Primers showing district products at the expected product size were kept and the rest were discarded as non-specific or faulty primers.

7.3.8 Polymerase Chain Reaction (PCR)

PCR was used to generate DNA fragments to detect target genes, to confirm RNA purity from DNA contaminations and to generate inserts of target genes. High fidelity polymerase was used to amplify selected target gene regions (Table 11 and 12). All reactions were performed in a Techne thermocycler (Techne, UK).

Table 11 Phusion High Fidelity PCR mix (Thermo, UK)

PCR Reaction Formula	**Volume (µL)**
5x Phusion Buffer	4
Forward Primer 20 mM	0.4
Reverse Primer 20 mM	0.4
DMSO	0.6
10 mM dNTPs	0.4
H_2O RNA-free	13.2
DNA template / gDNA	1
	Total Volume 20 µL

Table 12 PCR program for Phusion High Fidelity polymerase (Thermo, UK)

Fragment	Temperature (°C)	Duration (seconds)
Initial denaturation	98	60
Cycle denaturation	98	10
Cycle annealing	62	15
Cycle extension	72	30/kbp
Final extension	72	300
Final hold	4	Until sample collection

7.3.9 Colony Polymerase Chain Reaction

Colony PCR was employed to verify target genes or chromosomal mutations. Overnight colonies were picked with a sterile toothpick from LB agar petri dishes. The tip of the toothpick was used to inoculate a new LB agar petri dish, to maintain the colony and then twisted repeatedly in a 1.5 ml tube containing 10 µL of RNA-free H_2O for a liquid culture from the same starter colony. The samples were boiled for 10 minutes at 95°C to lyse the cells and release bacterial DNA. The tubes were spun at 13000 RPM for 2 minutes to pellet the cell material. A 1 µL aliquot of the supernatant was used later as DNA template for target gene detection in colony PCR.

Two master mixes for colony PCR were used depending on availability; 2x MyTaq from Bioline, UK or Thermo PCR Master Mix from Thermo, UK. In each case, the method was similar to that shown on

Table 13. The target gene was amplified using the respective program (as described in table 14 and 15) in Techne PCR Thermal Cycler for 35 cycles.

Table 13 Colony PCR Reaction Mix

PCR Reaction Formula	Volume (µL)
2x PCR Master Mix	10
(2x MyTaq or 2x Thermo PCR)	
Forward Primer 20 mM	0.4
Reverse Primer 20 mM	0.4
H_2O RNA-free	8.2
DNA template / gDNA	1
	Total Volume 20 µL

Table 14 PCR program for 2x MyTaq

Fragment	Temperature (°C)	Duration (seconds)
Initial denaturation	95	60
Cycle denaturation	95	15
Cycle annealing	60	15
Cycle extension	72	30/Kbp
Final extension	72	300
Final hold	4	Until sample collection

Table 15 PCR program for Thermo PCR

Fragment	Temperature (°C)	Duration (seconds)
Initial denaturation	94	120
Cycle denaturation	94	20
Cycle annealing (Tm-2)	58	30
Cycle extension	72	60/Kbp
Final extension	72	300
Final hold	4	Until sample collection

Table 16 Thermo PCR master mix formula

Ingredient	Amount
ThermoPrime Taq DNA Polymerase	0.625 units
Tris-HCl (pH 8.8 at 25°C)	75 mM
$(NH_4)_2SO_4$	20 mM
$MgCl_2$	1.5 mM
Tween 20	0.01% (v/v)
dATP, dCTP, dGTP and dTTP	0.2 mM each

7.3.10 Quantitative Real Time Polymerase Chain Reaction (qRT-PCR)

Real time quantitative PCR was employed to determine the relative transcription of selected genes. RT-PCR was carried out in 96 well plates (Bioline, UK) in 20 µL reaction volumes. The quantification of the transcripts was carried out using SensiFast SYBR NO-ROX polymerase mix (Bioline, UK) and a C1000 thermal cycler (Biorad, UK) equipped with a CFX-96 detection system (Table 17 and 18).

A 2 µg of total RNA were reversed transcribed using SuperScript II and random primers in a total volume of 20 µL, according to the supplier's instructions. The resulting cDNA was diluted 5 fold with water and 1 µl was loaded in a well according to the reaction mix described in table 17. Three technical replicates from each three biological replicates were used to quantify the target gene expression using the PCR program as described in table 18.

The relative fold change in transcription was calculated using amplification efficiencies taken from a standard curve of serially diluted genomic DNA from *P. denitrificans*. Technical replicates with an inefficient melt curve and or a standard deviation ≥ 0.2 were discarded as technically faulty replicates. The transcripts were normalized to a housekeeping gene *polB* encoding DNA polymerase B in *P. denitrificans*. The amplification efficiency was calculated based on known amounts of gDNA standards.

Table 17 Real Time PCR master mix with SensiFAST polymerase

Compound	Volume per reaction (µL)	Volume for 25 reactions (µL)
2x SensiFAST No-ROX mix	10	250
20 µM forward primer	0.4	10
20 µM reverse primer	0.4	10
Template (cDNA or gDNA)	1	---
H_2O RNA-free	8.2	205
total	20	475

Table 18 PCR program for Real Time PCR detection

Fragment	Temperature (°C)	Duration (seconds)
Initial denaturation	95	180
Cycle denaturation	95	5
Cycle annealing	60	10
Cycle extension	72	5

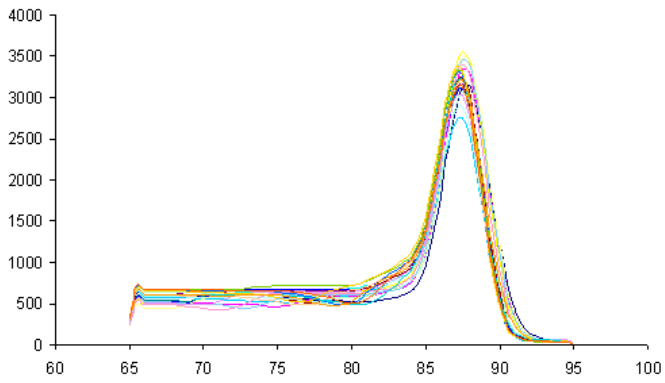

Figure 5 Typical melt curves in RT-PCR. Melting curve analysis is an assessment of the dissociation-characteristics of double-stranded DNA during heating which is characteristic of the primers and amplification efficiency.

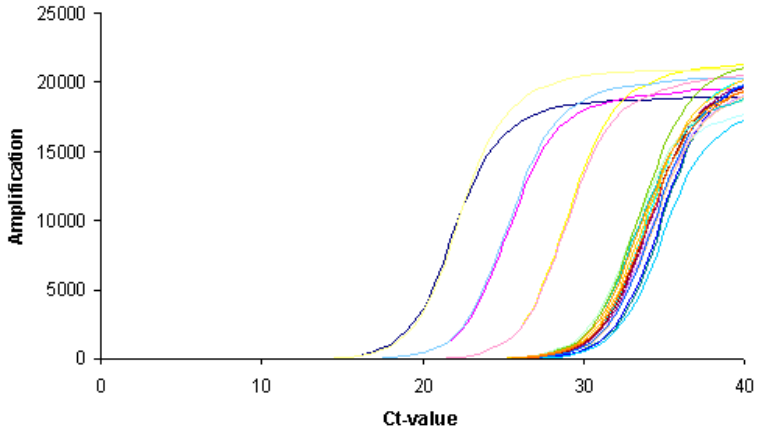

Figure 6 Typical amplification curves in RT-PCR. In real-time PCR, reactions are characterized by the point in time during cycling when amplification of a target is first detected (C_t value) rather than the amount of target accumulated after a fixed number of cycles.

7.3.11 RT-PCR comparative quantification

The ΔΔCt (or $2^{-\Delta\Delta CT}$ method) and the Pfaffl (2001) method were used to make gene comparisons on the relative gene expression. The ΔΔCt method is provided within the CFX Manager software (version 1.1, Biorad). The Pfaffl method takes into account the efficiency of the RT-PCR reaction and the Ct value in both target and reference genes (Equation 11). The ΔΔCt method assumes similar efficiencies in the target and reference genes and uses only the Ct values, as shown in

equation **10**.

$$\text{Fold difference} = 2^{-\Delta\Delta Ct}$$

$$\Delta\Delta Ct = \Delta Ct_{sample} - \Delta Ct_{control}$$

$$\Delta Ct_{sample} = Ct_{GOI-sample} - Ct_{HKG-sample}$$

$$\Delta Ct_{control} = Ct_{GOI-control} - Ct_{HKG-control}$$

Equation 10 Equations to calculate the relative expression based on the $\Delta\Delta C_t$ method. Where ΔCt is the difference of the Ct value between the gene of interest (GOI) and the housekeeping gene (HKG) for the sample and control condition.

$$\text{Fold difference} = \frac{E_{sample}{}^{\Delta Ct_{sample}}}{E_{control}{}^{\Delta Ct_{control}}}$$

$$E = 1 + \frac{E\%}{100}$$

$$\Delta Ct_{sample} = Ct_{GOI-sample} - Ct_{HKG-sample}$$
$$\Delta Ct_{control} = Ct_{GOI-control} - Ct_{HKG-control}$$

Equation 11 Equations to calculate the relative expression based on the Pfafll method. Where E is the efficiency of amplification and ΔCt is the difference of the Ct value between the gene of interest (GOI) and the housekeeping gene (HKG) for the sample and control condition.

7.3.12 Microarray and microarray data manipulation

Type II microarray techniques were used for transcriptional analyses following the method of Sullivan et al. (2013); each microarray slide contained two signals, a CY3-dCTP (Amersham, UK) labeled signal for genomic DNA from *P. denitrificans* and a CY5-

dCTP (Amersham, UK) labeled signal for the experimental sample. Total RNA was reversed transcribed to cDNA using AffinityScript reverse transcriptase (Aligent, UK) and random primers (Invitrogen, UK). The labeled DNA was mixed and hybridized in custom microarray slides (Aligent, UK). The array slides and the samples were allowed to hybridize at 55oC for approximately 60 h. Subsequently the hybridized slides were washed to remove excess dyes, dried and scanned using a GenePix 4000B scanner (Axon Instruments, USA). The raw and normalized signals at 532 and 635 nm as well as the signal ratio were quantified and corrected for background noise using the supplied scanning software (GenePix Pro, Axon Instruments, USA). The extracted datasets from the array images were normalized using Babar an algorithm written in R (Alston *et al.* 2010) that uses cyclic loesses to normalize the complete dataset. Post analyses were performed using GeneSpring 7 (Aligent, UK) and genes were filtered with a ≥ 2 fold expression filter ($p \leq 0.1$).

7.3.13 Genomic DNA extraction

Genomic DNA extraction was based on the Qiagen Genomic DNA handbook 2001. A pellet from a 9 ml overnight bacterial culture was resuspended in 3.5 ml of buffer B1 containing RNaseA. Then 80 µL of freshly-made lysozyme stock (100 $mg.ml^{-1}$) were added together with 100 µL of Qiagen Protease K. The sample was incubated at 37^{o}C for at least 30 minutes. After that 1.2 ml of buffer B2 was added and the solution was mixed well by inversion. The lysate was incubated at 50^{o}C for 30 minutes and then spun for 10 minutes at 6000 RPM. The supernatant was transferred to an activated midi column and was allowed to flow throw by gravity (1-3 hours). The flow through was discarded and 7.5 ml of buffer QC was added twice and was allowed to flow by gravity. The collection tube was replaced with a clean one and the genomic DNA was washed with 5 ml of buffer QF that was pre-heated to 50^{o}C. 3.5 ml of isopropanol were added to the eluate. After vigorous shaking for 2 minutes, the precipitated genomic DNA was collected with a wide diameter tip (clipped-off P1000 tip) and transferred to a 1.5 ml tube. The tube was spun for 30 minutes at max speed (12000 RPM) and the supernatant was discarded. The remaining pellet was washed with 700 µL of 70%

Ethanol in H_2O mix, spun for 2 minutes and the supernatant was removed carefully. The pellet was let to air-dry for 5 minutes and then redissolved in 100 µL of RNA-free H_2O. The pellet was fully dissolved after two-hour incubation at 50^{o}C. Genomic DNA was stored at -20oC for further use and analyses.

7.3.14 Plasmid DNA extraction (mini-prep)

Plasmid DNA extraction (mini-prep) was performed using the Qiagen Kit #27104, following the supplier's protocol as explained below. A 5 ml aliquot of overnight culture was spun at 6000 RPM for 10 minutes. The resulting supernatant was removed and discarded. The bacterial pellet was resuspended in 250 µL of buffer P1; for buffer contents see Table 19. The whole content was then transferred to a 1.5 ml tube and 250 µL of buffer P2 was added to initiate cell lysis. The mixture was well mixed by inversion and was let still for not more than 5 minutes. When a pH indicator was included in the P1 buffer, the mixture turned blue. The lysed cells were neutralized with buffer N3. The cell mixture was well mixed by inversion, until colourless. Then, it was spun at 13000 RPM for 10 minutes. The supernatant was transferred in the spin column and the cell pellet was discarded. The spin column was spun briefly for 60 seconds at max speed and the flow through eluate was discarded. 500 µL of buffer PB was added to the column, spun for 30 seconds, and discarded the flow through. 750 µL of buffer PE was added spun for 30 seconds and the flow through eluate was discarded. An additional centrifugation was performed for 1 minute to remove any remaining residual buffers, after that the spin columns were transferred into clean 1.5 ml tubes and 50 µL of RNA-free H_2O was added. The spin columns containing the H_2O and the plasmid DNA were let still for 2 minutes and then spun for 1 minute at max speed. The eluent containing the plasmid DNA was stored at -20 ^{o}C for further analyses.

7.3.15 Plasmid DNA extraction (midi-prep)

Plasmid DNA extraction (midi-prep) was performed using the Qiagen Kit #12143 following the supplier's protocol. A 100 ml overnight culture was split in two 50 ml tubes and spun for 15 minutes at 6000 RPM. Meanwhile the midi-columns were equilibrated by allowing 4 ml of equilibration buffer QBT, see buffer formulas on Table 19, to flow through the column matrix by gravity. The supernatant was removed and discarded and the cell pellet was resuspended in 4 ml of buffer P1. Then 4 ml of buffer P2 were added and the mixture was gently mixed by inversion, and cell lysis was initiated. The mixture was incubated for less than 5 minutes, then 4 ml of ice-cold buffer P3 were added, gently mixed by inversion and the mixture was incubated on ice for 30 minutes. After that, the mixture was centrifuged for 30 minutes at 20000 RPM. The supernatant was transferred to another clean tube and spun again for 15 minutes at max speed to settle down any remaining cell debris. Then the supernatant was applied carefully to the midi-columns and allowed to flow through the column matrix by gravity. The column was washed twice with 10 ml of buffer QC and the collection tubes were replaced by new ones. The plasmid DNA was eluted with 5 ml of buffer QF and collected. The eluate was then precipitated with the addition on 3.5 ml isopropanol. The precipitated eluate was distributed in equal volumes in 1.5 ml tubes that were later spun for 30 minutes at max speed. The eluent was discarded and the precipitated plasmid pellets were combined in one 1.5 ml tube. The tube was spun again for 15 minutes and any residual isopropanol was removed. The pellet was washed with 70 % Ethanol in H_2O mixture, spun for 10 minutes and the supernatant was removed. The pellet was allowed to air-dry for 10 minutes. Then the pellet was re-hydrated with 70 µL of RNA-free H_2O and stored in -20 ^{o}C for further use and analyses.

7.3.16 Formulas for Qiagen Kit Buffers

Table 19 Formulas for Qiagen Kit Buffers

Buffer	Buffer Contents
Buffer P1	50 mM Tris-HCl pH 8.0 10 mM EDTA 100 µg/ml RNaseA.
Buffer P2	200 mM NaOH 1% SDS.
Buffer P3	3.0 M potassium acetate pH 5.5
Buffer B1 (lysis buffer)	50 mM Tris-HCl pH 8.0 50 mM EDTA pH 8.0 0.5% Tween-20 0.5% Triton-X100 RNAse A 200 µg/l
Buffer B2 (lysis buffer)	3 M Gu-HCl 20% Tween-20
Buffer N3	4.2 M Gu-HCl 0.9 M potassium acetate pH 4.8
Buffer PB	5 M Gu-HCl 30% isopropanol
Buffer PE	10 mM Tris-HCl pH 7.5 80% ethanol
Buffer QBT (equilibration buffer)	750 mM NaCl 50 mM MOPS pH 7.0 15% isopropanol 0.15% triton X-100
Buffer QC (wash buffer)	1.0M NaCl 50 mM MOPS pH 7.0 15% isopropanol
Buffer QF (elution buffer)	1.25M NaCl 50 mM Tris-HCl pH 8.5 15% isopropanol

7.3.17 DNA digestions

Plasmid DNA and DNA fragments were digested with FastDigest restriction enzymes (Thermo, UK). A 20 µL total volume sample was incubated in a 37^{o}C water bath for 30 m and a subsequent heat-deactivation of the restriction enzymes (10 m at 75^{o}C). A subsample of 5 µL was loaded on Ethidium Bromide stained gel to test the efficiency of the digestion when required.

Table 20 Digestion mix formula for FastDigest restriction enzymes (Thermo, UK)

Compound	Amount (µL)
Restriction enzyme FastDigest*	1
10x buffer FastDigest	2
Template (containing <500 ng total DNA)	17

*When multiple restriction enzymes were used the sample volume was decreased accordingly

Table 21 Digestion mix formula for restriction enzymes (Promega, UK)

Compound	Amount (µL)
Restriction enzyme*	1
10x buffer	2
Template (containing <500 ng total DNA)	17

*When multiple restriction enzymes were used the sample volume was decreased accordingly

Table 22 Restriction enzymes used in this study

Restriction Enzyme	Restriction Site
NdeI	5'...C A↓T A T G...3'
	3'...G T A T↑A C...5'
XmaI	5'...C↓C C G G G...3'
	3'...G G G C C↑C...5'
XbaI	5'...T↓C T A G A...3'
	3'...A G A T C↑T...5'
EcoRI	5'...G↓A A T T C...3'
	3'...C T T A A↑G...5'
PstI	5'...C T G C A↓G...3'
	3'...G↑A C G T C...5'
NsiI	5'...A T G C A↓T...3'
	3'...T↑A C G T A...5'

7.3.18 Plasmid dephosphorylation

Enzymatically linearized plasmids were dephosphorylated using rAPid Alkaline Phosphatase from Roche, UK (#04898117001), this enzymatic treatment prevents the DNA strands from self-ligating (self-circularization and concatenation) by removing the phosphate group from the 5' ends. Dephosphorylation was performed according to the supplier's instructions.

Table 23 Dephosphorylation reaction mix formula

Contents	Amount (µL)
Digested vector	17
10x rAPid Buffer	2
rAPid Alkaline Phosphatase	1

7.3.19 DNA ligations

Custom designed DNA fragments were ligated to plasmid DNA using T4 DNA Ligase in a 10 µL volume reaction. For each ligation three molar insert-to-vector ratios were used and the resulting ligation reactions were incubated at 4°C overnight. However, for routine ligations three volume based ratios were used. An additional reaction was set up as negative controls containing a digested plasmid without any insert.

Table 24 DNA ligation mix formula

Contents	Inset-to-Vector ratio*			Negative Control
	1:1	1:3	1:7	
Vector	1	1	1	1
Insert	1	3	7	0
T4 DNA Ligase	1	1	1	1
Ligase Buffer 10x	1		1	1
H_2O	6	4	0	7

*amounts in µL

7.3.20 Preparation of competent cells

E. coli strains JM101 or 803 were made competent by using a modified procedure of based on $CaCl_2$ addition. Fresh cultures of 10 ml LB were incubated overnight at 37°C with 200 RPM agitation, and then 1% inoculum was used for 50 ml LB cultures. The new cultures were incubated for 2 hours at 37°C with 200 RPM agitation. The cultures were harvested in mid-exponential phase (OD_{600}=0.4) and centrifuged at 6000 RPM for 10 minutes. The resulting pellet was re-suspended in 15 ml ice-cold $CaCl_2$ and was allowed to incubate on ice for 30 minutes. Then the samples were spun down at 6000 RPM for 10 minutes (4°C) and the resulting pellet was resuspended in 2 ml of $CaCl_2$. The

samples were let on ice for 2 hour minimum. Subsequently, the competent cells were kept at 4°C for further use or kept frozen in 25% glycerol for future use.

7.3.21 Transformation competent cells

Competent cells were transformed with a heat based shocking technique. The ligated DNA and negative controls were added to 200 µL aliquots of competent cells. As negative controls, two extra aliquots were used; one containing only competent cells and one containing competent cell and the linear vector. The aliquots were incubated on ice for 30 minutes and then quickly sub-merged in a 42°C water bath for 3 minutes. After that, the samples were placed on ice for 1 minute and 500 µL of sterile LB was added. The samples were incubated at 37°C for 1 hour, centrifuged at 13000 RPM for 4 minutes. Approx. 600 µL of the supernatant were removed and the remaining supernatant approx. 100 µL was used to re-suspend the cell pellet before being spread on selective petri dishes and incubated at 37°C overnight. An additional control was included containing the digested vector.

7.3.22 Tri-parental mattings - Conjugations

Two methods were used within this study for constructing trans-conjugate cells. The first method is based on a mixture of cells growing and matting on a filter layer on the top of LB agar dish. The receiver strain, *P. denitrificans* was incubated at 37°C (200 RPM) overnight without any antibiotic in a 50 ml LB flask, the helper strain *E. coli* pRK2013 and the donor strain were incubated overnight (37°C, 200 RPM) with the appropriate antibiotic in 10 ml LB bottles. Two 50 ml LB flasks were inoculated with 1 ml of the helper and donor strain and were incubated for 4 and 7 hours respectively (37°C, 200 RPM). The cells were washed with sterile LB to remove any residual antibiotic. A 50 ml aliquot culture of each strain (receiver, helper and donor) was pelleted sequentially on the same tube (6000 RPM for 15 minutes). The resulting pellet was dissolved in 500 µL LB and carefully pipetted out on a nitrocellulose filter layered

on the surface of an LB petri dish. The dish was let still for 1 hour at room temperature and then was incubated at 30^{o}C overnight.

The second method of Tri-parental mattings is based on cross-patches of the helper, donor and receiver strains. A LB petri dish was divided in quarters and in each quarter a loop full of the respective strain was added, resulting in the following combinations: 1st helper-donor-receiver, 2nd helper-donor, 3rd receiver-donor and 4th helper-receiver. Then the strains of each quarter were mixed in a circular fashion and the dish was incubated at 30^{o}C overnight.

7.3.23 Construction of the narR mutant (PD2345)

An unmarked deletion mutant defective in narR (Pden_4238) was constructed by allelic replacement using pK18mobsacB. This mutant was made by PCR-amplifying and ligating the 5' and 3' flanking regions, 600 and 826 bp in size respectively, using primers designed to contain specific restriction enzyme sites (

Table 25). The resulting insert was cloned in to pK18mobsacB. Each suicide plasmid was verified by sequencing and conjugated into *P. denitrificans* PD1222 via triparental mating using the helper plasmid pRK2013, selecting for single cross-over recombination events using the appropriate antibiotics. These primary kanamycin resistant transconjugants were then grown to stationary phase in the absence of kanamycin, and double cross-over recombination events were selected by serial dilution and plating cells onto a modified LB-agar recipe (10 $g.L^{-1}$ tryptone, 5 $g.L^{-1}$ yeast extract, and 4 $g.L^{-1}$ NaCl) supplemented with 6% sucrose (w/v). Sucrose resistant deletion mutants that had lost kanamycin resistance were then screened by PCR, using primers external to the deletion. PCR products spanning the deletion were then sequenced for confirmation.

Table 25 Primers used for amplifying and checking a defective insert of *narR* for allelic gene exchange mutation.

Primer ID	Sequence	Restriction Site
narR_5flnF1	GA**GAATTC**gtccagacacccaggatcag	EcorI
narR_5flnR1	GA**TCTAGA**gggaaagacctggtcatagg	XbaI
narR_3flnF1	GA**TCTAGA**cccaacaccctgctggatac	XbaI
narR_3flnR1	GA**CTGCAg**aaagcggtcctggaagtc	PstI
narR_ChkF1	gcatcgggggaaaggaact	
narR_ChkR1	gaaagtggaacgggctcag	

7.3.24 DNA sequencing

The DNA fragments were sequenced by Eurofins MWG Operon, DE. Each plasmid or PCR sample contained 75 or 5 ng.µL^{-1} of DNA in a total volume of 15 µL, respectively. Sequencing primers were also submitted with the sequencing samples to the sequencing service centre (Eurofins MWG Operon, DE) at a concentration of 10 pmol.µL^{-1} per sequencing reaction. The sequencing results were retrieved either clipped (fasta format) or in the original *.ab1 file format which gives the possibility to further analyse data traces.

Table 26 Primer used for sequencing DNA fragments

Vector	Primer ID	Sequence
pGG001N10	pLMB509_1F	cgcccaactggactcatcta
	pLMB509_1R	ctgttgtttgtcggtgaacg
pGG002F01	pLMB509_1F	cgcccaactggactcatcta
	pLMB509_1R	ctgttgtttgtcggtgaacg
pK18*mobSacB*:Δ*narR*	narR_ChkF1	gcatcgggggaaaggaact
PD2345 (Δ*narR*)	narR_ChkR1	gaaagtggaacgggctcag

7.4 *In-silico* Techniques and Bioinformatics

7.4.1 General Use of Databases

Sequence databases of *P. denitrificans* (PD1222) were accessed through the NCBI Entrez server (www.ncbi.clm.nih.gov/Entrez) and a local file was downloaded separately for each chromosome and plasmid (Table 27). The viewing of the genome and retrieval of DNA and protein sequences were implemented with Artemis; a genome browser and annotation tool (http://www.sanger.ac.uk/resources/software/artemis/).

Table 27 Accession numbers for the DNA sequences of the *P. denitrificans* chromosomes and plasmids

Genome	Accession Number	Sequence Size (Mbp)
Chromosome 1	CP000489	2.852282
Chromosome 2	CP000490	1.730097
Plasmid	CP000491	0.653815
	Total	5.236194

Illustrations of the genome map or selections of the genome map (e.g. gene clusters) were based on the genome map of *P. denitrificans* on the Kegg genome database (http://www.genome.jp/).

7.4.2 Plasmid design using APE

APE is a plasmid editor supplied freely by W. Davis at the University of Utah (http://biologylabs.utah.edu/jorgensen/wayned/ape/). The deposited sequence of pLMB509 was retrieved from NCBI (GenBank: JQ895027.1) and added to APE. The *gfp* was virtually digested and removed at the NdeI site and the *narR, fnrP* and *nnrR* were virtually ligated resulting into to three plasmid sequences. The pK18*mobSacB* vector

(GenBank: FJ437239.1) was used to construct mutations in *P. denitrificans* by allelic gene exchange. The 5' and 3' flanking regions of *narR* were ligated to the vector at the *Eco*RI and *Pst*I restriction site.

7.4.3 Analysis of sequence data

The sequence data (*.ab1) were retrieved from the Eurofins MWG Operon (DE) data server and were aligned with the virtual plasmid sequences of pGG001N10, and pGG002F01 and pK18*mobSacB*:Δ*narR* respectively, *in-silico* using APE.

7.4.4 BLAST

The selected nucleotide or amino acid sequences from *P. denitrificans* were used as templates to search for similar sequences using BLAST. Sequence matches or 'Hits' are ranked according to a statistical parameter called the 'Expect value' (E-value). The E-value corresponds to the probability of the sequence similarity occurring by chance. BLAST was accessed from the NCBI Entrez server or directly from the Kegg database. The parameters used for the BLAST searches performed in this study are given in Table 28.

Table 28 BLAST parameters

Kegg Blast Attribute	**Value**
Blast	sequence as FASTA
Maximum number of database sequences to be reported	500
Maximum number of alignments to be displayed	250
Algorithm	BLOSOM62
Alignment	Pair-wise

7.4.5 Motif Search using MEME

DNA sequences of 200 bp upstream of highly expressed or repressed genes were submitted for potential pattern analysis (motifs) using MEME (http://meme.nbcr.net/meme/intro.html). MEME represents motifs as position-dependent letter-probability matrices which describe the probability of each possible letter at each position in the pattern. Individual MEME motifs do not contain gaps. Patterns with variable-length gaps are split by MEME into two or more separate motifs. These motifs are aligned against known motifs of transcriptional regulators.

7.4.6 Genome wide motif search Pattern Locator

Known DNA patterns (motifs) of the NNR, FNR and NarR, where submitted to the Pattern Locator (http://www.cmbl.uga.edu/software.html) to analyse the *P. denitrificans* genome for motif occurrence. Motifs located within the intragenic region were discarded.

7.4.7 Protein functional groups prediction

The functional structure of unknown amino-acid sequences was estimated using the PROSITE (http://prosite.expasy.org/prosite.html) Proteins or protein domains belonging to a particular family generally share functional attributes and are derived from a common ancestor. The PROSITE algorithm searches for conserved domains or profiles within a given FASTA sequence.

7.4.8 Protein topology

The location of proteins within the cell was predicted using the PSORT program (http://www.psort.org/psortb/index.html). The prediction algorithm utilizes the attributes such as the hydrophobicity of the proteins amino acids, signal peptides, and the primary structure e.g. membrane-spanning alpha-helices, to estimate the topology of the protein from a given FASTA sequence.

7.5 Statistical Techniques

7.5.1 Accuracy, reproducibility and coefficient of variation

A well accepted way of defining the accuracy of an analytical measurement is closeness of the agreement between the result of a measurement and a true value. However, this definition is theoretically impossible as the true value of each measurement is never known. The reading of the value always contains error. To simplify this concept, the accuracy of the HPLC and GC is estimated as the percentage difference of the reading with an assigned true value (equation 12); this is done during the calibration of the analytical equipment. Error values lower than 5% were regarded as acceptable.

$$e\% = 100 * \frac{|x_i - x|}{x}$$

Equation 12 Error, where *e%*= error expressed as percentage, x_i= measurement or reading value and *x*= true or assigned value.

To measure the reproducibility or repeatability of a measurement using the HPLC and GC, standard samples were measured repeatedly and the percent coefficient of

variation was calculated (equation 13). CV values smaller than 5% were regarded as acceptable.

$$\boldsymbol{CV\%} = \mathbf{100} * \frac{\boldsymbol{\sigma}}{\boldsymbol{\mu}}$$

Equation 13 Coefficient of variation, where *CV%* = Coefficient of variation expressed as percentage, σ= standard deviation and μ= mean.

7.5.2 Standard deviation and precision

The standard deviation (SD) of a set of values shows how much variation or dispersion from the average value exists (equation 14 and 15). SD may serve as a measure of uncertainty. The SD of a set of repeated values gives the precision of those values. A low standard deviation indicates that the data points tend to be very close to the mean or expected value whereas a high standard deviation indicates that the data points are spread out over a large range of values. Each treatment was replicated three times (n=3, biological replicates) and two or three technical replicates were taken. The sample bias of both equations (equation 14 and 15) of standard deviation is equally significant for small populations (n<10), for that reason the standard deviation of the sample was used to interpret the results. When analysing the qRT-PCR results, technical replicates having a SD> 0.2 were discarded as technically unacceptable.

$$SD = \sqrt{\frac{\Sigma(x_i - \mu)^2}{n}}$$

Equation 14 Standard deviation of the sample of a finite population, where *SD*= standard deviation, x_i= value, μ=mean and n=size of observations (population).

$$s = \sqrt{\frac{\Sigma(x_i - \mu)^2}{N - 1}}$$

Equation 15 Corrected sample standard deviation, where *s*= standard deviation, x_i= value, μ=mean and *N-1*= degrees of freedom.

The SD, as well as the mean, is a statistical description of the observations; the SD describes the degree to which an observation within the group of observations differs from the average value (mean).

7.5.3 Standard Error

The standard error is usually estimated by the sample estimate of the sample standard deviation divided by the square root of the sample size while assuming statistical independence of the values in the sample.

$$SE = \frac{SD}{\sqrt{n}}$$

Equation 16 The sample standard error, where SE= standard error, SD=standard deviation and n= size of the observations.

Standard error is probabilistic statement estimating how the number of observations (or samples) will provide a better bound on estimates of the population mean or the probability of the closeness of the population mean to the mean of an observation.

7.5.4 Volcano Plot Analysis

7.5.5 Principal Component Analysis

Principal Components Analysis (PCA) is an exploratory method that covariance analysis is performed to reduce data dimensionality. Dimensionless axes illustrate the trends and explains the variability of the gene data sets based on samples or conditions. PCA The eigenvectors and eigenvalues relevant to the data were calculated using a covariance matrix. Eigenvectors can be thought of as “preferential directions” of a data set, and eigenvalues can be thought of as quantitative assessment of how much a component represents the data. Simply, the eigenvalues represent the level of explained variance as a percentage of total variance. PCA was performed using the standard PCA tools of GeneSpring.

7.6 Primers used

7.6.1 Primers used for qRT-PCR detection

Table 29 Primer oligonucleotide sequences used for qRT-PCR detection in this study

Annotation	Gene ID	Forward	Reverse
narG	Pden_4236	gcgaggaggtctgctacaac	atccattcgtggtcctggta
nasB		cctataaatgggtggccaag	cgatagaccgactggctgat
nirS	Pden_2487	aattcggcatgaaggagatg	tccagatcccagtcgttttc
norB	Pden_2483	tatgtcagcccgaacttcct	ttcgggcaggatgtaatagg
nosZ	Pden_4219	ccgttcagttcctgatagtcg	cttttcgacctcctacaactcg
napA	Pden_4721	tggatccaggtgaacaacaa	gtccgagacgacgatgaaat
napB	Pden_4722	gctggaccgaacccatgtcc	tgttcaccgtcagctggtag
Aa3	Pden_4321	gctggatcatttcgtgctct	agggtccagatcacctcgat
qoxB	*Pden_5107*	cgtgttttccgaagtcacct	gcccatggtgaagaagtgat
ctaE	*Pden_4317*	cgtgctctacgtcatgttcg	acaggatgaagccgtattgc
ctaDI	*Pden_3028*	gctgatctcggtcacactca	taggtcacgacgacattcca
cycA	*Pden_1937*	cagcatctatgccactctcg	caagccttgcacttgttgaa
ctaDII	*Pden_1938*	gcctgatctcggtatgcttc	catgacgttccacaggtgtc
ccoN	*Pden_1848*	ccatgctgcatatcgtcaac	cataccaccattgcgtcatc
ccoO	Pden_1847	aaagcacaaggtcctggaaa	gcacctttcgatggtgttt
ccoQ	*Pden_1846*	Cttctgctgctggtggtctt	cgtctcgttacggaagatgc
uspA	*Pden_1849*	aagggctccttcagctcatc	gctattccgacctggtggt
narR	*Pden_4238*	agggctatcgcaacttcgt	Ccggtatcgagcgatcttt

Table continues in the next page

Annotation	Gene ID	Forward	Reverse
fdsA	Pden_2856	gcggtctttcacaacaacaa	gtcggtatcatcgaccgaat
ccbS	Pden_1700	gatgatggagctggacgaat	aggacatcatcaccgtctcc
ccpA	Pden_0893	tgcaagcctttatcgagacc	ggtctggctgatctcgtagc
fbcB	Pden_2306	ttgtgctggtcgtgttcttc	agggcaggaaataccattcc
cydB	Pden_4011	ggcatcagcatctttcccta	aggatgatcgggatgatgaa
cydA	Pden_4010	ctgttcgggatgaacaaggt	cgtctgcatccagctgttta
nodA	pden_1689	aggttccggtgcattacatc	gtctggtggaaatcggtgac

References

Alston, M., J. Seers, J. Hinton and S. Lucchini (2010). "BABAR: an R package to simplify the normalisation of common reference design microarray-based transcriptomic datasets." BMC Bioinformatics **11**(1): 73.

Baker, S. C., S. J. Ferguson, B. Ludwig, M. D. Page, O. M. Richter and R. J. van Spanning (1998). "Molecular genetics of the genus *Paracoccus*: metabolically versatile bacteria with bioenergetic flexibility." Microbiology and Molecular Biology Reviews **62**(4): 1046-1078.

Felgate, H. (2010). Nitrous oxide emissions in chemostats - 2nd year transfer report. Norwich, Univerisity of East Anglia.

Felgate, H., G. Giannopoulos, M. J. Sullivan, A. J. Gates, T. A. Clarke, E. Baggs, G. Rowley and D. J. Richardson (2012). "The impact of copper, nitrate and carbon status on the emission of nitrous oxide by two species of bacteria with biochemically distinct denitrification pathways." Environ Microbiol **14**(7): 1788-1800.

Figurski, D. H. and D. R. Helinski (1979). "Replication of an origin-containing derivative of plasmid RK2 dependent on a plasmid function provided in trans." Proceedings of the National Academy of Sciences **76**(4): 1648-1652.

Hoskisson, P. A. and G. Hobbs (2005). "Continuous culture – making a comeback?" Microbiology **151**(10): 3153-3159.

Hungate, R. E. (1969). A roll tube method for cultivation of strict anaerobes. New York, Academic Press.

Koutny, M. and L. Zaoralkova (2005). "Miniaturized kinetic growth inhibition assay with denitrifying bacteria *Paracoccus denitrificans*." Chemosphere **60**(1): 49-54.

Olson, B. J. S. C. and J. Markwell (2001). Assays for Determination of Protein Concentration, John Wiley & Sons, Inc.

Pfaffl, M. W. (2001). "A new mathematical model for relative quantification in real-time RT–PCR." Nucleic Acids Research **29**(9): e45.

Saunders, N. F. W., J. J. Hornberg, W. N. M. Reijnders, H. V. Westerhoff, S. de Vries and R. J. M. van Spanning (2000). "The NosX and NirX Proteins of *Paracoccus denitrificans* are functional homologues: their role in maturation of nitrous oxide reductase." Journal of Bacteriology **182**(18): 5211-5217.

Schafer, A., A. Tauch, W. Jager, J. Kalinowski, G. Thierbach and A. Puhler (1994). "Small mobilizable multi-purpose cloning vectors derived from the Escherichia coli plasmids pK18 and pK19: selection of defined deletions in the chromosome of Corynebacterium glutamicum." Gene **145**(1): 69-73.

Sears, H. J., S. Spiro and D. J. Richardson (1992). "Effect of carbon substrate and aeration on nitrate reduction and expression of the periplasmic and membrane-boundnitrate reductases in carbon-limited continuous cultures of *Paracoccus denitrificans* Pdl222." Microbiology **9971**: 3767-3774.

Sullivan, M. J., A. J. Gates, C. Appia-Ayme, G. Rowley and D. J. Richardson (2013). "Copper control of bacterial nitrous oxide emission and its impact on vitamin B12-dependent metabolism." Proceedings of the National Academy of Sciences.

van Spanning, R. J. M., A. P. N. de Boer, W. N. M. Reijnders, H. V. Westerhoff, A. H. Stouthamer and J. van der Oost (1997). "FnrP and NNR of *Paracoccus denitrificans* are both members of the FNR family of transcriptional activators but have distinct roles in respiratory adaptation in response to oxygen limitation." Molecular Microbiology **23**(5): 893-907.

Vishniac, W. and M. Santer (1957). "The *Thiobacilli*." Bacteriological Reviews **21**(3): 195-213.